The role of epigenetic modulators on circadian rhythms and metabolism



DPhil candidate: Dragos Ionut Mosneagu

Supervisor: Dr. Sridhar Vasudevan
Co-Supervisor: Professor Russell Foster

DTP Director and Programme supervisor: Dr. Esther Becker

Trinity Term 2020

New College,
Department of Pharmacology,
University of Oxford

Doctoral Training Centre (DTC),
Rex Richards Building,
University of Oxford

Wordcount: 49,900



OXFORD INTERDISCIPLINARY BIOSCIENCE
Doctoral Training Partnership

This DPhil thesis was submitted as part of the DPhil in Interdisciplinary Bioscience - Pharmacology 2016-2020 programme curriculum

LIST OF ABBREVIATIONS

Abbreviation	Full annotation
2DG6P	2-deoxyglucose-6-phosphate
ABCA1	ATP-Binding Cassette A1
ACC	Acetyl-CoA Carboxylase
ACF1	ATP-dependent Chromatin Remodelling Protein 1
AgRP	Agouti-Related Peptide
AMP	Adenosine monophosphate
AMPK	5'-AMP-activated protein kinase
ANOVA	Analysis of Variance
AP-1/2	Adaptor Protein Complex 1/2
ARNT	Aryl-Hydrocarbon Receptor Nuclear Translocator
ATCC	American-Type Culture Collection
ATP	Adenosine triphosphate
B-Act	B-Actin
BAT	Brown Adipose Tissue
BD	Bromodomain family
BDZ	Benzodiazepine
BET	Bromo- and Extracellular domain
BHLHE40/41	Basic helix-loop-helix Class E 40/41 (aka DEC1/DEC2)
BMAL1	Brain and Muscle ARNT-Like 1
BMI	Body-Mass Index
BRD	Bromodomain
BRDT	Bromodomain Testis-Associated
CAF	Cafeteria Diet
cAMP	Cyclic Adenosine Monophosphate
CBHA	m-Carboxycinnamic Acid Byshydroxamide
CD36	Cluster of Differentiation 36
CEBPα	CCAAT/Enhancer-Binding Protein A
ChIP-Seq	Chromatin Immunoprecipitation Sequencing
Ck1	Casein Kinase 1
CRPC	Castrate-Resistant Prostate Cancer
CRY1/2	Cryptochrome 1/2
CCG	Clock-Controlled Gene
CCL2	C-C Motif Chemokine 2
cDNA	Complementary DNA
CLOCK	Circadian Locomotor Output Cycle Kaput
CMV	Cytomegalovirus
CoA	Coenzyme A
COX7A1	Cytochrome C Oxidase 7A1
CREB	cAMP Response Element-Binding Protein
CT	Circadian Time
CVD	Cardiovascular Disease
DAPI	4'-6-diamidino-2-phenylindole
DBP	D-Box Binding PAR BZIP Transcription Factor
DDIT3	DNA Damage Inducible Transcript 3
DEC1/2	Deficient in oesophageal cancer (aka BHLHE40/41)

DIO	Diet-induced obesity
DIO2	2-Iodothyronine Deiodinase
DMEM	Dulbecco's Modified Eagle Medium
DMSO	Dimethyl Sulfoxide
DNA	Deoxyribonucleic Acid
DNMT	DNA Methyltransferases
DPP-4	Dipeptidyl peptidase-4 inhibitor
E-Box	Enhancer Box
EC_{50}	Efficacy Concentration 50
EBV	Epstein-Barr Virus
ECAR	Extracellular Acidification Rate
EGR1	Growth Response Protein 1
ELISA	Enzyme-linked immunosorbent assay
ELK1	ETS-Like-1 Protein
EMSA	Electrophoretic Mobility Shift Assay
EMA	European Medicines Agency
EPO	Erythropoietin
ER	Oestrogen Receptor
ESCs	Embryonic Stem Cells
Ex/Em	Excitation/Emission
FAD_2	Flavin Adenine Dinucleotide
FAS	Fatty Acid Synthase
FBS	Foetal Bovine Serum
FCCP	Carbonyl cyanide-4 phenylhydrazone
FDA	Food and Drug Administration
FNNS	Familial Natural Short Sleepers
GABA	Gamma Aminobutyric Acid
GAPDH	Glyceraldehyde 3-phosphate dehydrogenase
GATA1	GATA-Binding Protein 1
GCK	Glucokinase
GDP	Gross Domestic Product
GFP	Green Fluorescent Protein
GLP-1	Glucagon-like peptide 1
GTP	Guanosine Triphosphate
GLUT1/2/4	Glucose Transporter Type 1/2/4
GOI	Gene Of Interest
GR	Glucocorticoid Receptor
GSK-3b	Glycogen Synthase Kinase 3b
GSV	GLUT4 Storage Vesicles
GTT	Glucose Tolerance Test
H&E	Haematoxylin and Eosin Stain
HEY1/2	Hairy Ears, Y-Linked
HAT	Histone Acetyl-Transferase
HbA1c	Glycated haemoglobin
HDAC	Histone Deacetylase
HDL	High Density Lipoprotein
HER2	Human Epidermal Growth Factor Receptor 2
HEY1	Hes Related Family BHLH Transcription Factor with YRPW Motif 1
HFD	High Fat Diet
HG19	Homo Sapiens genome assembly GRCh37
HIF1	Hypoxia Inducible Factor 1
HIV	Human Immunodeficiency Virus

HKII	Hexokinase II
HKG	House-Keeping Gene
HLIP	Hepatic Lipase
HMT	Histone Methylation Enzymes
HNF1A/4A	Hepatic Nuclear Factor 1 α
HOMER	Hypergeometric Optimization of Motif Enrichment
HRE	Hypoxia-Response Element
HSL	Hormone Sensitive Lipase
HSPA1A	Heat Shock 70 kDa Protein 1A
HSV	Herpes Simplex Virus
HTS	High Throughput Screen
IBMX	3-isobuty-1-methylxanthine
IDH3A	Isocitrate Dehydrogenase α
IL-1b/6	Interleukin 1b/6
IR	Insulin Receptor
ITT	Insulin Tolerance Test
KDM	Histone Lysine Demethylases
KLF4	Kruppel-Like Factor 4
KMT	Histone Lysine Methyltransferases
LB	Lysogeni Broth
LD_{50}	Lethal Dose 50
LDL	Low Density Lipoprotein
LPL	Lipoprotein Lipase
MACS2	Model Based Analysis of ChIP-Seq 2
MAPQ	Mapping Quality
MBP	Methylation Binding Protein
MLL1	Mixed Lineage Leukaemia Protein 1
MODY	Maturity-Onset Diabetes in the Young
mRNA	Messenger RNA
MTF1	Metal Regulatory Transcription Factor 1
NAD(P)H	Nicotinamide Adenine Dinucleotide (Phosphate) Hydrogen
NAFLD	Non-Alcoholic Fatty Liver Disease
NASH	Non-Alcoholic Steatohepatitis
NCoR1	Nuclear Receptor Corepressor 1
NF Y/Kb	Nuclear Factor Y / Kb
NHS	National Healthcare System
NPAS2	Neuronal PAS Domain Protein 2
NPY	Neuropeptide Y
NR1D1	Nuclear Receptor subfamily 1 group D member 1
NSCLC	Non-Small Cell Lung Cancer
NTC	Non-Targeting Control
NUT	Neuronal Protein in Testis
OCR	Oxygen Consumption Rate
OCT4	Octamer-Binding Transcription Factor 4
Opti-MEM	Reduced Serum Media (Eagle's Minimum Essential Media)
OxPhos	Oxidative Phosphorylation
PAS domain	Per-Arnt-Sim domain
PER1/2/3	Period 1/2/3
PGC1A	PPARɣ-Coactivator 1-α
PNPLA3	Patatin-like phospholipase domain containing protein 3
PPARA/G	Peroxisome Proliferator-activated receptor α/gamma
PPARɣC1A	Peroxisome Proliferator-Activated Receptor Gamma Coactivator 1a

POMC	Proopiomelanocortin
PSAT1	Phosphoserine Aminotransferase 1
PUFAs	Polyunsaturated Fatty Acids
PVN	Paraventricular Nucleus
P/S	Penicillin Streptomycin
(q/RT)PCR	(Quantitative/Real-Time) Polymerase Chain Reaction
RBP-Jk	Recombinant Binding Protein for Immunoglobulin Kappa J Region
RETN	Resistin
RISC	RNA-Induced Silencing Complex
RLT	RNeasy Lysis Buffer
RNA	Ribonucleic Acid
ROS	Reactive Oxygen Species
SAHA	Suberonylanilide Hydroxamic Acid
SAM	S-Adenosyl Methionine
SAR	Structure Activity Relationship
SARS	Severe Acute Respiratory Syndrome
SCD1	Stearoyl-CoA Desaturase 1
SCN	Suprachiasmatic Nucleus
SCRD	Sleep and Circadian Rhythm Disruptions
SD	Standard Deviation
SEM	Standard Error of the Mean
SGLT	Sodium-glucose cotransport protein
shRNA	Short hairpin RNA
siRNA	Small interfering RNA
SIRT1	Sirtuin 1
SP1	Specificity Protein 1
SLC2A1/4	Solute Carrier Family 2 Member 1
T1D	Type-1 Diabetes
T2DM	Type-2 Diabetes Mellitus
TBP	TATA-Binding Protein
TF(BS)	Transcription Factor (Binding Sites)
TFEB	Transcription factor EB
TIEG1	Transforming Growth Factor-β Inducible Early Gene 1
TM6SF2	Transmembrane 6 Superfamily 2
TNBC	Triple Negative Breast Cancer
TNFα	Tumour Necrosis Factor A
TSS	Transcription Start Site
TTFL	Transcriptional Translational Feedback Loop
TZDs	Thiazolidinediones or glitazones
U2OS	Human osteosarcoma cells
UCP1/2	Uncoupling Protein 1/2
USF1/2	Upstream Stimulatory Factor 1/2
VCaP	Vertebral-Cancer of the Prostate
VEGF	Vascular Endothelial Growth Factor
VLDL	Very Low Density Lipoprotein
WAT	White Adipose Tissue
WHO	World Health Organization
XBP1	X-Box Binding Protein 1
YY1	Yin and Yang 1 Protein
ZNF	Zinc-Finger Domain
ZT	Zeitgeber Time

TABLE OF CONTENTS

LIST OF ABBREVIATIONS 2

TABLE OF CONTENTS 6

ABSTRACT 10

ACKNOWLEDGEMENTS 11

COVID-19 IMPACT ON RESEARCH 12

1 GENERAL INTRODUCTION 13

1.1 Recurrent rhythms in biology 13

1.2 Circadian rhythms in physiology and behaviour 14

1.3 Components of the molecular clock 16

1.4 The DEC1/DEC2-driven control of circadian rhythms 17

1.5 Tissue-specific control of the circadian genes 18

1.6 Impact of zeitgebers on epigenetics 19

1.7 Intrinsic and extrinsic epigenetic control of circadian rhythms 20

1.8 Importance of amplitude regulation in circadian gene expression 24

1.9 The metabolic syndrome 26

1.10 Impact of obesity 27

1.11 Aetiology of diabetes 28

1.12 Non-alcoholic fatty liver disease (NAFLD) and NASH 29

1.13 Current pharmacological therapies for the metabolic syndrome 30

1.14 Circadian rhythm disruptions in cardiometabolic regulation 33

1.15 Epigenetic modulation of metabolic phenotypes 36

1.16 Hypothesis and aims of this study 37

2 MATERIALS AND METHODS 39

2.1 Cells used for *in-vitro* experiments 39

2.2 Gene reporter system: *Per2*::Luc and *BMAL1::*Luc U2OS cells 39

2.3 Transient transfection protocol 40

2.4 siRNA knockdown transfection protocol 41

2.5 PrestoBlue cell-viability assay 42

2.6 Bacterial transformation and selection and plasmid preparation 42

2.7 RNA extraction, purification and sample preparation 43

2.8 RNA conversion and DNA quantification through PCR 44

2.9 Cignal transcription factors screen assay 45

2.10 Assessment of IBET-762 TF-activation on circadian rhythms 51
2.11 *Sp1::*Luc and *Hre::*Luc promoter reporter drug-induced activity 52
2.12 Transfac analysis of BMAL1 promoter regions 52
2.13 ChIP-Seq data analysis 53
2.14 Adipocyte differentiation protocol of 3T3-L1 54
2.15 Lipid-staining protocol in adipocytes 55
2.16 Nuclear-staining protocol in adipocytes 55
2.17 Lipolysis assay in 3T3-L1 differentiated adipocytes 56
2.18 Glucose-uptake assay in 3T3-L1 differentiated adipocytes 56
2.19 Lactate-uptake assay in 3T3-L1 differentiated adipocytes 57
2.20 ATP-production analysis in 3T3-L1 differentiated adipocytes 58
2.21 NAD^+/NADH ratio in differentiated 3T3-L1 adipocytes 59
2.22 High fat diet induced obesity mouse experimental setup 60
2.23 Glucose and insulin tolerance tests 62
2.23 Liver weight analysis 63
2.24 Tissue cryosection and histological staining 64
2.25 Ex-vivo plasma metabolite quantification 66
2.26 Data analysis and statistics 68

3 Chapter I: EPIGENETIC MODULATION ON CIRCADIAN RHYTHMS 72
3.1 INTRODUCTION 72
3.1.1 Epigenetic mechanisms in eukaryotes 72
3.1.2 DNA methylation mechanisms 73
3.1.3 Histone methylation mechanisms 75
3.1.4 Histone acetylation mechanisms 76
3.1.5 Bromodomains in epigenetic regulation 78
3.1.6 Bromodomain inhibitors as epigenetic drugs 79
3.2 RESULTS 81
3.2.1 Epigenetic drugs influence circadian rhythm gene expression 81
3.2.2 Effects of acetylation modulators on U2OS Bmal1::Luc expression 85
3.2.3 Effects of HDACs on circadian period and amplitude 88
3.2.4 Identification of bromodomain inhibition as circadian modulator 90
3.2.5 Effects of IBET-762 on circadian amplitude 92
3.2.6 Effects of IBET-762 on transiently-transfected clock genes 94
3.2.7 Circadian gene expression quantification following IBET-762 96
3.3 DISCUSSION 100

4 Chapter II: SP1-MEDIATED MOA OF BD-1 IN CIRCADIAN RHYTHMS 110
4.1 INTRODUCTION 110
4.1.1 Transcription factor interaction on promoter and enhancer regions 110
4.1.2 Bromodomains and transcription factor interaction 111
4.1.3 SP1 transcription factor and its interactions with bromodomains 113
4.1.4 HIF1 in cellular functionality and circadian rhythms 116
4.1.5 Pathophysiological role of bromodomains 118
4.1.6 Bromodomains in non-oncologic indications 120
4.1.7 TF activation and methods to study their activity 122
4.2 RESULTS 126
4.2.1 Effects of BRD-specific knock-down on circadian rhythms 126
4.2.2 BRD-knockdown effectiveness and specificity on U2OS cells 129
4.2.3 Evaluating the mechanisms behind BRD4 inhibition 131
4.3.4 Regulatory gene modulation by IBET-762 (motif enrichment) 133
4.2.5 Pathway gene ontology modulation by IBET-762 in VCaP cells 136
4.2.6 Early-gene modulation following IBET-762 administration 139
4.2.7 Effects of IBET-762 on TF modulation (U2OS screen) 141
4.2.8 Circadian effects of IBET-762 on upregulated TFs knock-down 143
4.2.9 Effects of IBET-762 on SP1 and HRE promoter activity 146
4.2.10 Epigenetic specificity of *Sp1*::Luc and *Hre*::Luc expression 148
4.2.11 *Bmal1* promoter transcription factor sites analysis (Transfac) 152
4.3 DISCUSSION 154

5 Chapter III: METABOLIC PHENOTYPING OF BET INHIBITORS 162
5.1 INTRODUCTION 162
5.1.1 Cellular hallmarks of adipocytes and obesity 162
5.1.2 White adipose tissue (WAT) and brown adipose tissue (BAT) 163
5.1.3 Cellular differentiation and functionality of adipocytes 165
5.1.4 Glucose-fuelled energy production in eukaryotic cells 167
5.1.5 Insulin regulation of cellular glucose uptake 169
5.1.6 HIF1 and SP1 in cellular metabolism 172
5.1.7 Impact of bromodomains on metabolism 176
5.2 RESULTS 178
5.2.1 Regulation of metabolic gene expression by IBET-762 178
5.2.2 Mediation of PPARɣ gene expression effects 180
5.2.3 Modulation of adipocyte differentiation by IBET-762 182

5.2.4 IBET-762 modulation of metabolic markers in adipogenesis 185
5.2.5 IBET-762 modulation of key metabolic pathways in adipocytes 188
5.2.6 IBET-762 modulation of metabolic regulation in adipocytes 191
5.2.7 Effects of IBET-762 on lipolysis and lactate production 193
5.2.8 CLOCK and SP1 effects of IBET-762 on adipocyte glucose uptake 195
5.2.9 Effects of IBET-762 on ATP energy production 197
5.2.10 Effects of IBET-762 on NAD^+ and NADH levels in adipocytes 201
5.3 DISCUSSION 203

6 Chapter IV: *IN-VIVO* EFFECTS OF IBET-762 ON METABOLISM 218
6.1 INTRODUCTION 218
6.1.1 Markers and types of diabetes 218
6.1.2 Circadian rhythms influence in diabetes 221
6.1.3 Models to study obesity and HFD in mice 223
6.2 RESULTS 227
6.2.1 Effects of IBET-762 on weight in chronic HFD mouse model 227
6.2.2 Effects of IBET-762 on glucose tolerance in chronic HFD mice 230
6.2.3 Effects of IBET-762 on insulin tolerance in chronic HFD mice 232
6.2.4 Effects of IBET-762 on liver weight and steatosis in HFD mice 234
6.2.5 Effects of IBET-762 on plasma metabolites in DIO mice 236
6.2.6 Adipogenesis markers expression in liver samples of DIO mice 238
6.2.7 Glucose regulation gene expression in liver samples of DIO mice 240
6.2.8 Glucose regulation gene expression in skeletal muscle of DIO mice 242
6.2.9 Metabolomic regulation gene expression visceral fat of DIO mice 244
6.2.10 Inflammatory markers gene expression in visceral fat of DIO mice 246
6.2.11 Effects of IBET-762 on the size of visceral adipocytes 246
6.2.12 Anorexigenic markers gene expression in PVN of DIO mice 248
6.3 DISCUSSION 250

7 FINAL DISCUSSION 265
7.1 Implications of circadian amplitude enhancement of BET inhibitors 265
7.2 SP1-mediated circadian amplitude increase of IBET-762 267
7.3 IBET-762 effects on cellular metabolism 268
7.4 Effects of IBET-762 on DIO C57BL/6 mouse model 271
7.5 Conclusions and final remarks 276

8 BIBLIOGRAPHY 279

ABSTRACT

The earth's rotation on its axis with a 24-hour period gave rise to circadian rhythms, which originated pervasive biologic fluctuations in gene expression, cellular physiology and whole-organism behaviour. The advancements in technology and culture accentuated behaviours and phenomena that implicated a disruption in the synchronisation between our inner circadian clock and the outer environment. This desynchrony was associated with a deregulated molecular clock and an increased incidence of metabolic disorders. We have identified circadian rhythm enhancers as a potential chronotherapeutic mechanism in tackling the circadian deregulations that could be key in the pathogenesis of these associated metabolic deregulations.

Here, we describe the characteristics and efficacy of bromodomain inhibitors, a novel class of epigenetic modulators, in enhancing the amplitude of mammalian circadian clock, with the aim of improving on the pathophysiologies correlated with dampened circadian rhythms. IBET-762, a selective and potent bromodomain inhibitor, is shown to enhance the expression of several clock genes including *Bmal1* and *Per2*, via BRD4 and Specificity Protein 1 (SP1), a transcription factor with widespread metabolic effects, and impact on metabolic pathophysiology at least partially through SP1.

IBET-762 reduces both glucose uptake and adipogenesis in 3T3-L1 cells, giving rise to the potential of being useful in tackling obesity and diabetes. The drug was further tested *in-vivo* in a C57BL/6 mouse model of diet-induced obesity, and showed to be efficacious in reducing weight gain and hepatosteatosis. This demonstrates the usefulness of BRD inhibitors in tackling obesity and non-alcoholic fatty liver disease (NAFLD). However, IBET-762 also induced a pre-diabetes like phenotype that was not associated to either insulin insensitivity or to β-cell toxicity, but rather to an acute inhibition of several genes involved in glucose metabolism and transport. It is therefore pivotal to further dissect the mechanism of action behind the metabolic effects of IBET-762 and identify the molecular mechanisms and pathways activated, such that one could be tackled independently from the deleterious effects of the others.

ACKNOWLEDGEMENTS

I would like to extend my appreciation to the Oxford University BBSRC Doctoral Training Programme for funding this DPhil and to everyone in the DTP16 cohort, professors, mentors and colleagues, for contributing towards a pleasant and stimulating learning environment.

Firstly, I would like to extend my gratitude to Dr. Sridhar Vasudevan, as he has shown an immense support throughout the past four years, both technically as well as personally. His input allowed me to grow both as a scientist and well-rounded individual. I will truly miss the long-lasting lunch chats related to science, current affairs and anything in between.

I would also like to thank former and present colleagues for their scientific and technical help, but also for rendering the laboratory a pleasant and enjoyable work environment: Dr. Dorota Nawrot, Dr. Harshmeena Sanghani, Zeinab Wakaf and Farid Ebrahimjee. I will truly miss our outdoor adventures and conference attendances, which often brought unforgettable memories. I am also grateful to Professor Grant Churchill, Professor Aarti Jagannath and the Jagannath lab members, for their help and support throughout my doctoral studies.

I would like to thank my friends for their companionship, moral support, and endless laughs, but also for their pharmacologic insight over a pint of Guiness. Thank you for making my permanence in Oxford such an unforgettable experience.

I would like to thank my parents and my partner, for their unconditional support throughout this period. Their unwavering advice has guided me throughout the years and have helped me to confidently become the person that I am today.

COVID-19 IMPACT ON RESEARCH

The Sars-Cov2 pandemic has caused the temporary closure of the Department of Pharmacology and The Oxford Molecular Pathology Institute, University of Oxford, between March and July 2020. These unforeseeable circumstances have prevented the possibility to run any of the experiments that were planned for this period:

1) RNA-Seq of *ex-vivo* liver and visceral fat samples from the diet-induced obesity C57BL/6 mice experiment. This experiment would have allowed the pathway analysis of the metabolic impact of IBET-762 in already collected samples, possibly aiding towards further understanding and dissociating the molecular impact of the drug on the mice phenotype.
2) Jet-lag experiment in a mouse model, to assess the *in-vivo* putative effects of IBET-762 as a circadian rhythm enhancer/resynchroniser, under the abrupt shift of the light-dark cycle.
3) Western Blot of Specificity Protein 1 (SP1), to characterize the protein levels and activity of the transcription factor, which was reputed central in the effects of IBET-762.

1 GENERAL INTRODUCTION

1.1 Recurrent rhythms in biology

Life on Earth has evolved as a function of Earth's rotation around the Sun and on its axis, giving rise to circa 365 days and 24 hours periods, respectively. The circa 365 days period, known as a circannual rhythms, gives rise to seasonal-specific behaviours in animals and plants, such as hibernation and morphological changes (Pengelley *et al.*, 1976), whereas the 24 hour period is known as diurnal rhythm. Biological rhythms are entrained by the environment and zeitgeber factors such as light, temperature, and food availability play a pivotal role in keeping these rhythms in check. However, to be defined as such, biological rhythms need to be endogenously self-sustaining, at least for a few cycles, when the environmental cues are removed (Aschoff, 1960).

Circadian rhythms are one of such example of circa 24-hour diurnal rhythms that are generated endogenously and are self-sustaining, even when the external zeitgebers, which can re-entrain the inner clock to the environment, are removed (Aschoff, 1965; Daan & Pittendrigh, 1976). These rhythms are driven by a circadian clock and are widely present in plants, animals, fungi, and cyanobacteria. They are ubiquitous in living systems and are found at different levels, regulating behavioural and physiological phenotypes. One distinguishing characteristic of circadian rhythms is temperature compensation, defined as the capacity of an internal clock to withstand differences in temperature without having an impact on its downstream effectors. This allows organisms to maintain an intact circadian rhythm even in presence of environmental temperature variations.

1.2 Circadian rhythms in physiology and behaviour

Virtually all aspects of mammalian physiology and behaviour display 24-hr oscillations, driven by an endogenous circadian clock. These 24-hr oscillations can be observed in fundamental physiological processes ranging from hormone secretion to complex processes such as cognition and memory formation. Other processes, such as thermoregulation, metabolic regulation, heart rate, and blood pressure all show a 24-hour circadian pattern (**Fig.1.1**). The oscillations are orchestrated by individual molecular clocks present in almost every cell within our body and these individual clocks are held in synchrony by a master clock located in the suprachiasmatic nucleus (SCN) (Weaver, 1998), in the hypothalamus, and is constituted by about 20,000 neurons in rodents and 100,000 neurons in humans (Abrahamson & Moore, 2001). The SCN clock is synchronised to the day/night cycle by photic input from the retina, and itself entrains the peripheral clocks of the body (Schibler & Sassone-Corsi, 2002), thereby resulting in coordinated rhythmic physiological and behavioural outputs (**Fig. 1.2**) in relation to the environment. Whilst the SCN dictates the phase entrainment of these peripheral clocks, interestingly, the molecular clocks within are self-sustaining oscillators capable of functioning even in the absence of the SCN; the peripheral clocks can keep an approximately 24-hour circadian cycle for a few days even in absence of SCN signalling before getting desynchronized. This system helps to predict and anticipate daily fluctuations in the environment, allowing appropriate physiological adaptation.

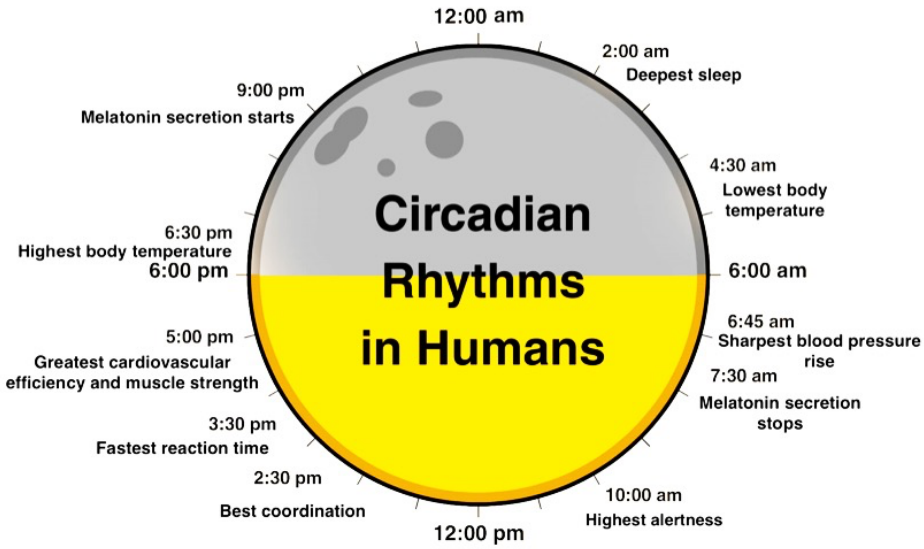


Figure 1.1 – Behavioural and physiological parameters that show a 24-hour temporal pattern. Several biological physiologies and behaviours show a specific time-of-day peak (or trough) in intensity, such as sleep but also other characteristics not directly associated with circadian rhythms, such as reaction time, coordination, alertness, body temperature, and cardiovascular functionality. Figure adapted from the open domain.

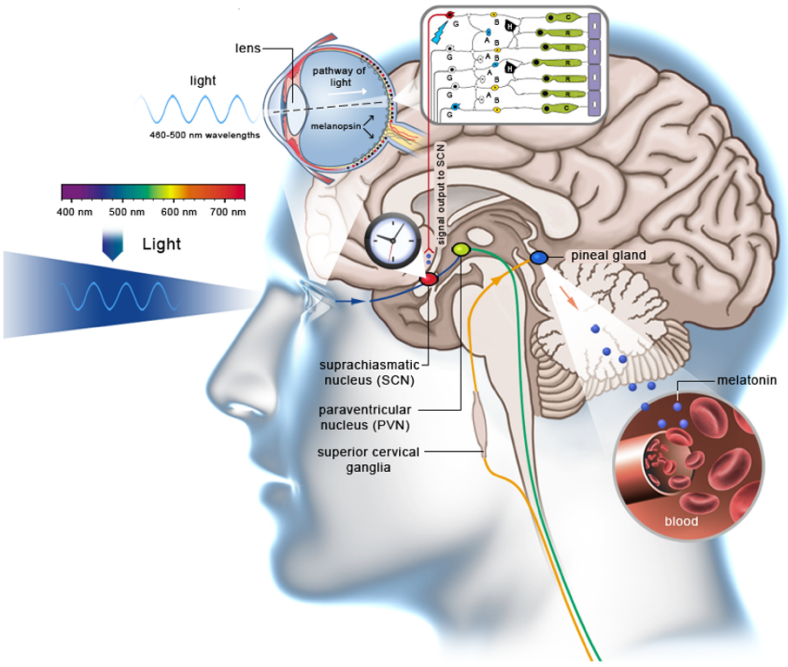


Figure 1.2 – Light entrains the SCN, which synchronizes all the other peripheral clocks. Light information is processed by the retinal ganglion cells and transduced into an electrical signal that is then processed in the SCN, in the hypothalamus. SCN is named as the master circadian clock and entrains the peripheral clocks around the body through ill-defined mechanisms, stimulating circadian physiology, such as the release of melatonin or leptin sensitivity in the paraventricular nucleus (PVN). Figure adapted from the open domain.

1.3 Components of the molecular clock

The first molecular clock genes were identified in the fruit fly *Drosophila melanogaster* in the 1980s, based on 1970s genetic studies (Konopka & Benzer, 1971), consolidating the hypothesis that a set of a few conserved genes should be driving the expression of circadian-controlled genes (dubbed the molecular clock). The discovery of the first clock genes by Jeffrey Hall, Michael Rosbash and Michael Young was indeed recognized with the 2017 Nobel Prize in Physiology or Medicine (Dibner & Schibler, 2018). It was later described in several organisms that the molecular circadian clock comprised of cell-autonomous transcriptional networks with integrated auto-regulatory feedback loops (TTFL: transcriptional–translational feedback loop). In mammals, the core clock proteins CLOCK (Circadian Locomotor Output Cycles Kaput) and BMAL1 (Brain and Muscle ARNT-Like 1) are transcriptional activators (positive arm of the clock) that drive the expression of many clock-controlled genes (CCGs) (Takahashi, 2017). CLOCK and BMAL1 heterodimerize and bind to E-boxes (sequence: CACGTG) within the promoters of CCGs to activate their expression (**Fig. 1.3**). Downstream of the TTFL, thousands of CCG's regulate cellular physiology in a rhythmic manner. For instance, it has been estimated that ~27% of β-cell transcriptome shows circadian expression and contribute to the circadian effect of insulin release (Perelis *et al.*, 2015). Among these CCGs there are other core clock proteins, PERIOD (PER1*,* PER2*,* PER3) and Cryptochromes (CRY1*,* CRY2) which constitute the negative arm of the clock. When CRY and PER proteins reach the threshold, they heterodimerize in the cytoplasm and translocate to the nucleus to inhibit CLOCK:BMAL1, forming a classical negative feedback loop. The dynamic interplay between the opposing effects of these two positive

and negative complexes generate circa 24-hour long circadian rhythms (Reppert & Weaver, 2002) at a cellular level.

For the core-clock to be self-sustaining in the absence of any input and keep to exact times, we have evolved additional auxiliary loops. One such loop is formed by REV-ERB and ROR. CLOCK and BMAL1 via E-boxes, drive the expression of REV-ERB (α, β) (*Nr1d1*) and *ROR* (α, β, γ), components of the 'auxiliary clock', enacting a further level of circadian regulation. REV-ERB and RORs represent nuclear receptors which possess opposed transcriptional activities governing *Bmal1* expression. REV-ERB represses transcription by binding to co-repressors such as the nuclear receptor co-repressor 1 – histone deacetylase 3 (NCoR1-HDAC3) complex (Yin & Lazar, 2005) and promoting condensation of targeted chromatin regions. REV-ERB therefore acts as a negative feedback upon *Bmal1* transcription. On the other hand, the ROR family can constitutively activate transcription through the ligand-independent recruitment of transcriptional co-activators. It also drives the expression of *Bmal1*, through a positive feedback mechanism (**Fig. 1.3**).

1.4 The DEC1/DEC2-driven control of circadian rhythms

DEC1 and DEC2 encoded by *Bhlhe40/Sharp2* and *Bhlhe41/Sharp1* are two paralogue genes that encode basic-helix-loop-helix proteins and repress the expression of CCGs by competing for E-Box element binding, including the *Per* gene (Honma *et al.*, 2002; Nakashima *et al.*, 2008). Moreover, the expression of DEC1/DEC2 is responsive to the environment and possibly links environmental factors to clock gene expression. For instance, light exposure acutely stimulates DEC1 expression during the subjective night (Honma *et al.*, 2002) whereas DEC2 is hypothesised to play a role in the timing, duration,

and quality of sleep. Indeed, in a GWAS study, a *DEC2* dominant mutation was associated with the Familial Natural Short Sleepers (FNNS) (He *et al.*, 2009).

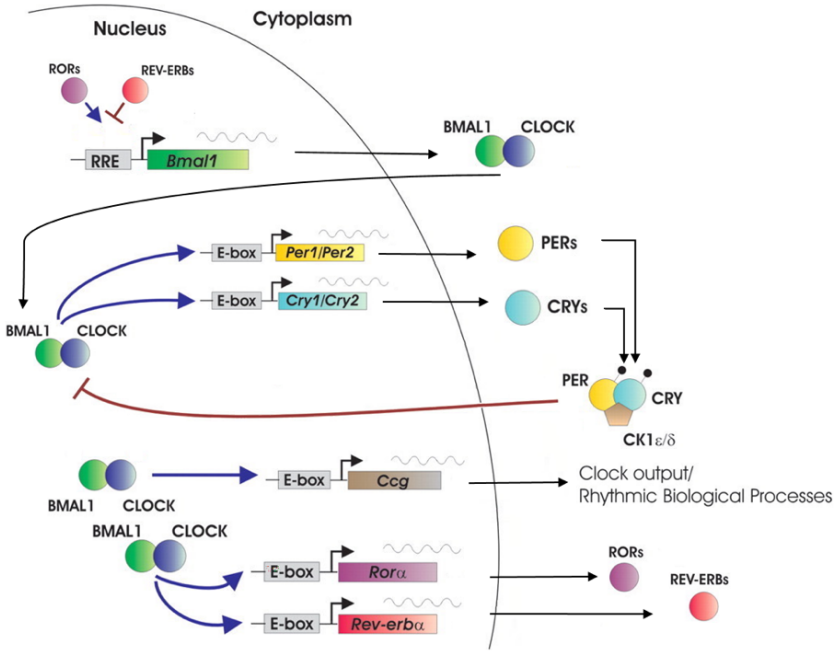


Figure 1.3 – Network of the main players involved in the transcriptional-translational feedback loop that constitutes the mammalian circadian clock. The circadian clock is formed by a conserved set of genes that cycles in a circa 24-hour cycle. The positive arm, constituted by CLOCK and BMAL1, dimerises and binds to E-Box regulatory regions throughout the genome, including to *Per* and *Cry* promoter regions, driving their expression and the expression of thousands of circadian and auxiliary clock genes such as *Rora* and *Rev-erbα*. PER and CRY dimerise and, inhibit the dimerization of CLOCK and BMAL1, as a negative feedback. Figure adapted from (Ko & Takahashi, 2006).

1.5 Tissue-specific control of the circadian genes

While research on circadian rhythms has made remarkable progress in understanding the fundamental basis of clock mechanisms and their contribution to physiological rhythms, there has been little progress in understanding the underlying mechanisms accounting for tissue-specific outputs, despite the core clock being the same. It has indeed been shown that about 10% of the transcriptome of each tissue is under the control of the circadian clock (Zhang *et al.*, 2014). As an example, it was noted that BMAL1 drives the circadian expression of about 2000 genes, in mouse liver (Rey *et al.*,

2011). In a recent study comparing the circadian gene expression from 14 rat tissues, it was observed that in any one of the tissues, the number of oscillating genes were around 10,000. In spite of the core clock being the same in all cells, the number of common CCGs showing circadian oscillations decreased drastically across these tissues, with only ~40 common genes oscillating in at least 8 out of 14 tissues, suggesting an intricate epigenetic regulation (Masri & Sassone-Corsi, 2010). Additionally, although both the SCN and the peripheral tissues share the same molecular clock, their entrainment mechanisms, and output are vastly divergent (Yamazaki *et al.*, 2000) and only few of the genes that oscillate in a circadian manner are actually controlled by the core circadian clock itself (Panda *et al.*, 2002). Chromatin remodelling could indeed be a key candidate for orchestrating the molecular interplay between the core clockwork and transcription to result in varied physiology (Ripperger & Schibler, 2006) and may constitute a key molecular signal that integrates endogenous and exogenous cues to maintain the period of biological clocks.

1.6 Impact of zeitgebers on epigenetics

Exogenous cues that entrain or synchronize our internal biological rhythms to the Earth's 24 hours light/dark cycles are defined as zeitgebers (or time-givers). The most common zeitgebers are light, temperature, food, social interaction and locomotion. Increasing evidence suggests that environmental factors could interact with our genetic code through epigenetic mechanisms, changing thus genomic function in a flexible but a stable way that could be transmitted from one generation of cells to another. Major epigenetic mechanisms include DNA methylation, post-translational histone modifications and post-transcriptional modification by microRNAs.

It was indeed shown that food, could act as both an entrainer for the circadian clock and an epigenetic modulator. As an example, a diet rich in polyunsaturated fatty acids (PUFAs) can generate free radicals and oxidative stress, which has been associated with epigenetic alterations (Lawless *et al.*, 2009). Furthermore, several types of molecules present in plants can actively modulate the epigenetic landscape (Dashwood & Ho, 2007). Certain vitamins, such as folate and vitamin B12 were also associated with the modulation of epigenetic characteristics (Kim *et al.*, 2009). Furthermore, its well acknowledged that various physiological and pathophysiological functions (e.g. abnormal weight gain) are directly under the control of the epigenetic pathways and nutrition, behaviour (e.g. exercise and stress) and several activities conducted on a daily basis has a profound impact on this (Palumbo *et al.*, 2018; Zhang *et al.*, 2011a).

1.7 Intrinsic and extrinsic epigenetic control of circadian rhythms

Several lines of evidence show how epigenetic mechanisms are pivotal in circadian rhythm modulation: the circadian transcription factor CLOCK has intrinsic histone acetyl-transferase activity (HAT) (Etchegaray *et al.*, 2003; Ripperger & Schibler, 2006); Sirtuin 1 (SIRT1), a class III histone deacetylase enzyme (HDAC), targets *Bmal1* and *Per2* (Asher *et al.*, 2008) directly via acetylation (Nakahata *et al.*, 2008), thus modulating circadian gene transcription. Further, HDAC1/2/3 were found to oscillate in a circadian manner (Alenghat *et al.*, 2008; Duffield *et al.*, 2002) and HATs/HDACs were shown to form complexes together with histone methylation enzymes (HMTs) and modulate circadian genes' expression (Etchegaray *et al.*, 2006; Katada & Sassone-Corsi, 2010).

Evidence also shows that epigenetic mechanisms are key in modulating the biology of circadian rhythms. It has indeed been shown that some HDAC Class IIa enzymes (eg. HDAC4 and HDAC5), have a role in sustaining circadian rhythms in *Drosophila melanogaster* and mammalian cells: HDAC5 has been shown to disrupt transcriptional rhythms of genes of the core clock and HDAC4 knockdown in flies impairs locomotor activity rhythms and dampens circadian function, at a more physiological level (Fogg *et al.*, 2014). Moreover, it has also been shown that the recruitment of HDAC3 to the genome displays circadian rhythmicity in mouse livers and that its absence can promote a reduction in REV-ERBa colocalization, both useful in regulating lipid homeostasis (Feng *et al.*, 2011). There is also evidence showing that DEC2 can recruit histone deacetylases such as HDAC1 and SIRT1 through specific C-terminal regions and inhibit gene expression in a HDAC-manner (Fujimoto *et al.*, 2007; Ow *et al.*, 2014). Moreover, the recruitment of NCoR-HDAC3 and eviction of the elongation factor bromodomain 4 (BRD4) at the REV-ERBa complex opposes functional loop formation between transcriptional enhancers and circadian gene promoters (Kim *et al.*, 2018). Histone methyltransferases were also shown to be circadian, as the mixed lineage leukaemia protein-1 (MLL1) was shown to form a complex with CLOCK-BMAL1 and be pivotal in circadian transcription and cyclic methylation of lysine 4 of histone 3 (Katada & Sassone-Corsi, 2010). Further, upon an interrogation of a genome-wide binding of the molecular clock genes, some distinct circadian features emerged: in the mouse liver, transcription factors and RNA Pol II binding and chromatin remodeling emerged to be modulated in a time-dependent fashion, following three main states: a CRY-driven transcriptionally poised state at circadian time 4 (CT4), a state of gene expression peak at CT15 given by CLOCK-BMAL1 binding, and a repressed state at CT16 to CT20

where CLOCK-BMAL1 binding decreases. It is also fundamental to underline the differential binding of several epigenetic histone markers at all three stages, including H3K9ac and H3K4me1 during the peak state and H3K4me3 and H3K27ac during the repressed state (Koike *et al.*, 2012) (**Figure 1.4**). The concomitant presence of specific histone markers centralizes the role of epigenetics in circadian gene expression regulation.

Moreover, epigenetics is thought to be an integral part in the regulation of circadian rhythms. It is hypothesized that environmental factors, such as light, temperature, stress, drugs, hormones, food, and age, act through epigenetic mechanisms to shape the circadian phenotype (Liu & Chung, 2015). Namely, the interaction between circadian rhythms and metabolic physiology was shown to display an epigenetic mechanism of action; loss of function of the NCor1-HDAC complex significantly alters the 24h oscillatory pattern of many metabolic genes as well as showing an aberrant regulation of the clock genes and the circadian behaviour (Alenghat *et al.*, 2008). Sirt1, can also be described as a metabolic sensor: it requires binding of its coenzyme NAD^+ for its activity. As the levels of NAD^+ oscillate over the circadian period (Nakahata *et al.*, 2009; Ramsey *et al.*, 2009), the enzymatic HDAC activity of Sirt1 oscillates, linking the metabolic state of the cell with the circadian clock, through an enzymatic feedback loop (**Fig. 1.5**). It has been shown that the SCN can integrate glucose sensing information from the hindbrain region and ultimately the periphery and affect adrenocorticotropic hormone and glucocorticoid responses (Watts & Donovan, 2010). Therefore, nutritional inputs and peripheral clock modulation might indirectly influence specific brain functions and feedback onto the master circadian clock, although the mechanisms through which this happens are still poorly understood (Masri & Sassone-Corsi, 2010).

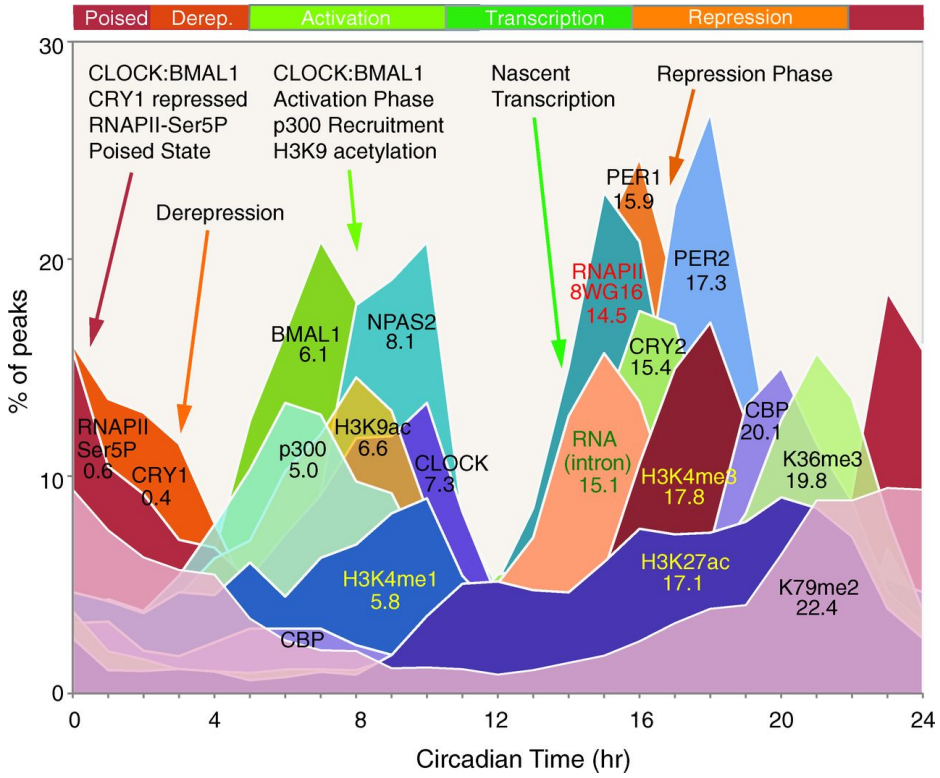


Figure 1.4 – **Epigenetic control of circadian gene expression in mouse liver**. Transcription factors and epigenetic markers are shown to peak in concomitance with several circadian proteins and distribute over 3 differential states over 24 hours: a poised state where circadian transcription diminishes, driven by CRY1 at CT0-4, a peak state where expression of circadian genes is driven by CLOCK-BMAL1 at CT15 and a repressed state during CT16-20 driven by Per1/2 and CRY2. It is fundamental to notice the differential concomitant presence of epigenetic markers at all three states, including H3K9ac, H3K4me1, H3K4me3 and H3K27ac, among others. Figure from (Koike *et al.*, 2012).

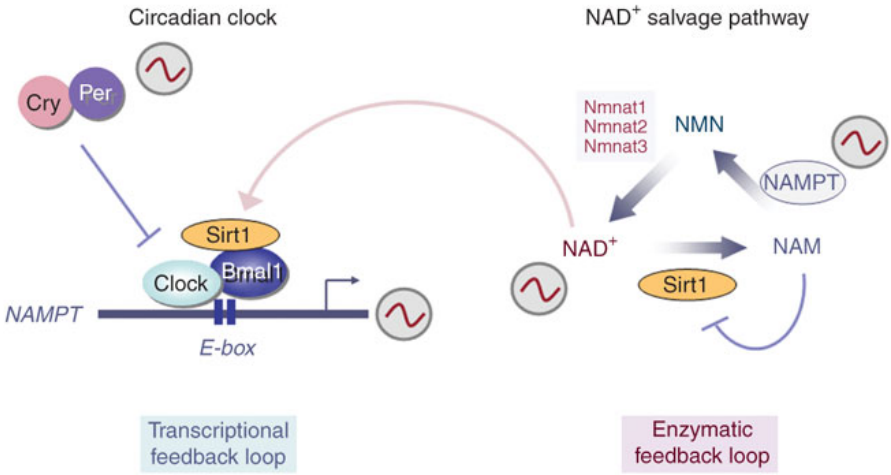


Figure 1.5 – **The NAD+ enzymatic feedback loop that connects the metabolic state and clock function**. Sirt1 is defined as a metabolic sensor of NAD^+, thus its circadian synthesis through NAMPT determines the circadian activation of the HDAC. Sirt1 was also shown to co-bind to E-box regions in partnership with Clock and Bmal1, determining an epigenetic mechanism of regulation of the circadian positive arm. Figure adapted from (Eckel-Mahan & Sassone-Corsi, 2009).

1.8 Importance of amplitude regulation in circadian gene expression

Circadian rhythms, given their widespread associated regulatory mechanisms and co-factors, were shown to influence a plethora of physiological functions across the body, and their disruption has been associated with several disorders, including the metabolic syndrome (Orozco-Solis & Sassone-Corsi, 2014). In order to tackle these diseases, a devised strategy is to re-synchronize circadian gene expression to limit the putative negative impact of circadian rhythm and sleep disorders (CRSD). The circadian clock can be altered by modulating several parameters, such as period, amplitude and phase of gene expression. Period is defined as the interval between two peaks or two troughs and circadian length was associated with circadian and sleep preferences and mood disorders, such as bipolar disorder (Hida *et al.*, 2013; Sanghani *et al.*, 2020). The amplitude of circadian gene expression, measured as the difference between the nadir and the zenith of the expression readout, is one of the most important elements of circadian biology regulation. External stimuli at an organism level can modulate amplitude, depending on the circadian responsiveness of the system: for example, it is acknowledged that light can boost (during subjective day) or dampen (during subjective night) circadian amplitude (Pulivarthy *et al.*, 2007). With respect to food intake and metabolism, increased body weight and the presence of various metabolic disorders were shown to dampen the blood concentration amplitude of several hormones: leptin, a hormone that is released by adipocytes following the ingestion of high-fat contents, was shown to be downregulated in amplitude in clinically obese patients (Matkovic *et al.*, 1997; Sinha *et al.*, 1996) and type-2 diabetes mellitus (T2DM) patients showed dampened melatonin amplitudes (Arendt *et al.*, 1982; Corbalan-Tutau *et al.*, 2014). Vice-versa, dampened circadian rhythms have been positively associated with diabetes, obesity and insulin-

resistance (Ando *et al.*, 2011; McMullan *et al.*, 2013) in the clinics and is further supported by animal models of circadian rhythm dysfunction (Sei *et al.*, 2008; Vitaterna *et al.*, 2006). Furthermore, circadian rhythm amplitude dampening is also associated with the natural phenomenon of ageing; it has been shown that the responsiveness to external stimuli is generally reduced in the aged circadian clock (Asai *et al.*, 2001; Kolker *et al.*, 2003). Among the hormones directly released by the SCN, melatonin and cortisol also show a decrease in circadian amplitude (Van Cauter *et al.*, 1996; Zhao *et al.*, 2002) (**Fig. 1.6**). Additionally, many metabolic rhythms also show progressive dampening with age, contributing to increased risks of metabolic diseases in older adults (Sohail *et al.*, 2015). As opposed to high-fat-and-sugar diets, chronic caloric restriction, known to extend lifespan, also increases the expression of several clock genes in peripheral tissues (Katewa *et al.*, 2016). Taken together its plausible that a clock with higher amplitude is beneficial for general health and physiology. Indeed frontline candidates that are believed to mediate these beneficial effects, such as SIRT1 are at very much at the interface of metabolism, aging and circadian rhythm regulation (Chang & Guarente, 2013; Wang *et al.*, 2016).

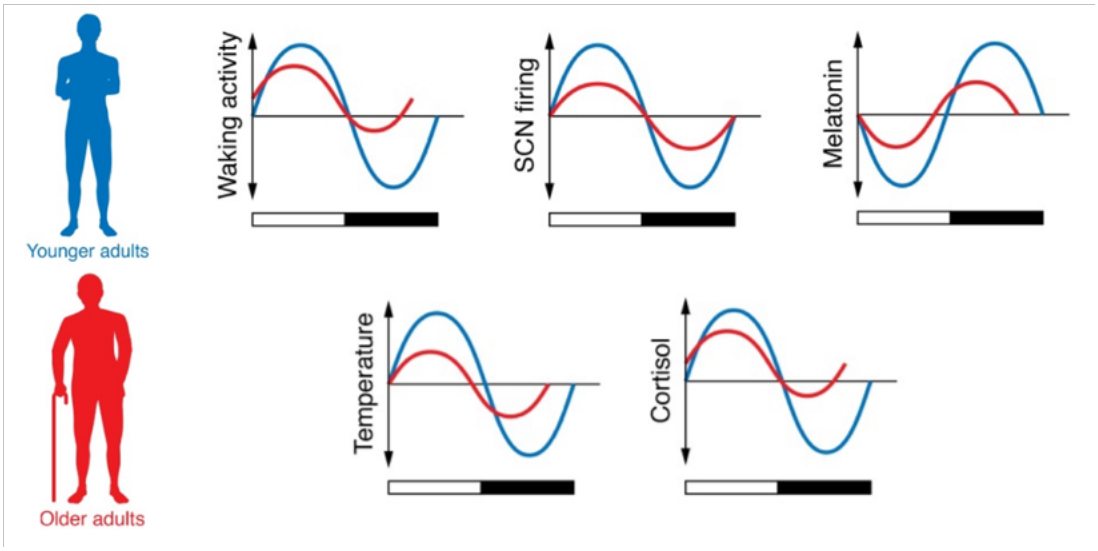


Figure 1.6 – Effects of aging on hormonal release. Circadian amplitude, defined as the difference between peak and trough of a 24-hour circadian process, is dampened in the elderly. Several physiological processes are impacted, including neuronal and behavioural activities (walking, SCN firing), hormonal release (cortisol, melatonin), bodily temperature, and metabolic activity. Adapted from (Hood & Amir, 2017).

1.9 The metabolic syndrome

The metabolic syndrome is defined as a cluster of three to five metabolic diseases (discussed below) that can occur together: abdominal obesity, high blood pressure, high blood glucose, high serum triglycerides, and low serum high density lipoprotein (HDL). The metabolic syndrome is associated with the risk of developing cardiovascular disease and T2DM, as obesity, or more specifically visceral obesity, is a major driving force of T2DM. The metabolic syndrome is diagnosed upon abnormal measurements of the waist circumference, blood pressure, fasting glucose and blood lipid levels. Therapies involve the tackling of each of the individuated correlated morbidities, including obesity, T2D and dyslipidaemia.

1.10 Impact of obesity

Obesity is a medical condition in which excess body fat has accumulated to the extent that it may have an adverse effect on health. Obesity can predispose towards serious metabolic diseases and cancer and it constitutes an important public health concern. In fact, it has been estimated that over 1.9 billion adults were overweight worldwide, of which over 650 million were considered clinically obese, accounting for 13% of the adult population (WHO obesity and overweight statistics, 2016). Moreover, these numbers will only exacerbate, as 38% and 20% of the world's population are estimated to become overweight and obese by 2030, respectively (Kelly *et al.*, 2008), possibly due to an increase in a sedentary lifestyle and the consumption of sugar- and fat-rich westernized diets. Overweight individuals are defined as all individuals that show a body-mass index (BMI) between 25 to 30, whereas individuals are diagnosed with obesity if their BMI is higher than 30 (Nuttall, 2015). Although the BMI can sometimes be a poor indicator of body fat percentage in a small number of individuals (eg. body-builders), it is widespread in its use as an universal risk factor calculator for the prevalence of several health disorders and in determining health policies, due to its ease of use (See **Formula 1.1** for the BMI calculation).

$$BMI = {Weight\ (kg)}\Big/{Height^2\ (m^2)}$$

Formula 1.1 – Body-mass index (BMI) formula.

Obesity can increase the risk of several diseases, such as disability, depression, type 2 diabetes, cardiovascular disease, dyslipidaemia, hepatic steatosis and cancer and therefore increase the mortality rates. It is thus considered to have a striking socio-

economic burden. In 2014, the economic burden of obesity was estimated at $2 trillion or 2.8% of the global GDP, in healthcare expenditure and lost productivity (Tremmel *et al.*, 2017).

1.11 Aetiology of diabetes

Diabetes mellitus (DM) is a metabolic disorder that occurs when blood glucose levels are too high over a prolonged period. If left untreated, it can cause several acute complications such as diabetic ketoacidosis, hyperosmolar hyperglycaemia and death (Kitabchi *et al.*, 2009) or more long-term complications such as foot ulcers, stroke, cardiovascular disease, nerve damage and cognitive impairment (Yang *et al.*, 2016). Diabetes is generally characterized by the inability of cells to uptake glucose from the blood and this can be either due to the pancreas not producing (or releasing) enough insulin as the ß-cells within the pancreas were destroyed (type I diabetes), or due to the cells not responding to insulin as they are desensitized or the pancreatic ß-cells not producing enough insulin due to an alteration in their activity (type II diabetes). Insulin is an anabolic hormone which is released from the pancreatic ß-cells and, among other functionalities, physiologically stimulates the uptake of glucose within cells in the liver, fat and skeletal muscle by activating the transfer of GLUT4 glucose transporters to the cellular membrane.

Diabetes affects over 450 million people worldwide and is expected to rise to over 700 million by 2040 (Saeedi *et al.*, 2019). This is primarily being attributed to increasingly lethargic lifestyle factors combined with overconsumption of fatty (Riserus *et al.*, 2009), highly caloric and sugary foods (Malik *et al.*, 2010), all of which can predispose towards

insulin resistance and type 2 diabetes mellitus (T2DM). T2DM accounts for about 90% of all diabetic cases (American Diabetes, 2009), though T1D is the most prevalent type in the youth (Patterson *et al.*, 2009). T1D can be either auto-immune (constitutes the majority of T1D cases in which host T-cells attack the pancreatic β-cells and promotes loss of insulin release), or idiopathic. As T2D progresses, it also mutates in a T1D-like phenotype as the higher levels of glucose stimulate pancreatic toxicity and β-cell dysfunction. In fact, hyperglycaemia results when an increased insulin secretion is unable to compensate for the initial insulin resistance (Kahn, 2003).

1.12 Non-alcoholic fatty liver disease (NAFLD) and NASH

NAFLD, although not strictly part of the metabolic syndrome, is increasingly seen as a pathological alteration correlated with the metabolic syndrome, with insulin resistance thought to be an aetiological cause of both (Godoy-Matos *et al.*, 2020). NAFLD is defined in relation to the presence of hepatic steatosis (adipocytes in the liver) equal or higher than 5% of the liver area, with an aetiology that is independent of alcohol consumption. The effects can be benign or can progress to more severe disorders such as steatohepatitis, cirrhosis and hepatocellular carcinoma. It is estimated that up to 25% of people present with NAFLD (Younossi *et al.*, 2016) in their lifetime. Although most people do not present noticeable symptoms at the early stages, upon repeated liver insults, the liver in these individuals can progress to non-alcoholic steatohepatitis (NASH), which is a severe state in which the steatosis is accompanied by an inflammatory and fibrotic liver profile. Metabolic comorbidities associated with NAFLD are obesity, type-2-diabetes, hyperlipidaemia, hypertension and the metabolic syndrome,

and, besides having a strong genetic aetiology, the presence of the disease is strongly correlated with obesity, as over 90% of severely obese patients (BMI >35 kg/m^2) were diagnosed with NAFLD (Machado *et al.*, 2006).

The specific mechanisms underlying NAFLD are currently unknown. In fact, even the fundamental mechanisms through which lipids accumulate in the liver, due to an imbalance between liver lipid deposition and removal, under the form of triglycerides is incompletely understood. Causally, a lot of cases can be ascribed to weight gain, and weight loss was shown to be one of the best interventions in ameliorating both NAFLD and NASH (Marchesini *et al.*, 2016). However, NAFLD can present itself in lean patients also, and it is associated with impaired insulin sensitivity, sedentary lifestyles and an increased cardiovascular risk. NAFLD and NASH also have a genetic component, with a higher risk of developing fibrosis in individuals that have family members affected by NASH (Friedman *et al.*, 2018). Specific single nucleotide polymorphisms have also been associated with increased chances of presenting NAFLD and with liver fibrosis, such as Patatin-like phospholipase domain-containing protein 3 (*Pnpla3*), a triacylglycerol lipase that mediates triacylglycerol hydrolysis in adipocytes and Transmembrane 6 superfamily 2 (*Tm6sf2*), of unknown functions *(Younossi et al., 2018).*

1.13 Current pharmacological therapies for the metabolic syndrome

The metabolic syndrome is a medical term that defines the cardiovascular risk given the concomitant presence of two or more risk factors, such as high blood pressure, obesity and diabetes. Currently, there are limited pharmacological interventions that can tackle these physio-pathological states.

Diabetes can be tackled depending on the type of diabetes diagnosed: for type 1 diabetes, the mainstream therapy is the administration of insulin, given that the ß-pancreatic cells are destroyed and the production of this hormone is halted. Several efforts focused on modifying the insulin peptide, adding adjuvants or improving on the means of administration such that it can be increasingly safer for patients. There are now several types of insulin on the market, with different times of action and half-lives (short-acting, long-acting etc). It is important to underline that type-2 diabetes patients may also need insulin administration, given that they can also develop a dysfunctional production of the hormone, as cells do not respond to insulin. However, type-2 diabetes can be also managed with insulin sensitizers, such as metformin (which works by lowering hepatic gluconeogenesis and improving the bodily sensitivity to insulin) and thiazolidinediones (such as rosiglitazone and pioglitazone). However, the latter ones were associated with weight gain, and given obesity is already endemic in individuals affected by type-2 diabetes, it can be a concerning side-effect in the affected population. It is important to underline that at least some of the thiazolidinediones' weight gain effects translate in weight redistribution from visceral to subcutaneous fat, which could be part of its mechanism of action as it improves insulin sensitivity (Miyazaki *et al.*, 2002). Another class of drugs that help the pancreas secrete more insulin are sulfonylureas (such as glyburide and glipizide) and meglitinides (such as repaglinide and nateglinide), though these can increase weight and cause low glucose levels as side effects. Other anti-diabetic drug classes help lower the blood sugar levels, such as the Dipeptidyl peptidase 4 (DPP-4) inhibitors, an enzyme which lowers incretin levels (incretins would normally stimulate the production of insulin, but also reduce liver gluconeogenesis) (eg. sitagliptin,

saxagliptin), Glucagon-like peptide 1 (GLP-1) receptor agonists (also known as incretin mimetics) (eg. exenatide, liraglutide and semaglutide) and Sodium-glucose cotransport protein 2 (SGLT2) inhibitors, which prevent renal reabsorption of glucose (canagliflozin and dapagliflozin). However, SGLT2 inhibitors increase the risk of diabetic ketoacidosis, as renal glycosuria might provoke a shift in substrate utilisation from carbohydrate to fat oxidation and hyperglucagonemia (Sanusi *et al.*, 2020).

Anti-obesity drugs are approved in patients with a BMI over 30 kg/m^2 or in individuals with a BMI≥28 kg/m^2, if they are affected by co-morbidities such as diabetes, hypertension, hyperlipidaemia or sleep apnoea (NHS Guidelines). Orlistat is the only anti-obesity drug approved in the United Kingdom to date. Its mechanism is action is based on lipase inhibition, thereby reducing caloric uptake. However, its effect is modest, with only 2-3kg of weight loss in addition to lifestyle changes, over the period of one year. However, it was shown the drug could lower the incidence of type-2 diabetes and improve cholesterol concentrations and blood pressure, with the main side-effects of gastrointestinal nature (Rucker *et al.*, 2007). Other drugs are approved by the European Medicines Agency (EMA), such as the repurposed naltrexone/bupropion combination, an opioid antagonist and a noradrenergic/dopaminergic re-uptake inhibitor anti-depressant respectively, were also shown to be effective in weight loss, possibly by reducing the activation of food craving and eating reward systems (Tek, 2016). However, this combination therapy can also bring serious side-effects and is not indicated in patients with a history of seizures, eating disorders and opioid use. Liraglutide, firstly approved in T2D, was also approved as an anti-obesity drug, given its weight-loss effects, due to appetite suppression. However, it can also have serious side effects, including the

possibility of an increased incidence of thyroid cancer, which is currently undergoing long-term investigations (Gallo, 2013).

NAFLD does not currently have any approved therapy, and the pharmacotherapy used is heavily based on drugs approved in other comorbidities, such as anti-obesity drugs, lipid-lowering agents such as statins, insulin sensitizers (as insulin resistance is a hallmark of NAFLD) and anti-oxidant agents. Specifically, thiazolidinediones showed improvements in metabolic end points and steatohepatitis, but were not able to promote a regression of fibrosis (Belfort *et al.*, 2006). Although statins showed to improve steatosis and slow down fibrosis progression when taken for longer periods of time (Ekstedt *et al.*, 2007), they were unable to promote regression of fibrosis in prospective studies (Athyros *et al.*, 2006; Nelson *et al.*, 2009). Although tremendous progress has been made to find pharmacological therapies for the treatment of the metabolic syndrome and its associated disorders, several of the drugs approved are limited to symptomatic treatment of the diseases, rather than tackling their etiological underpinnings. It is thus pivotal to further enhance our biologic understanding of these diseases to stimulate research and progress towards new disease-modifying therapies.

1.14 Circadian rhythm disruptions in cardiometabolic regulation

Circadian rhythm dysfunction has recently been shown to be intimately interlinked with an increased risk of diabetes and cardiovascular diseases. In addition to the observation that heart rate and blood pressure demonstrate a marked circadian physiology (Clarke *et al.*, 1976; Floras *et al.*, 1978), it is known that myocardial infarction, ventricular

arrhythmias and sudden cardiac death are more likely to occur at specific times of the day (Martino & Sole, 2009; Muller *et al.*, 1985), with shift work being considered a risk factor in developing cardiometabolic disorders, including T2DM (Brundtland, 2002). Given up to 15-20% of the overall workforce is employed in shift-work (Haus & Smolensky, 2006) and up to 70% of the western population suffers of social jet-lag, circadian disruptions have been hypothesised to be one of the reasons for the increase in cases of obesity and T2D (Knutson *et al.*, 2007; Roenneberg *et al.*, 2012). In fact, T2D has reached very high proportions in the general population and projected to reach about 440 million people and become the seventh cause of death by 2030 (Shaw *et al.*, 2010), creating considerable public health concerns for the future.

Support for the correlation between circadian rhythm disruptions and metabolic disorders comes from numerous epidemiological studies; glucose levels display circadian oscillations (Arslanian *et al.*, 1990) and disruptions of circadian oscillation of insulin secretion is a hallmark of T2D (Polonsky *et al.*, 1988). Furthermore, the expression of key rate-limiting enzymes involved in the regulation of glycolysis, fatty acid oxidation and oxidative phosphorylation are regulated by the circadian clock (Panda *et al.*, 2002). From a molecular perspective, the impact of circadian rhythm disruptions on metabolism is evident on its effects on T2DM, as disruptions in both CLOCK and BMAL1 in the rodent liver and pancreas have shown to lead to hyperinsulinemia and diabetes, as the timely oscillation of genes involved in glucose metabolism and insulin signalling is disrupted (Jacobi *et al.*, 2015; Marcheva *et al.*, 2010; Petrenko *et al.*, 2020). Muscle-specific BMAL1 knock-down showed defective muscle glucose uptake and a change in gene expression of glucose utilisation, such as the GLUT4 receptor and

pyruvate dehydrogenase (Dyar *et al.*, 2014). In fat tissue, BMAL1 knock-down showed an increase in obesity in mice and a shift towards day-time feeding (Paschos *et al.*, 2012). Mouse models carrying the $CLOCK^{D19/D19}$ mutation also showed attenuated diurnal feeding rhythms, hyperphagia, hyperlipidaemia, hyperglycaemia, hepatic steatosis and hyperinsulinemia (Turek *et al.*, 2005) and loss of rhythmicity of key metabolic components necessary for glucose and lipid homeostasis (McCarthy *et al.*, 2007).

Other directly circadian-regulated proteins can also influence and impact on energy metabolism, such as the peroxisome proliferator activated receptor (PPARA/G) (Sancar & Brunner, 2014) and the Sirtuins (Masri, 2015), both modulating the CLOCK:BMAL1 activity and their effects (Froy & Miskin, 2007). Transcription factor EB (TFEB), a basic helix-loop-helix protein that competes for the same E-Box regions to which the clock genes bind to, has been shown to regulate the transcription of *PPARɣ* in adipocytes and influence on adipogenesis and the adiponectin and glucose levels in mice (Salma *et al.*, 2017). The cellular redox status is also impactful on the circadian function, as CLOCK proteins can only bind more effectively to the DNA in presence of reduced NADH and NADPH (Rutter *et al.*, 2001). Adenosine triphosphate to monophosphate (ATP/AMP) ratio can also link energy metabolism to circadian rhythms, as 5'-AMP-activated protein kinase (AMPK) was shown to induce the degradation of Per2 and shorten the circadian phase (Um *et al.*, 2007).

At a physiological level, circadian misalignment induced glucose intolerance under a forced desynchrony (Buxton *et al.*, 2012) and a shift-work (Morris *et al.*, 2015) protocol, in humans, by stimulating an increase in postprandial glucose levels possibly due to a

decrease in insulin sensitivity. These effects were shown to be independent from sleep loss (Leproult *et al.*, 2014). Besides sleep-patterns, food-intake patterns are also a major zeitgeber of circadian alignment in both animals and humans and erratic food-intake timings impacts on the amplitude of gene expression (Vollmers *et al.*, 2009) and could influence the onset of several *metabolic* syndromes such as obesity (Garaulet & Gomez-Abellan, 2014) and glucose-intolerance (de Goede *et al.*, 2019). Moreover, the composition of the diet can also affect the circadian clock, with a high-fat diet shown to promote changes in locomotor activity and circadian gene expression profiles in mice (Kohsaka *et al.*, 2007). Taken together, there is clear evidence that circadian rhythm disruptions, both at a molecular and physiological level, negatively influence metabolic pathways and possibly increase the likelihood of developing metabolic disorders.

1.15 Epigenetic modulation of metabolic phenotypes

One important case study of the Netherlands 1944-1945 wartime winter famine showed, that children born from mothers during the nutrient-deprived times were more likely to become obese and develop type 2 diabetes, compared to their siblings born in more privileged times (Kyle & Pichard, 2006), implicating a possible epigenetic mechanism of metabolic control in the surviving children. More recently, studies showed that maternal prenatal diet and underlying metabolic diseases influenced the diet and body weight of offspring (Brion *et al.*, 2010; Plagemann *et al.*, 1997), and that low-birthweight children are more likely to develop type-2 diabetes subsequently, independently of body mass at the time of diagnosis (Hales *et al.*, 1991; Soto *et al.*, 2003). Taken together, these studies suggest that both hypocaloric and hypercaloric gestational diets as well as underlying

metabolic phenotypes can influence the body weight and development of metabolic disorders in the progeny. The theory proposed by scientists is that an adverse food-availability environment, either determined by under- or over-nutrition during prenatal development impacts on the energy homeostatic mechanisms in foetuses. These adverse conditions could therefore result in aberrant metabolic regulation, potentially culminating in obesity and diabetes, especially if these individuals were further predisposed to deleterious diets during adult life (Hales & Barker, 2001). The impact of aberrant prenatal diet on the offspring could be possibly due to leptin resistance and insulin signalling disruptions, as showed in several animal studies (Campodonico-Burnett *et al.*, 2020; Ferezou-Viala *et al.*, 2007; Page *et al.*, 2009). These changes could be mediated by epigenetic mechanisms: a pro-methylation diet was shown to reduce the transgenerational amplification of body mass in mice (Waterland *et al.*, 2008) and mice exposed to a high fat diet showed an increase in histone acetylation of key enzymes involved in fatty acid and glucose metabolism (Alrob *et al.*, 2014).

1.16 Hypothesis and aims of this study

Given well-known intricate links between cellular metabolism and circadian rhythms, combined with the fact that there is an ever increase in circadian rhythm disruptions due to social jet lag and shift-work patterns, we hypothesized we could target the circadian system to improve metabolic health. By enhancing circadian gene expression and downstream effectors, we would therefore better subdivide time-dependent physiological functionalities across the 24-hour period and potentially improve on putative disorders associated with a dampened, desynchronised and misaligned clock.

In order to tackle this, we had the following objectives:

1) Screen an epigenetic library of drugs. This was used as a starting point as epigenetic modulation is one of the most common means of translating the effects of the environment onto our genetic code and owning to its intertwined nature with circadian rhythms.

2) Focus on identifying small molecule amplitude enhancers of circadian gene expression. This is due to the fact that a weak circadian clock has been reported in several pathophysiological alterations, such as the metabolic syndrome.

3) Evaluate the effects of these molecules through *in-vitro* and *in-vivo* models of metabolic dysfunction. The cellular and animal work will provide translational evidence of the metabolic impact of the amplitude enhancers.

2 MATERIALS AND METHODS

All materials for solutions, buffers and media were obtained from Life Technologies Limited, unless otherwise stated.

2.1 Cells used for *in-vitro* experiments

All cell and tissue procedures were performed in sterile conditions under a HEPA-filtered containment level II microbiological safety cabinet (Gelaire). Cells were maintained in incubators at 36˚C with 5% CO_2 concentration and 70% humidity (Panasonic) to limit media evaporation.

Human osteosarcoma cells (U2OS) and mouse pre-adipocytes cells (3T3-L1) obtained from American Type Culture Collection (ATCC) were used for the *in-vitro* experiments. For the PCR experiments, unmodified U2OS and 3T3-L1 cells were employed. For the reporter gene assays, stably transfected U2OS cells with *Per2*::Luc or *BMAL1*::Luc (gift from Patrick Nolan, MRC Harwell UK) were employed. Cells were grown and maintained from passage 2-30, after which they were discarded and replaced. For the reporter gene assays, the luciferase was placed under the control of either the *Per2* or *Bmal1* promoters, thus reporting their promoter activation and by proxy their gene expression levels.

2.2 Gene reporter system: *Per2*::Luc and *BMAL1*::Luc U2OS cells

U2OS cells stably transfected with a *Per2*::Luc or *Bmal1*::Luc reporter were cultured in Dulbecco's Modified Eagle Medium (DMEM) supplemented with 10% Foetal Bovine Serum (FBS) and 1% Penicillin Streptomycin (P/S). For the circadian gene expression

experiments, cells were seeded at 20,000 per well into 96-well white-bottom plates (Greiner) for 24h to attain confluence. Twenty-four hour following seeding, the cells were synchronized with 200 nM dexamethasone for an hour (Balsalobre *et al.*, 2000) and reconstituted with recording media (phenol-red free DMEM supplemented with B-27, Thermo Fisher Scientific) and 400 μM luciferin potassium salt (Promega Inc). The investigated drugs were added to the media at pre-specified concentrations, keeping the solvent volume constant across all treatments. Following this, the plate was left for an hour in the incubator to restore CO_2 levels, and then sealed and placed in a plate luminometer. *Per2*::Luc or *Bmal1*::Luc rhythms were recorded with a BMG Labtech Omega plate reader maintained at 36°C with readings being taken from each well every 30 minutes, for at least 96 hours (circa 4 days).

The reporter luciferase assay used is a well-validated model for screening genes and small molecule modulators and functions based on the random genetic insertion of luciferase, where luciferase expression is driven by the transcriptionally-activated promoter region of a specific gene of interest, such as *Bmal1*. Therefore, whenever a drug modulates the binding of transcriptional factors to the promoter of a gene, its transcriptional activity is regulated and measured through the amount of light produced through the interaction between the luciferase and luciferin, its substrate.

2.3 Transient transfection protocol

For the transient transfection experiments, cells were seeded at 10,000 per well into white 96-well plates for 16-24 hours and transfected with 50ng/well of plasmid-DNA

following a 1h incubation with antibiotic free DMEM and 1:4 ratio Viafect (Promega Inc. USA), together with Reduced Serum Media (opti-MEM). The transfection was allowed to continue for 24-hours, following which, the cells were synchronized, treated, and recorded as in **Methods 2.2**. As a transfection negative control, we transfected the cells with a plasmid backbone that closely resembled the one used experimentally, without expressing the gene or promoter of interest.

2.4 siRNA knockdown transfection protocol

For siRNA transfections, cells were seeded at 10,000 per well onto white 96-well plates. 16-24 hours following this, the cells were transfected with 20nM siRNA following an hour media change with antibiotic free DMEM. Lipofectamine RNAiMAX (Thermofisher Inc. USA) 0.4μL/well, together with Reduced Serum Media (opti-MEM) up to a volume of 10% of the final well media, and P/S-free DMEM were employed for the transfections and left to react for 24-hours, after which the media-mix was removed. The cells were then synchronized, treated, and rhythms were recorded similarly to as described in **Methods 2.2**. The siRNAs used (Dharmacon, Horizon Discovery, UK) were a mixture of four different siRNAs targeting the same mRNA of interest pooled together. Their sequences were determined through *in-silico* screening against the mRNAome to guarantee both a high efficacy of at least 75% knockdown as well as a low off-target effect and thus high specificity. As a transfection negative control, we transfected the cells with a non-targeting siRNA mix that did not inflict on circadian rhythm expression nor on other genes. As a transfection positive control, we treated the

cells with a siRNA against Casein Kinase 1 (*Ck1*), which was shown to significantly lengthen circadian period when knocked-down (Meng *et al.*, 2010).

2.5 PrestoBlue cell-viability assay

To assess cell viability, following the completion of the cell luminescence experiments, a PrestoBlue (Life Technologies, Thermo Fisher Scientific) cell-viability assay was performed according to the company's published protocol and the results were read using a BMG Labtech Omega Fluorimeter equipped with 544nm excitation and 590nm emission filters. Results were normalized over non-treated wells (as positive control) and no-cell wells (as negative control).

2.6 Bacterial transformation and selection and plasmid preparation

Plasmids carrying a promoter:luciferase reporter used in this study (*Bmal1*::Luc, *Per1*::Luc, *Per2*::Luc, *Cry1*::Luc, *Cry2*::Luc *Sp1*::Luc, *Hre*::Luc) were grown and selected in bacterial growths. Samples of the plasmids were used to transform Top10 OneShot competent E. Coli cells (ThermoFisher Scientific). 5µL of the plasmid sample were added onto 45µL of the competent cells and allowed to react on ice, for 30 minutes, followed by a 30 seconds heat shock at 42ºC, and a further 2 minutes on ice. After adding 250µL of S.O.C. media (Melford Laboratories Ltd, UK), the transformed bacterial cells were shaken for 2 hours at 37ºC and 225rpm. 100µL of media and cells were then removed from the tube and either kept at the same concentration or diluted 1:10 to allow for a better spread of the bacterial growths on the agar plates, at 30ºC overnight. Bacterial

growths were then selected and inoculated in Lysogeni Broth (LB) growth media with the addition of the selective agent, either 60μg/mL kanamycin or 100μg/mL carbenicillin (Sigma). The selection agent was specific to the gene in the backbone of the plasmid that gave resistance to the specific antibiotic, such that only the bacteria that were transformed would grow. Successful colonies were then further expanded in LB media.

Bacterial mini-preps (Qiagen) were then performed on the selected colonies, according to the manufacturer's protocol. Confirmation of the presence of the plasmid was confirmed by sequencing (Sanger sequencing services, Source Bioscience).

2.7 RNA extraction, purification and sample preparation

Cells were seeded and grown in 12-well transparent plates were synchronized with 200nM dexamethasone and washed as described in **Section 2.2**. After washing, phenol-free DMEM media was added to the plates along with drugs or controls, constituting of 0.25% v/v dimethyl sulfoxide (DMSO). After 24 hours, RNA was extracted from each plate. The RNA was extracted by lysing the cells with 600μL of RNeasy Lysis (RLT) Buffer (containing 0.1% ß-mercaptoethanol). The extract was immediately frozen on dry-ice and stored at -80°C until later use.

Total RNA was purified using the microRNeasy column method (QIAGEN, Hilden, Germany), following their protocol and instructions. Quality and quantity of RNA were

measured using an Agilent Bioanalyzer and a Nanodrop1000 (Thermo Fisher Scientific, Waltham, MA USA), respectively.

2.8 RNA conversion and DNA quantification through PCR

RNA quantities were normalized to 600ng/well for each of the samples. Complementary DNA (cDNA) was synthesized with a qScript cDNA synthesis kit (Quanta Biosciences, Gaithersburg, MD), following their protocol. A small quantity of all cDNA samples was mixed and serially diluted 1:2 to provide for the 8-point standard curve. The curve was used to assess the efficiency of the primers and therefore transcription: efficiencies between 0.9 and 1.1 were reputed good (data not shown); gene-of-interests' (GOIs) efficiencies were required to be within 0.05 of the house-keeping gene (HKG). Primer sequences are provided in **Table 2.1.** Real Time polymerase chain reaction (qPCR) was conducted with SYBR Green I and an SDS7700 thermal cycler (Applied Biosystems, Foster City, CA) and all reagents were used according to manufacturer's instructions. SYBR green is a dye that binds to dsDNA and emits fluorescence when intercalated between the double strand, becoming less mobile and allowing for an increased emission of fluorescence. The fluorescence increases thus with the concentration of DNA and is measured. The amplified sequence is quantified by dissecting its fluorescence intensity from the baseline emitted by non-amplified genomic DNA. SYBR green real-time PCR is a versatile method that can be used to monitor the amplification of any sequence, as long as specific forward and reverse primers are used. There is no need for probes, reducing assay setup time and costs. However, it may generate unspecific results if primers are not well designed and amplify undesired secondary sequences, though this

risk should be minimised by performing a melt curve analysis. During the melt curve, the dsDNA dissociates and lowers the fluorescence intensity of SYBR green at temperatures specific to the sequence of the DNA that has dissociated. The difference in melting temperatures between different DNA sequences is due to the intensity of hydrogen bonds between bases: G-C base pairing have three hydrogen bonds, whereas A-T base pairing have only two hydrogen bonds, allowing thus for discrimination among different DNA sequences.

2.9 Cignal transcription factors screen assay

U2OS cells were seeded and transfected in antibiotic-free DMEM at a density of 10,000 cells/well in a 96-well plate. Viafect Transfection Reagent (Promega Inc. USA) was used together with Reduced Serum Media (opti-MEM). The transfection was allowed to continue for 24 hours, following the Cignal reporters assay kit specifications (Qiagen). The rationale was to test the reporter::luciferase activity of several transcription factors, upon administration of 0.5μM IBET-762 in 0.01% volume of DMSO. This assay provided information about the quantitative activity of 45 signaling transduction pathways, by measuring the activation of downstream activation pathways. The reporters comprise a combination of specific transcription factors and basic promoter elements (placed in tandem repeat), driving the expression of a firefly luciferase, placed under a basal promoter element, a TATA box (**Figure 2.1A**). The negative control is represented by a constitutively-active TATA-box-powered expression of a firefly luciferase, outside of the regulation of specific promoters (**Figure 2.1B**), whereas the positive control is represented by a mix of *Cmv*-immediate early enhancer/promoter driving the expression of both Green Fluorescent Protein (GFP) and firefly luciferase (**Figure 2.1C-D**). The

change in activity of the analyzed transcription factors can be assessed both if augmented or diminished. This dual-luciferase system is constituted by a basal (renilla-based) and experimental (firefly-based) luciferase. The basal renilla-luciferase acts as an internal control, which normalizes for potential variability in the transfection rate, cytotoxicity, technical variability (**Figure 2.1E**). U2OS cells were transfected with the transfection-ready DNA-based vectors in a 96-well plate, over a 16-hour period. A baseline of transfection was then assessed over a 6-hour window until the activity levels stabilized. Transfected cells were then treated with 0.5µM IBET-762 in duplicate, and the effects of the drug were assessed over 4 hours of incubation, as a function of the luminescence emitted and collected by a luminescence plate-reader. Cells were lysed and the renilla luciferase activity was subtracted from the experimental firefly-luciferase emission. The results were expressed as a percentage of the negative control.

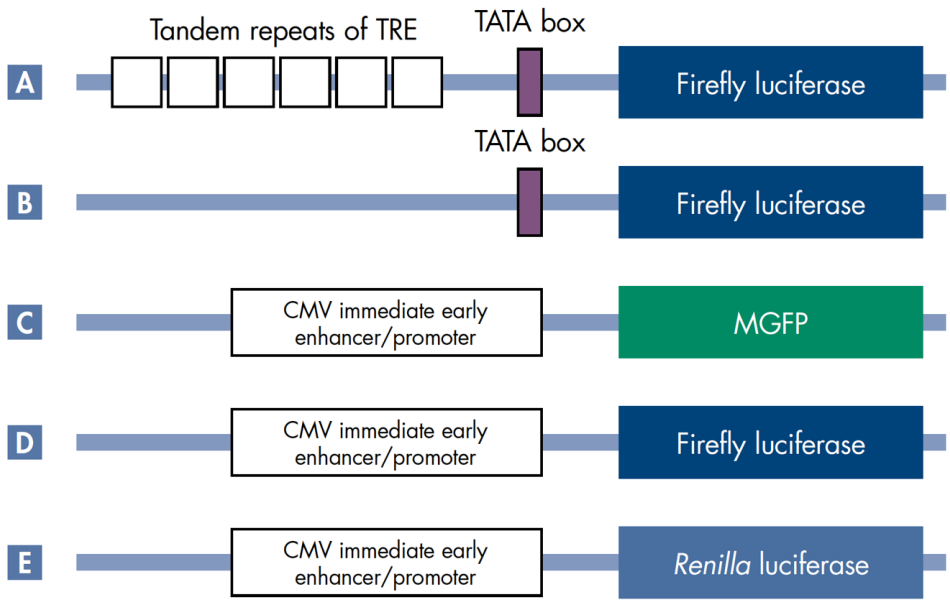


Figure 2.1 – Representation of constructs included in Cignal Reporter Assay kit – Each assay contains a pathway-focused TF-responsive firefly luciferase (A), a non-inducible firefly luciferase as a negative control (B), a constitutively-expressed mix of GFP and firefly-luciferase (C-D) as a positive control, a constitutively-expressed Renilla-luciferase construct as a normalization baseline. Source: Cignal reporter assay kit protocol, Qiagen.

Species	Gene	Direction	Sequence
Homo Sapiens	CLOCK	Forward	5'- GGCACCACCCATAATAGGGTA -3'
Homo Sapiens	CLOCK	Reverse	5'- TGTTGCCCCTTAGTCAGGAAC3 -3'
Homo Sapiens	Bmal1	Forward	5'- GCCCATTGAACATCACGAGTAC -3'
Homo Sapiens	Bmal1	Reverse	5'- CCTGAGCCTGGCCTGATAGTAG -3'
Homo Sapiens	Per1	Forward	5'- TCTGTAAGGATGTGCATCTGGT -3'
Homo Sapiens	Per1	Reverse	5'- CAGGCAGTTGATCTGCTGGT -3'
Homo Sapiens	Per2	Forward	5'- AGTTGGCCTGCAAGAACCAG -3'
Homo Sapiens	Per2	Reverse	5'- ACTCGCATTTCCTCTTCAGGG -3'
Homo Sapiens	Cry1	Forward	5'- ACAGGTGGCGATTTTTGCTTC -3'
Homo Sapiens	Cry1	Reverse	5'- TCCAAAGGGCTCAGAATCATAACT -3'
Homo Sapiens	Cry2	Forward	5'- CGTCTTCCCAAGGCTGTTCA -3'
Homo Sapiens	Cry2	Reverse	5'- CTCCGTCACTACTTCCACACC -3'
Homo Sapiens	B-Actin	Forward	5'- CATGTACGTTGCTATCCAGGC -3'
Homo Sapiens	B-Actin	Reverse	5'- CTCCTTAATGTCACGCACGAT -3'
Homo Sapiens	GAPDH	Forward	5'- AAGGTGAAGGTCGGAGTCAT -3'
Homo Sapiens	GAPDH	Reverse	5'- GAAGATGGTGATGGGATTC -3'
Homo Sapiens	18S	Forward	5'- GTAACCCGTTGAACCCCATT -3'
Homo Sapiens	18S	Reverse	5'- CCATCCAATCGGTAGTAGCG -3'
Homo Sapiens	TBP	Forward	5'- TGGGCTTCCCAGCTACCTACTG -3'
Homo Sapiens	TBP	Reverse	5'- GGAAATAATTCTGGCTCATAG -3'
Homo Sapiens	BRD2	Forward	5' – GTGGTTCTCGGCGGTAAG –3'
Homo Sapiens	BRD2	Reverse	5'- ACACCCCGGATTACATACCC -3'
Homo Sapiens	BRD3	Forward	5'- CCTCAGGGAGATGCTATCCA -3'
Homo Sapiens	BRD3	Reverse	5'- ATGTCGTGGTAGTCGTGCAG -3'
Homo Sapiens	BRD4	Forward	5'- AGCAGCAACAGCAATGTGAG -3'

Homo Sapiens	BRD4	Reverse	5'- GCTTGCACTTGTCCTCTTCC -3'
Homo Sapiens	TFEB	Forward	5'- CCAGAAGCGAGAGCTCACAGAT -3'
Homo Sapiens	TFEB	Reverse	5'- TGTGATTGTCTTTCTTCTGCCG -3'
Homo Sapiens	BHLHE40	Forward	5'- GACCGGATTAACGAGTGCAT -3'
Homo Sapiens	BHLHE40	Reverse	5'- TGCTTTCACATGCTTCAAGG -3'
Homo Sapiens	BHLHE41	Forward	5'- GCATGAAACGAGACGACACC -3'
Homo Sapiens	BHLHE41	Reverse	5'- ATTTCAGATGTTCAGGCAGT -3'
Homo Sapiens	HEY1	Forward	5'- GGATCACCTGAAAATGCTGCATAC -3'
Homo Sapiens	HEY1	Reverse	5'- CCGAAATCCCAAACTCCGATAG -3'
Homo Sapiens	SIRT1	Forward	5'- TGCTGGCCTAATAGAGTGGCA -3'
Homo Sapiens	SIRT1	Reverse	5'- CTCAGCGCCATGGAAAATGT -3'
Homo Sapiens	PPARɣ	Forward	5'- AGGCGAGGGCGATCTTGACAG –3'
Homo Sapiens	PPARɣ	Reverse	5'- GATGCGGATGGCCACCTCTTT -3'
Homo Sapiens	PGC1A	Forward	5'- TGCCCTGGATTGTTGACATGA -3'
Homo Sapiens	PGC1A	Reverse	5'- TTTGTCAGGCTGGGGGTAGG -3'
Homo Sapiens	SP1	Forward	5'- TTGAAAAAGGAGTTGGTGGC –3'
Homo Sapiens	SP1	Reverse	5'- TGCTGGTTCTGTAAGTTGGG -3'
Homo Sapiens	HIF1A	Forward	5'- TGCTTGGTGCTGATTTGTGA -3'
Homo Sapiens	HIF1A	Reverse	5'- GGTCAGATGATCAGAGTCCA -3'
Mus Musculus	Retn	Forward	5'- GGCTTAAATTGCTGGACAGTC -3'
Mus Musculus	Retn	Reverse	5'- TCTATCCTTGCACACTGGC -3'
Mus Musculus	CD36	Forward	5'- GATGACGTGGCAAAGAACAG -3'
Mus Musculus	CD36	Reverse	5'- TCCTCGGGGTCCTGAGTTAT -3'
Mus Musculus	CEBPα	Forward	5'- CAAGAACABCAACGAGTACCG -3'
Mus Musculus	CEBPα	Reverse	5'-GTCACTGGTCAACTCCAGCAC
Mus Musculus	AdipoQ	Forward	5'- CCCAAGGGAACTTGTGCAGGTTGGATG -3'
Mus Musculus	AdipoQ	Reverse	5'- GTTGGTATCATGGTAGAGAAGAAAGCC -3'

Mus Musculus	FAS	Forward	5'- CTGAGATCCCAGCACTTCTTGA -3'
Mus Musculus	FAS	Reverse	5'- GCCTCCGAAGCCAAATGAG -3'
Mus Musculus	Leptin	Forward	5'- CTCCATCTGCTGGCCTTCTC -3'
Mus Musculus	Leptin	Reverse	5'- CATCCAGGCTCTCTGGCTTCT -3'
Mus Musculus	HSL	Forward	5'- GGACGCCATTCATACCTT -3'
Mus Musculus	HSL	Reverse	5'- ATCAACTCGCCGATGTCT -3'
Mus Musculus	PPARɣ	Forward	5'- CCACCAACTTCGGAATCAGCT -3'
Mus Musculus	PPARɣ	Reverse	5'- TTTGTGGATCCGGCAGTTAAGA -3'
Mus Musculus	Psat1	Forward	5'- TGGAACGGTGAACATTGTCC -3'
Mus Musculus	Psat1	Reverse	5'- GTCAGGTACGAAGTCAAACTCC -3'
Mus Musculus	COX7A1	Forward	5'- TGTGGCAGAGAAGCAGAAG -3'
Mus Musculus	COX7A1	Reverse	5'- AGCCCAAGCAGTATAAGCAG -3'
Mus Musculus	PGC1A	Forward	5'- CATTTGATGCACTGACAGATGGA -3'
Mus Musculus	PGC1A	Reverse	5'- GTCAGGCATGGAGGAAGGAC -3'
Mus Musculus	IDH3A	Forward	5'- ACGGAAGGAGAATACAGTGG -3'
Mus Musculus	IDH3A	Reverse	5'- GTACTCGAAGGCAAACTCTG -3'
Mus Musculus	UCP1	Forward	5'- GAGCTGGTAACATATGACCTC -3'
Mus Musculus	UCP1	Reverse	5'- GAGCTGACAGTAAATGGCA -3'
Mus Musculus	DIO2	Forward	5'- CTGTGTCTGGAACAGCTT -3'
Mus Musculus	DIO2	Reverse	5'- CACTGGAATTGGGAGCAT -3'
Mus Musculus	PPARA	Forward	5'- ACGCATGTGAAGGCTGTAAG -3'
Mus Musculus	PPARA	Reverse	5'- CACTTGTGAAAACGGCAGTAC -3'
Mus Musculus	GLUT1	Forward	5'- GGTGTGCAGCAGCCTGTGTA -3'
Mus Musculus	GLUT1	Reverse	5'- CAACAAACAGCGACACCACAGT -3'
Mus Musculus	GLUT4	Forward	5'- CTGTGCCATCTTGATGACCGTG -3'
Mus Musculus	GLUT4	Reverse	5'- GTTGGAGAAACCAGCGACAGC -3'
Mus Musculus	GCK	Forward	5'- AGGGAACAACATCGTGGGAC -3'

Mus Musculus	GCK	Reverse	5'- TCACATTGGCGGTCTTCATA -3'
Mus Musculus	DBP	Forward	5'- AATGACCTTTGAACCTGATCCCGCT -3'
Mus Musculus	DBP	Reverse	5'- GCTCCAGTACTTCTCATCCTTCTGT -3'
Mus Musculus	InsR	Forward	5'- TTTGTCATGGATGGAGGCTA -3'
Mus Musculus	InsR	Reverse	5'- CCTCATCTTGGGGTTGAACT -3'
Mus Musculus	SCD1	Forward	5'- TTCTTACACGACCACCACCA -3'
Mus Musculus	SCD1	Reverse	5'- GCAGGAGGGAACCAGTATGA -3'
Mus Musculus	IRS1	Forward	5'- TCCTATCCCGAAGAGGGTCT –3'
Mus Musculus	IRS1	Reverse	5'- TGGGCATATAGCCATCATCA -3'
Mus Musculus	IRS2	Forward	5'- GTAGTTCAGGTCGCCTCTGC -3'
Mus Musculus	IRS2	Reverse	5'- TTGGGACCACCACTCCTAAG -3'
Mus Musculus	HNF1A	Forward	5'- GCCCTACCTGATGGTTGGAG –3'
Mus Musculus	HNF1A	Reverse	5'- CCCATCGTCATCCGTGTCAT -3'
Mus Musculus	HNF1B	Forward	5'- GGCCTACGACCGGCAAAAGA -3'
Mus Musculus	HNF1B	Reverse	5'- GGGAGACCCCTCGTTGCAAA -3'
Mus Musculus	GCK	Forward	5'- AGGGAACAACATCGTGGGAC -3'
Mus Musculus	GCK	Reverse	5'- TCACATTGGCGGTCTTCATA -3'
Mus Musculus	HNF4A	Forward	5'- GGTAGGGGAGAATGCGACTC -3'
Mus Musculus	HNF4A	Reverse	5'- AAACTCCAGGGTGGTGTAGG -3'
Mus Musculus	TFEB	Forward	5'- AAGGTTCGGGACGTATCTGTCTG–3'
Mus Musculus	TFEB	Reverse	5'- GGGTTGGAGCTGATATGTAGCA-3'
Mus Musculus	IL6	Forward	5'- TCTCCAGCAACGAGGAGAAT -3'
Mus Musculus	IL6	Reverse	5'- TGTGATCTGAAACCTGCTGC -3'
Mus Musculus	TNFA	Forward	5'- CCACATCTCCCTCCAGAAAAGA –3'
Mus Musculus	TNFA	Reverse	5'- GCTGGGTAGAGAATGGATGAAC -3'
Mus Musculus	CCL2	Forward	5'- TTAAAAACCTGGATCGGAACCAA -3'
Mus Musculus	CCL2	Reverse	5'- GCATTAGCTTCAGATTTACGGGT -3'

Mus Musculus	Resistin	Forward	5'- CCATCGACAAGAAGATCAAACAAG -3'
Mus Musculus	Resistin	Reverse	5'- GGAGACTGTCCAGCAATTTAAGC-3'
Mus Musculus	POMC	Forward	5'-TAGATGTGTGGAGCTGGTGC -3'
Mus Musculus	POMC	Reverse	5'- CCAGCGAGAGGTCGAGTTTG -3'
Mus Musculus	HSPA1A	Forward	5'- TGGTGCAGTCCGACATGAAG –3'
Mus Musculus	HSPA1A	Reverse	5'- GCTGAGAGTCGTTGAAGTAGGC -3'
Mus Musculus	AGRP	Forward	5'- CTTTGGCGGAGGTGCTAGAT -3'
Mus Musculus	AGRP	Reverse	5'- AGGACTCGTGCAGCCTTACAC -3'
Mus Musculus	NPY	Forward	5'- CAGATACTACTCCGCTCTGCG –3'
Mus Musculus	NPY	Reverse	5'- GGGCTGGATCTCTTGCCATA-3'
Mus Musculus	XBP1	Forward	5'- ACACGCTTGGGAATGGACAC -3'
Mus Musculus	XBP1	Reverse	5'- CCATGGGAAGATGTTCTGGG -3'
Mus Musculus	Ddit3	Forward	5'- GGAGCTGGAAGCCTGGTATG –3'
Mus Musculus	Ddit3	Reverse	5'- GGATGTGCGTGTGACCTCTG -3'

Table 2.1 – Sequences of the primers used in this study.

2.10 Assessment of IBET-762 TF-activation on circadian rhythms

The putative transcription factors that could be influential in increasing circadian amplitude in response to IBET-762, were sequentially knocked-down. Furthermore, IBET-762 was administered at a concentration of 0.5μM in 0.25% volume of DMSO, to assess the amplitude increasing impact of the drug over 92 hours. The amplitude increasing effects of IBET-762 over a mock gene knock-down were then compared to the effects of IBET-762 in the specific gene-of-interest knock-down, and expressed as a percentage of the control.

2.11 *Sp1::*Luc and *Hre::*Luc promoter reporter drug-induced activity

Sp1::Luc and *Hre*::Luc promoter reporters were transiently-transfected in U2OS cells, following the methodology described above. Furthermore, the transfection baseline was assessed over the first six hours, until the promoter activity stabilized. Then drugs were added to the media at a 1μM concentration, in 0.5% volume of DMSO, and the reporter activity was assessed over 6 hours for *Sp1*::Luc and 12 hours for *Hre*::Luc promoters. The luminesce activity was reported as a percentage change of the DMSO-negative control.

2.12 Transfac analysis of BMAL1 promoter regions

The human promoter sequence of *Bmal1* gene and the *Bmal1*::Luc mouse gene promoter were analyzed using Transfac. Transfac is a database of more than 23,000 eukaryotic transcription factors, their genomic binding sites and DNA-binding profiles. Promoter reports with mapped annotated Transcription Factor (TF) binding sites were generated. High-throughput chromatin immunoprecipitation sequencing (ChIP-Seq) data is also annotated, where available, with an 'E', underlining the availability of experimental evidence of transcription factors binding to the specific DNA sequences, based on a database of 2,000 High Throughput Screen (HTS) TF binding sites ChIP-Seq experiments.

2.13 ChIP-Seq data analysis

ChIP data from Asangani *et al.*(Asangani *et al.*, 2014) was re-analysed as part of this project, as follows: reads were aligned to the *Homo sapiens* genome assembly GRCh37 (HG19) reference genome using Bowtie2 (Langmead & Salzberg, 2012) with all default settings. Quality control was performed with FASTQC, and the alignments with a quality over 20 Mapping Quality (MAPQ) were over 92%. Aligned reads were sorted, exact duplicates and likely misalignments with a MAPQ score under 20 were removed using Samtools (Li *et al.*, 2009). To compare the genome-wide distribution of BRD2, BRD3, and BRD4 peaks in DMSO vs IBET-762 treatments, peaks and summits were called for each of the proteins using Model Based analysis of ChIP-Seq 2 (MACS2) (Zhang *et al.*, 2008) with all default settings (FDR<0.01), in a paired-end fashion. For each protein (BRD2, BRD3, BRD4) we assessed quantitative changes in their respective enrichment levels upon drug treatment (IBET-762) relative to the levels in the DMSO control. As BET-inhibitors work through a mechanism that is expected to decrease BRD DNA-binding peaks, the DMSO treatment was used as the higher-peak condition. Enriched motifs with lengths between 8 and 16bp were searched with Hypergeometric optimization of motif enrichment (HOMER) 4.9 on the narrow peak file outputs. The enriched motifs represent the DNA sequences which show a reduced binding of bromodomains, following IBET-762 treatment. The searching window was set to 200bp in size, and the background was masked using the background peak file output from MACS2 to minimise false positives. Gene ontology was also run to find representations of genes within peaks, and highlight biological processes of genes regulated by IBET-762.

2.14 Adipocyte differentiation protocol of 3T3-L1

3T3-L1 cells are an established pre-adipose fibroblast-like mouse-derived cell line, which under the right conditions, differentiates into an adipocyte-like phenotype. When the cells show an adipocyte-like phenotype, they increase the synthesis and accumulation of triglycerides and acquire the morphology of adipocytes. The cells also become sensitive to lipogenic and lipolytic hormones, can be transfected and are responsive to drugs of metabolic effects (Green & Kehinde, 1975).

To chemically induce 3T3-L1 cells to differentiate into adipocytes, a series of drugs must be added in their media: IBMX (3-isobutyl-1-methylxanthine, a methylated xanthine derivative at a 0.5mM final concentration), dexamethasone (a corticosteroid at a 1μM final concentration) and insulin (10ug/mL final concentration). A PPARɣ-agonist, such as rosiglitazone, can be added as an additional prodifferentiative agent, to achieve a higher grade of 3T3-L1 differentiation (2μM final concentration) (Zebisch *et al.*, 2012).

The established protocol sees seeding pre-adipocyte 3T3-L1 cells at $3x10^3$ cells/cm^2 in a six-well plate and allow to reach 70% confluency. The DMEM media, with the above-mentioned added prodifferentiative agents, will be changed every 2-3 days, for two-three cycles, after which the prodifferentiative agents will be replaced with insulin alone for an extra cycle, then replaced by DMEM with no prodifferentiative agents for other 2-3 days, to allow for stabilisation and remove the acute effects of insulin and other prodifferentiative agents on the cell line (Reed & Lane, 1980).

2.15 Lipid-staining protocol in adipocytes

Nile red (9-diethylamino-5H-benzo[α]phenoxazine-5-one) is a lipophilic stain used to stain intracellular lipid droplets that will emit an intense fluorescence when in a lipid-rich environment, with varying colours from deep red (for polar membrane lipids) to strong yellow-gold (for neutral lipids in intracellular storages). The emission/excitation wavelengths is 450-500/>528nm for yellow-gold fluorescence and 515-560/>590nM for red fluorescence (Greenspan *et al.*, 1985). The dye is very soluble in lipids and does not dissolve them. Nile red can also identify neutral lipid deposits, which are not generally seen with other dyes commonly used for lipid staining (Fowler & Greenspan, 1985). The application of the dye followed the experimental protocol by Sigma-Aldrich.

2.16 Nuclear-staining protocol in adipocytes

DAPI (4',6-diamidino-2-phenylindole) is a fluorescent stain that strongly binds adenine-thymine rich regions within the DNA, and can stain both live and fixed cells. When bound to dsDNA, DAPI shows an absorption maximum at 358nM (ultraviolet) and an emission maximum at 461nM (blue) (Kapuscinski, 1995). DAPI can therefore be used to stain nuclei and assess cellular morphology, based on the disposition of nuclei. Importantly, DAPI staining showed no structural changes due to the dye itself (Tarnowski *et al.*, 1991). The application of the dye followed the experimental protocol by Thermofisher. Fluorescence was assessed through a microplate-reader and the values were used for normalisation of the lipid-staining readings (as a proxy of number of cells viable).

2.17 Lipolysis assay in 3T3-L1 differentiated adipocytes

Lipolysis is the hydrolysis of triglycerides into glycerol and free fatty acids, which are then released into the culture media. Lipolysis is active at baseline and can also be induced by catecholamines, such is isoproterenol, which activate β-adrenergic receptors, leading to the activation of adenylyl cyclase. Its activation catalyses the conversion of ATP to Cyclic Adenosine Monophosphate (cAMP), which then activates the hormone-sensitive lipase, hydrolysing the triglycerides. The lipolysis assay kit (provided by Abcam, ab185433), is a quantitative colorimetric assay that quantifies the amount of glycerol released, at a >540nm wavelength. Lipolysis activity was therefore analysed as a function of the concentration of glycerol released in the culture media (Schweiger *et al.*, 2014). The baseline was removed and the values were fit on a standard curve, to allow for the calculation of absolute values of glycerol, released in the media at 1 hour, 4 hours and 24 hours after IBET-762 or DMSO treatment.

2.18 Glucose-uptake assay in 3T3-L1 differentiated adipocytes

Glucose-uptake-Glo™ (Promega) is a simple, plate-based, bioluminescence assay which measures glucose uptake within cells, based on the detection of 2-deoxyglucose-6-phosphate (2DG6P). 2DG is picked up by cells from the culture media through present glucose transporters, and the hexokinase phosphorylates it to 2DG6P through the first step of glycolysis. This process is interrupted by the stop buffer. A detection reagent is then added, which quantifies the presence of 2DG6P within the cells, as a proxy of a

reaction which reduces NADP+ to NADPH, which is then used to convert pro-luciferin to luciferin, the substrate of a luciferase which produces light (see **Figure 2.2**).

Luminescence was quantified through the aid of a microplate-reader and analysed by removing the baseline and fitting the values on a standard curve, to allow for the calculation of absolute concentrations of 2DG6P, as a proxy of glucose-uptake, at 24 hours after IBET-762 or DMSO treatment.

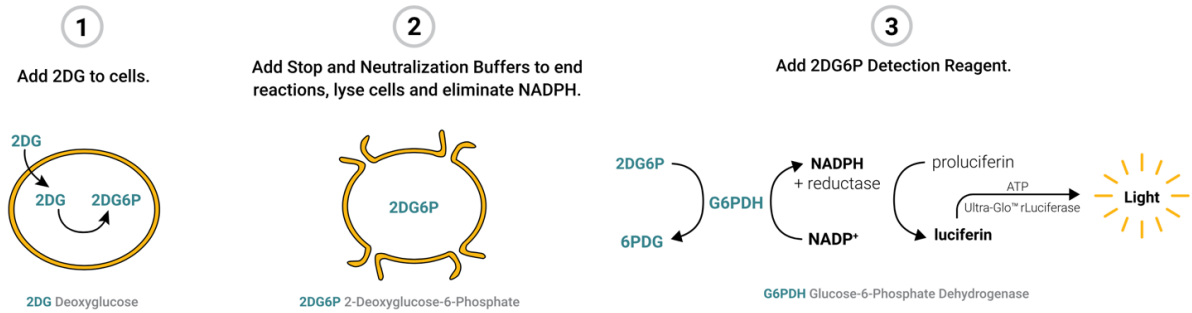


Figure 2.2 – Glucose-uptake Glo™ assay principle. Cells are added a 2DG substrate, which is then phosphorylated by the hexokinase. A stop and neutralisation buffers ensure the end of cellular reactions and lyse the cells and a detection reaction quantifies the presence of 2DG6P through the emission of light, as luciferin is produced concentration-dependently.

2.19 Lactate-uptake assay in 3T3-L1 differentiated adipocytes

Lactate-Glo™ (Promega) is a bioluminescent assay for the detection of L-lactate in biological samples. Lactate is produced by glycolysis, especially in conditions of low cellular oxygen (hypoxia). A selective L-lactate dehydrogenase is added, which uses L-lactate and NAD+ as a substrate to produce pyruvate and NADH. NADH levels are then quantified by the activity of a reductase, which converts pro-luciferin in luciferin, which is then used in a luciferase reaction, to produce light.

Luminescence was quantified through the aid of a microplate-reader and analysed by removing the baseline and fitting the values on a standard curve, to allow for the calculation of absolute concentrations of lactate, at 24 hours after IBET-762 or DMSO treatment.

2.20 ATP-production analysis in 3T3-L1 differentiated adipocytes

To analyse ATP production in live adipocytes and to assess energy production levels within, we have used a Seahorse XF Analyzer assay (Agilent). The Seahorse XF analyser assay measures the oxygen consumption rate (OCR) (pmol/minute) and extracellular acidification rate (ECAR) (mpH/minute) of live cells, informing thus on cellular functions such as mitochondrial respiration and glycolysis. Upon analysing basal levels of OCR and ECAR, drugs can be added to the media to inhibit certain pathways and allow for specific readings (Divakaruni *et al.*, 2014).

Oligomycin inhibits ATP synthase (complex V), resulting in a reduction in mitochondrial respiration (OCR). This decrease can be linked to cellular ATP production. Carbonyl cyanide-4 phenylhydrazone (FCCP) is then added, which collapses the proton gradient and disrupts the mitochondrial membrane potential, allowing a maximal electron flow and oxygen consumption by complex IV, and can be used to calculate spare respiratory capacity (difference between maximal respiration and basal respiration), and relates to the cellular ability to respond to increased energy demand or stress. The third injection is a mix of rotenone (complex I inhibitor) and antimycin A (complex III inhibitor),

shutting down mitochondrial respiration, enabling the calculation of nonmitochondrial respiration (**Figure 2.3).**

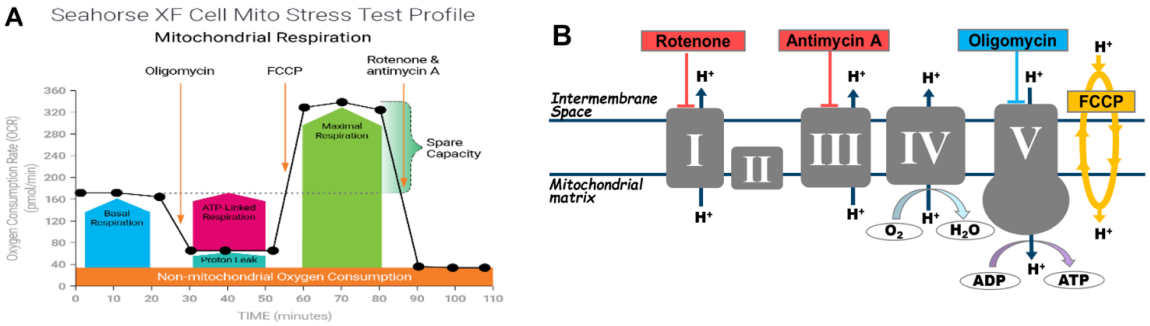


Figure 2.3 – Seahorse XF Analyzer assay. Levels of basal respiration are assessed (**A**), then a series of drugs are added sequentially, such as oligomycin, FCCP and rotenone and antimycin A, modulating the activity of specific cellular mitochondrial respiration complexes (**A, B**). OCR and ECR activities were assessed at regular intervals and after the addition of each of the drugs.

2.21 NAD^+/NADH ratio in differentiated 3T3-L1 adipocytes

The NAD/NADH-Glo assay (Promega) allows for the quantification of NAD and NADH, through a bioluminescence mechanism. As NAD cycling enzyme converts NAD^+ to NADH, a reductase reduces a pro-luciferin substrate to luciferin, which is detected through the emission of light when interacting with a rLuciferase. The light emitted is collected by a microplate reader and is proportional to the concentration of NAD^+ and NADH levels. NAD^+ and NADH levels can be measured separately by an acid treatment and a basic treatment respectively, according to the manufacturer's protocol.

2.22 High fat diet induced obesity mouse experimental setup

48 C57BL/6 4-week old male mice (Envigo) were caged in groups of four, in a total of 12 cages with ad libitum feeding and housed in a 12:12 house dark cycle at 20-22ºC and 40% humidity. The mice were subdivided in 3 experimental groups (vehicle high-fat diet control, diet control and IBET-762 20mg/kg-treated mice) of 4 cages (or 16 mice) in each cohort (**Figure 2.4**), with food available *ad libitum*.

Experiments were performed in accordance with the United Kingdom Animals Act (Scientific Procedures) of 1986, following national and international ethical standards and in accordance with the Three Rs (Replacement, Reduction and Refinement, wherever possible).

Diet: The Vehicle Control cohort group and IBET-762-treated cohorts was given a high-fat diet (HFD) chow (60%Kcal fat, D12492 by Research Diets) *ad libitum* until the end of the experiment. This allowed for the testing of our main outcome, that is the effects of IBET-762 on high-fat-diet-induced weight gain. The diet control was administered as a normocaloric control diet (standard chow diet, D12450J by Research Diets) that is a control match to the HFD in macro and micronutrients, except the fat content, which was limited to 10%kcal (see **Table 2.2**). This will allow for a comparison of the high-fat diet effectiveness in increasing the body mass of the mice, as compared to the normocaloric diet-control.

	High fat diet (D12492)	Control Diet (D12450J)
Protein content	20% KCal	20% KCal
Fat content	60% KCal	10% KCal
Carbohydrate content	20% KCal	70% KCal
Energy density	5.21 KCal/g	3.82 KCal/g

Table 2.2 – Energetic content of diets used in the DIO rodent study

Intervention: All mice were treated with drug/vehicle on daily basis (7 days/week), via gavage, for a maximum period of 10 weeks. Each mouse was administered 100μL of a 15% Koliphor saline solution (0.9% NaCl) containing either the vehicle or drug. IBET-762 was dissolved in Koliphor to be administered to mice at a concentration of 20mg/kg. The gavage injection was carried out daily at ZT7 - ZT9, to allow for a time-sensitive intervention. Mice were monitored for their weight, food consumption, and general standards, on a weekly basis. At the end of the 10th week, their sensitivity towards glucose and insulin was tested, and all animals except 8 of the IBET-762-treated mice were sacrificed for tissues collection for further gene expression and image-based analysis. The group of 8 IBET-762-treated mice were allowed to carry on a high fat diet, without any further drug administration. The treatment was thus halted but the HFD was kept, to allow for a dissection of the effects of the treatment halt. The 8 IBET-762 mice were culled at week 18, after 8 weeks of HFD-only intervention.

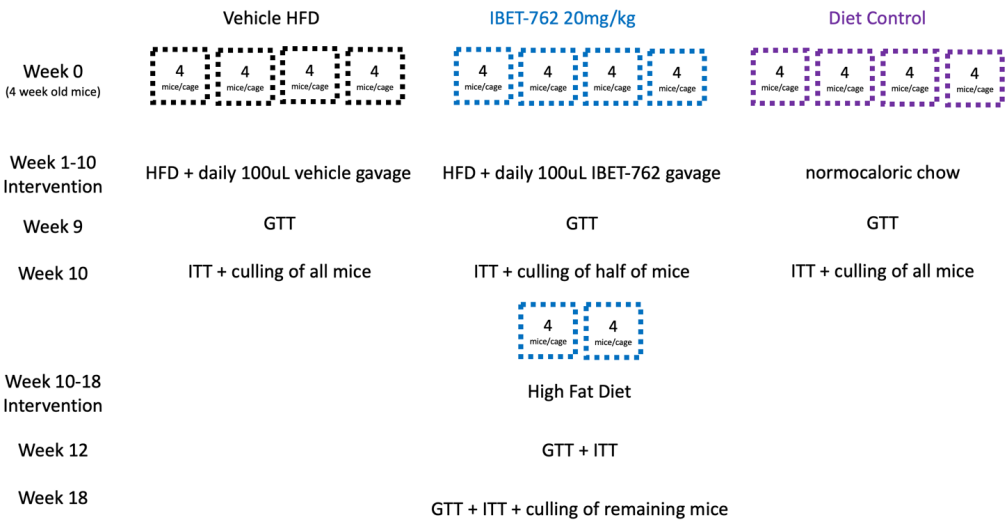


Figure 2.4 – Experimental paradigm of high-fat diet-induced obesity in C57BL/6 mice; mice were fed a high fat diet *ad libidum*, except the diet control group, which had access to a normocaloric chow. The HFD-fed subjects were administered with a 100uL daily gavage for week 1-10, either a control or 20mg/kg IBET-762. Animals were tested for glucose and insulin tolerance between week 9 and 10 and were culled at week 10, besides half of IBET-762 treated mice. These last ones were fed high-fat-diet over week 10-18, during which GTT and ITT were repeated at week 12 and week 18. They were also culled at week 18.

2.23 Glucose and insulin tolerance tests

Glucose and insulin tolerance tests were performed at week 9-10. This allowed for a quantification of glucose after a challenge of glucose and insulin, to further understand the diabetic-phenotype of the mice. IBET-762 were further subdivided into two groups of 8 mice each: group 1 was culled after 10 weeks of HFD + IBET-762 administration, whereas group 2 was kept under a HFD-only regimen for a further 8-week period, with no IBET-762 administration. Group 2 was also tested for glucose and insulin tolerance at week 12 and week 18, before culling. This allowed for a further comparison after IBET-762 treatment halt.

Glucose tolerance test (GTT) (week 10, week 12, week 18):

Procedure: ZT2, after 16-hour overnight fasting (food removed at ZT10 the day before) - 8 mice per cohort were given a bolus of glucose (1g/kg) to be administered orally and a drop of blood (~10ul) was collected at various time points to cover for a time course (e.g. 0, 15, 30, 60, 90 and 120 min) for plasma glucose analysis using αTRAK 2 (Zoetis, United States).

Insulin tolerance test (ITT) (week 10):

Procedure: at ZT8, after 5 hours fasting (food removed at ZT3 the same day) - 8 mice per group were given a bolus of 1.0 U/kg insulin to be administered intraperitoneally and a drop of blood collected at various time points to cover a time course (e.g. 0, 15, 30, 60 and 90 min) for plasma glucose using αTRAK 2.

2.23 Liver weight analysis

Livers were dissected from mice immediately *post-mortem* and were weighted, after which they were processed for further experimentation. To allow for a normalisation of different physiognomies among mice, we have normalised their weights on each subject's tibial length, which has been extensively used in the past to normalise weights of different organs, independently of the body weight of the subject (Nunes-Souza *et al.*, 2016; Yin *et al.*, 1982). The measures were calculated in g/cm and expressed as a

percentage difference over the vehicle control. The results were statistically tested through a one-way ANOVA and Dunnett-powered multiple comparisons analysis.

2.24 Tissue cryosection and histological staining

Tissue sections were removed from mice *ex-vivo*, upon culling, in a consistent manner and fixed by immersion in formaldehyde (10% neutral buffered formalin), for 48 hours. Formaldehyde was used as a cross-linking agent, to prevent tissue decay and promote fixation, for future examination. Upon fixation, the tissue was immersed on a 30% sucrose/PBS solution overnight, to help prevent the formation of ice-crystals in tissues when water freezes and expands. Tissues were then embedded in Optimal Cutting Temperature (OCT, Fisher Scientific UK Ltd) compound, which provides a matrix for the tissue for cryostat sectioning at low temperatures, and were frozen at -80ºC until future use. The tissues were later cryosectioned with a cryotome, at an optimal temperature for the tissues between -21 and –25ºC and optimal thickness of 8μm for the liver sections and 20μm for the visceral fat sections. They were placed onto glass slides suitable for imaging (Superfrost, VWR International Ltd) and dried at room temperature. Sections were then double fixed with formaldehyde (10 minutes), rinsed in PBS (5 minutes) and air-dried. The tissue slices were then stained according to specific protocols dependent on type of tissue and the target to highlight. After staining, tissues were dehydrated through four changes of alcohol (100%, 95%, 80%, 60%), from the least concentrated to the most concentrated one.

Liver sections staining and quantification procedure

Liver sections were stained by immersing slides in Oil Red O and haematoxylin (Mayer's Haematoxylin Solution, Merck Chemicals Ltd) to highlight the presence of fatty acids and cellular nuclei, respectively, following their protocol. The tissue slides were then cleared using xylene and mounted using DPX Mountant (Merck Life Science UK Ltd), a distyrene and xylene mixture used as a synthetic resin mounting media. The coloured structures were then observed on the tissue sections under microscopy and imaged at magnifications of 40X.

Oil Red O staining was then quantified using the ImageJ software as follows: the image was transformed in the YIQ colour space using the Colour Transformer plugin (by Maria E. Barilla, University of Birmingham, UK) and was then converted in a 8-bit image format. Q channel levels were adjusted and a threshold was applied such that the Oil Red O stain would now be visualized in a black and white contrast. The black pixels were then quantified as a percentage of the total area of the image.

Visceral fat sections staining procedure

Visceral fat sections were stained by immersing slides in haematoxylin (Mayer's Haematoxylin Solution, Merck Chemicals Ltd), to stain the nuclei of a blue-purplish colour, and eosin, an acidic dye that stains negatively charged organelles, such as the cytoplasm, of a pink colour. The tissue slides were then cleared and covered with a water soluble mounting agent (SlowFade Diamond antifade Mountant, Life Technologies Ltd),

to avoid dissolving the oily stains. The coloured structures were then observed on the tissue sections under microscopy and imaged at magnifications of 20X.

2.25 Ex-vivo plasma metabolite quantification

Metabolite levels were quantified using the indicated assays following 5 hours of caloric restriction.

Insulin quantification

Plasma insulin quantification was conducted using the Abcam Insulin Enzyme-linked immunosorbent assay (ELISA) kit (ab100578), following the manufacturer's protocol. Signal output was read with a microplate reader (BMG Labtech), and colorimetric quantification was identified at 450nm. All experiments were conducted in parallel with a standard curve to aid accurate quantification and the results are expressed in uIU/ml. Statistical significance was tested through a one-way ANOVA and Dunnett-powered multiple comparisons analysis.

Free fatty acid quantification

Plasma free fatty acid quantification was conducted using the Abcam's free fatty acid assay kit (ab65341), which offer fully quantitative results from the enzyme-based analysis of long-chain free fatty acids in plasma (C-8 and longer). Fatty acids are converted to their Coenzyme A (CoA) derivatives, which are subsequently oxidized, leading to the formation of colour/fluorescence. The free fatty acid assay was previously used to

successfully quantify free fatty acids in mouse plasma (Becares *et al.*, 2019). We followed the producer's protocol in analysing and quantifying the results. All experiments were conducted in parallel with a standard curve to aid accurate quantification using palmitic acid and the results are expressed as mmol/L. Signal output was read with a microplate reader (BMG Labtech) and fluorometric quantification was identified at Ex/Em 535/587nm. Statistical significance was tested through a one-way ANOVA and Dunnett-powered multiple comparisons analysis.

Total cholesterol quantification

Total cholesterol quantification was conducted using Cellbiolabs's cholesterol assay kit (STA-391), which offer fully quantitative results from total cholesterol in plasma (cholesteryl esters and free cholesterol). Cholesteryl esters are converted to cholesterol through an esterase and then oxidised in presence of a fluorescence probe, leading to the formation of fluorescence. The assay was previously used to successfully quantify cholesterol in mouse plasma (Ko *et al.*, 2020). We followed the producer's protocol in analysing and quantifying the results. All experiments were conducted in parallel with a standard curve to aid accurate quantification and expressed as mg/dl. Signal output was read with a microplate reader (BMG Labtech) and fluorometric quantification was identified at Ex/Em 530-570/590-600nm. Statistical significance was tested through a one-way ANOVA and Dunnett-powered multiple comparisons analysis.

Triglyceride quantification

Plasma triglycerides quantification was conducted using Abcam's Triglyceride assay kit (ab178780), which offer fully quantitative results of plasma triglycerides. In this assay, triglycerides are hydrolysed to glycerol and fatty acids. The glycerol then reacts with an enzyme mix to form an intermediate product which reacts with a fluorescent probe to generate fluorescence. The assay was previously used to successfully quantify triglycerides in mouse plasma (Yisireyili *et al.*, 2019). We followed the producer's protocol in analysing and quantifying the results. All experiments were conducted in parallel with a standard curve to aid accurate quantification and expressed as mmol/L. Signal output was read with a microplate reader and fluorometric quantification was identified at Ex/Em 535/587nm. Statistical significance was tested through a one-way ANOVA and Dunnett-powered multiple comparisons analysis.

2.26 Data analysis and statistics

Data from the gene reporter experiments were analysed using MultiCycle, software developed by Actimetrics (http://actimetrics.com/products/multicycle). The first hours were not considered, to avoid disturbances due to cell manipulation and temperature changes. Data was baseline-subtracted and smoothed by a 6-hours moving average. Graphs were plotted with the help of GraphPad Prism 8. An unpaired one-way ANOVA analysis was performed on all conditions that did not show toxicity. A multiple comparison Bonferroni post-hoc test between treated cells and control followed. The post-hoc test was corrected for multiple comparisons: confidence intervals and

significance. Dose response curves were also built using standard non-linear regression analysis, showing the percentage amplitude (and period) change effects of the conditions used. Data was presented in the form of an average ± Standard Error of Mean (SEM).

Data from the qPCR experiments was analysed through relative quantification of transcript levels. This was pursued following a published method (Peirson *et al.*, 2003). The expression of the genes of interest was normalized over the expression of the housekeeping genes, given an optimal efficiency of the primers, as described in **2.7**. For the 36-hour qPCR experiments, graphs were plotted on Prism using a modified sine equation (see **Equation 2.1**), and constraining its wavelength to 20 hours. An extra sum-of-squares F test statistical comparison analysis assessed the divergence between the two datasets considered (treated vs control). If the data did not cycle in a circadian-manner, a two-way ANOVA analysis was performed (time and treatment) with a subsequent multiple-comparison post-hoc in between treatments, within each timepoint.

Equation 2.1 $Y = BaseLine + Amplitude^{(-K * X)} * \sin((2 * pi * X / Wavelength) + PhaseShift)$

The choice of statistical tests employed was mainly dictated by the number of conditions analysed; if two different treatments were analysed, then a T-Test was employed to study their statistical difference (paired if the groups of samples were the same and the treatments different, unpaired if both groups of samples and treatments were different). ANOVA analyses were employed to study the statistical significance among the means of three or more treatments. Specifically, one-way ANOVAs were employed to study the statistical significance among three or more groups of data on one specific factor or

independent variable, whereas two-way ANOVAs were employed when two-independent variables were studied. Post-hoc tests were then employed to dissect which specific condition and variable are responsible for the difference between the datasets. A legend was used to represent the levels of statistical significance found through the various tests: ns=$p \geq 0.05$, *=$p<0.05$, **=$p<0.01$, ***=$p<0.001$ and ****=$p<0.0001$.

CHAPTER I

EFFECTS OF EPIGENETIC MODULATION ON CIRCADIAN RHYTHMS

main findings:

epigenetic mechanisms are key to circadian rhythm modulation

acetylation as a pivotal mechanism of amplitude increase in circadian rhythms

JQ-1 and IBET-762 promote amplitude increase of circadian clock genes

3 Chapter I: EPIGENETIC MODULATION ON CIRCADIAN RHYTHMS

3.1 INTRODUCTION

3.1.1 Epigenetic mechanisms in eukaryotes

All the different cells within our body contain the same primary genetic material (DNA sequence/chromosome etc.) but upon differentiation, they develop different phenotypes optimised to conduct specialised biological functions. This epigenetic differentiation within an individual is driven by heritable changes in gene expression that are not due to alterations in the DNA sequence (Holliday, 1987). The DNA is packaged into a highly-condensed histone-rich structure, called chromatin (Luger *et al.*, 2012). The chromatin is dynamic and highly regulated by a series of processes that render it more accessible or inaccessible (see **Fig. 3.1.1**) DNA methylation as well as histone modifications are the best-defined phenomena of epigenetic modification mechanisms (Kouzarides, 2007).

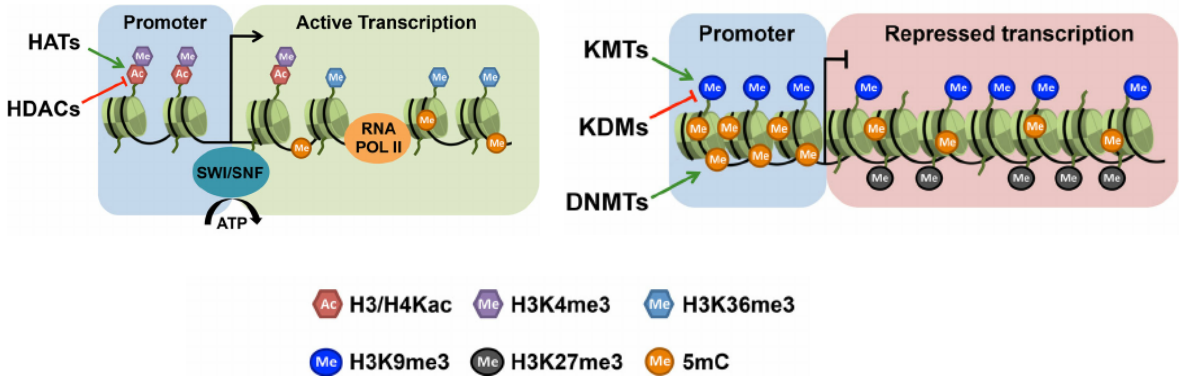


Figure 3.1.1 – Mechanisms of epigenetic regulation. Histone acetyltransferases (HATs) and histone deacetylases (HDACs) modulate histone acetylation mechanisms, whereas histone lysine methyltransferases (KMTs), histone lysine demethylases (KDMs) modulate histone methylation mechanisms. DNA methyltransferases (DNMTs) modulate methylation on the DNA strands. Adapted from (Mirabella *et al.*, 2016).

3.1.2 DNA methylation mechanisms

DNA methylation is a process through which methyl groups are added to the DNA molecule and can change the expression of genes without changing the DNA sequence of a cell. DNA methylation is involved in both repression of genes (specifically when promoter regions are methylated) but is also associated with an activation of gene transcription. The effect of DNA methylation on gene expression is largely dependent on the site of methylation and the change in dynamics of protein-to-DNA interaction, where the proteins can be constituted by both regulatory and transcription factors. In the mammalian genome, DNA methylation involves the transfer of a methyl group onto the C5 position of the DNA cytosine to form 5-methylcytosine. High methylation levels within the DNA are usually found in CpG islands (regions of DNA where a cytosine nucleotide is followed by a guanine nucleotide, repeated in a linear sequence with high enrichment over other nucleotides). DNA methylation in or near promoter regions has

shown to participate in transcriptional regulation. Currently, most models underline a repression-based mechanism of DNA methylation (Buck-Koehntop & Defossez, 2013). Typically, a DNA-methylated cytosine is bound by a methylation binding protein (MBP) and blocks the interaction of DNA with some but not all transcription factors, and subsequent transcription initiation. However, these interactions can also alter the binding potential of transcriptional repressors or modulators, adding several degrees of complexity to the DNA-methylation functional outcomes (Jin *et al.*, 2016). To illustrate this complexity; recently it was show that the binding of transcription factors to methylated non-CpG regions can promote differential effects in gene expression, with glucocorticoid receptor (GR) binding being enhanced and BMAL1-CLOCK binding being reduced. Similarly, oestrogen receptor (ER) TF binding to DNA was unaltered by methylation-based mechanisms (Jin *et al.*, 2016). Several enzymes can promote changes of the DNA methylome and all belong to the class of DNA methyltransferases (DNMTs), such as DNMT1, DNMT2, DNMT3a, DNMT3b, and DNMT3l, which are required for the establishment and maintenance of DNA methylation patterns. DNA demethylases are also pivotal in maintaining methylation patterns by removing 5-methyl groups, essential in epigenetic reprogramming of genes. Our views of CpG islands being the only centres for methylation control is changing based on recent evidence showing that CpG moieties within 'non-CpG' islands are abundantly methylated in embryonic stem (ES) cells (Lister *et al.*, 2009).

Indeed, DNA methylation is fundamental during the developmental stages, playing a critical role in cell fate, from totipotent zygotes towards a fully functioning organism and in cellular reprogramming. Advancements in the understanding of these epigenetic

mechanisms could also be fruitful in the differentiation of stem-like pluripotent progenitors in regenerative medicine (Seisenberger *et al.*, 2013) and potentially in modulating gene expression paradigms. The importance of methylation in disease has been widely recognized, such as the DNA hypomethylation patterns seen in some types of cancers.

3.1.3 Histone methylation mechanisms

Methyl groups can also be added to amino acids of histone proteins that make up the nucleosome, in a process called histone methylation. Methylation of histones can either increase or decrease the expression of a gene, based on which amino acids are methylated and the number of methyl groups added. Methylation is generally associated with transcriptional repression. Methyl groups are added onto histone tails by histone methyltransferases, a class of enzymes which transfer methyl groups from S-Adenosyl methionine (SAM) onto the arginine or lysine residues of histone 3 and 4. As a general criterion, methylation events that weaken the interaction between histone tails and DNA, allow for an increased access of transcriptional factors to the DNA and promote gene transcription, whereas events that encompass the histone tails around the DNA, restrict the access to the genome and decrease gene transcription (Greer & Shi, 2012).

Histone methylation is generally associated with transcriptional repression; however, it can also exceptionally result in transcriptional activation (eg. methylation of lysine 4 of histone 3, and arginine residues on histone 3 and 4). Although histone methylation was initially thought to be irreversible, it was later shown to be in fact dynamic (Shi *et al.*,

2004). Biologically speaking, histone methylation is fundamental as a response following both developmental as well as environmental events. In fact, methylation of different lysine residues has divergent turnover rates, providing for both reversible and irreversible changes (Zee *et al.*, 2010).

3.1.4 Histone acetylation mechanisms

Lysine acetylation of histones is one of the main and widely-studied modifications occurring in histone tails. The central role of lysine acetylation is reflected by the large amount of acetylation sites identified in proteins, especially those present in the cell nucleus, suggesting a key role of acetylation in the regulation of chromatin and control of transcription (Choudhary *et al.*, 2009). Lysine acetylation is also seen as one of the most dynamic protein post-translational modifications, regulating vast cellular processes (Choudhary *et al.*, 2009). Histone acetylation is the process where an acetyl functional group is transferred from one molecule (acetyl-Coenzyme A) to another, the histones, which are alkaline proteins within eukaryotic cell nuclei that package the cellular DNA into a structured form within the chromatin. There are four core histone classes: H2A, H2B, H3, and H4 which exist as dimers, resulting in an octameric core entwining approximately 146bp. On the other hand, the classes H1 and H5 have a nucleosome-linking function enabling linkage of nucleosomes into higher order structures. The addition of an acetyl-moiety to the sidechain lysine leads to neutralisation of charges, which in turn dramatically alters the chromatin structure. Lysine modification is reversibly controlled by histone acetyltransferases and deacetylases.

Thus, histone acetylation (promoted by histone acetyltransferases, HATs, which add an acetyl group onto histones) mainly promotes the relaxation of the chromatin (euchromatin) hence exposing the DNA to polymerases and transcription factors, associated with greater levels of gene transcription. On the other hand, histone deacetylation (promoted by histone deacetylases - HDACs, remove an acetyl group from histones) and promotes chromatin condensation (heterochromatin) (Allfrey *et al.*, 1964; Pazin *et al.*, 1994). Moreover, acetylation of histones promotes binding of proteins, as they can attract proteins to the elongated chromatin market by acetyl groups, potentially for transcriptional activation (Cheung *et al.*, 2000). The histone code hypothesis states that fingerprints of posttranslational histone modifications, collectively, can direct specific cellular phenotypes, as these modifications can be distinctly interpreted by transcription factors and complexes. HDACs are divided into five main subgroups, based on sequence homologies: Class I (HDAC1, HDAC2, HDAC3 and HDAC8), Class IIA (HDAC4, HDAC5, HDAC7, HDAC9), Class IIB (HDAC6, HDAC10), Class III (Sirtuins), and Class IV (HDAC11). These epigenetic markers allow information to be encoded in chromatin and together they act in regulating gene expression, DNA repair, and replication. Histone modification is considered a major regulatory mechanism that is involved in many different stages of genetic functions and the modification patterns can be collectively maintained in mitosis and meiosis to modify both short term and possibly long-term gene expression (Turner, 2000). Histone acetylation was shown to have fundamental roles in developmental processes and their deregulation has been correlated to different human pathologies, such as several types of cancers (Timmermann *et al.*, 2001).

3.1.5 Bromodomains in epigenetic regulation

Bromodomains are 110 amino acid long protein domains that recognize acetylated lysine residues, such as those on the *N*-terminal tails of histones. There are two major bromo- and extra-terminal domain (BET) families: BD1 and BD2, which are both included in the BRD2/3/4 and BRDT domains. Although BRDT is primarily expressed in germ cells, BRD2/3/4 are ubiquitously expressed. BD1 and BD2 are N-terminal protein structures that drive the interaction with acetylated lysine residues on histone tails. Bromodomains can be viewed as lysine acetylation readers and might be responsible in transducing the signal carried by acetylated lysine residues and translating it into various phenotypes. Bromodomain-containing proteins can have a wide variety of functions, ranging from HAT activity and chromatin remodelling to transcriptional mediation and co-activation (Ntranos & Casaccia, 2016). The human proteome contains 46 different bromodomain-containing proteins, with most of these recognizing acetylated histones and regulating gene expression. Bromodomain-containing proteins can act as scaffolds, facilitating the assembly of larger protein complexes, such as Mediator complexes or transcription factors, which will modulate the transcription of a gene. For example, bound BRD4 recruits p-TEFb, promoting transcriptional elongation through Ser2 phosphorylation on RNA Pol II (Jonkers & Lis, 2015). A recent study showed that BRD4 can be recruited to the E-Box regions through BMAL1 acetylation by TIP60 (Petkau *et al.*, 2019). Unlike BRD4, BRD2 provides a scaffold and stimulates the binding and interaction of HATs, HDACs and E2F. Bromodomain-proteins can also perform catalytic functions themselves, such as acting as methyltransferases, chromatin-remodelling complexes and other chromatin modifications. In fact, most histone

acetyltransferases have been shown to have bromodomains, in addition to acetyl-transferase domains, and these seem to have a major role in target recognition (Dhalluin *et al.*, 1999). It is known that BRDs tether HATs to transcriptional sites and regulate the activities of chromatin remodelling complexes (Barbieri *et al.*, 2013). Members of the BET families have been implicated as targets in several cancer disorders (Jung *et al.*, 2015) and multiple sclerosis (Gacias *et al.*, 2014).

3.1.6 Bromodomain inhibitors as epigenetic drugs

Several bromodomain inhibitors have been developed in recent years, such as JQ-1 (Filippakopoulos *et al.*, 2010) and I-BET (Nicodeme *et al.*, 2010). Both BET inhibitors engage the bromodomain pocket in a manner that is competitive with acetylated peptide binding, thereby causing the displacement of all BET proteins from chromatin (Prinjha *et al.*, 2012), thus interfering with the transcriptional machinery (**Fig. 3.1.2**). JQ-1 was one of the first BD1 and BD2 specific inhibitors identified, a small molecule that binds the BD-containing proteins with high affinity. JQ1 has two stereoisomers, (+)-JQ-1 and (-)-JQ1-; (+)-JQ-1 was shown to selectively bind the BET family, whereas (-)-JQ1 showed no interaction with any bromodomain, thus constituting a valid negative control (Filippakopoulos *et al.*, 2010). IBET-762, another bromodomain inhibitor discovered through lead optimization structure-activity relationship studies (SAR) was shown to have greater selectivity, a longer half-life and are clinically safe (Mirguet *et al.*, 2013).

Bromodomain inhibitors are currently being studied in several types of cancers, as the BET family of proteins have been shown to regulate transcription of oncogenes such as

MYC and the Neuronal Protein in Testis (NUT) fusion oncoprotein. Disruption of binding of BET proteins reduces cellular proliferation and induces apoptosis (Stewart *et al.*, 2013), and has shown potential in several hematologic malignancies and types of leukaemia (Dawson *et al.*, 2011; Zuber *et al.*, 2011). Besides leukaemia, JQ-1 is also studied, as an experimental drug, in solid cancers such as medulloblastoma, a malignant brain tumour in children, characterized by the amplification of MYC (Henssen *et al.*, 2013; Venkataraman *et al.*, 2014) and glioblastoma in adults (Cheng *et al.*, 2013), and has showed to reduce tumour growth in colorectal cancers (Zhang *et al.*, 2018b), breast cancers (Borbely *et al.*, 2015) and castration-resistant prostate cancer (Lochrin *et al.*, 2014).

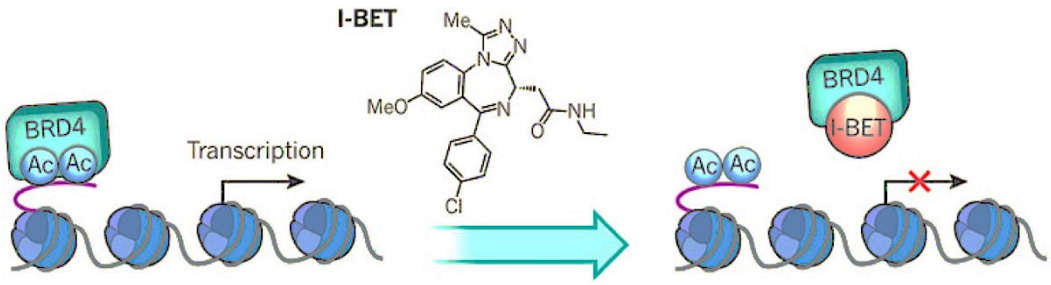


Figure 3.1.2 – Mechanistic hypothesis for IBET drugs in inhibiting gene transcription. Bromodomains are known as 'readers' of acetylated histones on the chromatin, and their binding stimulates the recruitment of the RNA Polymerase II and other transcription factors, which can modulate transcription. The inhibition of bromodomains binding (eg. BRD4) through IBET would block the recruitment of the RNA polymerase and transcription factors and thus inhibit gene transcription.

3.2 RESULTS

3.2.1 Epigenetic drugs influence circadian rhythm gene expression

Epigenetics has long been known to be a pivotal mechanism of regulation within circadian biology (**Introduction 3.1.1-3.1.6**). However, although methylation and acetylation are known to be important in circadian rhythm modulation (Sahar & Sassone-Corsi, 2013), little is known about the effects of specific epigenetic proteins/targets on circadian gene expression. Here we studied the effects of several epigenetic modulators, targeting a wide range of proteins on cellular circadian rhythms with amplitude and period, as the two main parameters modulated by changes in circadian modulation. In order to evaluate the role of epigenetic targets on circadian rhythms, we conducted a drug based screen comprising of 80 specific and well-validated epigenetic modulators on circadian phenotypic assay with the *Bmal1*::Luc U2OS cells.

Upon a screen of a library of 80 epigenetic modulators, several of these were shown to influence the luciferase expression driven by the Bmal1-promoter in U2OS cells. The drugs were administered at a 1μM concentration and repeated on three separate occasions followed by luminescence recording and analysis. A significance threshold of three standard deviations from the DMSO control was set (± 0.46 hours). The analysis demonstrated 50% of the molecules to be capable of altering the circadian period (**Figure 3.2.1**). These molecules on average increased the period within a range of 0.6 (JGB1741, a Sirtuin inhibitor) to 7.9 hours (CBHA, m-carboxycinnamic acid byshydroxamide, an HDAC inhibitor). None were shown to significantly reduce period.

Likewise, a significance threshold of three standard deviations from the DMSO control was set at 1.41 times increase in amplitude with respect to the DMSO control.

The analysis showed a hit rate of 65% in amplitude increase (**Figure 3.2.2**). The epigenetic modulators significantly increased the amplitude within a range of 1.46 (garcinol, a HAT inhibitor) to 2.5 times (SAHA, Suberonylanilide Hydroxamic Acid, an HDAC inhibitor), with respect to the DMSO control. The significance of this could perhaps be appreciated when comparing this with data from a previous screen within our lab with 5000 regulatory agency approved drugs: of these, only ~0.5% showed to statistically increase circadian amplitude (data not shown). This potentially highlights the importance of epigenetic modulators within circadian modulation.

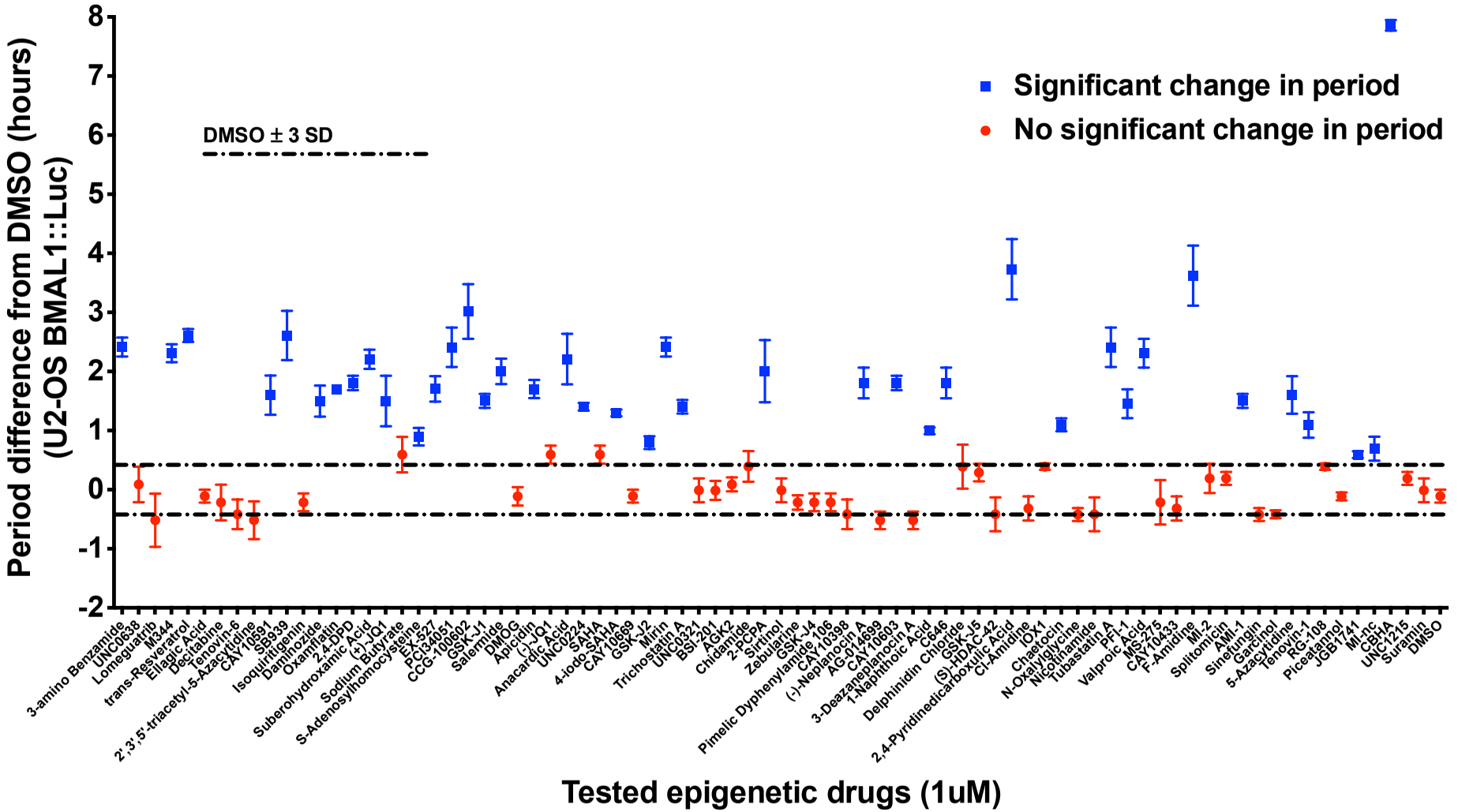


Figure 3.2.1 - Effects of epigenetic modulators on *Bmal1* promoter period. U2OS cells were stably-transfected with a *Bmal1*::Luc promoter and period was assessed over 92 hours of luminescence following the addition of 1µM of drug. Data was analyzed with the aid of the Multicycle software and was expressed as a difference over DMSO (mean ± SEM). Significance threshold was set at DMSO + 3 SD (demarked by an interrupted line at y=±0.46 hours).

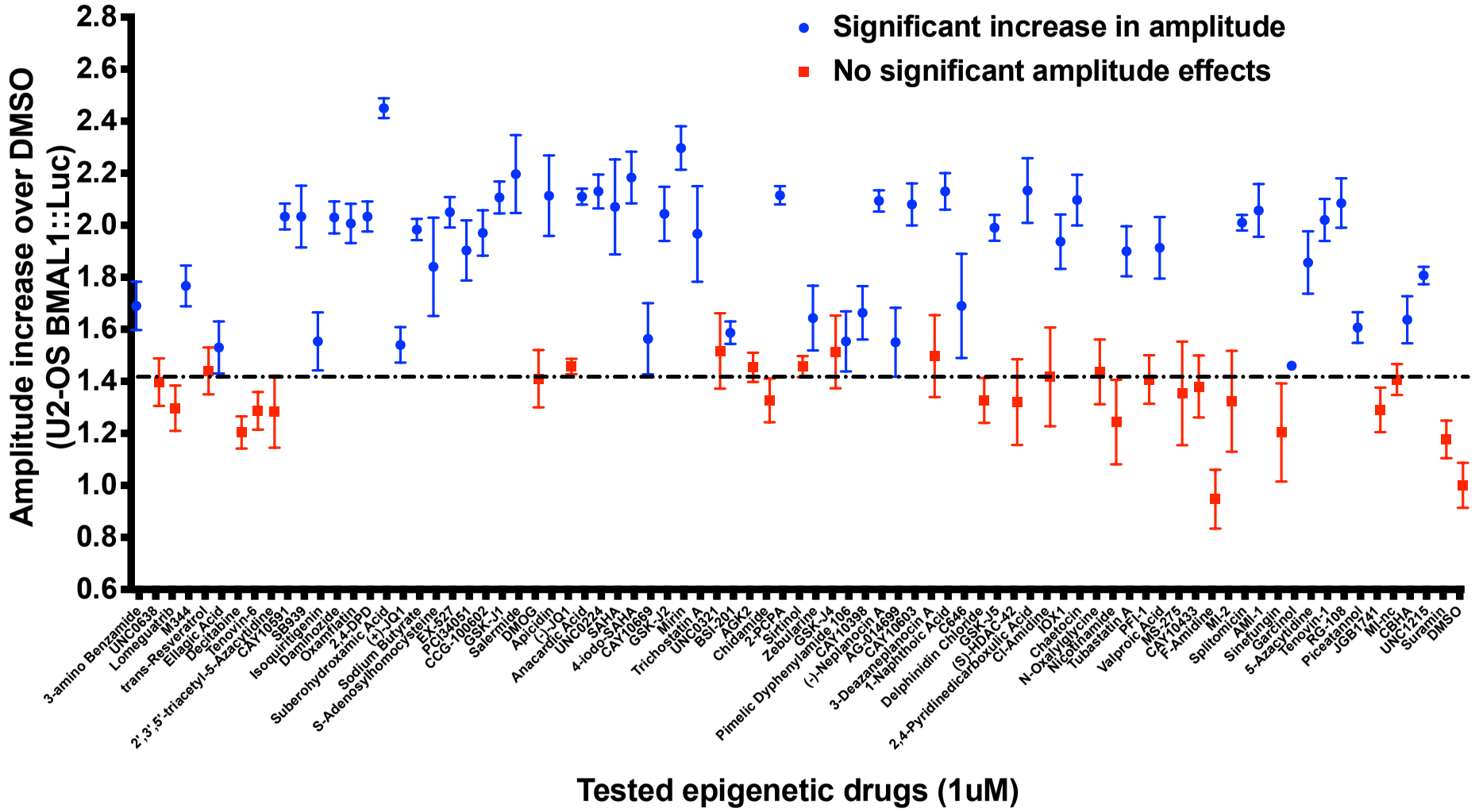


Figure 3.2.2 - Effects of epigenetic modulators on *Bmal1* promoter amplitude. U2OS cells were stably-transfected with a *Bmal1:*:Luc promoter and amplitude was assessed over 92 hours of luminescence following the addition of 1µM of drug. Data was analyzed with the aid of the Multicycle software and was expressed as a difference over DMSO (mean ± SEM). Significance threshold was set at DMSO + 3 SD (demarked by an interrupted line at y=+1.41).

3.2.2 Effects of acetylation modulators on U2OS Bmal1::Luc expression

Following the completion of the initial screen we conducted a 8-point dose-response study by selecting molecules covering a wide range of targets, demonstrating the greatest potency in the initial screen. As we can see in **Fig. 3.2.3**, notable examples portrayed are SB939 (**Fig. 3.2.2A**) and Neplanocin-A (**Fig. 3.2.3B**). SB939 increased period by up to 2.82 hours when compared to the DMSO and an EC_{50} of about 1μM (**Fig. 3.2.3C**), whereas Neplanocin-A increased the circadian period by up to 5.75 hours, with an EC_{50} of 29nM (**Fig. 3.2.3D**).

To exclude the possibility that the increase in period was specific to *Bmal1*::Luc U2OS cells, we also tested these compounds on U2OS *Per2*::Luc cells. As can be seen in **Fig. 3.2.4**, notable examples are the suberoylanilide hydroxamic acid (SAHA) **(Fig. 3.2.4A)**, CAY10603 **(Fig. 3.2.4C)** and SB939 **(Fig. 3.2.4E)**. Besides assessing the period increase, amplitude was also analyzed and its increase was shown as dose-dependent in all three scenarios. The EC_{50} was calculated at 1.32μM for SAHA **(Fig 3.2.4B)**, at 740nM for CAY10603 **(Fig. 3.2.4D)** and at 80nM for SB939 **(Fig. 3.2.4F)**, following a nonlinear regression curve fit analysis.

As all three confirmed epigenetic modulators share a HDAC inhibition as their mechanism of action, we decided to focus our attention on acetylation as a major mechanism in circadian rhythm amplitude increase.

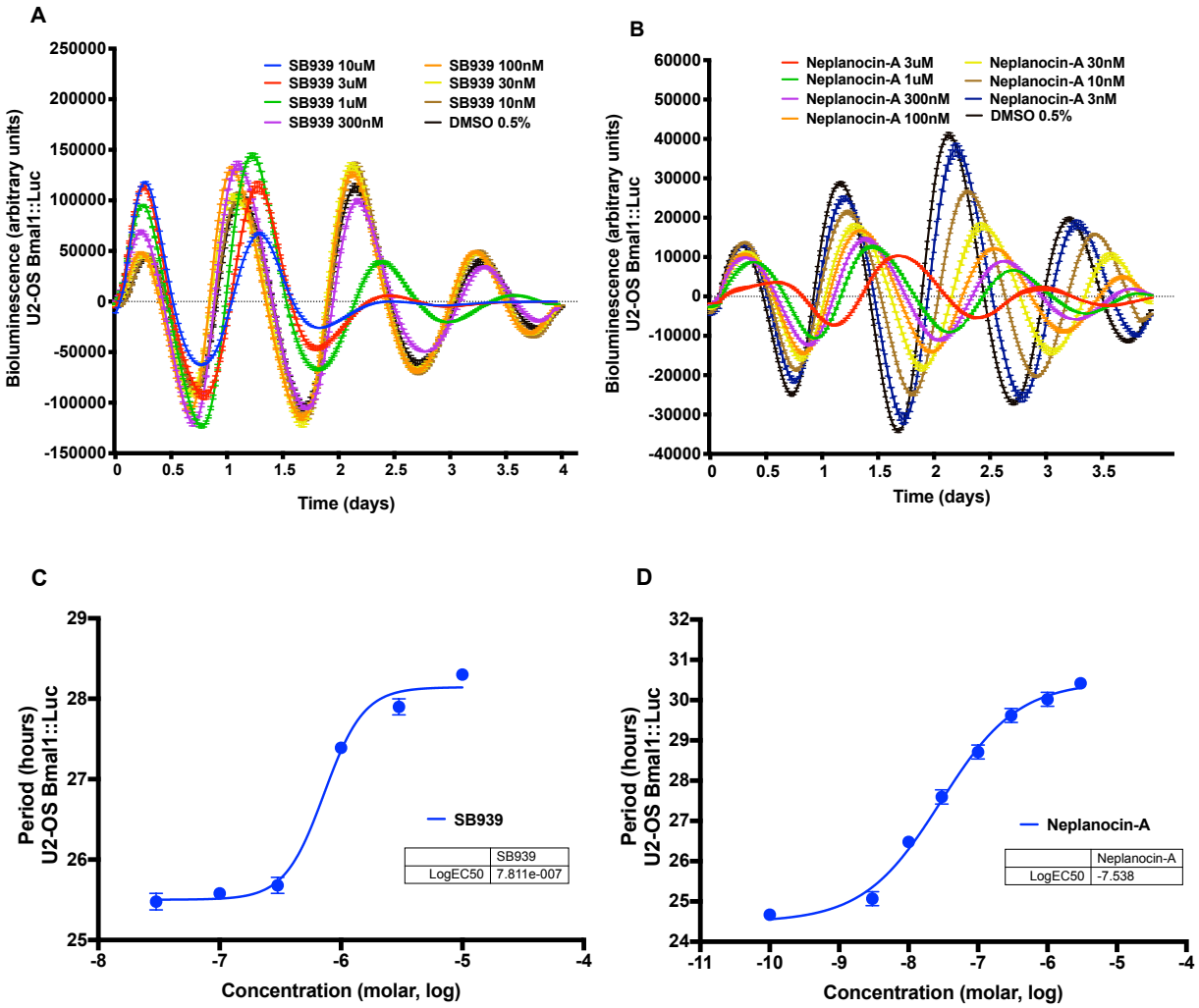


Figure 3.2.3 - Effects of epigenetic modulators on *Bmal1*::Luc promoter period. U2OS cells were stably-transfected with a *Bmal1*::Luc promoter and period and amplitude were assessed over 92 hours of luminescence following a pharmacological dose-response treatment with epigenetic modulators that were found as hits from the epigenetic screen. The traces of two HDAC inhibitors are portrayed, namely SB939 **(A)** and Neplanocin-A **(B)**. Data was analyzed with the aid of the Multicycle software and was expressed in absolute mean values ± SEM and directly compared to the DMSO control 0.5%. A dose-response curve was fit for SB939 **(C)** and Neplanocin-A **(D)**, and their EC_{50} in amplitude increase calculated.

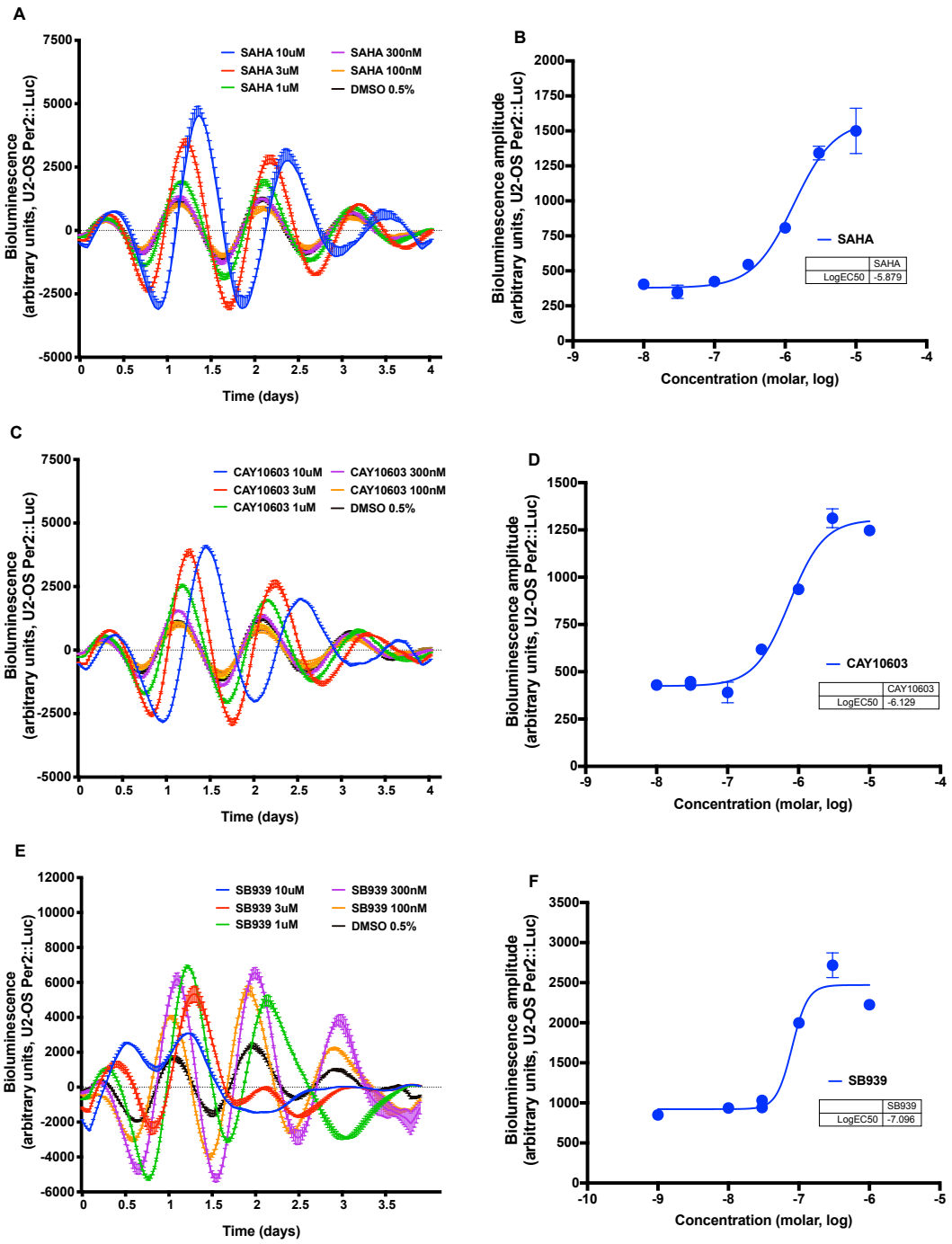


Figure 3.2.4 - Effects of epigenetic modulators on *Per2*::Luc promoter amplitude. U2OS cells were stably-transfected with a *Per2*::Luc promoter and period and amplitude were assessed over 92 hours of luminescence following a pharmacological dose-response treatment with epigenetic modulators that were found as hits from the epigenetic screen. The traces of two HDAC inhibitors are portrayed, namely suberoylanilide hydroxamic acid (SAHA) **(A),** CAY10603 **(C)** and SB939 **(E)**. Data was analyzed with the aid of the Multicycle software and was expressed in absolute mean values ± SEM and directly compared to the DMSO control 0.5%. A dose-response amplitude curve was fitted for SAHA **(B)**, CAY10603 **(D)** and SB939 **(F)**, and their EC_{50} in amplitude increase calculated.

3.2.3 Effects of HDACs on circadian period and amplitude

To assess the importance of acetylation mechanisms on the expression of circadian genes and confirm our aforementioned findings, we transfected a series of siRNAs aimed at downregulating the expression of *Hdac* genes and assess their effects on the circadian gene expression (**Figure 3.2.5**). **Figure 3.2.5A**, demonstrates the effects of HDACs on period, with 9 out of the 18 HDACs showing to significantly increase period (*Hdac2*, *Hdac3*, *Hdac6*, *Hdac7*, *Hdac10*, *Hdac11*, *Sirt3*, *Sirt5*, *Sirt7*) with a range of 0.41 hours (*Hdac2*, *Hdac3*) to 1.62 hours (*Hdac7*), as tested through a one-way ANOVA powered by a Dunnett post-hoc multiple comparisons analysis.

Of the 18 HDACs evaluated, 11 demonstrated a significant increase in amplitude, (*Hdac6, Hdac7, Hdac8, Hhdac9, Hdac10, Hdac11, Sirt1, Sirt2, Sirt3, Sirt4, Sirt6*). The amplitude increase ranged from a minimum of 12% (*Sirt5*) to a maximum of 56% (*Hdac11*), with respect to the non-targeting control (non-targeting siRNA transfection). The most significant targets comprising of *Hdac7* (**Figure 3.2.5C**), *Hdac11* (**Figure 3.2.5D**) and *Sirt3* (**Figure 3.2.5E**) are shown for visual representation and in all experiments Casein Kinase 1 knockdown was used as a positive control along with a non-targeting siRNA as negative control.

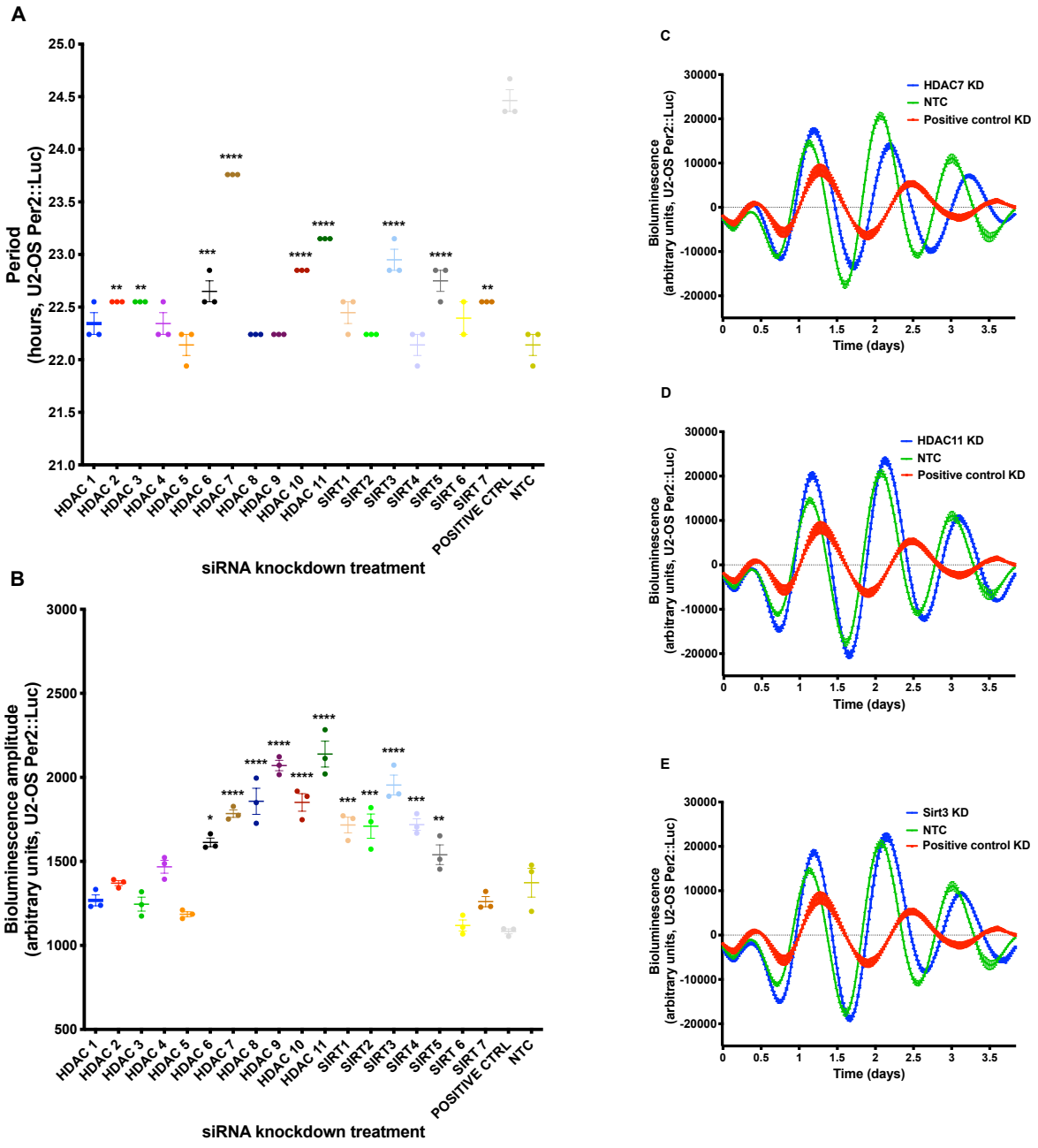


Figure 3.2.5 - Effects of HDACs on *Per2*::Luc promoter period and amplitude. U2OS cells were stably-transfected with a *Per2*::Luc promoter and period **(A)** and amplitude **(B)** were assessed over 92 hours of luminescence following a transient-transfection knock-down treatment with 20nM siRNA of a mix of targeting inhibitors. Data was analyzed with the aid of the Multicycle software and was expressed in absolute mean values ± SEM and directly compared to the non-targeting control treatment (NTC). Significance was calculated through a one-way ANOVA powered by a Dunnett post-hoc multiple comparisons analysis and, when found, was signalled appropriately. Representative traces of *Hdac* knockdown along with the non-targeting control and a CK1-kd positive control is shown (**C, D, E**).

3.2.4 Identification of bromodomain inhibition as circadian modulator

Given that drugs targeting acetylation were over represented in the drug screen and validated using siRNA, coupled with the fact that the bromodomain (acetylation reader) targeting drug JQ-1 was one of the most potent modulators in the screen capable of altering the circadian period and amplitude, we decided to focus on this class. Selection of this class was further aided by the fact that, bromodomain inhibitors are considered safer in comparison to the wider epigenetic modulators available at present, following studies in both rodents and humans. We show that the effects of JQ1 are dose-dependent **(Fig. 3.2.6A)**, and promote an increase in circadian amplitude. To establish that the effects of JQ-1 on circadian rhythms were through the inhibition of bromodomains, we evaluated the effects of (-)JQ-1 on amplitude increase. (+)JQ1 was shown to selectively bind to the BET family, whereas its stereoisomer (-)JQ-1, had no significant interaction with the bromodomains, thus constituting an incredibly powerful negative control. The results showed that only (+)JQ-1 was active as an amplitude enhancer (p<0.0001, F=16.16), whereas (-)JQ-1 had no effect (ns, p>0.2) (see **Fig. 3.2.6A/B**), suggesting the mechanism of amplitude increase to be BRD-mediated. It is worth noting that doses of 1μM, 700nM, and 300nM are toxic to cellular health. (+)JQ-1 at its highest not toxic dose demonstrated up to 50% increase in *Bmal1* amplitude. A dose-response study with (+)JQ-1 demonstrated the EC_{50} to be 30nM, in line with its reported value (see **Fig. 3.2.6C**). Further, a cell viability assay revealed (+)JQ-1 is toxic at higher doses (0.1μM-1μM) **Fig. 3.2.6D**, and that this effect is mediated through active BRD-binding, as its stereoisomer (-)JQ1 did not demonstrate any toxicity at those doses, confirming the amplitude dampening results of the highest three doses of (+)JQ-1.

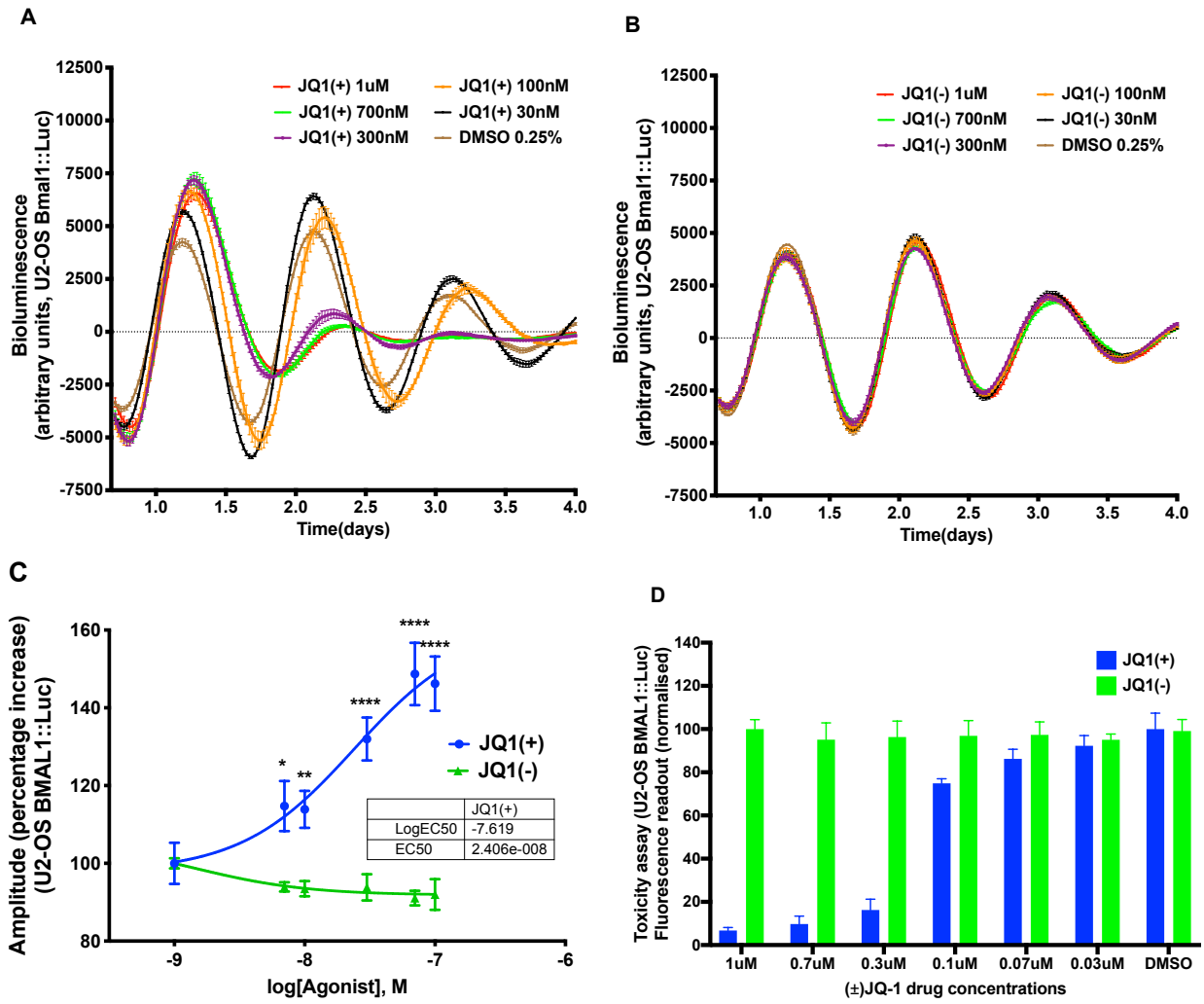


Figure 3.2.6 – Dose response study of (+)JQ1 and (-)JQ1 in U2OS cells stably-transfected with *Bmal1*::Luciferase. Doses of 1µM to 0.07µM of (+)JQ1 **(A)** and (-)JQ1 **(B)** were administered and the amplitude effects were compared against a 0.25% DMSO control. (+)JQ1 administration showed a maximal effect of 50% increase in *Bmal1* amplitude and expressed arbitrary units ± SEM (N=3-4). One-way ANOVA analysis showed statistical significance of the treatment with (+)JQ1 in U2OS BMAL1::Luc (p<0.0001, F=16.16) but not with (-)JQ1 (ns, p>0.2) **(A,B)**. A multiple-comparisons Bonferroni post-hoc test showed significance in amplitude increase at all concentrations of (+)JQ1, compared to the DMSO control. A dose-response curve results showed an EC_{50} of (+)JQ1 of around 30nM **(C)**. A survival analysis showed toxicity of (+)JQ1 at doses between 1 to 0.1µM, but not for (-)JQ1, indicating a BRD-mediated toxicity MOA **(D)**.

3.2.5 Effects of IBET-762 on circadian amplitude

As JQ-1 proved to be toxic at higher doses (see **Fig. 3.2.6AD**) and owning to its very short *in vivo* half-life, we tested an alternative bromodomain inhibitor alternative, IBET-762, that is currently under clinical evaluation for NUT-midline carcinoma. The effects of IBET-762 as an amplitude enhancer of the circadian clock genes were elucidated using a dose-response study (**Figure 3.2.7**). Doses from 0.03μM to 1μM of IBET-762 were used and the amplitude increase were compared against a 0.25% DMSO control. The EC_{50} of IBET-762 was ~45nM in both U2OS *Per2*::Luc and *Bmal1*::Luc cells in line with its reported potency as bromodomain inhibitor. IBET-762 administration showed a maximum effect of 87% and 30% increase in *Per2* and *Bmal1* amplitude respectively.

These data suggest that IBET-762 has a higher effect on the magnitude-increase of expression of *Per2* than *Bmal1* (3-fold higher), but this might be due to differences in gene insertion between the two stably-transfected cell-lines. However, the dosage at which the maximum effects take place is similar, quantified here through the EC_{50}, the concentration that promotes half of the maximal effect. Both genes were upregulated by 50% at about 45nM, suggesting the expression increase in both genes is due to a common effector. The one-way ANOVA analysis showed statistical significance of the treatment in both U2OS *Per2*::Luc ($p<0.0001$, $F=26.95$) and U2OS *Bmal1*::Luc ($p<0.05$, $F=5.09$).

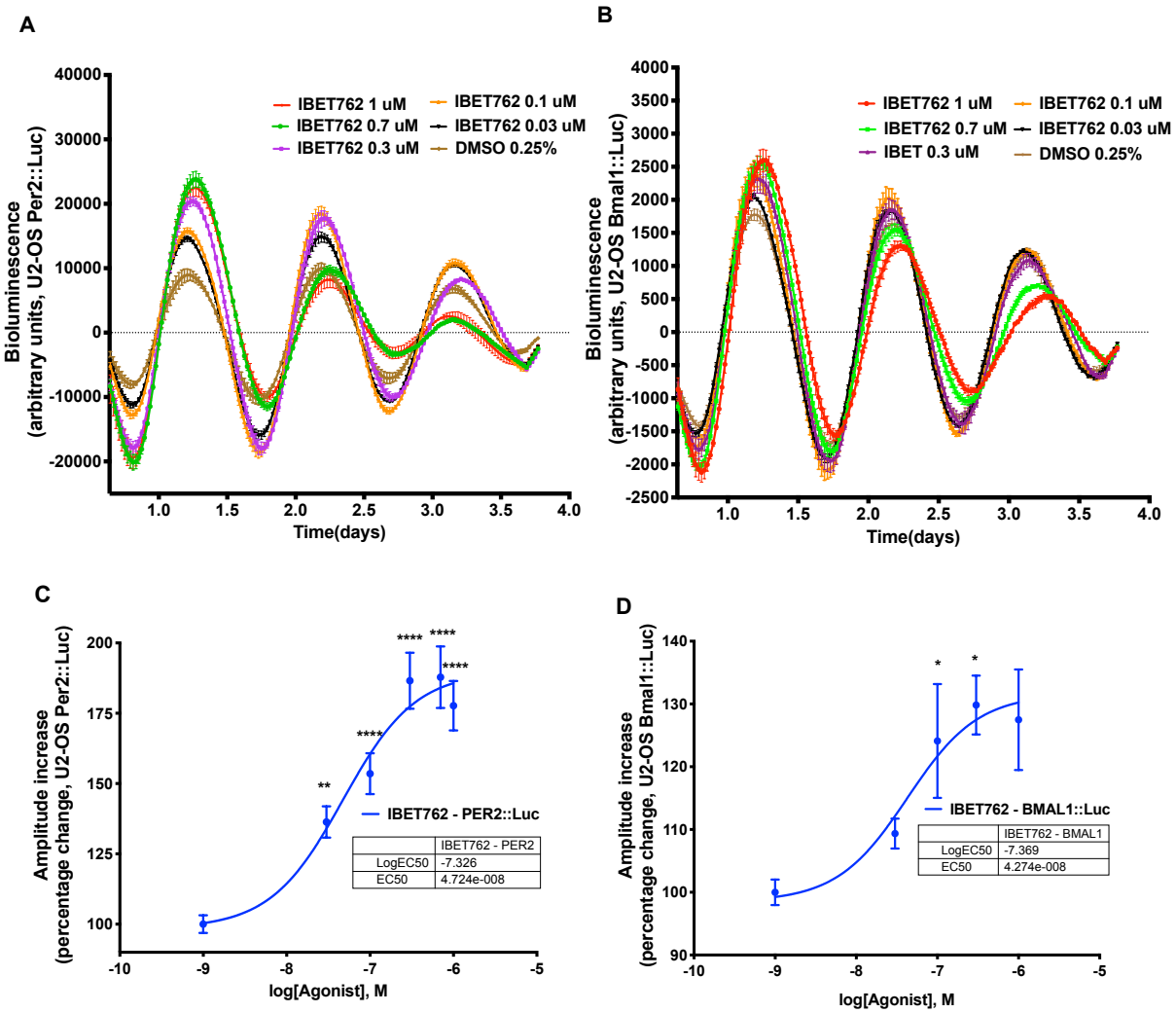


Figure 3.2.7 – Dose response curves of IBET-762-treatment in U2OS cells stably transfected with *Per2*::Luciferase and U2OS *Bmal1*::Luciferase. Varying doses of IBET-762 were administered and the amplitude effects were compared against a 0.25% DMSO control (**A, B**). IBET-762 administration showed a maximum effect of 87% increase in *Per2* amplitude and of 30% increase in *Bmal1* amplitude, expressed in arbitrary units ± SEM (N=3-4). One-way ANOVA analysis showed statistical significance of the treatment in U2OS *Per2*::Luc (p<0.0001, F=22.78) (**A**) and U2OS *Bmal1*::Luc (p<0.05, F=5.09) **(B)**. A multiple-comparisons Bonferroni post-hoc test showed significance in amplitude increase of IBET-762 at all concentrations in U2OS *Per2*::Luc and at 0.3-1μM in U2OS *Bmal1*::Luc, compared to the DMSO control. A dose-response curve results showed an EC_{50} of IBET-762 of around 47nM in U2OS *Per2*::Luc cells (**C**) and of 43nM in U2OS *Bmal1*::Luc cells (**D**).

3.2.6 Effects of IBET-762 on transiently-transfected clock genes

The previous experiment assessed whether IBET-762 promoted gene expression changes in both *Per2* and *Bmal1* stably transfected promoters. However, as IBET-762 is an epigenetic modulator, the epigenetic makeup of the flanking regions around the promoter can be of extreme importance regarding the expression of the inserted promoter itself. As the promoter insertion used in generating a stable cell line is inserted in an uncontrolled fashion, it was pivotal to exclude the possibility of the promoter being under the control of epigenetic markers that are not related to *Per2* and *Bmal1* respectively. Thus, a transient transfection experiment was devised, in which the promoters of *Bmal1* **(A)**, *Per2* **(B)**, *Bhlhe40* **(C)**, *Cry1* **(D)** and a *Cmv* control **(E)** attached to a luciferase gene, were transfected within an U2OS cell-line in the form of a plasmid, and the effects of 0.5μM of IBET-762 were assessed following the luminescence emitted by the associated luciferase (see **Fig. 3.2.8**). The levels of transfection were assessed by measuring baseline luminescence for the three hours prior to drug-addition and no differences between the two groups were noticed (see **Fig. 3.2.8F**). The administration of the drug confirmed a general upregulation of the main circadian genes. The results are overall in line and further expand on the outcomes gathered from the stably-transfected U2OS cell line experiments. As the circadian clock genes are upregulated, it is to be hypothesized that the effector of the increase in gene expression of the circadian clock might have a common mechanism. Further, the lack of increase in *Cmv*-Luc luminescence excludes the possibility of the IBET-762 being a luciferase activator.

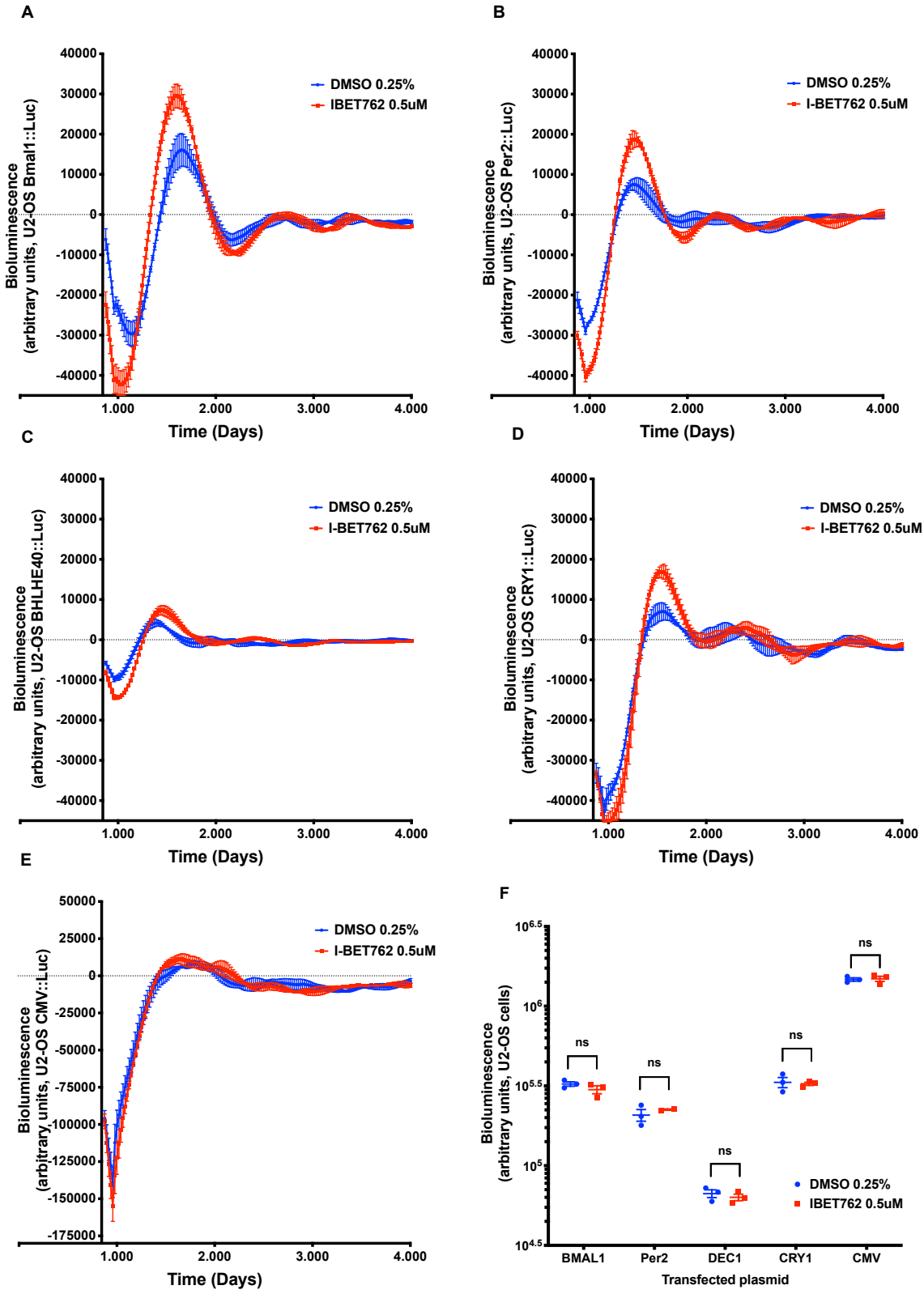


Figure 3.2.8 – Effects of IBET-762-treatment in U2OS cells transiently transfected with different clock genes plasmids. A dose of 0.5µM of IBET-762 was administered and the amplitude effects were compared against a 0.25% DMSO control (n=3) **(A-D)**. A CMV promoter control was used to investigate potential artefacts **(E)**.The transfection control is constituted by the backbone plasmid expressing luciferase under a CMV promoter. **(F)** Baseline values before drug addition are expressed on a $\log_{10}$ scale, to assess the baseline of circadian genes' transient transfection. No difference was noted in between DMSO and IBET-762-treated samples.

3.2.7 Circadian gene expression quantification following IBET-762

As the stably-transfected cell lines only report the promoter activity of the circadian genes, it was pivotal that we confirmed that the expression of the underlying clock gene changed in tandem using qPCR. Moreover as the promoter sequence was randomly inserted within the genome of the cells during the creation of the *Per2*::Luc and *Bmal1*::Luc cell lines, it is plausible that the promoter could have been inserted in areas of the genome that might have greater accessibility and as a result a different epigenetic background.

As can be seen in **Figure 3.2.9**, the gene expression of *Bmal1* (**Fig. 3.2.9A**) both at baseline expression levels (+39%) and overall amplitude (+75%) was increased following 1 μM IBET-762 administration, (compared to the controls). The statistical comparison following the extra sum-of-squares F test procedure showed that the two datasets corresponding to treated and control samples respectively, differ in between, confirming that they constitute separate curves ($F_{(5, 77)}$=17.09, p<0.0001). *Per1* gene expression was also increased, following IBET-762 administration (**Fig. 3.2.9B**). However, in this case, only the baseline expression was increased (+49%), whereas the amplitude was decreased (-19%), in comparison to the controls. As before, the statistical comparison showed that the two datasets differ in between, ($F_{(5, 80)}$=10.59, p<0.0001). Conversely, for the *Per2* gene expression, the results were different, as there was no statistical difference between the two datasets ($F_{(5, 72)}$=0.7773, p=0.5693) (**Fig. 3.2.9C**). *Nr1d1* gene expression decreased in amplitude after IBET-762 administration (by 10%) and the statistical comparison showed that the two datasets differ in between ($F_{(5, 77)}$=4.22,

p<0.0019) (**Fig. 3.2.9D**). *Cry1* and *Cry2* gene expression also showed an increase in expression following IBET-762 administration (**Fig. 3.2.10A/B**). From the sine wave analysis, the baseline was increased (+50% and +40% respectively) whereas the amplitude was decreased in both cases. The statistical comparison showed that the two datasets differ in between ($F_{(5,\ 71)}$=26.07, p<0.0001 and $F_{(5,\ 76)}$=11.12, p<0.0001 respectively).

We then analysed the auxiliary genes of the circadian clock, which are pivotal in controlling cellular circadian function, such as *Bhlhe40* and *Bhlhe41*. The results show an amplitude and baseline increase effect of 49% and 65% respectively, on *Bhlhe40* (DEC1), following the administration of IBET-762. On the other hand, the drug administration procured a reduction in both amplitude and baseline of *Bhlhe41* (DEC2) gene expression of 20% and 68% respectively. The statistical comparison showed that the two datasets differ in between (*Bhlhe40*: $F_{(5,\ 77)}$=77.37, p<0.0001 and *Bhlhe41*: $F_{(5,\ 80)}$=32.00, p<0.0001).

These results largely confirm and support the data gathered from the stably-transfected U2OS *Bmal1*::Luc and *Per2*::Luc cell-lines and the transient-transfected experiments, as there is a general increase in several of the circadian genes, namely *Bmal1*, *Cry1/2*, *Per1/2*, although there were some discrepancies regarding the upregulation of *Per1/2*.

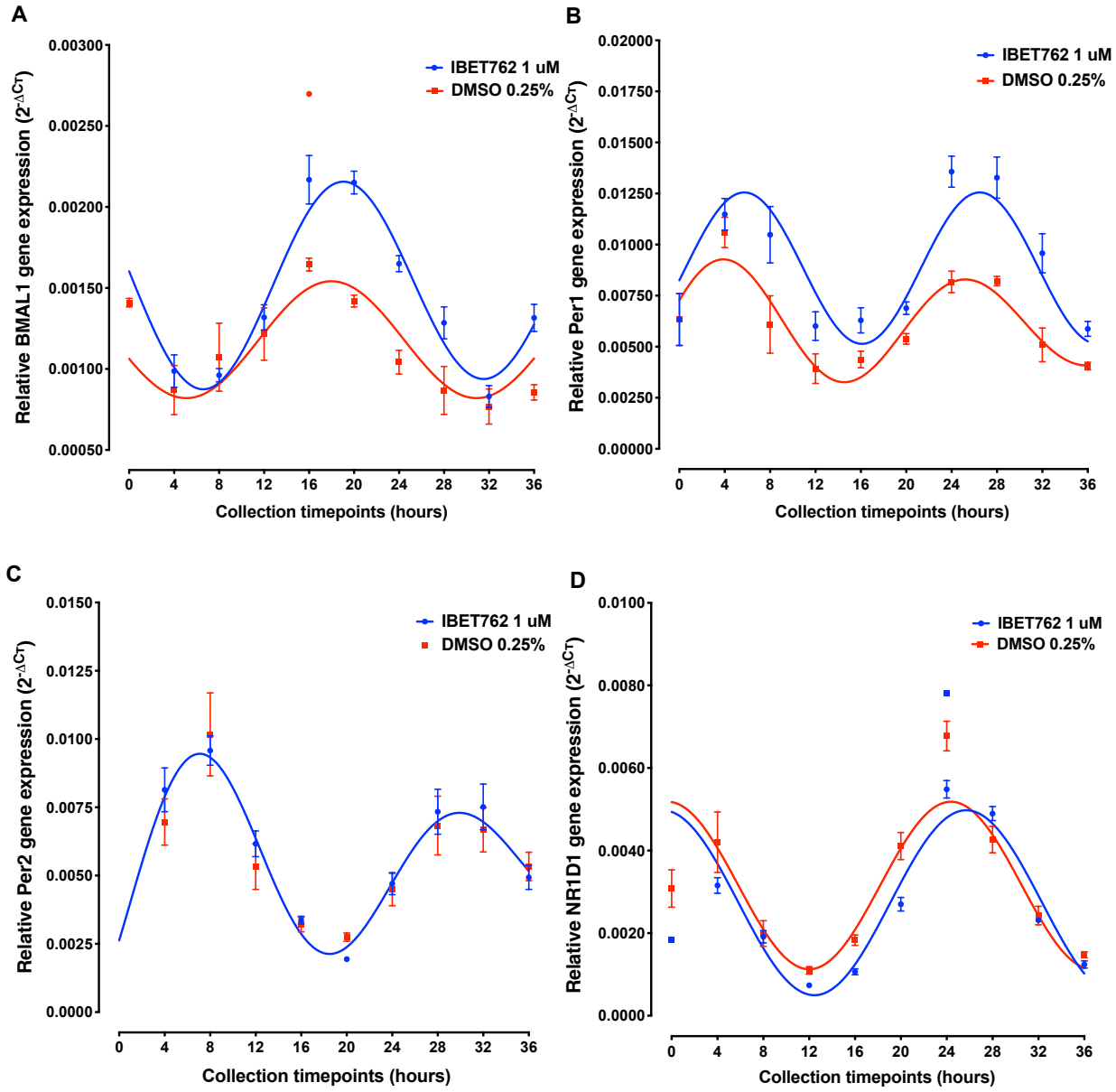


Figure 3.2.9 – Effects of 1μM IBET-762 on the circadian gene expression of *Bmal1* (**A**)*, Per1* (**B**)*, Per2* (**C**)*, Nr1d1* (**D**) in U2OS cells (qPCR); data was expressed as average ± SEM (n=5). The data was analysed using a non-linear regression modified dampen sine wave and the possible divergence between the two curves was statistically tested using the extra sum-of-squares comparison. The null-hypothesis (one curve fits all dataset) verified in all instances and parameters such as Baseline and amplitude were reported.

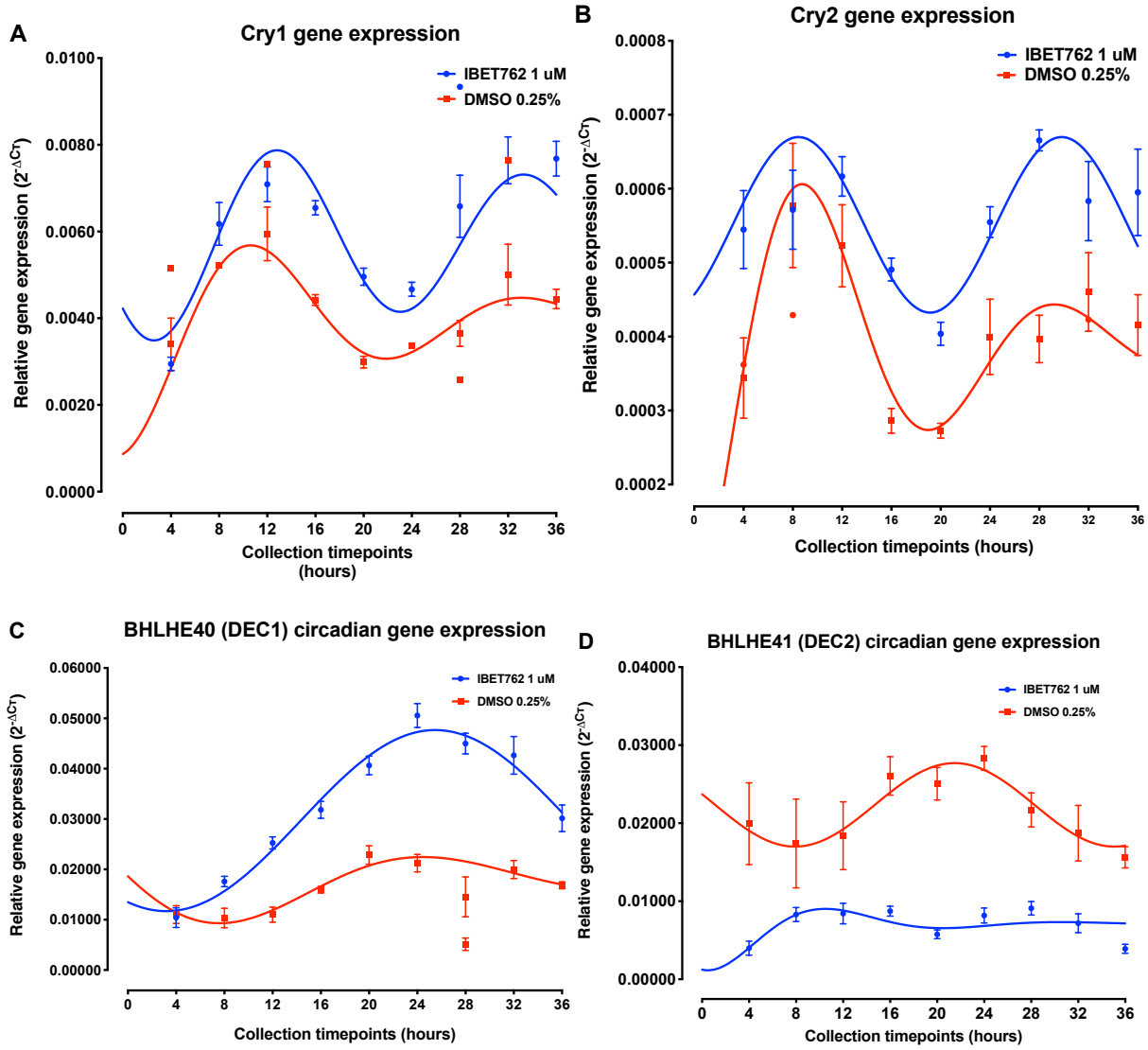


Figure 3.2.10 – Effects of IBET-762 on the circadian gene expression of *Cry1* (**A**)*, Cry2* (**B**)*, Bhlhe40* (**C**) and *Bhlhe41* (**D**) in U2OS cells (qPCR); data was expressed as average ± SEM (n=5). The data was analysed using a non-linear regression modified dampen sine wave and the possible divergence between the two curves was statistically tested using the extra sum-of-squares comparison. The null-hypothesis (one curve fits all dataset) verified in all instances and parameters such as Baseline and amplitude were reported.

3.3 DISCUSSION

As depicted in **Figure 3.2.1-3.2.2**, epigenetic modulators were shown to impact gene expression of *Bmal1*, a key gene of the positive loop of the circadian clock. The high proportion of period increasing and amplitude increasing drugs (50% and 65% respectively), out of the 80 epigenetic modulators tested, underlines the importance of epigenetic modulation and its effects on the circadian clock gene expression. It is important to note that, less than 1% of drugs tested within our lab (of a total of 3000 FDA-approved drug of different libraries) demonstrated an impact on circadian rhythms (data not shown). Similarly, recent data showed that only 5% of over 1000 Food and Drug Administration (FDA) -tested compounds were able to inflict changes on the circadian period, in stably-transfected U2OS *Bmal1* cells (Tamai *et al.*, 2018). However, the effects could not be clearly ascribed to a specific epigenetic mechanism. This might be due to the fact that epigenetic modulators have multiple targets, especially at a concentration of 1μM, as used during the drug screening process. Moreover, many of the acute changes brought forward by these drugs can also influence chronic and secondary responses based on different epigenetic mechanisms. The widespread effect of epigenetic modulators on the circadian clock can be traced to the extensive evidence showing the role of epigenetic alterations on rhythmic biology. It has indeed been shown that the SCN adaptation to the time of the day is dependant on DNA methylation patterns that inflicts on the expression of circadian clock genes and pivotal downstream pathways. These changes were reversible after re-entrainment, and Zebularine, a methyltransferase inhibitor, was able to suppress period changes (Azzi *et al.*, 2014). Furthermore, histone acetylation modifications were also shown to be pivotal in the cyclical transcription of genes of the circadian clock (Etchegaray *et al.*, 2003) with

CLOCK showing histone acetyltransferase activity itself (Doi *et al.*, 2006) and circadian histone acetylation described in the mouse liver (Le Martelot *et al.*, 2012). Similarly, Trichostatin A, an HDAC inhibitor, was shown to influence the circadian expression of genes of the molecular clock, across several murine tissues (Naruse *et al.*, 2004).

Nothwistanding the widespread effects of the epigenetic modulators of several classes, we decided to focus our attention on acetylation, given its importance in epigenetics as a regulator at the forefront between genome and environmental factors and its more reversible and flexible mechanism of action upon pharmacologic intervention. We have confirmed through a dose-finding study, that the effects of several histone deacetylase inhibitors (HDACs) are dose-dependent and that the EC_{50} is in the nanomolar range (**Figure 3.2.3**), suggesting the likely effects are due to the specific targets under investigation as opposed to off-target effects. These confirmatory results have also been replicated on an alternative cell/promoter U2OS *Per2*::Luc stably-transfected cell line (**Figure 3.2.4**). *Per2* is a gene of the negative feedback-loop of the circadian clock, whose expression is driven by BMAL1:CLOCK protein levels. Its increase confirms that the effects of the drugs bring about an increase in the protein levels of BMAL1 as well, as it has a measureable downstream effect.

To further confirm the aforementioned results, we have knocked-down all known genes expressing histone deacetylases, sequencially (**Figure 3.2.5**). Both period and amplitude changes were portrayed and shown to be common to several of the HDAC inhibitors. Although some of the HDAC products have been previously reported as important in circadian rhythm regulation, such as HDAC3, HDAC4, and HDAC5 (Feng *et al.*, 2011;

Fogg *et al.*, 2014), as well as SIRT1, SIRT3, and SIRT6 (Masri, 2015), several that are shown here to promote circadian effects are novel and show an impact on both circadian period and amplitude. Among these novel genes associated with circadian rhythm disruptions, we can specifically pinpoint *Hdac6*, *Hdac7*, *Hdac10*, *Hdac11,* and *Sirt7*, whose knockdown showed a period increasing effect, and *Hdac7*, *Hdac8*, *Hdac9*, *Hdac10*, *Hdac11,* and *Sirt2*, *Sirt4*, *Sirt5*, whose knockdown promoted an amplitude increase effect. Therefore, some of these genes, when knocked-down, promoted both a period and amplitude increase: *Hdac7*, *Hdac10*, *Hdac11*.

The HDAC knockdown was performed through the use of silencing RNA (siRNA). Cellular gene knockdown can be carried out either through genetic modification or through inhibition of translation of a gene through complementary sequences to the messenger RNA (mRNA) transcript of the specific gene. The modification of genetic material that determines a lower expression of a gene is a permanent knock-down, whereas a transient knockdown takes place when the change in expression is defined by an oligonucleotide that binds to the gene's mRNA and inhibits its translation, but does not modify the genetic sequence of the gene. As genetic knockout requires a long process of modification and optimization, it was considered impractical considering the early exploratory nature of this investigation. Therefore, for one-off experiments, we have employed the more practical method of knockdown of a gene of interest with the use of oligonucleotides. Although gene knockdown is not a complete inhibition of the gene, it often downregulates it enough to impact on its studied physiology without bringing about toxic or compensatory effects correlated to a complete eradication of its expression. Interference RNA can be either generated from hairpin forming precursors

(shRNA) or introduced exogenously as silencing RNA (siRNA). siRNA is a dsRNA structure homologous to the mRNA produced by our gene of interest. In cells, the siRNA is processed by the endoribonuclease Dicer and then by the RNA-induced silencing complex (RISC), that locates the targeted mRNA, which is then cleaved by a ribonuclease (Bernstein *et al.*, 2001). Moreover, the specificity and efficiency of siRNA knockdown has also improved, given the use of *in-silico* rational design in using pools of siRNAs that are more accurate in targeting the mRNA of interest, with a high likelihood of silencing (Mittal, 2004).

Further, we focused our attention on the effects of *Hdac* knockdown on amplitude, given amplitude decrease was strongly correlated to environmental factors such as induced phase shifts (Dijk *et al.*, 2012) and old age (Nakamura *et al.*, 2011). It was indeed shown that a stoichiometric increase in components of the molecular clock can be critical for the robustness of the circadian clock (Lee *et al.*, 2011) and a robust circadian clock was correlated with an improvement on pathophysiological statuses. For example, time-restricted feeding can lead to the enhancement of the expression and amplitude of core clock genes and the improvement of lipid homeostatis and extension of life span (Manoogian & Panda, 2017). Further, bight light was shown to improve levels of melatonin, together with cognitive and noncognitive functions in elderly (Riemersma-van der Lek *et al.*, 2008), underlining thus the benefits of a stronger molecular clock on pathophysiology and behaviour.

More specifically, we focused on bromodomain inhibitors, as they are a novel class of epigenetic readers of acetylation changes within our genome. Although it has been

shown that BRD4 can interact with P300 and promote histone acetylation (Wu *et al.*, 2018), the general bromodomain read-out functionality allows for a reduced interference with the acetylation mechanisms, when compared to HDAC inhibitors. Therefore, bromodomain inhibitors were shown to be safer and were employed extensively in clinical trials (Alqahtani *et al.*, 2019). We firstly confirmed that the effects of JQ-1 were dose-dependent and had an EC_{50} of about 25nM (**Figure 3.2.6A/C)**, then we confirmed that the circadian effects we saw in stably-transfected USO2 *Bmal1*::Luc cells were bromodomain-dependent (**Figure 3.2.6B/C)**, as we used a drug that lacks a group which is essential for binding to the KAc group on bromodomains, as a negative control (Filippakopoulos *et al.*, 2010). Calculating the LC_{50} on the same cell line, we found that it was about 10 times higher than the EC_{50}, thus not allowing for a toxic effect at the amplitude and period increasing concentrations.

We have further tested a different bromodomain inhibitor, which was shown to be less toxic and safer in animals and humans and have a longer half-life: IBET-762. The drug was tested and shown to be efficacious in increasing amplitude in both stably-transfected USO2 *Per2*::Luc and *Bmal1*::Luc cells (**Figure 3.2.7A/B**). We can see both the 1μM and 0.7μM concentrations promoted the highest amplitude effect in both U2OS *Per2*::Luc and *Bmal1*::Luc cells in the first day of analysis, however the amplitude decreases in subsequent days, as the gene expression levels start to decline. A plausible explanation would be that these two higher doses can have a toxic effect over a longer period. Moreover, IBET-762 had a 3-fold stronger amplitude impact on *Per2*::Luc than on *Bmal1*::Luc cells. This might be due to the fact that the different cell lines have a different number of promoter::Luc copies inserted within their genome, at different locations that

can be differently expressed and regulated under different enhancers and silencers. This hypothesis is supported by the very similar amplitude-increasing EC_{50} in both cell lines (**Figure 3.2.7C/D**), indicating that the amplitude enhancing effector is of common origin. Another explanation could be that the PER-CRY negative feedback complex could be less abundant than the BMAL:CLOCK positive regulator complex in the U2OS cells, thus changes in its expression would influence the former one more heavily, thus allowing for a bigger increase in activity. This was shown that it was the case in mouse embryonic fibroblasts, with CRY2, PER1 and PER2 proteins only half as abundant as CLOCK, BMAL1 and CRY1 (Lee *et al.*, 2011).

However, as stably-transfected cells have the promoter-copies inserted randomly within the genome, we wanted to test whether their putative location could have an artifactual effect on the expression of the genes. We have therefore tested IBET-762 on transiently-transfected U2OS cells. IBET-762 was shown to increase circadian amplitude on *Bmal1*, *Per2* and *Cry1* promoters, with a similar fold increase (**Figure 3.2.8A/B/D**), and with a lower fold increase, on *Bhlhe40* (Dec1) (**Figure 3.2.8C**). These results confirm our findings in stably-transfected U2OS cells and give us confidence that the increase is not due to aberrant activation of transcription due to the position of the promoter inserts within the genome.

To further confirm the results we gathered so far on IBET-762-mediated amplitude enhancing effect on genes of the circadian clock, we have also tested if the gene expression was increased in blank U2OS cells. To do so, we have treated U2OS cells with 1μM of IBET-762 over 36 hours and have assessed the effects of the drug through

RT-PCR. This was to avoid possible artefacts due to luminescence reading and interaction of the luciferase with the DMSO and administered drug. Moreover, this allowed us to evaluate the effect of the drug on the physiological number of gene copies present within the genome.

The RT-PCR results confirmed the enhancing effects of IBET-762 on *Bmal1* and *Per1* in both baseline and amplitude, however they did not confirm an increase in *Per2* (**Figure 3.2.9A/B/C**). *Nr1d1* (REV-ERBa) has also shown a period-shift effect (**Figure 3.2.9D**). Furthermore, *Cry1* and *Cry2* were also shown to be increased, as well as *Bhlhe40* (DEC1), a gene of the auxiliary circadian clock (**Figure 3.2.10A/B/C**). As *Per1* is an immediate early gene, it is possible *Per2* gene might take longer than the examined time-frame, to increase in expression. *Bhlhe41* (DEC2), a gene that acts as a negative-feedback loop to *Bmal1* transcription, was found to be reduced, confirming the general hypothesis of an amplitude increase of the genes of the circadian clock (**Figure 3.2.10D**).

Bromodomain inhibitors, such as IBET-762 and JQ-1, were synthesized from a scaffold of a diazepine attached to a isostere of benzene, which is similar to the benzodiazepine (BDZ) structure. The benzodiazepine scaffold is considered as a 'priviledged structure', given its activity towards numerous cellular targets, such as the Gamma aminobutyric acid (GABA) receptor. Many BDZ-based molecules were developed as therapeutics such as anti-convulsants, sedatives, and anxyolytic purposes (Richter *et al.*, 2012). Beyond GABA receptor modulation, BDZ-based drugs were also shown to bind to farnesyltransferases, mitogen activated protein kinase-activated protein kinase 2, hepatitis C polymerase, and histone deacetylases, among others (Anderson *et al.*, 2009;

Loudni *et al.*, 2007; McGowan *et al.*, 2009; Reid & Beese, 2004). Similarly, the benzodiazepine and thienodiazepine-related IBET-762 and JQ-1 bromodomain inhibitors, respectively, bind to and inhibit the bromodomains of the BET family (Filippakopoulos *et al.*, 2010; Mirguet *et al.*, 2013), and additional groups added to the core BDZ-like structure help to prevent off-target interactions and increase affinity for BET moieties (**Figure 3.3.1**). Studies also showed an effect of Alprazolam, a benzodiazepine, in inhibiting BRD4 at higher 2.5μM concentrations, underlining the importance of the 1,2,4-triazole moiety in eliciting the BET-I effects, possibly as an acetyl-lysine mimetic (Filippakopoulos *et al.*, 2012a). Further, our data showing the circadian amplitude enhancing effects of bromodomain inhibitors is confirmed by previous findings which marked the effects of several benzodiazepine-based molecules in modulating molecular circadian rhythm activity across different tissues (Chen *et al.*, 2012b). These findings suggest the BDZ-related structure could be essential in mediating the circadian amplitude enhancing effects of IBET-762 and JQ-1.

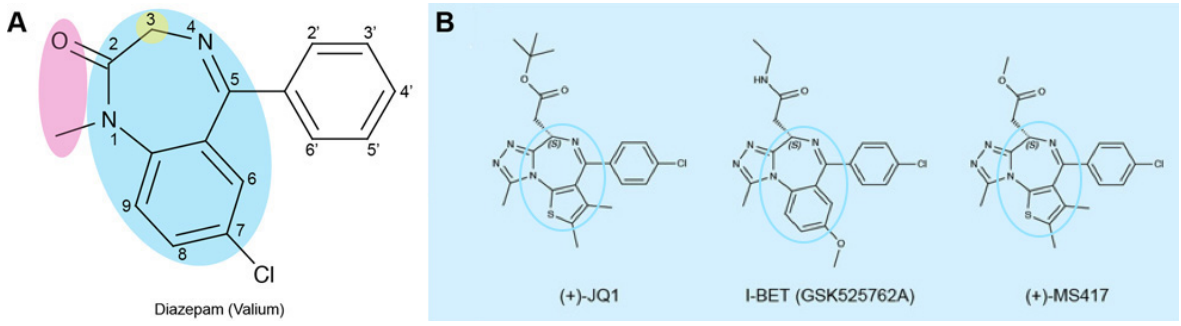


Figure 3.3.1 – Chemical structure and similarity sites of benzodiazepine-based molecules. (**A**) Molecular structure of Diazepam, a benzodiazepine that is known to activate GABA receptors and produce calming effects and has been used to treat anxiety, muscle spasms and seizure fits, contains a benzene and diazepine group used as scaffolds in the discovery of other molecules with different activities. Among these, of interest are bromodomain inhibitors such as IBET-762, JQ-1 and MS417 (**B**), which were shown to inhibit BET proteins and were confirmed by us as circadian rhythm amplitude enhancers. Figure adapted from Smith *et al.*, 2014.

Taken together, we have shown how epigenetic mechanisms are influencial in modulating the expression of key genes of the circadian clock. More specifically, we have individuated histone acetylation as an important target in epigenetic modulation and have further narrowed our focus on a specific class of acetylation readers, bromodomain inhibitors, as a novel class of epigenetic modulators. JQ-1 was shown to dose-dependently enhance circadian amplitude, and its effects were mediated by bromodomains. We further tested IBET-762, a safer alternative to JQ-1, which produced similar effects on circadian amplitude enhancement. IBET-762 was indeed shown to modulate the amplitude of gene expression of *Bmal1*, *Per1/2*, *DEC1/2,* and *Cry1/2*, suggesting a widespread circadian effect.

CHAPTER II

SP1-MEDIATED MOA OF BROMODOMAIN INHIBITION IN CIRCADIAN RHYTHMS

main findings:

BRD4 knockdown increases circadian amplitude of PER2::Luc

IBET-762 modulates binding to enriched E-Box motifs in bHLH and circadian genes

BRD4 domain likely to mediate modulation of the positive arm of the circadian clock

SP1 is the transcription factor responsible for IBET-762's increase in circadian amplitude

SP1-binding sites are found in the promoters of circadian clock genes, such as BMAL1

4 Chapter II: SP1-MEDIATED MOA OF BD-1 IN CIRCADIAN RHYTHMS

4.1 INTRODUCTION

4.1.1 Transcription factor interaction on promoter and enhancer regions

Transcription factors account for over 3200 proteins in the human genome (Babu *et al.*, 2004) and their activity controls the rate of transcription of genetic information into RNA and protein translation and impact on cellular physiology. Transcription factors work alone or in complexes, and bind to regions of the DNA and RNA Polymerase II (RNA Pol II) in modulating the expression of specific genes (Roeder, 1996). However, their regulation can be compromised, with the possible advancement of serious pathologies, thus it is pivotal to further understand their activation and pathological implications.

As bromodomain proteins bind to acetylated lysines on histone tails, they recruit a series of transcription factors which are pivotal in the regulation of transcription, thus their physiological role is carried out in collaboration with transcription co-factors. The nature of this interaction can be either activation or repression depending on their partners (co-activators and co-repressors), which in turn is dictated by the binding regions. Bromodomains can bind to acetylated histones present on promoters, as well as on enhancers, distal regulatory elements of transcriptional activity and efficiency, to exert

their functionality in regulating the likelihood of gene expression (Di Micco *et al.*, 2014; Loven *et al.*, 2013).

Enhancers are short (20-400bp) segments of DNA subject to binding by transcription factors that modulate the transcription of a specific gene (Bondarenko *et al.*, 2003), and are recognized as critical components in transcriptional regulation. Enhancers occur up to 1Mbp downstream or upstream from the transcriptional start site (TSS), and regulate the transcription of a gene by interacting with the TSS through DNA-looping, facilitated by mediators and co-factors. Thus, although enhancer regions are far from the TSS at a sequence level, DNA-coiling allows for close spatial interactions between different genetic loci (Kulaeva *et al.*, 2012; Vologodskii & Cozzarelli, 1996). Flanking of enhancers are marked by histone modifications H3K27ac1 and H3K4me1 whenever active, whereas inactive enhancers are market by H3K4me1 alone (Calo & Wysocka, 2013).

4.1.2 Bromodomains and transcription factor interaction

The human proteome contains over 46 bromodomain-containing proteins, conserved across mammals. These are classified in 8 families on structural topologies and sequence similarities (Filippakopoulos *et al.*, 2012b). Bromodomain proteins are expressed across several tissues with variable and location-dependent expression profiles, thus their modulation is thought to have a considerable impact on specific cellular pathophysiology (Kim *et al.*, 2014b). Among these, we can find the bromodomain and extra-terminal domain proteins (BET) family II, which contains the four bromodomains BRD2, BRD3, BRD4 and BRDT. BET proteins contain two N-terminal bromodomain modules (BD1

and BD2), which are connected by a flexible linker. BET inhibitors were shown to discriminate between the active sites BD1 and BD2 domains, but not among the four conserved family members (Filippakopoulos & Knapp, 2014).

As previously discussed, bromodomains can also act as a scaffold and aid the binding of other transcription factors, both repressive and activatory in nature. The final result on gene transcription depends thus on the changes in the chromatin structure and the overall stimulatory effect of gene transcription, given the binding of several transcription factors with possibly counteracting activities. As an example, it is known that Brd2 co-represses PPARɣ target genes in adipocytes, but it also co-activates the expression of cyclin A in proliferating cancerous cells, through HAT recruitment (Greenwald *et al.*, 2004; Wang *et al.*, 2009a).

The vast majority of BET interactions are with acetylated histones, however several examples of BET interacting with acetylated non-histones have been described. Among these, it was shown that bound BRD4 recruits P-TEFb, promoting transcriptional elongation (Jonkers & Lis, 2015). BRD4 was also shown to interact with the Mediator complex, a coactivator that links transcription factors to RNA Polymerase II activation (Jiang *et al.*, 1998; Wu & Chiang, 2007) (**Figure 4.1.1**). Moreover, BRD4 can be recruited to the E-Box regions through BMAL1 acetylation by TIP60 (Petkau *et al.*, 2019). TIP60 is a histone acetylase that was shown to activate transcription factor expression, such as E2F (Van Den Broeck *et al.*, 2012) and c-Myc (Patel *et al.*, 2004) and its modulation can be relevant in several pathologies such as various types of cancers (Chen *et al.*, 2012a; Sakuraba *et al.*, 2011) and viral infections (Hong *et al.*, 2015; Kamine *et al.*, 1996).

Furthermore, BRD4 could regulate transcription by associating with the demethylase Jmjd6 (Liu *et al.*, 2013) and the methyltransferase Nsd3 (Rahman *et al.*, 2011).

In this chapter, we focussed our attention on the role of two transcription factors, Specificity-Protein 1 (SP1) and the Hypoxia-Inducible Factor 1 (HIF1). We focused on SP1 and HIF1 as pivotal transcription factors in BRD4's effects as we highlighted it as potentially central in relaying the circadian amplitude-enhancing effects of IBET-762.

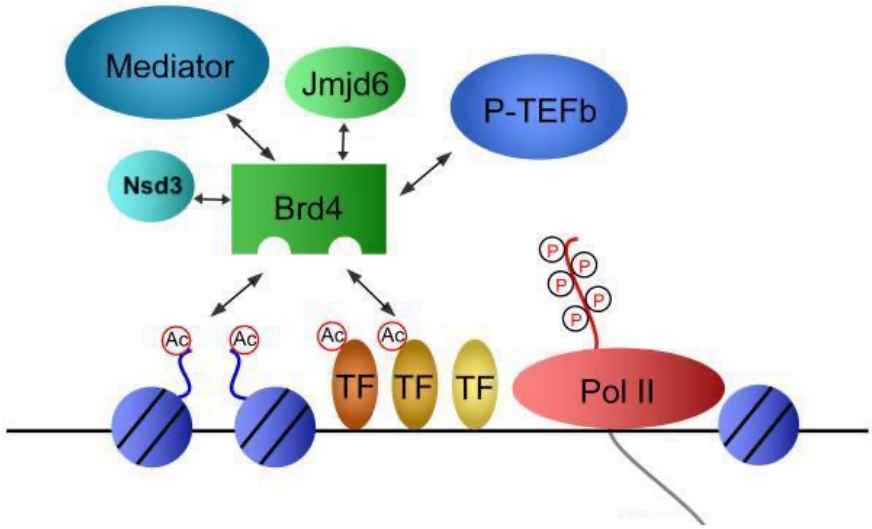


Figure 4.1.1 – Interaction between BRD4 and known transcription factors and complexes. Graphic representation of the interaction between BRD4 and various complexes such as Mediator and P-TEFb and methylation regulators such as Jmjd6 and Nsd3. Adapted from (Shi & Vakoc, 2014).

4.1.3 SP1 transcription factor and its interactions with bromodomains

Specificity-Protein 1 (SP1) is a zinc-finger transcription factor which belongs to the SP/KLF (Kruppel-Like Factors) family, characterized by the presence of three conserved Cys2-His2-type zinc finger DNA binding domains in its C-terminus (Beishline & Azizkhan-Clifford, 2015). Each of the three zinc fingers in SP1 has a

specific sequence preference, and all three are required for high-affinity binding. The zinc fingers help DNA-binding but are also necessary to nuclear localisation (Ito *et al.*, 2010). The SP1 protein is 785 amino acids long, has a molecular weight of 81kDa, and is ubiquitously expressed from the *Sp1* gene in mammalian cells (Wierstra, 2008). It binds to GC-rich promoters and consensus sequences 5'-(G/T)GGGCGG(G/A)(C/T)-3' of various genes and enhances transcription. SP1-binding sites are widespread throughout the genome, counting up to 12,000 in the human genome (Zhang *et al.*, 2019). In line with its expression, SP1 plays a significant role in processes ranging from cellular growth, cell cycle regulation, and differentiation, hormonal activation, apoptosis, angiogenesis, cancer (Black *et al.*, 2001) and metabolic functions (Roy *et al.*, 2017).

Several lines of evidence show that BRD4 could indirectly interact with SP1 through c-Myc, as c-Myc is thought to sequester SP1 in eliciting its oncogenic effects (Gartel *et al.*, 2001). In fact, other genes were also found to be modulated in expression on *Sp1*-binding sites, through BRD4. It was shown that BRD4 can bind and interact to the *Sp1*-binding sites and regulate the transcription of genes, such as the inducible heme oxygenase 1 (*Hmox1*). In fact, BRD4 could both augment as well as reduce its expression, depending on other interacting elements and environmental stressors (Hussong *et al.*, 2014), underlying the versatility of bromodomains as transcriptional regulators. Additionally, a screen of protein-protein interactions between BRD4 and transcription factors further demonstrated BRD4 to associate directly with several transcription factors and chromatin-modifying enzymes, such as p53, Yin and Yang 1 Protein (YY1), Adaptor Protein Complex 2 (AP2), c-Jun, c-Myc, CCAAT/enhancer binding protein α (CEBPα), ATP-dependent chromatin assembly factor 1 (Acf1) as well as G9a, and found no

protein-protein interaction between SP1 and BRD4 (Wu *et al.*, 2013b). However, it was previously shown that the transcriptional factor E2F associates with both BRD4 and SP1 (Lin *et al.*, 1996), further leading to their binding to SP1-binding sites and transcription activation. Drawing parallels from these studies, it can be evinced that inhibition of BRD4 can allow for an increase in binding of SP1 (Wong *et al.*, 2005) (**Figure 4.1.2).**

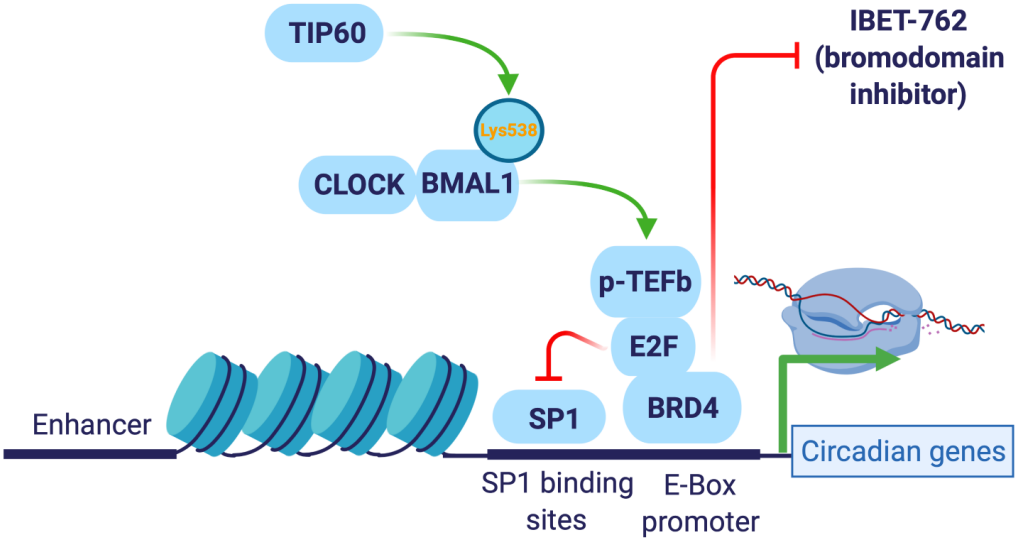


Figure 4.1.2 – Mechanism of action of bromodomain inhibitors on the circadian clock. Acetylation of BMAL1 at lysine 538 by TIP60 stimulates the binding of the pTEFb and BRD4 at E-Box regions that regulate the transcription of circadian genes. E2F interacts with BRD4 and supresses the binding of SP1 to SP1-binding sites. A bromodomain inhibitor, such as IBET-762, would therefore inhibit the binding of the pTEFb-E2F-BRD4 complex to the E-box regions and allow the binding of SP1 to SP1-binding sites, eliciting its stimulatory action on the expression of circadian genes.

4.1.4 HIF1 in cellular functionality and circadian rhythms

The hypoxia-inducible factors are transcription factors that respond to a lowering in cellular oxygen availability and hypoxic conditions. The highly conserved HIF1 complex is a heterodimer composed of an α (HIF1α, HIF2α, HIF3α) and a β subunit, with the latter being constitutively-expressed (Wang *et al.*, 1995),(Wang & Semenza, 1995). Both subunits form part of the basic-helix-loop-helix (bHLH) family. HIF1α contains an activation domain that binds to HRE-elements 5'-RCGTG-3'(Semenza *et al.*, 1996). HIF1α expression levels increase exponentially with decrease of oxygen availability, but can also increase due to a direct activation of gene transcription (Jiang *et al.*, 1996).

The physiological role of HIF1 signalling activation is to mediate the effects of cellular hypoxia. HIF1α, the most extensively studied isoform, was shown to promote inhibition of further differentiation and proliferation (Goda *et al.*, 2003), stimulate apoptosis (Carmeliet *et al.*, 1998), and the formation of new blood vessels. Angiogenesis was mediated by the activation of transcription of erythropoietin (*Epo*) and vascular endothelial growth factor (*Vefg*) genes, supporting the delivery of oxygen to hypoxic area (Lemus-Varela *et al.*, 2010). The HIF1α increase in activity was also associated with several pathological states, such as cancerous growths, where cells at the centre of the mass are under a low oxygen exposure thus evolve to activate HIF1 signalling for survival. Some of these effects were correlated with the HIF1-induced modulation of Octamer-binding Transcription Factor 4 (*Oct4*) expression, a gene implicated in differentiation and cancer growth (Covello *et al.*, 2006).

Hypoxia and HIF1 are essential in promoting angiogenesis and trigger metabolic adaptation in cancer growths, as well as a shift towards glycolysis, an anaerobic way of producing ATP (Marsin *et al.*, 2002). As bromodomain inhibitors were shown to be effective in various forms of haematic and solid cancers, they were also applied in studies looking at their modulation of the hypoxic and HIF1 signalling. It was shown that JQ-1 and OTX015, both BET inhibitors, partially modulate the hypoxia-induced genes, including *Ca9* and *Vegfa* expression, and could be a mechanism through which exert its anti-cancer effect in triple-negative breast cancer (TNBC) (da Motta *et al.*, 2017; Vazquez *et al.*, 2017). TNBC is an aggressive form of breast cancer that tests negative for oestrogen receptors, progesterone receptors and excess Human Epidermal Growth Factor Receptor 2 (HER2) protein.

Several lines of evidence point towards the impact of hypoxia and HIF1 on circadian gene expression (**Figure 4.1.3**)**.** Most importantly, HIF1α belongs to the same protein family as the core circadian proteins, the bHLH-motif containing the Per-Arnt-Sim (PAS)-domain signal sensors (Gu *et al.*, 2000). Specifically, it has been shown that PAS domains in PER proteins were found to form heterodimers with other PAS-containing proteins, such as the Aryl-Hydrocarbon Receptor Nuclear Translocator (ARNT, or HIF1β), suggesting that their functionality may overlap in certain scenarios (Gu *et al.*, 2000). It has indeed been shown that PER2 facilitates the recruitment of HIF1α, the most extensively studied isoform, to the hypoxia-response-element (HRE), increasing its activity (Kobayashi *et al.*, 2017). Moreover, circadian clockwork was found to regulate HIF1α nuclear localisation (Button *et al.*, 2017); BMAL1 and HIF1α were indeed shown to co-localise at HRE-sites on the *Per2* promoter, with its binding enhancing *Per2*

amplitude (Peek *et al.*, 2017) in the skeletal muscle. Also, the BMAL1-CLOCK complex were also shown to bind to E-Box sequences within the promoter of HIF1α, supporting a bidirectional interaction between the circadian clock and hypoxia (Wu *et al.*, 2017).

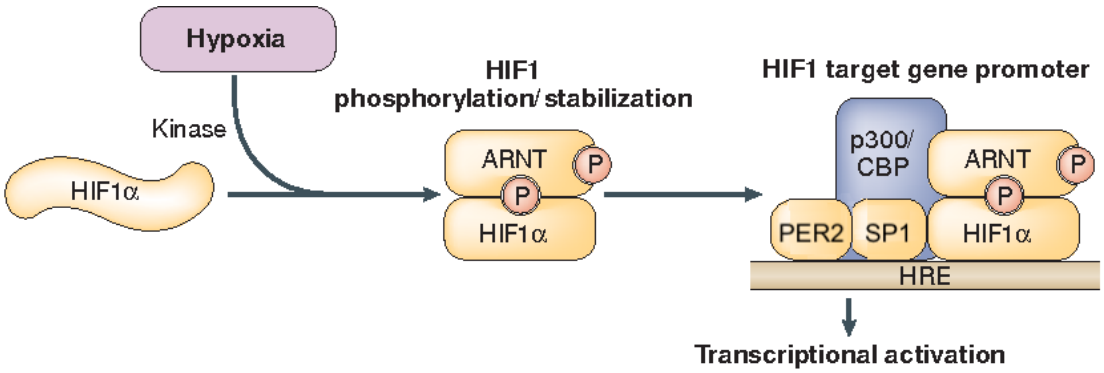


Figure 4.1.3 – Role of HIF1 at the interaction between metabolic functionalities and circadian rhythms. The graph depicts the role of hypoxia, circadian genes (PER2) and transcription factors (SP1) on the binding of HIF1 to hypoxia-responsive elements (HRE). The transcriptional activation has a variety of effects, amongst which a regulation of metabolic functionalities that are implicated in obesity, insulin signaling and glucose intolerance. Adapted from (Sharp & Bernaudin, 2004).

4.1.5 Pathophysiological role of bromodomains

As we study bromodomain inhibition in circadian rhythm modulation, it is pivotal to underline previous lines of study of these molecules, specifically of IBET-762, as they were tested for their efficacy in pathophysiological alterations.

BET proteins are of extensive focus in pathophysiology, given the discovery of several BET-targeting bromodomain inhibitors, such as IBET-762 and JQ-1. The BET-family forms the focus of this study, as BET-inhibitors such as IBET-762 and JQ1 were shown to enhance circadian amplitude in U2OS cells. All BET proteins play differential physiological roles in different cells: for example, BRD2 is involved in neuronal

development and cell cycle progression in neuroepithelial cells (Tsume *et al.*, 2012), whereas it was found to affect gene splicing in HeLa cells (Hnilicova *et al.*, 2013). BRD3 has a role in erythropoiesis by regulating specific erythroid genes through GATA-Binding Protein 1 (GATA1) (Lamonica *et al.*, 2011). Furthermore, BRD4 was shown to be involved in coding and enhancer RNA transcript elongation through p-TEFb (Kanno *et al.*, 2014). BRDT was shown to have a role in spermatogenesis (Shang *et al.*, 2007). These effects underline the differential role of BET bromodomains in cellular and tissue physiology and suggest BET-inhibition could impact on the whole organism physiological processes through different pathways.

Given the link to key oncogenic transcription factors, efforts mainly converged on studying BET-inhibitors in cancer pathologies (Xu & Vakoc, 2017). Moreover, neoplastic cells seem to depend on BET-expressing gene activity for their survival, and their overexpression occurs in several human cancers (Baratta *et al.*, 2015; Zuber *et al.*, 2011). BET proteins promote in fact aberrant expression of MYC oncogene in several types of leukaemia and lymphomas. It has indeed been shown that inhibition of BET proteins significantly reduces cellular proliferation in these cancer cells (Dawson *et al.*, 2011). NUT midline carcinoma is specifically targeted by bromodomain inhibitors: NUT carcinoma is given by the genetic fusion of the NUT gene to the BET gene BRD4 on chromosomes 15 and 19, respectively. This fusion stimulates the overexpression of NUT oncogene driven by the BRD4 promoter, and is considered pivotal in the pathogenesis of this type of cancer (French *et al.*, 2008).

BET-overexpression was also associated with other cancers. As an example, BRD4 was shown to interact with WHSC1, a histone H3K36 methyltransferase that acts as a positive regulator of oestrogen receptor α (ERα), which is upregulated in tamoxifen-resistant breast cancer, raising hopes for bromodomain inhibitors as part of a combination therapy in this type of cancer (Feng *et al.*, 2014). A role of BET-inhibitors was also postulated in a combination-treatment in castrate-resistant prostate cancer (CRPC), by downregulating androgen-receptor signalling in cells (Asangani *et al.*, 2014). Furthermore, BET proteins were found to be overexpressed in glioblastomas (Pastori *et al.*, 2014), gastric cancer (Montenegro *et al.*, 2016) and KRAS-mutant non-small cell lung cancer (NSCLC) (Shimamura *et al.*, 2013), with disruption of the BET proteins reducing aberrant cell proliferation.

JQ-1 is unsuitable for clinical trials due its short half-life. IBET-762 is currently being studied in phase I and phase II clinical trials in metastatic NUT midline carcinoma, lymphoma, pancreatic cancer, and other solid tumours that are either metastatic or refractory (NCT03925428 and NTC04116359). In spite of being well-tolerated in patients (Piha-Paul *et al.*, 2020), side-effects brought forward by IBET-762 in clinical trials include reversible thrombocytopenia, fatigue, gastrointestinal symptoms, and hyperbilirubinemia.

4.1.6 Bromodomains in non-oncologic indications

Given the preclinical work that has been reported so far, BET-inhibitors are also postulated to be potentially useful in non-oncologic indications. BET inhibitors were

shown to reverse septic shock in mice and to have anti-inflammatory properties (Tough *et al.*, 2016). Their effects were shown to be potentially useful in periodontitis patients, with inflammation of the gums, where JQ-1 suppressed the transcription of various inflammatory cytokines, such as Interleukins *Il-1β*, *Il-6*, Tumour Necrosis Factor A (*Tnfα*) and Nuclear Factor kβ (*Nfkβ*) (Maksylewicz *et al.*, 2019; Meng *et al.*, 2014). Evidence also showed that brd2$^{+/-}$ haploinsufficiency extended lifespan and healthspan in C57BL/6 mice, possibly by reducing molecular and cellular damage (Pathak *et al.*, 2020).

Furthermore, BET-inhibitors were shown to be potentially therapeutic in reducing the incidence of myopathies, and even reversing cardiac damage in heart failure, by suppressing both inflammation and fibrotic mechanisms (Duan *et al.*, 2017). RVX-208 is the only BET-I drug studied as a potential protective factor against cardiovascular morbidities, with a phase III clinical trial looking at reducing the number of cardiovascular events in patients affected by high cardiovascular disease risk and type-2 diabetes (Gilham *et al.*, 2016; Nicholls *et al.*, 2018). Clinical trials have also shown the effects of RVX-208 in improving the blood glucose profile upon a glucose tolerance test with a potential as a protective agent against developing type-2 diabetes (Siebel *et al.*, 2016). It is so far unclear whether the putative effects of RVX-208 are due to its selectivity towards BD2 vs BD1 or not (Picaud *et al.*, 2013).

BET-inhibitors also have a potential as anti-viral therapies. They were indeed shown to reactivate the latent human immunodeficiency virus (HIV) and herpes simplex virus (HSV1 and HSV2), by modulating its transcription, and thus possibly allowing for its definite degradation by the immune system in conjunction with antiretroviral therapies

(Li *et al.*, 2013; Lu *et al.*, 2016; Ren *et al.*, 2016). On the other hand, BET-inhibitors were also shown to reduce viral replication and genome integration in Epstein-Barr virus (EBV), by blocking the expression of early lytic viral genes (Keck *et al.*, 2017). BET-inhibition was shown to be of potential usefulness in inhibiting parasite development in Trypanosoma Brucei (Schulz *et al.*, 2015) and BRD4 downregulation also showed to boost a rapid immune response and increase host response to viral infections by activating a DNA damage response mechanism (Wang *et al.*, 2020).

Early reports in 2020 also show that the Severe Acute Respiratory Syndrome SARS-CoV-2, the virus that can bring about an infectious, debilitating and possibly dangerous acute respiratory syndrome known as Covid-19, expresses protein E that directly interacts with the host BRD2/4 proteins (Gordon *et al.*, 2020). The small envelope protein (E protein) plays a role in the production and maturation of the virus and is involved in assembly, budding, envelope formation and pathogenesis (Schoeman & Fielding, 2019). RVX-208 was reported to potentially inhibit this interaction in preclinical studies and efforts towards starting clinical trials were underway (Press Release, AP News, Resverlogix Corp, June 1 2020).

4.1.7 TF activation and methods to study their activity

Understanding transcription factor activation is pivotal to study the regulation of transcription under environmental and localized factors (Lemon & Tjian, 2000). Environmental factors that can modulate the activation of transcription factors are the binding of other transcription factors, histone modifications and chromatin remodelling.

Efforts were held to identify and validate the binding sites of transcription factors throughout the human genome, as well as their modulatory transcriptional effects in pathophysiology.

Methodologies to study the activation of specific transcription factors binding sites can be varied, however, functional analyses through TF-binding-sequence luciferase reporters have been widely used in understanding the activation of mapped TF binding sequences (Trinklein *et al.*, 2003). This methodology allows the use of a plasmid containing a luciferase reporter attached to the predicted binding sequence of a transcription factor. The TF sequence can be predicted either through computational studies and ChIP-Seq experimentation (Whitfield *et al.*, 2012). In the luciferase-driven reporter assays, the binding of the TF sequence activates the expression of the luciferase which then uses luciferin as a substrate to produce luminescence, which is measured and analysed in intensity. The results can be further validated by mutating the binding sites and re-assessing and comparing luciferase activity (Myers *et al.*, 1986).

Other methodologies to study the activation of transcription factors can be through measuring the quantity of activated protein through western blot or immunoprecipitation and probe-based methodologies such as TF arrays, electrophoretic mobility shift assays (EMSAs) or enzyme-linked immunosorbent assays (ELISAs). All have advantages and disadvantages with respect to several parameters of efficacy, predictiveness and ease-of-use. With respect to the reporter-luciferase library assays, screening for the activation of several TF binding sites is practical to carry out, and allows for a quantitative analysis of activation of several transcription factor binding sites at the

same time, when analysed against baseline measures. Furthermore, the results are functional as the activation is carried out in living cells. However, the luciferase assay can also have important limitations that need to be taken into account; firstly, it has a limited translational efficacy, as we look at the reporter activation outside of the control of normal regulatory chromatin structures, thus the effects should be possibly validated in a phenotypical assay. Secondly, we cannot know which proteins drive the activation of the binding site, but only if it is driven or not. Thus, the activation mechanisms can be multiple and are generally predicted from the literature. These should be further validated in other targeted experiments, such as immunoprecipitation studies.

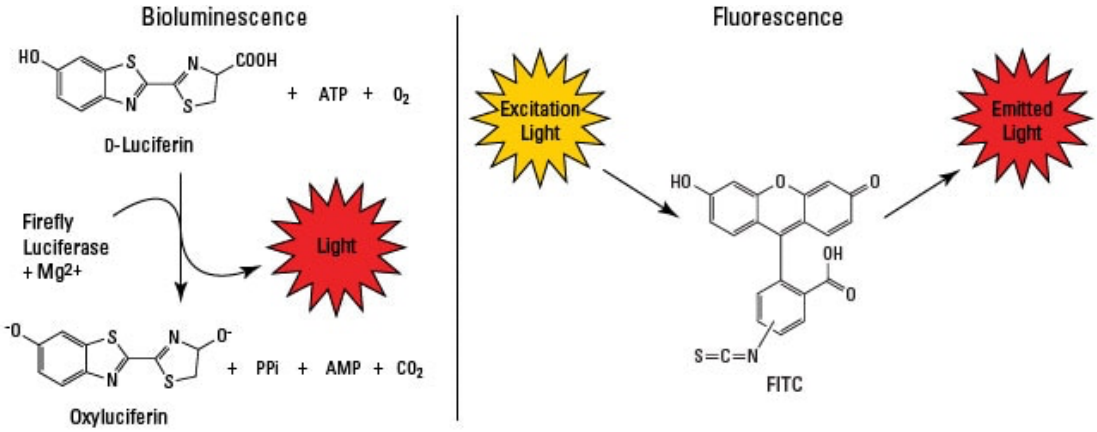


Figure 4.1.4 – Principles of fluorescence and bioluminescence. Bioluminescence uses luciferin as a substrate for its reaction and light emission, whereas fluorescence uses light excitation at a specific wavelength, allowing for a more limited sensitivity.

Regarding the luminescence technology employed by the reporter-luminescence assays, it differs from other technologies such as colorimetric and fluorometric assays on several aspects. Firstly, as opposed to fluorescence, the excitation energy is supplied by an enzymatic reaction rather than another source of light, allowing for an increase in sensitivity and wider dynamic range, given that fluorescence reporters are subject to

photo bleaching (**Figure 4.1.4**). Fluorescent reporters are less responsive to real-time changes, and can be perturbed by natural cellular fluorescence, which gives a higher background noise. Moreover, fluorescent reporters are better studied in live cells as they do not require co-factors for their activity (such as luciferin, ATP and magnesium), and are more stable for a longer period of time. The luciferin we use in our experiments originates in fireflies and is more suitable for cell-based gene reporter experiments , when compared to Renilla Coelenterazine, due to its shorter half-life and increased dynamicity. Furthermore, the glow type luciferase assay used, is better at keeping comparability between wells as it takes longer to degrade. However it can be less sensitive than the flash type luciferase.

4.2 RESULTS

4.2.1 Effects of BRD-specific knock-down on circadian rhythms

The BET family is formed by 4 main bromodomain members, BRD2, BRD3, BRD4 and BRDT. To test the hypothesis that the effects of IBET-762 are via BRDs, and not via off-target effects, we knocked-down each of the bromodomains using siRNA. Given that IBET-762 acts as a bromodomain inhibitor, the knock-down effects should mimic the bromodomain inhibitor effects. As shown in **Figure 4.2.1** the bromodomain knock-down promotes amplitude enhancement only in the case of BRD4 knock-down, as assessed on U2OS *Per2*::Luc cells (**Fig. 4.2.1G**). Moreover, BRD4 knock-down seems to have a period-increase effect in both U2OS *Per2*::Luc and *Bmal1*::Luc cells (**Fig. 4.2.1G and C)**. BRD-T knock-down, on the other hand, induces a decrease in circadian amplitude, in both *Bmal1*::Luc (**Fig. 4.2.1D**) and *Per2*::Luc (**Fig. 4.2.1H**) stably-transfected cells. BRD4-specific knock-down was shown to increase circadian amplitude significantly in U2OS *Per2*::Luc cells (20% increase, p=0.0052) (**Figure 4.2.2B**), mimicking the effects of IBET-762 circadian effects. Other treatments were shown to decrease circadian amplitude significantly, such as the BRD-T knockdown treatment, on both the *Per2*::Luc (47% decrease, p<0.0001) and *Bmal1*::Luc (33% decrease, p<0.0001) stably-transfected cell lines. The latter amplitude decreasing effect is not in line with the effects with IBET-762 on the circadian clock. A more general dampening effect was observed by BRD2-3-4 knock-down on *Bmal1*::Luc stably-transfected cells (23-21% decrease, p<0.0001). This effect is also not a mimic of the effects of IBET-762 on circadian amplitude.

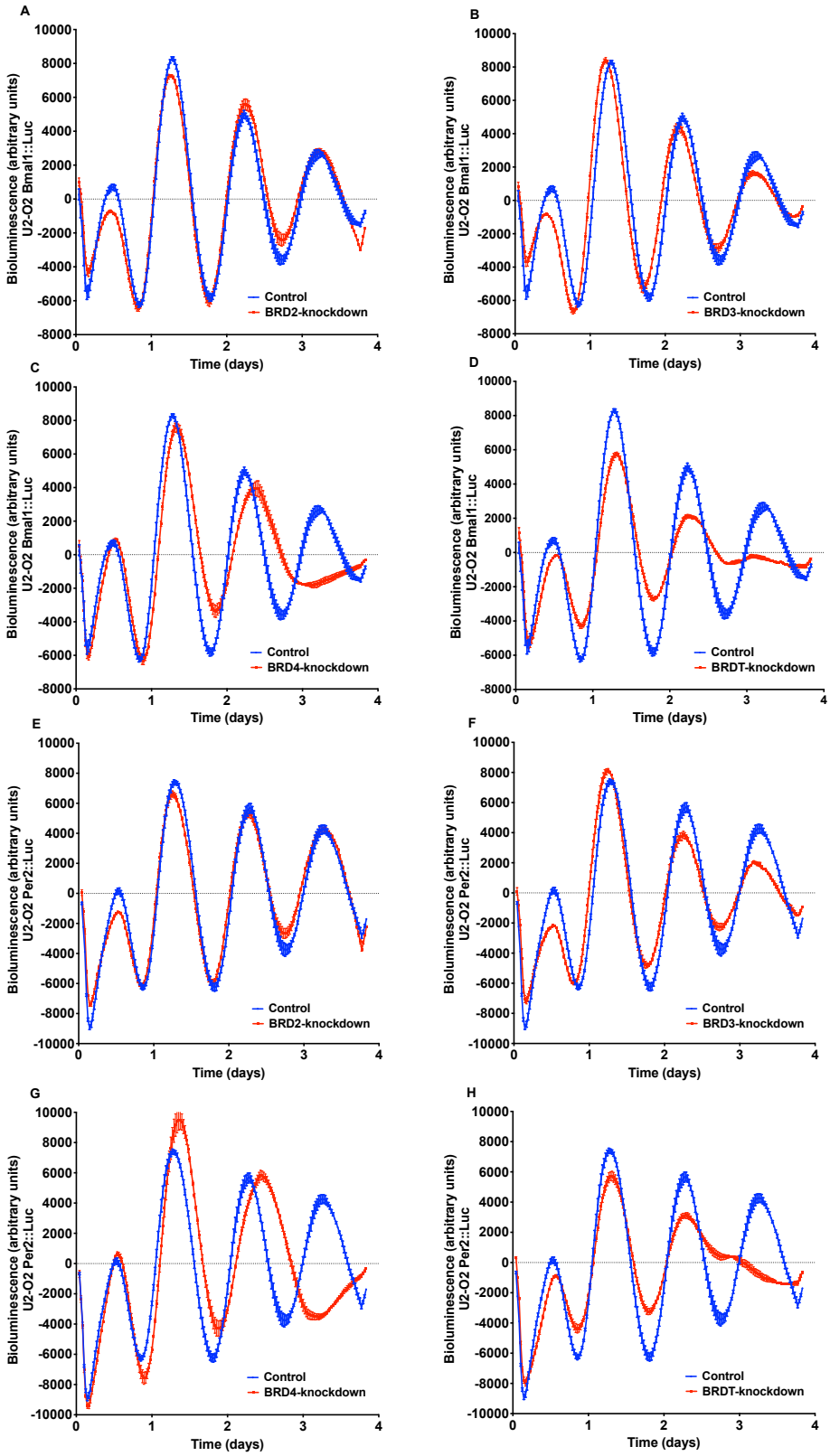


Figure 4.2.1 - Effects of bromodomain knock-down on circadian rhythms. U2OS cells were stably-transfected with a *Bmal1*::Luc (**A-D)** or *Per2*::Luc (E-**G**) promoter and period and amplitude were assessed over 92 hours of luminescence, following a 24-hour knockdown of bromodomain-genes BRD2 (**A, E**), BRD3 (**B, F**), BRD4 (**C, G**) and BRDT (**D, H**) (**Methods 1.2.4)**. Data was analyzed with the aid of the Multicycle software and was expressed in absolute mean values ± SEM and directly compared to the non-targeting control (n=4).

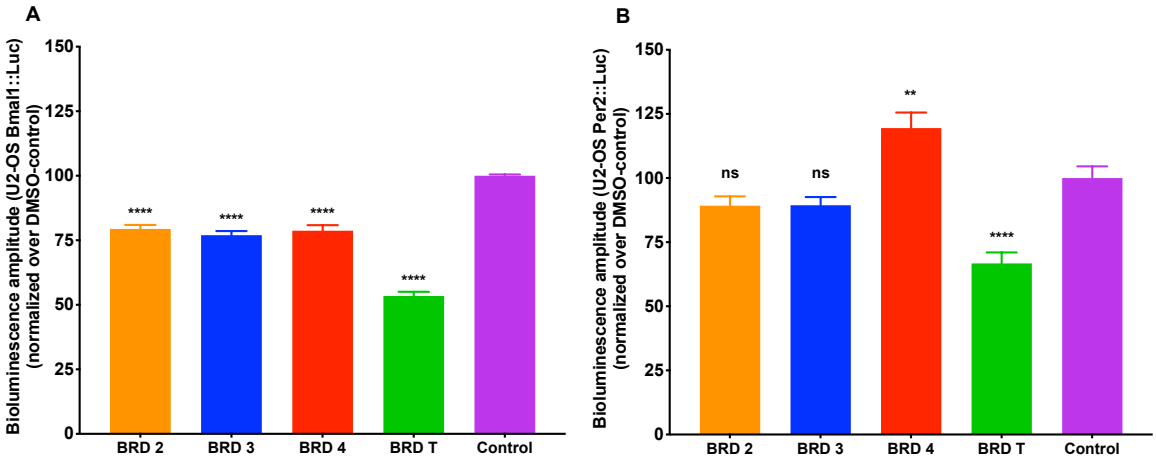


Figure 4.2.2 - Analysis of bromodomain knock-down on circadian rhythm amplitude. *Bmal1*::Luc (**A**) and *Per2*::Luc (**B**) stably-transfected U2OS cells were treated for 24-hours with siRNA for the knockdown of bromodomain-genes BRD2, BRD3, BRD4 (**Methods 1.2.4**)**.** Data was analyzed with the aid of the Multicycle software and the amplitude values were normalized on the DMSO-control and were expressed as absolute mean values ± SEM (n=4). A one-way ANOVA and a Sidak-powered post-hoc multiple-comparison were performed to test the effects of BRD-knockdown on amplitude (p<0.05).

4.2.2 BRD-knockdown effectiveness and specificity on U2OS cells

To assess the knock-down efficiency, we measured the expression of the gene under investigation, both as an absolute expression and normalised over the DMSO-control, as a percentage change (**Figure 4.2.3A**). As could be seen, the knockdown was efficacious in reducing bromodomain expression (BRD2 knocked-down by 82%, BRD3 by 86% and BRD4 by 88%) when compared to their DMSO-control counterpart ($p<0.0001$).

Furthermore, to ensure the knock-down was specific to the intended target, following the knock-down of a specific bromodomain, we analysed the expression of all other bromodomains (**Figure 4.2.3B-D**). Upon statistical analysis, we have shown that down-regulations were specific to their intended targets within the bromodomain range, with the exception of BRD2-knockdown, which also showed to partially downregulate BRD3 expression (reduction of 19%, $p=0.0027$) (**Figure 4.2.3B**). Taken together, the effects of BRD knockdown were significant and specific to the target of interest.

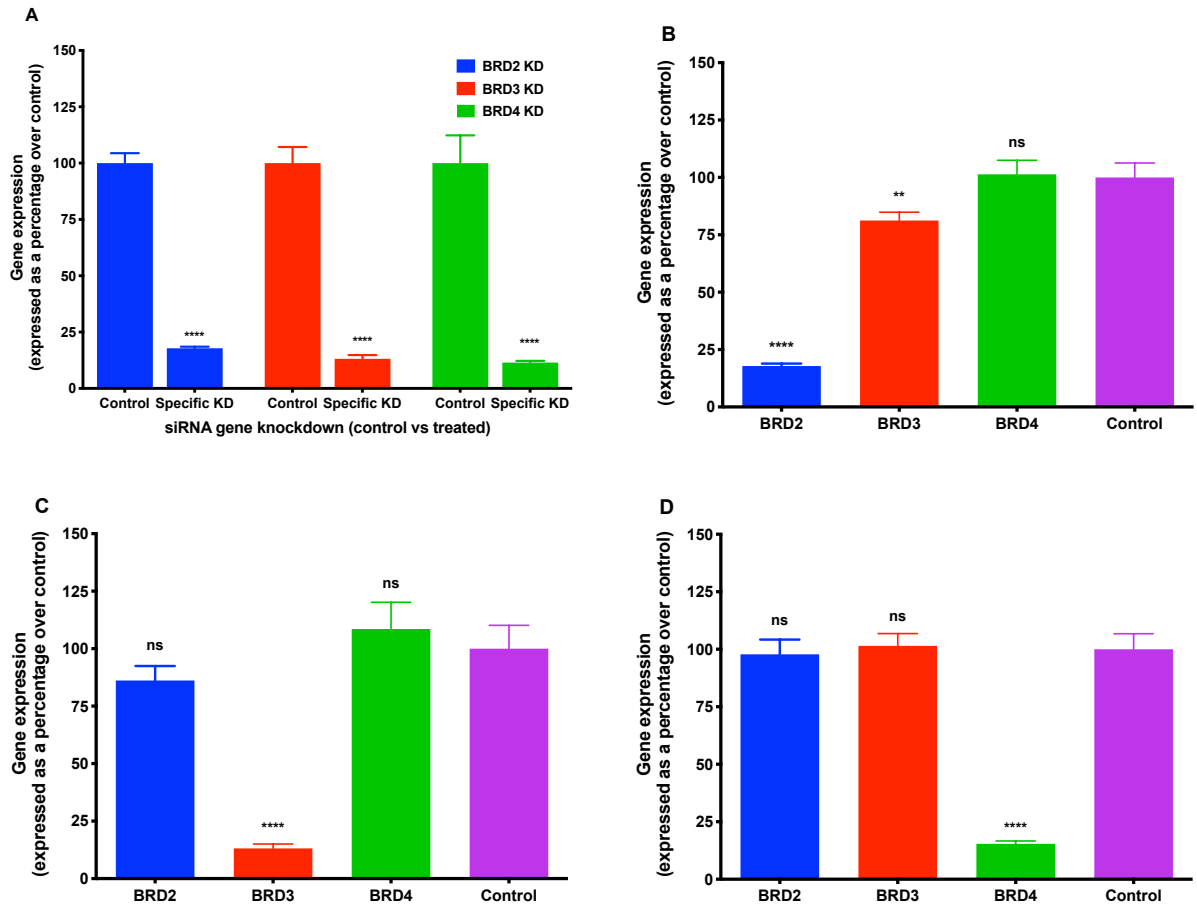


Figure 4.2.3 - Specificity of siRNA bromodomain knock-down on gene expression. U2OS cells were treated for 24-hours with siRNA for the knock-down of bromodomain-genes BRD2, BRD3, BRD4. The expression of BRD2, BRD3 and BRD4 were quantified as a knockdown percentage over control transfection **(A)**. The knock-down of BRD2 (**B**), BRD3 (**C**) and BRD4 (**D**) were quantified in relation to the knock-down of the other bromodomains, to rely knockdown specificity. the data was expressed as average ± SEM (n=4). A one-way ANOVA and a Sidak-powered post-hoc multiple-comparison were performed to test the efficacy and specificity of BRD-knockdown (p<0.05).

4.2.3 Evaluating the mechanisms behind BRD4 inhibition

Having ensured that the effects of IBET-762 were specifically mediated via bromodomains and possibly through BRD4, we next evaluated the mechanism of this inhibition. Bromodomains have two main dominant structures that are pivotal in the interaction with acetylated lysine residues on histone tails: BD1 and BD2. To evaluate whether the effects on circadian rhythms were mediated by either BD1 or BD2 or both, we took a pharmacological approach and used two bromodomain inhibitors, Olinone and RVX208. Olinone shows a 100-times inhibitory specificity towards BD1 versus BD2 (Chiang, 2014), whereas RVX208 has about 170-fold selectivity towards BD2 versus BD1 (Picaud *et al.*, 2013).

They both showed to increase circadian amplitude with an EC_{50} in the nanomolar range, at about 80nM for Olinone (**Figure 4.2.4C**), and about 50nM for RVX208 (**Figure 4.2.4D**). Moreover, RVX208 increased the circadian period at doses of 3μM and 1μM, though these doses might promote cellular toxicity, given the decrease in amplitude after 24 hours of exposure (**Figure 4.2.4B**). Olinone does not seem to increase period (**Figure 4.2.4A**) and has shown a limited increase in amplitude.

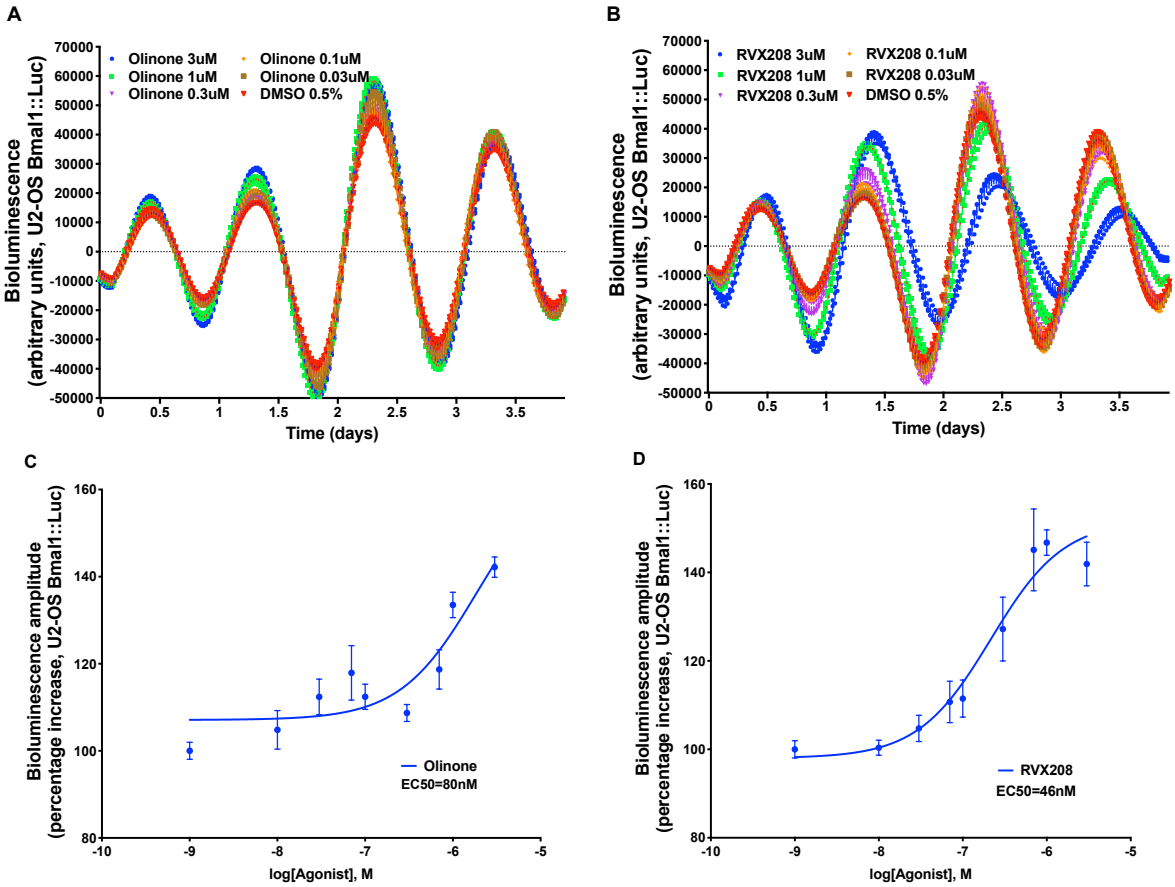


Figure 4.2.4 - Effects of bromodomain inhibitors on *Bmal1*::Luc promoter amplitude. U2OS cells were stably-transfected with a *Bmal1*::Luc promoter and period and amplitude were assessed over 92 hours of luminescence following a pharmacological dose-response treatment with specific BD1 (Olinone) and BD2 (RVX208) inhibitors. Representative traces of the two bromodomain inhibitors are portrayed, namely Olinone **(A)** and RVX208 **(B)** are shown. Data was analyzed with the aid of the Multicycle software and was expressed in absolute mean values ± SEM and directly compared to the DMSO control 0.5%. A dose-response curve was drawn for Olinone **(C)** and RVX208 **(D)**, on a semi-logarithmic scale and their EC_{50} in amplitude increase was calculated.

4.3.4 Regulatory gene modulation by IBET-762 (motif enrichment)

As shown above, bromodomains, and specifically BRD4, mediate the effects of IBET-762 on circadian amplitude (**Figure 4.2.1-4.2.2**). To further understand the DNA regions of bromodomain-binding inhibition by IBET-762 administration, we conducted a bioinformatic analysis on the ChIP-Seq data from a previous study completed by Asangani *et al.* The study performed chromatin immunoprecipitation followed by sequencing (ChIP-Seq) with antibodies against BRD2/3/4 in Vertebral-Cancer of the Prostate (VCaP) cells treated with 0.5μM IBET-762 (Asangani *et al.*, 2014). By analyzing the peak sequences, we performed a differential motif enrichment analysis following IBET-762, and DMSO treatment on the binding modulation of each of the three bromodomains. The top 10 results of motif-enrichment were reported below, for the individual bromodomains (**Figure 4.2.5**), including both known motif enrichment (**Figure 4.2.5A/B/C**), as well as *de-novo* motif enrichment (**Figure 4.2.5D/E/F**).

This unbiased known motif analysis showed a statistically significant enrichment of the 'CACGTG' sequence, the Enhancer-Box (E-box) region found in eukaryotes across different tissues, acting as a transcription-binding sequence for initiation of gene transcription. The E-box binding proteins usually contain a basic helix-loop-helix structural motif, which is typical of several transcription factors and circadian genes, such as BMAL1, and DEC1/2. The 'CACGTG' sequence was found to be differentially enriched in BRD2 binding, with p=1e-29 (**Figure. 4.2.5A**) and in BRD4 binding, with p=1e-11 (**Figure 4.2.5C**). A further significant sequence that was enriched in IBET-762

differential binding was 'ACGTG' (hypoxia-response element) which is known to be bound by HIF1, in both BRD2-binding (p=1e-24) and BRD4-binding (p=1e-7).

In line with the above analysis, the *de-novo* motif analysis largely confirmed known motif enrichment results, with E-Box DNA-binding sequences ('CACGTG') showing a statistically-significant-enrichment for BRD2 (p=1e-39, **Figure 4.2.5D**) and BRD4 (p=1e-11, **Figure 4.2.5F**) precipitation. Furthermore, protein-binding sequences for other transcription factors such as OCT (octamer binding transcription factor, important in development and stem cells) was shown in both BRD2 (p=1e-33, **Figure 4.2.5D**) and BRD3 (p=1e-16, **Figure 4.2.5E**), the zinc-finger domain (ZNF) in both BRD3 (p=1e-13, **Figure 4.2.5E**), and BRD4 (p=1e-10, **Figure 4.2.5F**), and SP1 in BRD4 (p=1e-9, **Figure 4.2.5F**), among others.

A BRD2 Homer known motif enrichment

Rank	Motif	Name	P-value
1		NPAS(bHLH)/Liver-NPAS-ChIP-Seq(GSE39860)/Homer	1e-29
2		HIF-1b(HLH)/T47D-HIF1b-ChIP-Seq(GSE59937)/Homer	1e-24
3		BMAL1(bHLH)/Liver-Bmal1-ChIP-Seq(GSE39860)/Homer	1e-23
4		CLOCK(bHLH)/Liver-Clock-ChIP-Seq(GSE39860)/Homer	1e-19
5		NPAS2(bHLH)/Liver-NPAS2-ChIP-Seq(GSE39860)/Homer	1e-18
6		c-Myc(bHLH)/LNCAP-cMyc-ChIP-Seq(Unpublished)/Homer	1e-16
7		bHLHE40(bHLH)/HepG2-BHLHE40-ChIP-Seq(GSE31477)/Homer	1e-14
8		n-Myc(bHLH)/mES-nMyc-ChIP-Seq(GSE11431)/Homer	1e-14
9		Max(bHLH)/K562-Max-ChIP-Seq(GSE31477)/Homer	1e-13
10		c-Myc(bHLH)/mES-cMyc-ChIP-Seq(GSE11431)/Homer	1e-13

B BRD3 Homer known motif enrichment

Rank	Motif	Name	P-value
1		OCT:OCT(POU,Homeobox)/NPC-OCT6-ChIP-Seq(GSE43916)/Homer	1e-7
2		c-Myc(bHLH)/LNCAP-cMyc-ChIP-Seq(Unpublished)/Homer	1e-7
3		Brn2(POU,Homeobox)/NPC-Brn2-ChIP-Seq(GSE35496)/Homer	1e-6
4		ZNF711(Zf)/SHSY5Y-ZNF711-ChIP-Seq(GSE20673)/Homer	1e-5
5		NPAS(bHLH)/Liver-NPAS-ChIP-Seq(GSE39860)/Homer	1e-5
6		Pit1(Homeobox)/GCrat-Pit1-ChIP-Seq(GSE58009)/Homer	1e-3
7		n-Myc(bHLH)/mES-nMyc-ChIP-Seq(GSE11431)/Homer	1e-3
8		CLOCK(bHLH)/Liver-Clock-ChIP-Seq(GSE39860)/Homer	1e-3
9		HIF-1b(HLH)/T47D-HIF1b-ChIP-Seq(GSE59937)/Homer	1e-3
10		Max(bHLH)/K562-Max-ChIP-Seq(GSE31477)/Homer	1e-3

C BRD4 Homer known motif enrichment

Rank	Motif	Name	P-value
1		NPAS(bHLH)/Liver-NPAS-ChIP-Seq(GSE39860)/Homer	1e-11
2		c-Myc(bHLH)/mES-cMyc-ChIP-Seq(GSE11431)/Homer	1e-7
3		HIF-1b(HLH)/T47D-HIF1b-ChIP-Seq(GSE59937)/Homer	1e-7
4		n-Myc(bHLH)/mES-nMyc-ChIP-Seq(GSE11431)/Homer	1e-6
5		BMAL1(bHLH)/Liver-Bmal1-ChIP-Seq(GSE39860)/Homer	1e-6
6		c-Myc(bHLH)/LNCAP-cMyc-ChIP-Seq(Unpublished)/Homer	1e-6
7		AR-halfsite(NR)/LNCaP-AR-ChIP-Seq(GSE27824)/Homer	1e-5
8		Max(bHLH)/K562-Max-ChIP-Seq(GSE31477)/Homer	1e-5
9		USF1(bHLH)/GM12878-Usf1-ChIP-Seq(GSE32465)/Homer	1e-4
10		ERG(ETS)/VCaP-ERG-ChIP-Seq(GSE14097)/Homer	1e-4

D BRD2 Homer de-novo motif enrichment

Rank	Motif	P-value	Best Match/Details
1		1e-52	PB0170.1_Sox17_2/Jaspar(0.688) More Information | Similar Motifs Found
2		1e-39	CLOCK/MA0819.1/Jaspar(0.867) More Information | Similar Motifs Found
3		1e-33	OCT:OCT(POU,Homeobox)/NPC-OCT6-ChIP-Seq(GSE43916)/Homer(0.605) More Information | Similar Motifs Found
4		1e-21	PB0207.1_Zic3_2/Jaspar(0.576) More Information | Similar Motifs Found
5		1e-18	BHLHE41/MA0636.1/Jaspar(0.651) More Information | Similar Motifs Found
6		1e-17	Arntl/MA0603.1/Jaspar(0.801) More Information | Similar Motifs Found
7		1e-17	EKLF(Zf)/Erythrocyte-Klf1-ChIP-Seq(GSE20478)/Homer(0.578) More Information | Similar Motifs Found
8		1e-16	STAT3/MA0144.2/Jaspar(0.732) More Information | Similar Motifs Found
9		1e-16	GLI2/MA0734.1/Jaspar(0.741) More Information | Similar Motifs Found
10		1e-16	PB0117.1_Eomes_2/Jaspar(0.575) More Information | Similar Motifs Found

E BRD3 Homer de-novo motif enrichment

Rank	Motif	P-value	Best Match/Details
1		1e-16	c-Myc(bHLH)/LNCAP-cMyc-ChIP-Seq(Unpublished)/Homer(0.738) More Information | Similar Motifs Found
2		1e-16	OCT:OCT(POU,Homeobox)/NPC-OCT6-ChIP-Seq(GSE43916)/Homer(0.708) More Information | Similar Motifs Found
3		1e-15	ZNF692(Zf)/HEK293-ZNF692.GFP-ChIP-Seq(GSE58341)/Homer(0.691) More Information | Similar Motifs Found
4		1e-15	ZBTB7A/MA0750.1/Jaspar(0.552) More Information | Similar Motifs Found
5		1e-14	PB0045.1_Myb_1/Jaspar(0.670) More Information | Similar Motifs Found
6		1e-14	Zfx/MA0146.2/Jaspar(0.607) More Information | Similar Motifs Found
7		1e-14	IRF7/MA0772.1/Jaspar(0.695) More Information | Similar Motifs Found
8		1e-13	PB0196.1_Zbtb7b_2/Jaspar(0.577) More Information | Similar Motifs Found
9		1e-13	ZNF692(Zf)/HEK293-ZNF692.GFP-ChIP-Seq(GSE58341)/Homer(0.517) More Information | Similar Motifs Found
10		1e-13	PB0110.1_Bcl6b_2/Jaspar(0.657) More Information | Similar Motifs Found

F BRD4 Homer de-novo motif enrichment

Rank	Motif	P-value	Best Match/Details
1		1e-13	EKLF(Zf)/Erythrocyte-Klf1-ChIP-Seq(GSE20478)/Homer(0.533) More Information | Similar Motifs Found
2		1e-11	ARNT::HIF1A/MA0259.1/Jaspar(0.718) More Information | Similar Motifs Found
3		1e-11	PB0199.1_Zfp161_2/Jaspar(0.531) More Information | Similar Motifs Found
4		1e-10	ZNF416(Zf)/HEK293-ZNF416.GFP-ChIP-Seq(GSE58341)/Homer(0.577) More Information | Similar Motifs Found
5		1e-10	ZNF416(Zf)/HEK293-ZNF416.GFP-ChIP-Seq(GSE58341)/Homer(0.672) More Information | Similar Motifs Found
6		1e-9	X-box(HTH)/NPC-H3K4me1-ChIP-Seq(GSE16256)/Homer(0.624) More Information | Similar Motifs Found
7		1e-9	PB0097.1_Zfp281_1/Jaspar(0.557) More Information | Similar Motifs Found
8		1e-9	Sp1(Zf)/Promoter/Homer(0.530) More Information | Similar Motifs Found
9		1e-8	TFAP2A(var.2)/MA0810.1/Jaspar(0.659) More Information | Similar Motifs Found
10		1e-8	PB0101.1_Zic1_1/Jaspar(0.621) More Information | Similar Motifs Found

Figure 4.2.5 - Motif enrichment data gathered through peak analysis with MACS2 and motif analysis with HOMER. Peaks were called with MACS2 with the DMSO treatment as the higher-peak condition and motifs were found and annotated with HOMER using the standard analysis cut-offs. Results are reported for the effects of 0.5uM IBET-762 on prostate cancer cells, BRD2 (**A, D**), BRD3 (**B, E**) and BRD4 (**C, F**) binding, through both a known motif and de-novo analysis.

4.2.5 Pathway gene ontology modulation by IBET-762 in VCaP cells

To understand whether the differential peak expressions found in the analysis of IBET-762 vs DMSO treatments in VCaP cells are enriched within the genes of pathways that have specific cellular functionalities and processes, we have carried out a gene ontology analysis. The input list of IBET-762-modulated genes allowed for a gene ontology annotation analysis with respect to their biological processes.

The analysis shows a series of pathways being modulated by IBET-762 through all three bromodomains it inhibits (**Figure 4.2.6**). For BRD2 (**Figure 4.2.6A**), we can see that white cell differentiation (p=4.6e-16) and regulation of glucose import (p=1.5e-6) to be important pathways modulated differentially by IBET-762, together with neurotransmitter transport (p=3.6e-8) and regulation (p=1.2e-8), post-embryonic morphogenesis (p=1.3e-7), osteoblast differentiation (p=2.5e-7), smooth muscle contraction (p=1.3e-4), and positive regulation of cyclase activity (p=1.8e-3).

Regarding BRD3 (**Figure 4.2.6B**), the most IBET-762-differentially modulated processes are general transcriptional and translational mechanisms, such as mRNA catabolic processes (p=8.3e-17), translational initiation (p=1.8e-16), and termination (p=1.1e-16), viral transcription (p=1.2e-16), as well as macromolecular complex disassembly (p=1.1e-15).

For BRD4 (**Figure 4.2.6C**), we can see processes modulated differentially by IBET-762 to be similar to the ones modulated through BRD3, such as transcriptional and translational mechanisms: chromatin assembly (p=1e-14), translational initiation

(p=2.5e-14), and termination (p=5.9e-13), viral gene expression (p=2.5e-13), mRNA catabolic processes (p=1.3e-12), and protein complex disassembly (p=2.4e-12). Moreover, other specific pathways were also shown to be differentially modulated by IBET-762, such as growth hormone secretion (p=2.1e-4), and positive regulation of circadian sleep-wake cycle (p=2.7e-3).

A	Term Name BRD2	Binom Rank	Binom Raw P-Value
	white fat cell differentiation	16	4.5870e-16
	regulation of neurotransmitter levels	143	1.2340e-8
	neurotransmitter transport	163	3.5929e-8
	post-embryonic morphogenesis	194	1.3313e-7
	negative regulation of osteoblast differentiation	210	2.4558e-7
	neuron fate commitment	224	3.3178e-7
	hindbrain morphogenesis	235	4.7902e-7
	amino acid transport	237	4.8994e-7
	cerebellar cortex formation	242	6.7795e-7
	cerebellar cortex morphogenesis	266	1.2498e-6
	regulation of glucose import	276	1.4968e-6
	cerebellum morphogenesis	318	3.4938e-6
	phasic smooth muscle contraction	538	1.3465e-4
	positive regulation of cyclase activity	866	1.7868e-3

B	Term Name BRD3	Binom Rank	Binom Raw P-Value
	nuclear-transcribed mRNA catabolic process, nonsense-mediated decay	2	8.2904e-17
	translational termination	3	1.0945e-16
	viral gene expression	4	1.2119e-16
	viral transcription	5	1.2197e-16
	translational initiation	6	1.7752e-16
	macromolecular complex disassembly	8	1.0513e-15
	protein complex disassembly	9	6.3892e-15
	mRNA catabolic process	10	6.4423e-15
	cotranslational protein targeting to membrane	13	2.0498e-14
	SRP-dependent cotranslational protein targeting to membrane	14	2.5852e-14
	nuclear-transcribed mRNA catabolic process	15	2.6530e-14
	cellular protein complex disassembly	16	5.3215e-14
	RNA catabolic process	18	7.8900e-14

C	Term Name BRD4	Binom Rank	Binom Raw P-Value
	nucleosome assembly	95	9.9927e-15
	chromatin assembly	97	1.5326e-14
	translational initiation	100	2.5249e-14
	nucleosome organization	103	4.3927e-14
	chromatin assembly or disassembly	108	8.3127e-14
	viral gene expression	112	2.4672e-13
	viral transcription	114	4.7444e-13
	translational termination	116	5.8551e-13
	nuclear-transcribed mRNA catabolic process, nonsense-mediated decay	122	1.2576e-12
	protein complex disassembly	125	2.3847e-12
	macromolecular complex disassembly	128	4.3007e-12
	cellular protein complex disassembly	134	2.2688e-11
	nuclear-transcribed mRNA catabolic process	151	1.0472e-10
	viral life cycle	155	1.6694e-10
	growth hormone secretion	447	2.0598e-4
	positive regulation of circadian sleep/wake cycle, sleep	648	2.7256e-3

Figure 4.2.6 - Gene ontology analysis on the BRD-mediated effects of IBET-762 on gene clusters. The gene enrichment analysis shows the gene-clusters and their specific function, which are modulated upon IBET-762 administration, on each of the specific bromodomains: BRD2 (**A**), BRD3 (**B**) and BRD4 (**C**).

4.2.6 Early-gene modulation following IBET-762 administration

To evaluate whether the genes shown to be modulated and enriched by IBET-762 binding to BRD4 in VCaP prostate cancer cells were relevant to the U2OS cells, we assessed and quantified the expression of several genes reported hitherto. The early expression was also assessed to understand whether any of these genes were potentially upstream of the effects seen by IBET-762. Here we show that several of the selected genes are indeed modulated following IBET-762 administration. More specifically, genes that were shown to be potentially modulated in the ChIP-Seq study (**Figure 4.2.5**), such as *Bhlhe41* (DEC2), Hes Related Family BHLH Transcription Factor with YRPW Motif 1 (*Hey1*), *Tfeb* and *Bhlhe40* (DEC1) were also shown to be modulated following IBET-762 treatment. As an example, *Bhlhe41* showed a reduction of its expression, which was significant one hour after drug administration (27% reduction, p=0.0022), and showed an increased effect after two hours (41% reduction, p<0.0001), after four hours (60% reduction, p<0.0001) and after six hours (60% reduction, p<0.0001) (**Figure 4.2.7A**). *Hey1* showed a reduction trend at one hour after drug administration (17% reduction, ns), two hours after (20% reduction, ns), four hours after (30% reduction, p=0.0142), and six hours after (26% reduction, ns) (**Figure 4.2.7B**). Thus, only after four hours following drug administration, the reduction was significant. *Tfeb* also showed a decrease in gene expression, which was significant from two hours after IBET-762 administration (25% reduction, p=0.0075), as well as after four hours (43% reduction, p<0.0001), and after six hours (38% reduction, p=0.0004) (**Figure 4.2.7C**). *Bhlhe40* was also shown to be modulated, however the change did not seem to be significant within the early-hours analysis (**Figure 4.2.7D**).

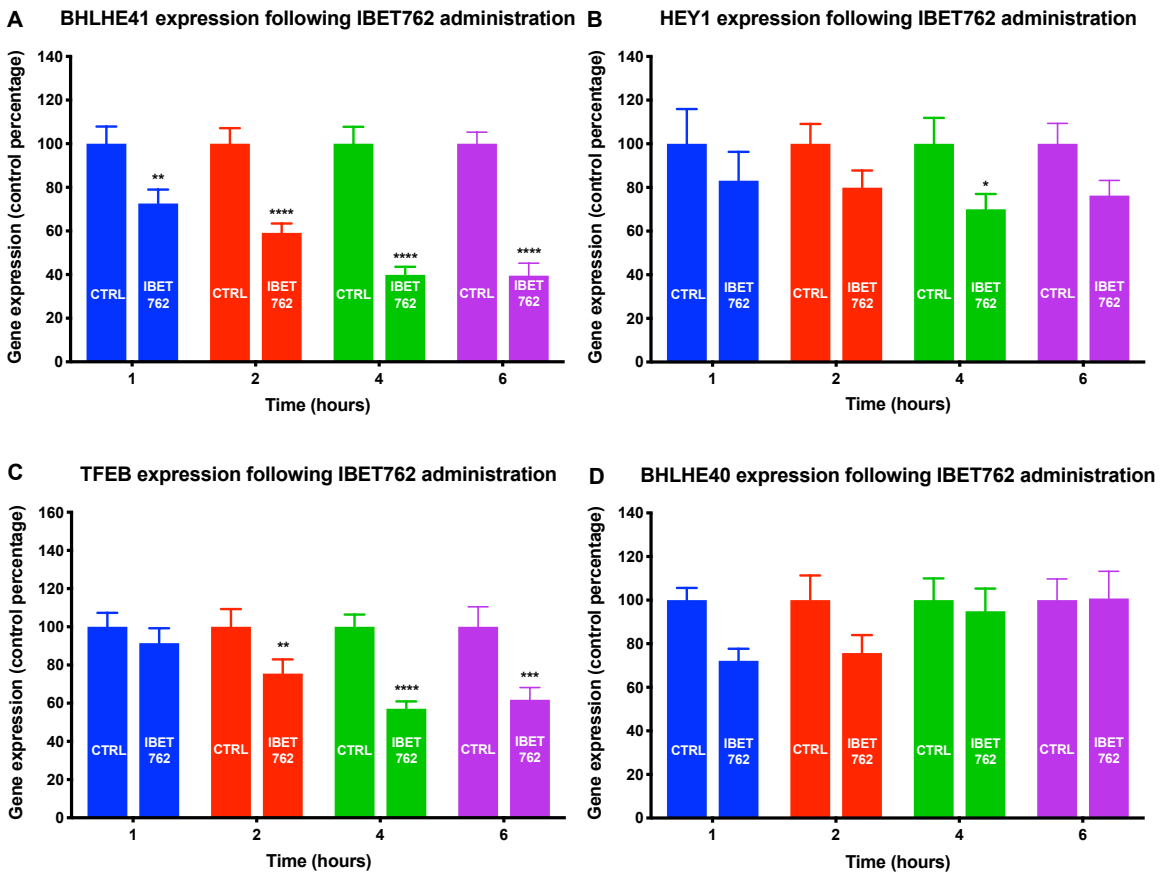


Figure 4.2.7 - Effects of IBET-762 on the early gene expression of selected genes, in U2OS cells (qPCR); data was expressed as average ± SEM (n=5). Potentially modulated genes were tested for their expression, including *Bhlhe41* (DEC2) (**A**), *Hey1* (**B**), *Tfeb* (**C**) and *Bhlhe40* (DEC1) (**D**). The data was analysed using a two-way ANOVA method and a Bonferroni posthoc multiple comparisons test. The data was normalized upon the levels of gene expression revealed for the DMSO treatment, within each timepoint, and the IBET-762 0.5µM modulation was expressed as an increase/decrease percentage over the DMSO treatment.

4.2.7 Effects of IBET-762 on TF modulation (U2OS screen)

To further assess the mechanism of action of IBET-762, and the transcription factors it modulates, we assessed the effects of 0.5μM IBET-762 on the most common eukaryotic transcription factors promoters, which have been transfected in a U2OS cell-line using a transcription factor reporter assay (**Figure 4.2.8**) . The results showed that IBET-762 was able to modulate the expression of a number of transcription factor binding sites; out of 45 transcription factors under evaluation, 13 were significantly modulated by IBET-762 (29% of all tested transcription factor binding sites). In order of magnitude, ETS-like-1 protein (*Elk1*) showed a 625% increase in expression (p<0.0001), Specificity Protein 1 (*Sp1*) showed a 620% increase (p<0.0001), Yin Yang 1 (*Yy1)* showed a 557% increase (p<0.0001), kruppel-like factor *4* (*Klf4*) showed a 410% increase (p<0.0001), activator protein 1 (*Ap-1*) showed a 363% increase (p<0.0001), early growth response protein *1* (*Egr1*) showed a 339% increase (p<0.0001), cAMP response element-binding protein (*Creb*) showed a 321% increase (p<0.0001), hypoxia-inducible factor 1 (*Hif1*) showed a 260% increase (p<0.0001), metal regulatory transcription factor 1 (*Mtf1*) showed a 200% increase (p<0.0001), CCAAT-enhancer-binding proteins (*C/ebp*) showed a 153% increase in expression (p<0.0001), whereas recombinant binding protein for immunoglobulin kappa J region (*Rbp-Jk*) showed a 110% increase (p=0.0059), and *Myc/Max* showed a 104% increase (p=0.012). The only transcription factor binding-site that was downregulated was nuclear factor Kb (*NfkB)*, which was significantly reduced (p=0.0014). The remaining of the transcription factor binding sites were non-significantly impacted by the drug addition.

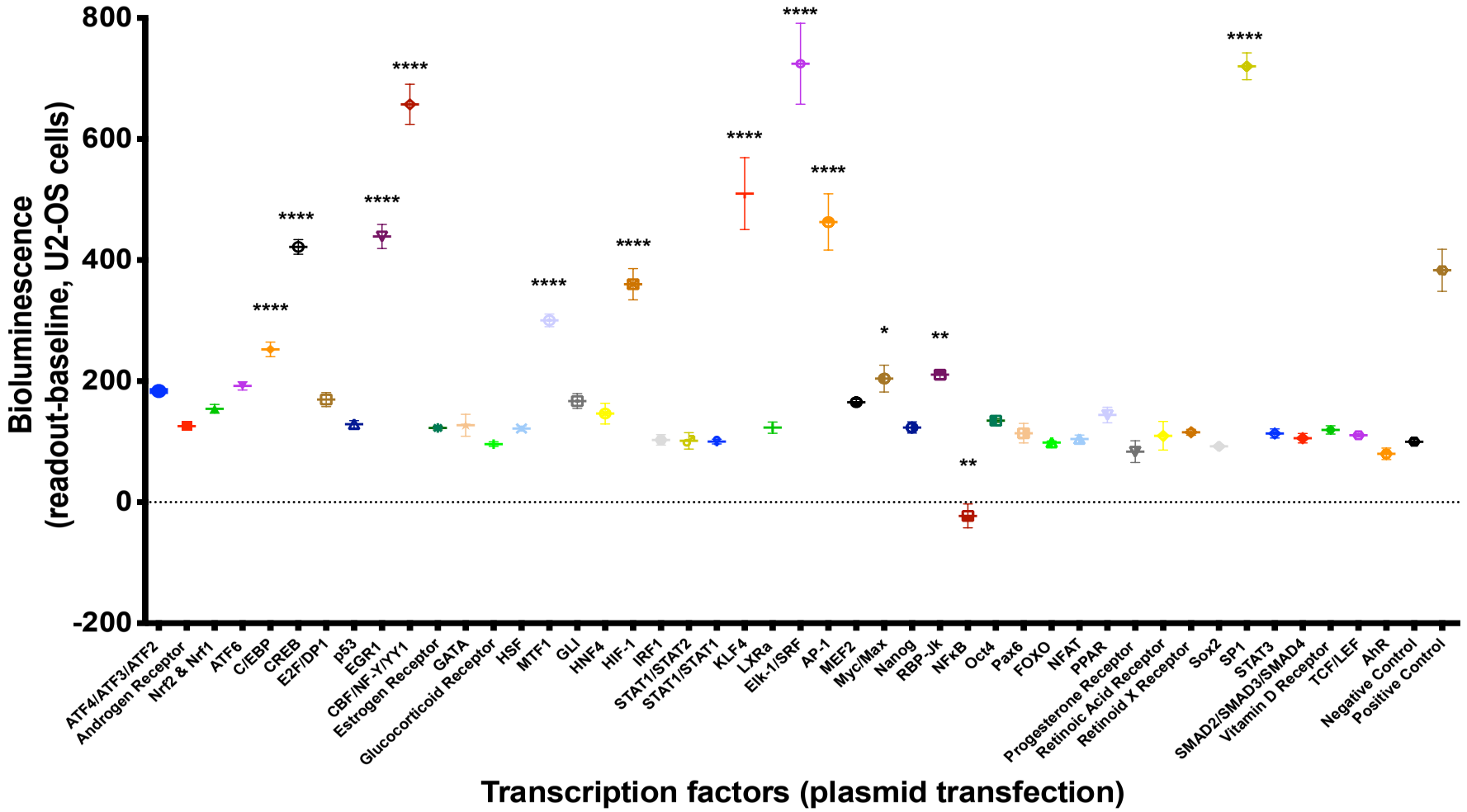


Figure 4.2.8 – TF modulation upon IBET-762 administration. 45 different TFs were transiently transfected in U2OS cells in duplicate. IBET-762 effects were evaluated as the drug was administered at a concentration of 0.5uM. The data was corrected upon a 6-hour baseline transfection, before the administration of the drug. The negative control consists of 0.5% DMSO, whereas the positive control is given by a transcription and luminescence activator. A one-way ANOVA and a Sidak-powered post-hoc multiple comparisons analysis tested the significance of the change in luminescence emission.

4.2.8 Circadian effects of IBET-762 on upregulated TFs knock-down

To evaluate which of the 13 TF identified above is important in mediating the circadian effects of IBET-762 treatment (**Figure 3.2.7**), we knocked-down selected transcription factors and evaluated the effects of IBET-762, on *Per2*:Luc U2OS cells (**Figure 4.2.9**). We tested the transcription factors' expression modulation by IBET-762, excluding the ones with minimal effects or affecting cell survival. We therefore tested the importance of MYC (**Figure 4.2.9A**), YY1 (**Figure 4.2.9B**), KLF4 (**Figure 4.2.9C**), SP1 (**Figure 4.2.9D**), MTF1 (**Figure 4.2.9E**), EGR1 (**Figure 4.2.9F**), ELK1 (**Figure 4.2.9G**), CEBPα (**Figure 4.2.9H**) and HIF1 (**Figure 4.2.9I**). Visually, we can assess that IBET-762 could still increase circadian amplitude under knock-down of MYC, YY1, KLF4, MTF1, EGR1, ELK1 and CEBPα, but its amplitude increasing effects were muted following knockdown of SP1 and HIF1. Furthermore, upon analysing the first day amplitude increase (**Figure 4.2.10**), we can see that only *Sp1* (6% decrease, ns), and *Hif1* (6% decrease, ns) knock-down eliminated the amplitude enhancing effects of IBET-762. *Egr1* (26% increase, p=0.0044), *Mtf1* (34% increase, p<0.0001), *Elk1* (24% increase, p=0.0018), *CEBPα* (20% increase, p=0.031), *Klf4* (48% increase, p=0.0005), *Yy1* (81% increase, p=0.0018), and *Myc* (44% increase, p=0.0018) have shown to be unrelated to the effects of IBET-762 on circadian amplitude increase, when compared to the IBET-762 increasing effects on the control group (39% increase, p<0.0001).

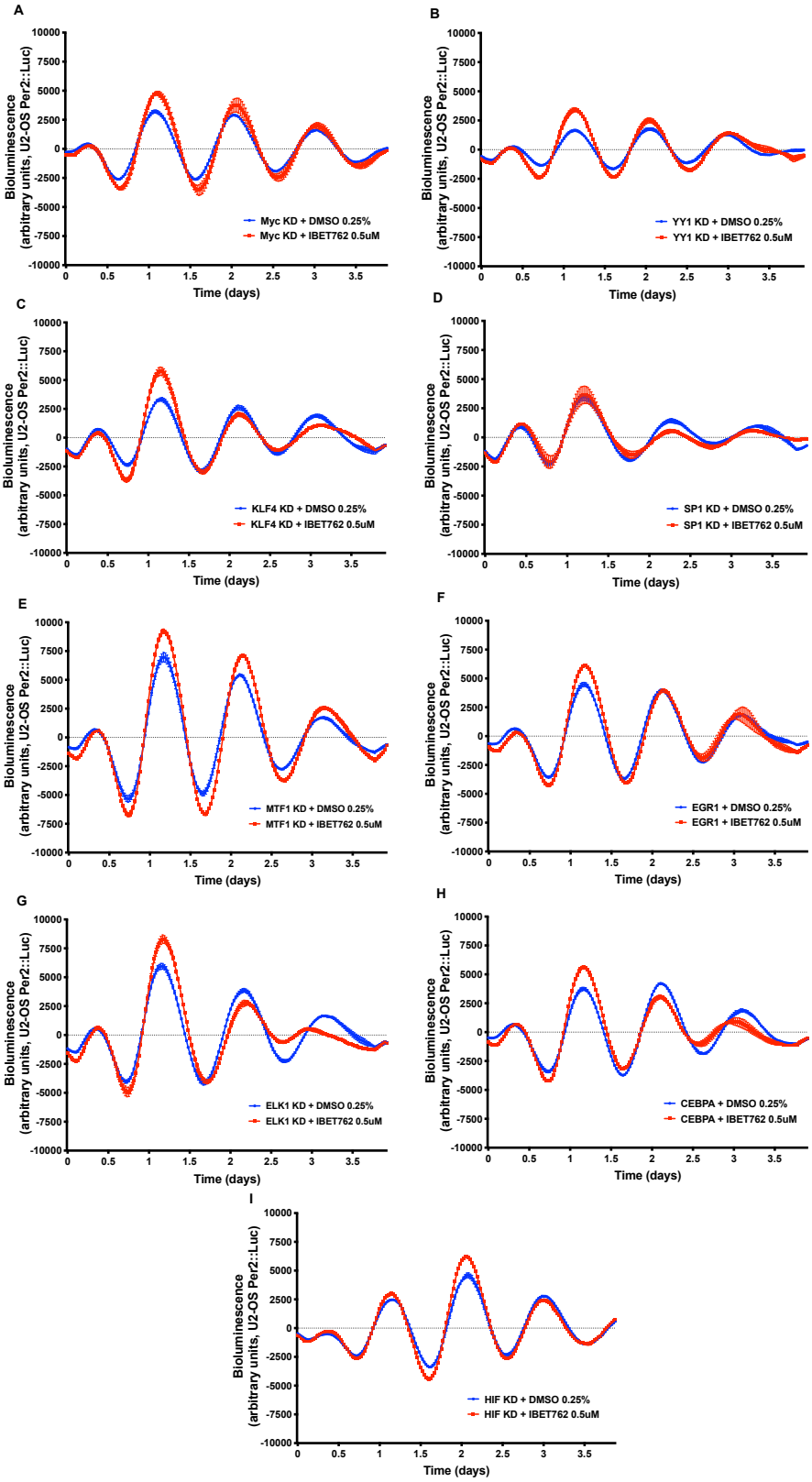


Figure 4.2.9 - Effects of transcription factor knock-down and IBET-762 0.5µM administration on circadian rhythms. U2OS cells were stably-transfected with a *Per2::*Luc promoter and period and amplitude were assessed over 92 hours of luminescence, following a 24-hour knockdown of transcription factors MYC (**A**), YY1 (**B**), KLF4 (**C**), SP1 (**D**), MTF1 (**E**), EGR1 (**F**), ELK1 (**G**), HIF1 (**H**) and CEBPα (**I**). Data was analyzed with the aid of the Multicycle software and was expressed in absolute mean values ± SEM and directly compared to the non-targeting control with or without IBET-762 administration (n=3).

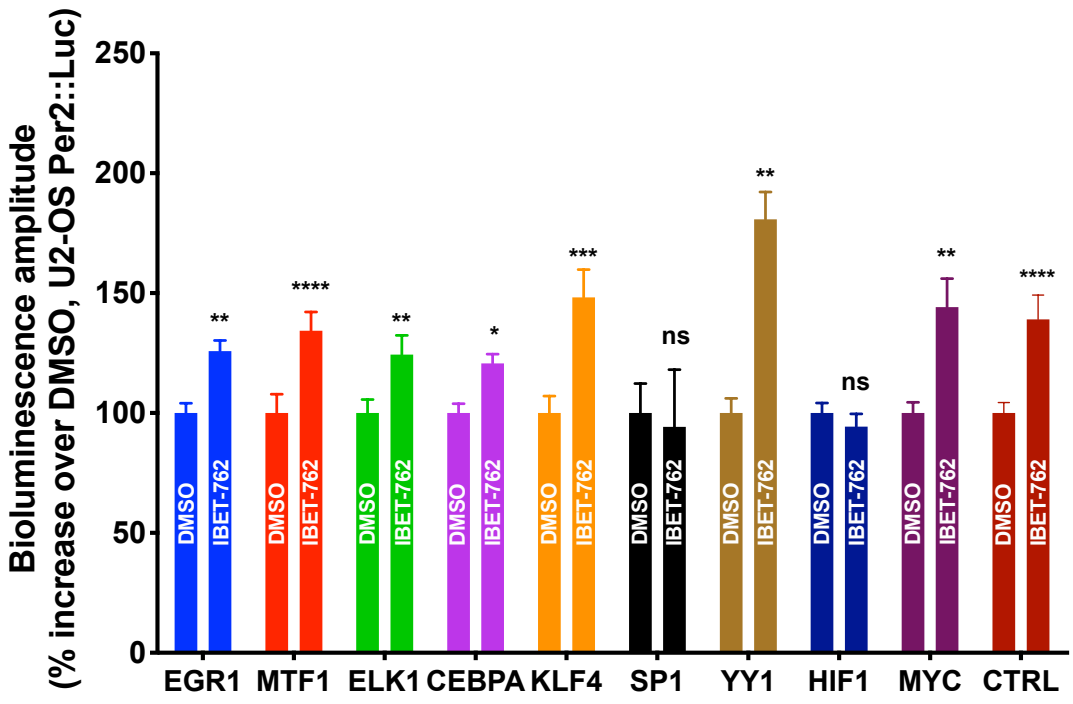


Figure 4.2.10 - Analysis of transcription factor knock-down over 0.5µM IBET-762 on circadian rhythms. U2OS cells were stably-transfected with a *Per2*::Luc promoter and period and amplitude were assessed over 92 hours of luminescence, following a 24-hour knockdown of transcription factors MYC, YY1, KLF4, SP1, MTF1, EGR1, ELK1, HIF1 and CEBPα. Data was analyzed through a two-way ANOVA and a Holm-Sidak post-hoc multiple comparison and the IBET-762 vs DMSO results were reported within each transfected group (n=3).

4.2.9 Effects of IBET-762 on SP1 and HRE promoter activity

To directly assess *Sp1* and *Hre* promoter activity and to interrogate the dose-dependency of IBET-762 administration, we conducted reporter luciferase assays with respective transcription factor element driving the expression of the luciferase reporter (**Figure 4.2.11**). With *Sp1*::Luc, IBET-762 caused a dose-dependent increase in expression of the luciferase reporter, with a maximum effect reached at 1μM with an 182% increase at ~30 min (p<0.0001) (**Figure 4.2.11A, 4.2.11C**), and a EC_{50} of $3.45e^{-6}$. The *Hre*::Luc assay showed a muted and delayed dose-responsive effect of IBET-762 (**Figure 4.2.11DB, 4.2.11D**), with the highest doses of 700nM and 300nM showing a 110% increase in amplitude (p<0.0001). Lower doses of 100nM and 70nM show a more contained increase of 30% (ns). The EC_{50} for the *Hre*::Luc activity increase was calculated at $2.56e^{-7}$. Given the dose-dependent effect of the drug on *Sp1*::Luc combined with the suboptimal increase of *Hre*::Luc, the drug seems to be more impactful on *Sp1* gene expression.

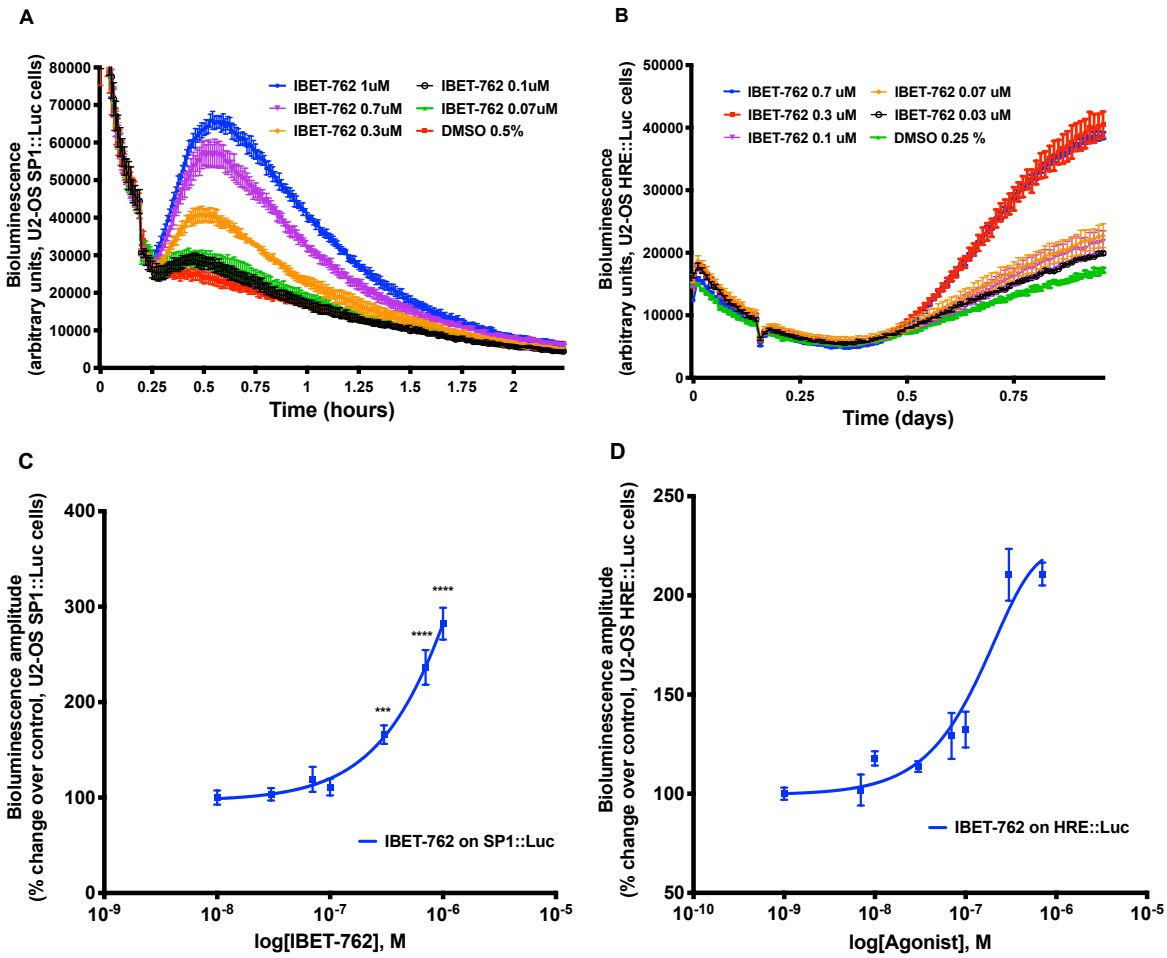


Figure 4.2.11 - Effects of IBET-762 on *Sp1*::Luc and *Hre*::Luc promoter expression. U2OS cells were stably-transfected with a *Sp1*::Luc or *Hre*::Luc promoter and gene expression were assessed over a short period of time, following a pharmacological dose-response treatment with IBET-762. The traces of luciferase gene expression are portrayed for IBET-762's effects on *Sp1*::Luc (**A**) and *Hre*::Luc (**B**) promoter. A dose-response curve was drawn for the effects of IBET-762 on *Sp1*::Luc (**C**) and Hre::Luc (**D**) promoter at peak expression, on a semi-logarithmic scale. Data was analyzed through a one-way ANOVA and a Dunnett post-hoc multiple comparison and the IBET-762 vs DMSO results were reported within each transfected group (n=3).

4.2.10 Epigenetic specificity of *Sp1*::Luc and *Hre*::Luc expression

To understand whether the *Sp1*::Luc and *Hre*::Luc activity are bromodomain dependant, or a generic response to epigenetic modulation, we investigated the role of several other epigenetic modulators in increasing the expression of the two reporter luciferases.

With regards to the *Sp1*::Luc analysis, we could find four drugs that were able to significantly increase the expression of the gene reporter at four hours after drug administration, (**Figure 4.2.12**). Three out of the four drugs that were able to significantly increase *Sp1*::Luc expression were bromodomain inhibitors (+)-JQ1 (38% increase, $p<0.0001$), PFI-1 (13% increase, $p=0.024$), and IBET-762 (116% increase, $p<0.0001$), with the exception of anacardic acid (10% increase, $p=0.0046$). Importantly, (-)-JQ1, the bromodomain-inactive variant of the drug, does not have any activity on the *Sp1*::Luc promoter (2% increase, ns). Regarding the *Hre*::Luc analysis, there were a few targets with respect to the increase in expression of the reporter luciferase, at 12 hours after drug administration (**Figure 4.2.13**).

The activity of the *Hre* reporter luciferase was enhanced by 15 out of the 80 tested drugs: among these, 8 were HDAC inhibitors, such as SB939 (518% increase, $p<0.0001$), suberohydroxamic acid (317% increase, $p<0.0001$), apicidin (184% increase, $p=0.0182$), 4-iodo-SAHA (333% increase, $p<0.0001$), CAY10398 (248% increase, $p<0.0001$), AGK2 (465% increase, $p<0.0001$), splitomicin (455% increase, $p<0.0001$), and CBHA (268% increase, $p<0.0001$), further confirming the impact of HDAC inhibition on hypoxia-mechanisms. Other hits shared demethylase inhibition as a mechanism of action, such as 2-PCPA (345% increase, $p<0.0001$), and 2,4-Pyridinedicarboxulic acid

(385% increase, p<0.0001), and others were methyltransferase inhibitors such as UNC0321 (337% increase, p<0.0001), chaetocin (290% increase, p<0.0001), and AMI-1 (366% increase, p<0.0001). Other two drugs did not fit within these three main categories, such as mirin (MRN-ATM complex inhibitor, prevents ATM activation following ds-DNA breaks associated with heterochromatin (Goodarzi *et al.*, 2008)) (334% increase, p<0.0001), and (-)-Neplanocin-A (SAH-hydrolase inhibitor, affecting cellular methylation mechanisms (Chiang, 1998)) (303% increase, p<0.0001). It is important to notice that bromodomain inhibition does not seem to play a decisive role in *Hre*::Luc regulation on the epigenetic modulation in stark contrast to *Sp1*::Luc activation.

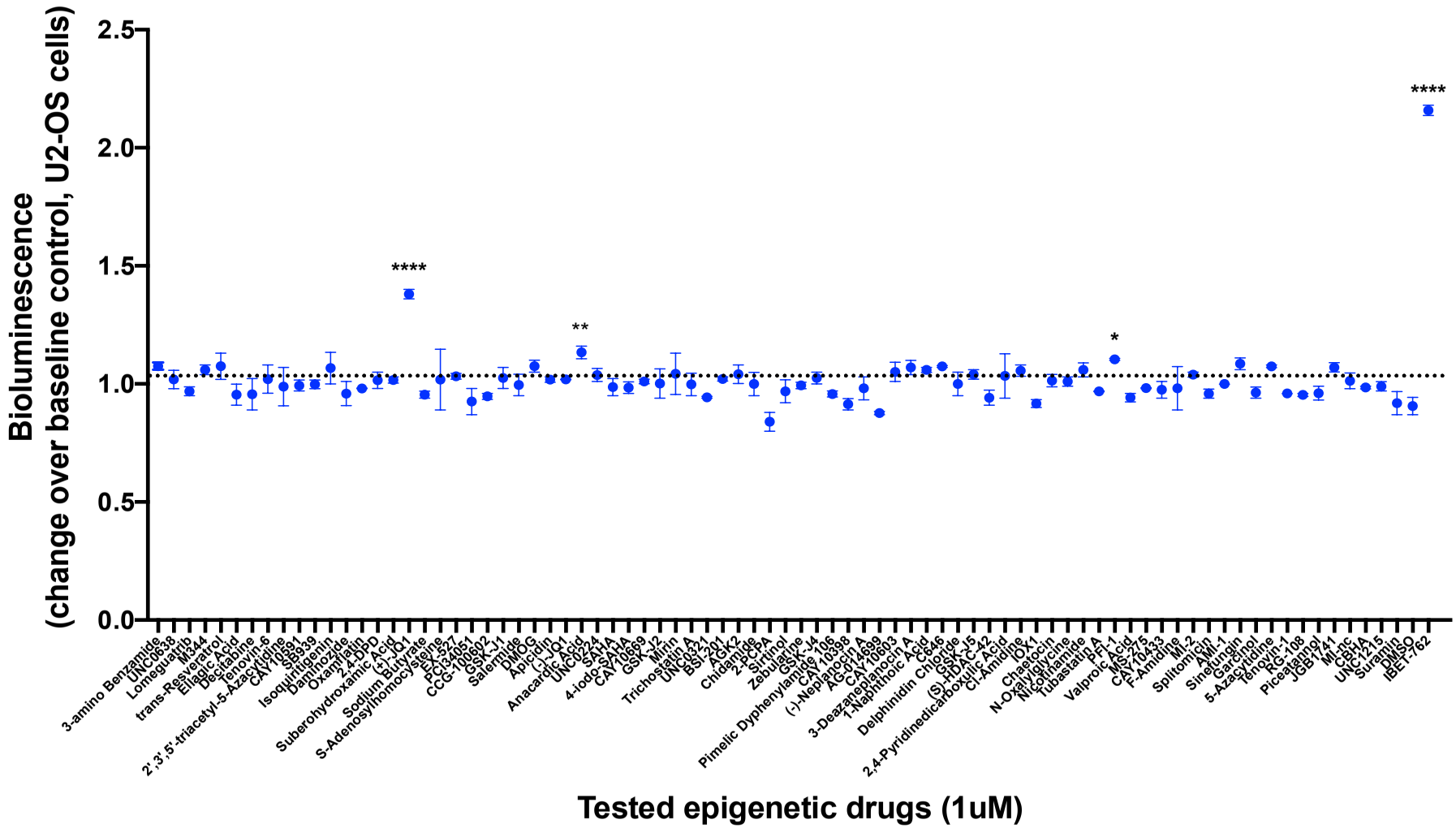


Figure 4.2.12 - Effects of epigenetic modulators on *Sp1*::Luc promoter expression. U2OS cells were transiently-transfected with an *Sp1*::Luc promoter and its expression was assessed before (as a baseline) and after the administration of 80 different epigenetic modulators, at an 1µM concentration. Data was normalized over the initial 3-5 hour baseline and was expressed as a % change over a DMSO control ± SEM. Significance threshold was set at DMSO + 3SD (demarked by an interrupted line).

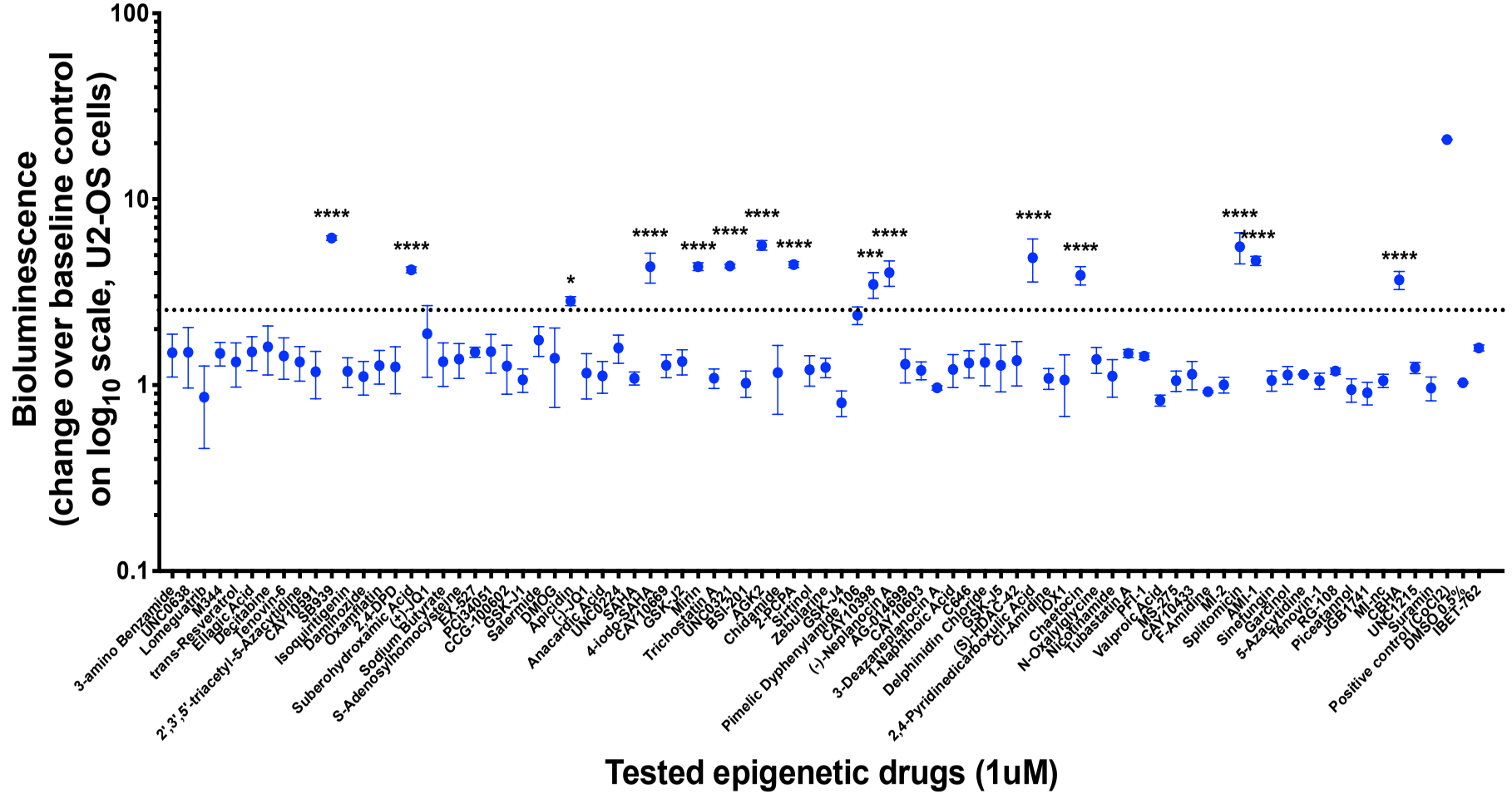


Figure 4.2.13 - Effects of epigenetic modulators on *Hre*::Luc promoter expression. U2OS cells were transiently-transfected with an *Hre*::Luc promoter and its expression was assessed before (as a baseline) and after the administration of 80 different epigenetic modulators, at an 1µM concentration. Data was normalized over the initial 3-5 hour baseline and was expressed as a % change over a DMSO control ± SEM. Significance threshold was set at DMSO + 3SD (demarked by an interrupted line).

4.2.11 *Bmal1* promoter transcription factor sites analysis (Transfac)

Given the importance and specificity of *Sp1*::Luc activity increase after administration of bromodomain inhibitors such as IBET-762 (**Figure 4.2.10**, **Figure 4.2.12**), we were interested to further understand whether there is evidence showing the presence of *Sp1* binding sites within the promoter of *Bmal1* gene, which was shown to be upregulated after IBET-762 administration (**Figure 3.2.7B/D**, **Figure 3.2.8A**, **Figure 3.2.9A**). More specifically, we wanted to understand whether there were *Sp1*-binding sites in the promoter of the gene that showed to be upregulated in circadian rhythm amplitude enhancer, such as *Bmal1*.

The Transfac analysis showed evidence of *Sp1*-binding sites on both the mouse sequence of the *Bmal1* promoter used in stably transfected U2OS cells (**Figure 4.2.14A**), as well as in the more generic promoter sequence of the *Homo Sapiens Bmal1* gene (**Figure 4.2.14B**). More specifically, the 'GGGCGGG' *Sp1*-binding sequence, a GC-box element, is shown to be located both in position -34bp and +2bp from the *Bmal1* transcription-start site (TSS) (**Figure 4.2.14A**). Besides being very close to the TSS and possibly modulating its transcription, there is also experimental ChIP-Seq evidence showing the physical binding of proteins on those specific sites. The 'GGGCGGG'-sequence can also be seen at the same location within the *Bmal1* promoter-sequence used in the stable transfection of U2OS cells (**Figure 4.2.14A**), further consolidating the role of SP1 in mediating the effects of *Bmal1* circadian amplitude increase.

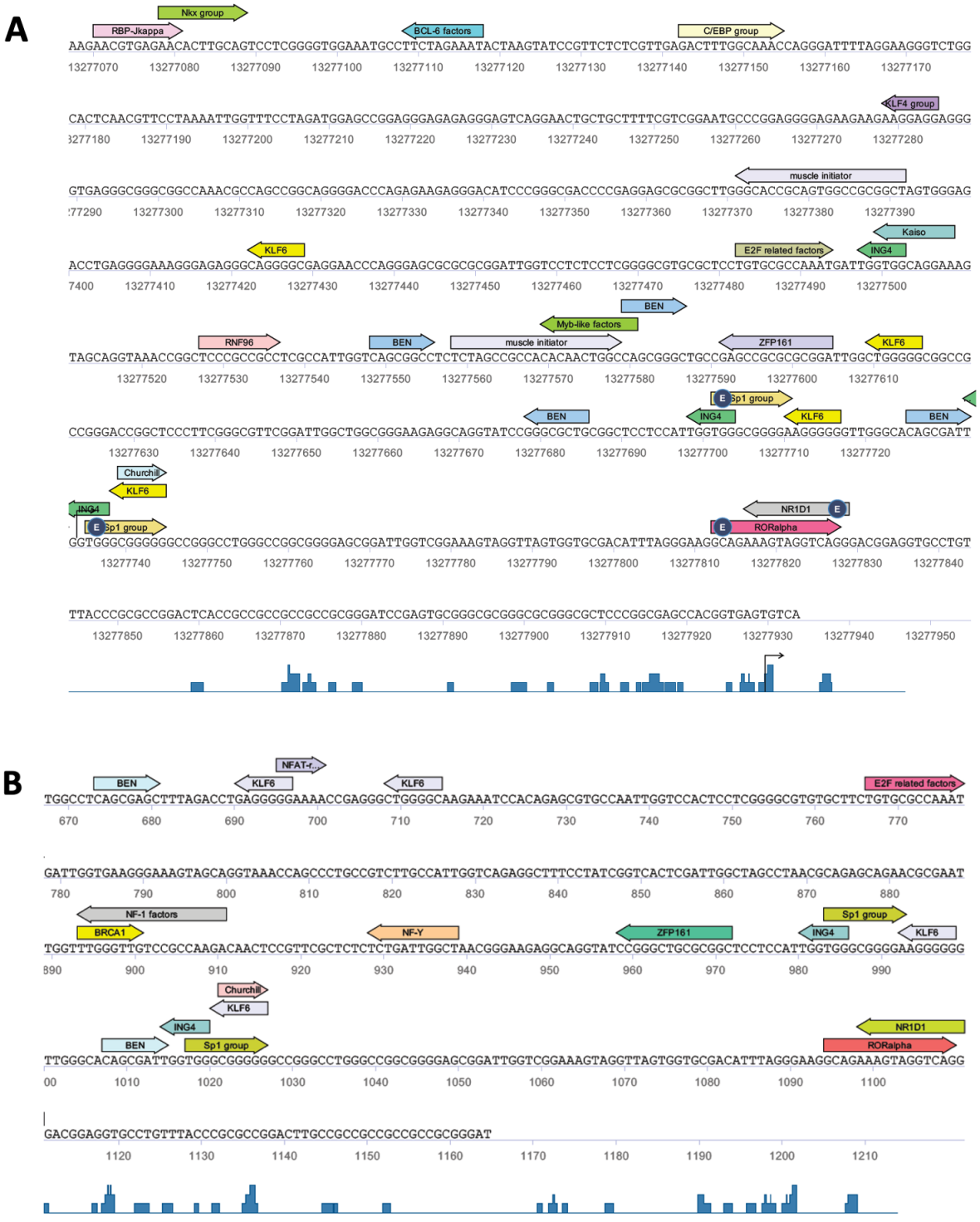


Figure 4.2.14 - Transfac analysis of transcription factor binding on the promoter region of *Bmal1*. The promoter region of *Arntl* (BMAL1) is portrayed with the binding sites of all known transcription factors highlighted (**A**). The SP1, NR1D1, and RORa binding sites show experimental evidence of binding from literature-based ChIP-Seq studies, near the transcription site. The promoter region stably-transfected within the U2OS *Bmal1*::Luc cell-line is also shown (**B**), with the theoretic binding sites of all transcription factors highlighted.

4.3 DISCUSSION

We have previously shown that the effects of bromodomain inhibitors on circadian amplitude are mediated specifically via bromodomains, given that the negative control of JQ-1, a bromodomain inhibitor, was not able to increase circadian amplitude (**Figure 3.2.6**). To understand which of the bromodomains can enhance circadian amplitude, we have sistematically knocked-down BRD2, BRD3, BRD4 and BRDT through siRNA, and assessed the effects of the knock-down on circadian gene reporter activity of *Bmal1* and *Per2* (**Figure 4.2.1**).

The knockdown results showed that the BRD4 knock-down was able to increase the amplitude of *Per2*::Luc expression significantly (**Figure 4.2.1G**, **Figure 4.2.2B**), but not of *Bmal1*::Luc (**Figure 4.2.1C, Figure 4.2.2A**). However, BRD4 knock-down qualitatively increased period in both *Bmal1* and *Per2* stably-transfected U2OS cells (**Figure 4.2.1C/G**). This is in line with our previous results showing the effects of (+)JQ-1, in both increasing amplitude and period of U2OS *Bmal1*::Luc transfected cells (**Figure 3.2.6A/C**), however BRD4 knock-down alone did not increase *Bmal1* amplitude. Given that IBET-762 also inhibits BRD2, BRD3 and BRDT, it is possible that the wider effects of the drugs could be given by the overarching inhibition of all bromodomains. It was indeed shown that BRD2 and BRD3 have some functional redundancy (LeRoy *et al.*, 2008), characteristic which can be possibly shared by BRD4 as well. Thus, the knock-down of BRD4 can be overcome by the input of the intact bromodomains. The effects of BRDT knock-down are also noticeable on circadian rhythms' gene activity of both *Bmal1* and *Per2* reporters, however the knock-down

decreased the amplitude of the reporter activity (**Figure 4.2.1D/H**, **Figure 4.2.2A/B**). As the BRDT knock-down results are not in line with the amplitude enhancing effects of IBET-762, this suggests that IBET-762 has little affinity for BRDT. If we examine the efficiency of bromodomain knock-down in U2OS cells, we can see that the silencing was specific and efficient (82% to 88% downregulated) (**Figure 4.2.3**). These results are considered acceptable to be able to observe the consequences of a specific gene on a phenotypic assay and for proof of concept. Collectively taken together our evidence indicate BRD4 is playing a dominant role in mediating the effects of IBET-762 on amplitude increase, though some of its effects could be overlapped with the effects of BRD2/BRD3 knockdown. Our results on BRD4 being the critical mediator if IBET-762 is further supported by evidence demonstrating BMAL1 could elicit the binding of BRD4-TEFb complex to regulatory regions of the chromatin, stimulating the expression of downstream circadian genes (Petkau *et al.*, 2019).

As all four bromodomain proteins of the BET family contain both BD1 and BD2 domains, to evaluate their relative importance in mediating the drug's effects, we used two drugs with very different specificities towards these domains present within BRD4 (**Figure 4.2.4**). In fact, it was shown that drugs that bind to the two domains with different selectivity, can have vastly differential biological effects; RVX-208 showed to reduce vascular inflammation in cardiovascular diseased (CVD) patients (Tsujikawa *et al.*, 2019) and Olinone showed to enhance oligodendrocite differentiation (Chiang, 2014).

As RVX-208 is more specific towards BD2 (Picaud *et al.*, 2013), it showed to mediate both amplitude and period increase. Olinone, a specific BD1-inhibitor (Chiang, 2014), although increased circadian amplitude, this was somewhat limited in its dose-dependency. Thus, BD2-binding is more likely to mediate the effects of bromodomain inhibitors on circadian rhythms.

To understand which DNA areas IBET-762 exerts its action as a bromodomain inhibitor, we have analyzed a ChIP-Seq study that looked at the binding of BRD2/3/4 to the human genome, in presence or absence of IBET-762 (Asangani *et al.*, 2014). The results showed that, unbiasedly, E-box regions (3'-CACGTG-5') were enriched in both BRD2 and BRD4 binding, in absence of IBET-762 (**Figure 4.2.5A/C**). The Homer analysis predicted that genes of the circadian clock, such as Neuronal PAS Domain Protein 2 (*Npas2*, a *Clock* paralogue), *Bmal1*, *Clock*, *Bhlhe40* (DEC1), *Bhlhe41* (DEC2), but also other bHLH-domain containing genes such as *c-Myc*, *Hif1* and Upstream Transcription Factor 1 (*Usf1*) could be modulated by IBET-762, through a bromodomain action. This confers confidence of the modulatory effects of IBET-762 on the circadian clock. The overlap in E-box modulatory effects of IBET-762 on BRD2 and BRD4 suggests that there might be some overlapping functionality of these two bromodomains. A further gene ontology analysis, looking at which of the three bromodomains (BRD2, BRD3 and BRD4) mediate the modulation of cellular functionalities, also underlined the importance of IBET-762 on the BRD4-mediated impact on the positive regulation of circadian sleep/wake cycle (**Figure 4.2.6C**). Other biological processes were also modulated by IBET-762's BRD2-binding inhibition on white fat cell differentiation, and the regulation of glucose import (**Figure 4.2.6A**),

aspects which will be further investigated as potentially related to the effects of circadian modulation.

To assess whether the E-Box-containing genes that were predicted to be modulated by IBET-762 from the ChIP-Seq study in VCaP prostate cancer cells, were also modulated by IBET-762 in U2OS cells, we assessed the early-stage modulation of several of these genes considered relevant to our study using RT-PCR (**Figure 4.2.7**). Some of the genes such as *Bhlhe41* and *Tfeb* were indeed found to be modulated within the first six hours of IBET-762 administration. This evidence shows that the effects of IBET-762 on important genes of the circadian clock, such as *Bhlhe41*, might bring forward a direct impact on the cellular circadian functionality.

To further characterise the mechanism of action of IBET-762, we evaluated the effects of 0.5μM of the drug on the activity of 45 common transcription factors (**Figure 4.2.8**). Of the 45 tested TFs, 12 demonstrated an increased activity and one reduced it. Out of the 13 modulated transcription factors, we tested 9 for their role in mediating the effects of IBET-762 on the circadian clock (**Figure 4.2.9**). The *Sp1* knock-down abolished the amplitude-increasing effect of IBET-762 (**Figure 4.2.9D**, **Figure 4.2.10**), whereas the *Hif1* knock-down limitedly abolished the effects of the drug only during the first day, but not during the subsequent days (**Figure 4.2.9I**, **Figure 4.2.10**). This underlines the importance of SP1 in mediating the effects of IBET-762 on the circadian clock. The putative importance of SP1 as a regulator of circadian rhythms is evinced from further evidence showing that GC-rich motifs (present in the SP1-binding sites) are significantly enriched in promoter regions of circadian controlled genes (Bozek *et al.*, 2009).

Additional evidence has pinpointed a number of transcription factors that could be influencial in the regulation of circadian oscillating genes in mouse tissues, including SP1 (Yan *et al.*, 2008).

To further assess the modulation of SP1 and HIF1 by IBET-762, we tested transiently-transfected U2OS cells with the two promoter reporters *Sp1*::Luc and *Hre*::Luc followed by IBET-762 administration (**Figure 4.2.11**). The effects of IBET-762 on the activity of *Sp1*::Luc and *Hre*::Luc were dose-dependent.

We also tested the specificity of both the *Sp1*::Luc and *Hre*::Luc increase in activity over an array of 80 epigenetic modulators (the same 80 epigenetic modulators assessed for effects in modulating circadian rhythms) (**Figure 3.2.1**, **Figure 3.2.2**). From the *Sp1*::Luc screen, bromodomain inhibitors were the only drugs to activate the expression of this promoter reporter within 4 hours following drug administration, making this an early response gene (**Figure 4.2.12**). The only other epigenetic modulator outside of BRD class that augmented the activity of *Sp1*::Luc significantly was anacardic acid, possibly due to non-specific effects of the drug (Park *et al.*, 2018). On the other hand, the *Hre*::Luc activity was modulated by several classes of epigenetic modulators, as 15 out of the 80 drugs tested were shown to increase activity significantly (**Figure 4.2.13**), indicating a generic effect of epigenetic modulation. Further, given the 12 hours delayed effect, we can attribute the *Hre*::Luc increase of epigenetic modulators to undirect mechanisms. Moreover, IBET-762 did not impact on the activity of *Hre*::Luc significantly, when assessed jointly with the rest of the epigenetic modulators. Given previous strong evidence of SP1 being a transcriptional modulator on hypoxia-response elements

(HREs), it is plausible that the HREs are modulated following SP1 activity increase, and acts on cellular mechanisms as a secondary effector (Iyer *et al.*, 1998; Kim & Park, 2010). Furthermore, past evidence shows that the expression of both SP1 and HIF1 are needed in order to elicit some of the HIF1's hypoxic effects and they serve a vital role as co-regulators in some cancers (Liu *et al.*, 2016) and HIF1 could influence the binding of SP1 to other transcription factors and the effects it elicits (Koshiji *et al.*, 2005). This evidence suggests an interlink between SP1 and HIF1, underlining their influence in co-regulating analysed aspects of the cellular and physiological impact of IBET-762.

To understand whether the *Sp1*-binding site was expressed in genes of the molecular clock, we examined the *Per2* and *Bmal1* promoters. The Transfac analysis showed the sequence sites which were predicted to bind specific transcription factors. Moreover, for the human *Bmal1* promoter, further information on experimental evidence from ChIP-Seq studies showed which transcription factors were actually bound to their DNA sequences of interest. Both the human and mouse *Bmal1* promoters showed two *Sp1*-binding sites at -34bp and +2bp from the TSS. Although the binding of the transcription factor could not be influencial in impacting on gene expression, taken together with previous evidence of E-box binding modulation and the SP1 TF importance, it is likely that the *Sp1*-binding sites could be of impact on the transcriptional regulation of the gene (**Figure 4.2.14**).

Further evidence of the putative importance of *Sp1*-binding sites in mediating the amplitude increase of IBET-762 come from previous work showing selenium to downregulate the binding of Transforming Growth Factor-B Inducible Early Gene 1

(TIEG1, a transcriptional repressor belonging to the SP1 family) to SP1-binding sites on the *Bmal1* promoter, driving thus *Bmal1*::Luc expression (Hirota *et al.*, 2010). An anti-toxicity effect was further shown in mice, with the effect being removed in Clock-mutant mice, suggesting the molecular clock is fundamental in mediating such protection (Hu *et al.*, 2011). Furthermore, the effect of selenium was shown to be tissue-specific, affecting the liver but not the SCN, allowing thus for an interdependent modulation of tissue physiology and an increased specificity of the drugs' effects. These findings are in line with other circadian modulators found to have different effects across several tissues, possibly owning it to the tissue-specific plethora of genes that are differentially expressed across tissues (Chen *et al.*, 2012b).

Taken together, the evidence suggests that IBET-762 regulates circadian gene transcription through the modulation of the activity of BRD4 and SP1 transcription factor (**Figure 4.1.4**). It would be important to assess what other implications the SP1 modulation brings about within a physiological system.

⇒ Amplitude enhancing effects of IBET-762 on *Bmal1* (**Fig. 3.2.7-9**)

⇒ Circadian amplitude enhancing effects of BRD4 KD (**Fig. 4.2.1**, **Fig. 4.2.2**)

⇒ Enrichment of E-Box sequences upon differential BRD motif analysis (**Fig. 4.2.5**)

⇒ Early upregulation of *Sp1*::Luc activity upon IBET-762 administration (**Fig. 4.2.8**)

⇒ SP1 knock-down on lack of IBET-762 amplitude enhancement (**Fig. 4.2.9-10**)

⇒ Presence of *Sp1*-binding sites (GC-boxes) within the *Bmal1* promoter (**Fig. 4.2.14**).

CHAPTER III

METABOLIC PHENOTYPING OF BROMODOMAIN INHIBITORS

main findings:

IBET-762 modulates expression of several metabolic genes in U2OS cells and adipocytes

IBET-762 decreases 3T3-L1 adipocyte differentiation and expression of adipogenesis markers

IBET-762 decreases SP1-mediated glucose uptake, lactate production and lipolysis

IBET-762 lowers glycolytic and mitochondrial ATP and increases NAD+/NADH ratio

5 Chapter III: METABOLIC PHENOTYPING OF BET INHIBITORS

5.1 INTRODUCTION

5.1.1 Cellular hallmarks of adipocytes and obesity

Obesity is characterised by an increase in the mass of the adipose tissue, by either an increase in the size of existing adipocytes (hypertrophy) or by the formation of new adipocytes (adipogenesis) through differentiation of precursors known as preadipocytes. Hypertrophy can increase the size of adipocytes to several hundred micrometres in diameter, and is believed to be the main cause of obesity in adults. However, recent rodent-studies have shown that new adipocytes can be formed through *de novo* adipogenesis, from precursors, and contribute to epididymal adipose tissue expansion, in long-term caloric-excess diets (Wang *et al.*, 2013). These pre-adipocyte precursors are fibroblast-like cells located in the perivasculature (Tang *et al.*, 2008). Hypertrophy of adipocytes is also associated with an increase in hypoxia in their cellular environment, which is mediated by HIF1. However, the lack of oxygen and action of HIF1 are not sufficient to explain the phenotype associated with obesity including tissue fibrosis, necrosis and inflammation (Skurk *et al.*, 2007). These factors can promote an unhealthy physiology of adipocytes, allowing for a reduction in their functionality and a subsequent increase in the concentration of blood sugars and fats, which can sediment on different organs as ectopic fat deposits (**Figure 5.1.1**), promote insulin resistance (Halberg *et al.*,

2009; Lonn *et al.*, 2010) and elevated lipolysis (Laurencikiene *et al.*, 2011), among other possible outcomes.

5.1.2 White adipose tissue (WAT) and brown adipose tissue (BAT)

The development of obesity in addition to being dependent on the balance between food intake and exercise, also depends on the balance between white adipose tissue (WAT) and brown adipose tissue (BAT). BAT and WAT have opposing functions, with WAT storing excessive fat as triglycerides, providing insulation and mechanical cushioning, and is responsible for driving the increase in obesity. BAT is specialised in dissipating its stored energy as heat, and is more common in small mammals and new-borns. More recently, it has been noted that BAT can also be found in adults, with higher quantities of BAT being associated with a lower body weight and potentially playing an active role in energy homeostasis. Moreover, higher levels of BAT activity can protect from obesity, insulin resistance and cardiovascular diseases (Mattson, 2010), possibly due to the brown adipocytes' active metabolism and their utilization of high amounts of glucose. Browning of WAT (beige fat) is also known to have anti-obesity and antidiabetic effects in rodents (Wu *et al.*, 2013a). Whilst WAT is known to form most of the subcutaneous and visceral fat, higher proportions of BAT can be found throughout the cervical, supraclavicular, axillary, paravertebral, mediastinal and upper abdominal regions (Wehrli *et al.*, 2007), including in adult humans, where it is seemingly activated by cold temperatures and sympathetic signalling (van Marken Lichtenbelt *et al.*, 2009; Virtanen *et al.*, 2009).

Besides their functionality differences, the two adipocytes are also different structurally. White adipocytes are spherical cells and their size is functional to the size of the lipid droplets that they store. This lipid droplet is formed of triglycerides and accounts for about 90% of the cell volume. Brown adipocytes contain multiple lipid droplets, of smaller sizes, and are typically polygonal and of variable sizes. BAT also packs numerous mitochondria and capillaries, due to their greater oxygen demand (Cinti, 2009). They produce heat by uncoupling mitochondrial oxidative phosphorylation from ATP production, as a consequence of a transmembrane proton leak mediated by uncoupling protein 1 (UCP1) (Gesta *et al.*, 2007).

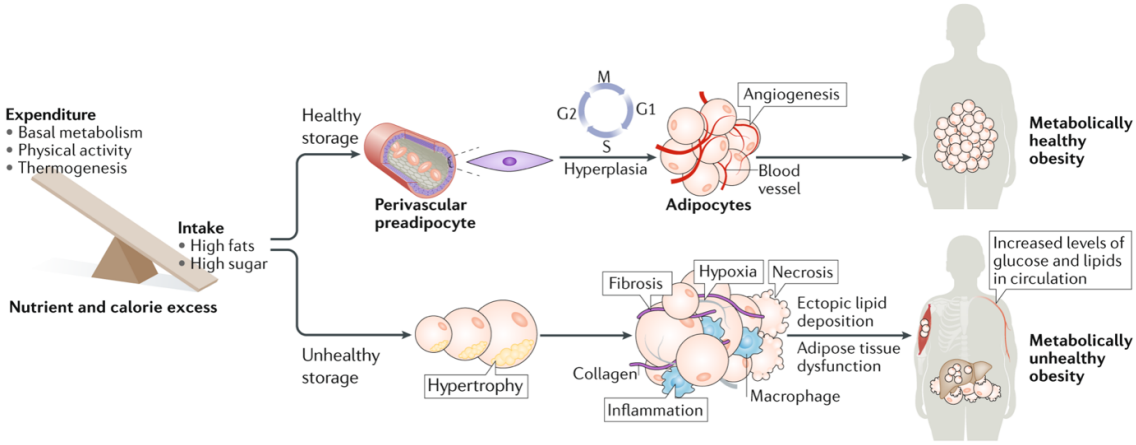


Figure 5.1.1 – Modalities of adipose tissue expansion. Different ways of adipocyte expansion through healthy storage (hyperplasia or formation of new adipocytes) or unhealthy storage (hypertrophy of existing adipocytes). Hypertrophy of adipocytes can stimulate inflammation and underperformance of the cells, allowing for an increased concentration of glucose and lipids in circulation. Adapted from Ghaben *et al.,* 2019

The localization and molecular characteristics of fat are also pivotal in understanding its impact on the whole body physiology; in fact, intra-abdominal visceral fat is associated with insulin resistance, whereas accumulation of subcutaneous fat has no adverse effects on the diabetic phenotype and may protect against the metabolic syndrome (Fox *et al.*, 2007; Tran *et al.*, 2008), with molecular rather than localization differences possibly explaining their opposing roles. Visceral adipocytes were indeed shown to have increased

rates of lipolysis and apoptosis (Lafontan & Girard, 2008), owning it possibly to differential gene expression signatures and response to environmental and genetic stimuli (Macotela *et al.*, 2012). Visceral fat is also characterised by a chronic low-grade inflammatory state, with higher-than normal levels in gene expression of several inflammatory cytokines, such as Tumour Necrosis Factor α (TNFα) (Hotamisligil *et al.*, 1993), as well as infiltrations of the adipose tissue with macrophages and leukocytes.

5.1.3 Cellular differentiation and functionality of adipocytes

As producers of leptin, adipocytes have been dubbed as whole-body regulators of energy homeostasis, and their overabundance was also correlated with certain cardiovascular disorders (Lau *et al.*, 2005). As addressed above, adipocytes have evolved to have a have specific cellular physiology, which can be pinpointed through the expression of a set of genes that are specific to their functionality. The expression of these genes is enhanced upon adipocyte differentiation, a process that has long focused on the role of the nuclear receptor peroxisome proliferator-activated receptor gamma PPARɣ and the CCAT-enhancer binding proteins (C/EBP) family members as master regulators. PPARɣ is known to be both necessary and sufficient for adipogenesis without which adipogenesis cannot be promoted, and several factors were shown to have an anti-adipogenic effect by inhibiting PPARɣ expression (Tong *et al.*, 2000; Tontonoz *et al.*, 1994). Furthermore, PPARɣ expression is also essential for the maintenance of the differentiated status in adipocytes (Imai *et al.*, 2004). C/EBP is also pivotal in stimulating adipogenesis, and this is thought to be due, in the case of the β and gamma isoforms, by stimulating PPARɣ expression (Tanaka *et al.*, 1997), however, the α isoform may stimulate adipogenesis independently (Linhart *et al.*, 2001). Furthermore, up to 60% of the gene expression

modulated by the two transcription factors overlap, underlying intricate co-regulatory mechanisms (Lefterova *et al.*, 2014; Wu *et al.*, 2013a). Cluster of differentiation 36 (*Cd36*) and resistin (*Retn*) are examples of WAT-specific genes whose expression is directly regulated by PPARɣ and C/EBP (Tomaru *et al.*, 2009), both exacerbating inflammation and insulin resistance in adipocytes (Cai *et al.*, 2012; Qatanani *et al.*, 2009).

The main role of adipocytes is to deposit lipid droplets, acting as energy storage. In circumstances of food intake surplus, as blood glucose, triglyceride and insulin levels rise, the body stimulates the storage of triglycerides as fat, through *de novo* biosynthesis of long-chain fatty acids (lipogenesis). This process is regulated by fatty-acid synthase (FAS) and other key enzymes (Chakravarty *et al.*, 2004). However, in times of nutrient deprivation, lipases such as the hormone-sensitive lipase (HSL) are activated to release fatty acids from the lipid droplets to counteract the lowered blood glucose levels. The adipose tissue also works as an endocrine organ, releasing several hormones into the blood stream: notable examples are leptin and adiponectin, known as adipokines. Leptin and adiponectin can work synergistically, with the former inhibiting hunger and diminishing fat storage in adipocytes when nutrients suffice (Brennan & Mantzoros, 2006), and the latter protecting against obesity-related diseases, such as hyperglycaemia and T2D, atherosclerosis, and inflammation, as it is involved in glucose regulation and fatty-acid oxidation (Diez & Iglesias, 2003).

The redox status is also key in adipogenesis, as oxidative stress was shown to inhibit adipocyte differentiation, possibly by inhibiting the G_1->S-phase transition during mitotic division (Findeisen *et al.*, 2011). Cytochrome C oxidase 7A1 (*Cox7a1*, catalyst of

the electron transfer from reduced cytochrome c to oxygen), isocitrate dehydrogenase α (*Idh3a*, an NAD+ to NADH reducing enzyme of the TCA cycle) and peroxisome proliferator-activated receptor gamma coactivator 1-α (*PPARγc1α),* a master regulator of Reactive Oxygen Species (ROS) scavenging enzymes are examples of markers activated during oxidative stress. The brown adipose tissue can be characterised by the upregulation of specific genes of mitochondrial respiration, such as uncoupling protein 1 (*Ucp1*, a protein that decreases the proton gradient generated in oxidative phosphorylation, allowing energy dissipation and heat production). Other genes that are preferentially expressed in BAT are the 2 iodothyronine deiodinase (*Dio2*) and the fatty-acid-activated receptor-α (*Pparα*), among others (Lo & Sun, 2013).

5.1.4 Glucose-fuelled energy production in eukaryotic cells

Glycolysis and oxidative phosphorylation (OXPHOS) are the two main mechanisms of cellular energy production from glucose. Following uptake of glucose into cells, it is phosphorylated to glucose-6 phosphate by glucokinase (GCK), dramatically lowering the likelihood of the molecule to exit the intracellular environment and regulating the release of insulin in the pancreas. GCK is a rate-limiting step enzyme in glycolysis and was recognised to play a pivotal role in sensing the blood glucose concentration. Alterations in its expression or activity have been associated with a diabetes-like phenotype in blood glucose concentrations called maturity-onset diabetes of the young (MODY), accounting for about 1 to 3% of all diabetes cases worldwide (Shields *et al.*, 2010). As glycolysis occurs in the cytosol, one molecule of glucose produces two molecules of pyruvate, of ATP and of NADH. Pyruvate can either be used to produce

lactate and restore the NAD^+ levels in hypoxic conditions, for further glycolysis, or to synthesize Acetyl Coenzyme A (AcetylCoA). The lactate produced by anaerobic glycolysis in muscles is transported to the liver, where it is converted to glucose through gluconeogenesis, in the Cori cycle. Otherwise, the two AcetylCoA molecules are further metabolised through the Krebs Cycle (or the citric acid cycle), producing two guanosine triphosphate (GTP, which can be converted into ATP), two Flavin Adenine Dinucleotide ($FADH_2$) and six NADH molecules. FADH2 and NADH are then used in oxidative phosphorylation to create a proton gradient which translates into a mitochondrial transmembrane electrical potential used to produce ATP, in presence of O_2 as an electron acceptor. Through oxidative phosphorylation, about 34 molecules of ATP are produced from the metabolites of one molecule of glucose, in contrast with the 4 ATP molecules produced through the glycolytic and Krebs Cycle (**Figure 5.1.2**). It is thus evident how important the aerobic vs anaerobic conditions can be towards guiding the energy production to a more or less efficient pathway of ATP production.

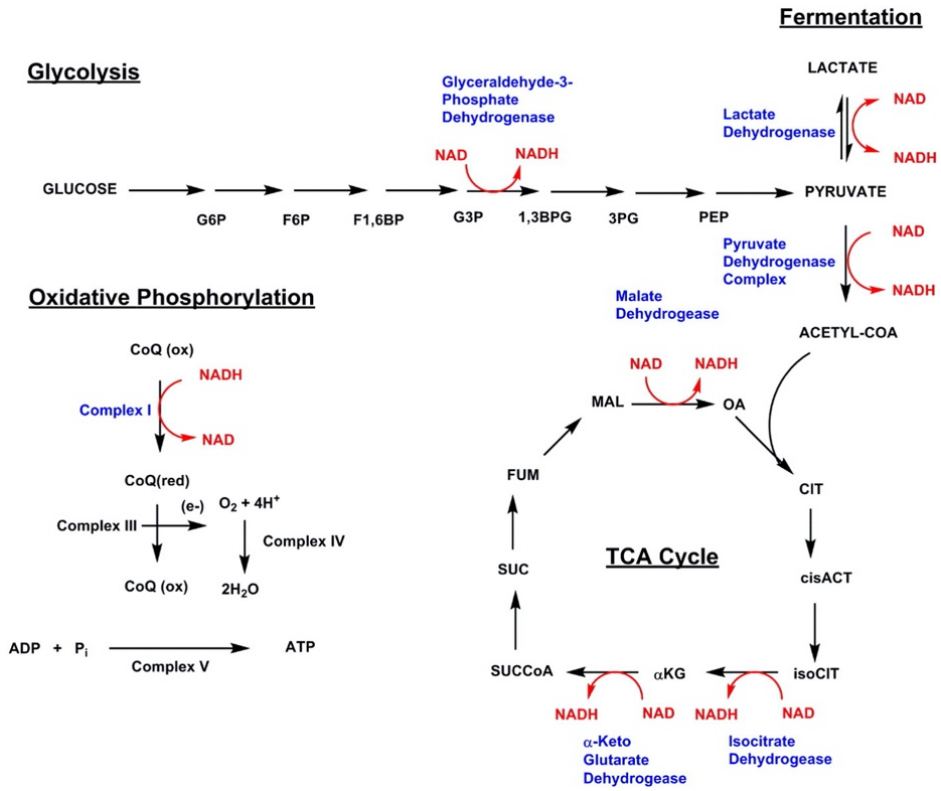


Figure 5.1.2 – Aerobic and anaerobic glucose metabolism. Glucose enters cytosolic glycolysis and produces ATP and pyruvate, which then either produces lactate anaerobically or is converted into AcetylCoA and produces ATP aerobically through the citric acid cycle and oxidative phosphorylation, both mitochondrial processes.

5.1.5 Insulin regulation of cellular glucose uptake

Glucose is one of the main energy sources used by our body, and its levels are maintained by homeostatic bodily processes. The main factors for keeping blood glucose within physiological limits are insulin and glucagon. Insulin is produced and released by Langerhans β-cells, whereas the glucagon is produced and released by the α-cells, within the pancreas. As glucagon works to raise the blood glucose concentration (and of fatty acids) when these are low, it is one of the main catabolic hormones of the body. Its release stimulates the liver to convert glycogen, a macromolecule that stores energy in form of compacted glucose molecules, back into glucose and release it into blood stream (glycogenolysis) and synthesis of *de novo* glucose through gluconeogenesis. Insulin, on

the other hand, is the main anabolic hormone with the opposite function of promoting the lowering of blood glucose concentration by stimulating its uptake largely by liver, fat and skeletal muscle cells (Sonksen & Sonksen, 2000).

Cellular glucose uptake engages several different sodium-glucose linked transporters (SGLTs) and facilitated diffusion glucose transporters (GLUTs), with slightly different localisation, sensitivity and role. SGLTs are generally localized on the surface of the small intestine and renal tubules, where they facilitate the absorption and re-absorption of glucose from diet and the glomerular filtrate, respectively. There are six different SGLT subtypes which are specific in affinity and localisation, all relying on the sodium concentration gradient generated by the sodium-potassium ATPase as a chemical potential (Navale & Paranjape, 2016). Furthermore, the Class I facilitated diffusion glucose receptors not requiring ATP, are present throughout the body, known to have distinct regulatory and kinetic properties: GLUT1, GLUT2, GLUT3 and GLUT4, all 12-transmembrane bidirectional transporters specialized in glucose homeostasis, have slightly different physiology and localization.

GLUT1 is present throughout the body and responsible for the low levels of basal glucose uptake required to maintain cellular respiration and is found upregulated in certain types of cancer (Ganapathy *et al.*, 2009). It also supplies glucose to cells of the central nervous system, and its upregulation is sought in stroke and cardiac infarction (Yu *et al.*, 2008). GLUT2 is a low-affinity transporter mainly present in the Langerhans β-islets within the pancreas where it functions as a glucose sensor, thus linking glucose concentration to the release of insulin, and within the liver where it transports glucose

needed for glycogenesis and glycolysis. Thus, a reduction in GLUT2 expression in pancreatic β-cells can prevent glucose-stimulated insulin secretion (Thorens *et al.*, 1990). GLUT3 is a major neuronal glucose transporter, with a high affinity for glucose, allowing for the transport of glucose even when it is found low concentrations.

GLUT4 is the insulin-regulated glucose transporter mainly expressed in adipose tissue and striatal muscle. More precisely, their translocation to the membrane was shown to be impaired in patients affected by type 2 diabetes mellitus (T2DM), whereby the cellular response to insulin does not translate into an increase in the activity of glucose uptake by the cells (Garvey *et al.*, 1998). GLUT4 is normally localised in GLUT4 storage vesicles (GSVs) and other intracellular membrane compartments, and it is translocated to the plasma membrane via an exocytic pathway upon insulin stimulation on the tyrosine-kinase insulin receptors (**Figure 5.1.3**). GLUT4-mediated glucose uptake was shown to have an important impact on glucose homeostasis, especially in skeletal muscle cells, as they account for up to 80% of postprandial plasma glucose uptake in healthy individuals (Thiebaud *et al.*, 1982), and if impaired, could promote early-stages insulin-resistance and hyperglycaemia (DeFronzo & Tripathy, 2009). In fact, separate GLUT4 knockdown in either adipocytes or muscle cells can cause widespread glucose dysregulations and type-2 diabetes-like phenotypes (Abel *et al.*, 2001; Zisman *et al.*, 2000).

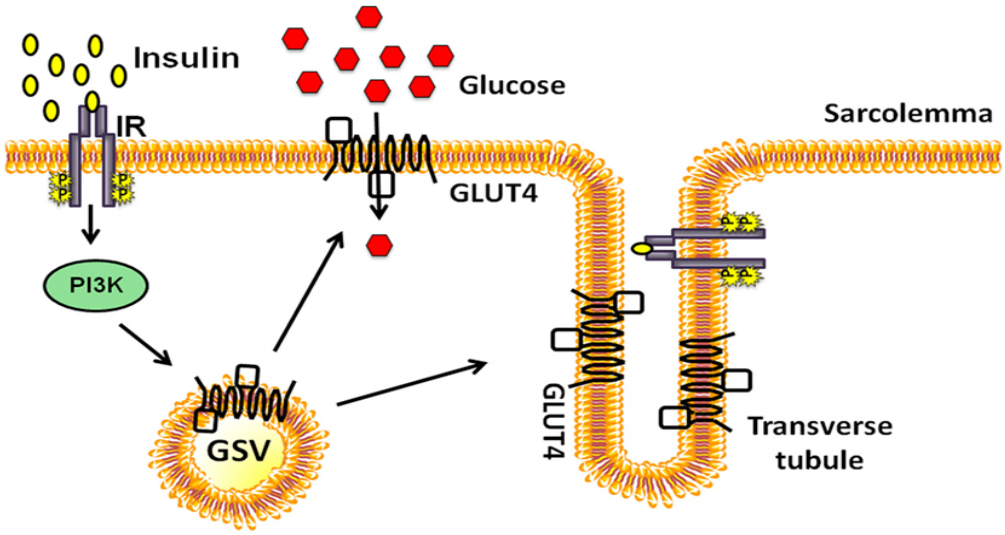


Figure 5.1.3 – Insulin regulation of glucose transport in skeletal muscle and adipocytes. Insulin acts on the tyrosine-kinase insulin receptors (IRs) which activate a PI3K-dependent pathway that promote the transport of glucose receptors GLUT4 to the plasma membrane. GLUT4 receptors, normally stored in GLUT4 storage vesicles (GSVs), are thus activated and ready to transport glucose across the membrane, in a facilitated diffusion fashion. Adapted from Tunduguru *et al.*, 2017.

5.1.6 HIF1 and SP1 in cellular metabolism

It has been shown that the transcription and translation of several genes for proteins with important metabolic functions is regulated by the binding of SP1 (**Figure 3.1.4**). The Hexokinase II, a rate limiting glycolytic enzyme, is shown to have an SP1-mediated increase in expression in cancer (Lee & Pedersen, 2003). SP1 binding was shown to regulate the transcription of Pyruvate Kinase, a final rate-limiting step in glycolysis, and specifically of its M isoform, enriched in the muscle and brain tissue (Schafer *et al.*, 1997). Fatty acid synthase (FAS) is normally expressed at a low level in cells, as human tissues uptake fatty acids from the diet, and was shown to have SP-1 binding sites within its promoter (Schweizer *et al.*, 2002). SP1 was shown to play a role in regulating *de novo* lipogenesis, as knocking down SP1 was shown to reduce FAS expression (Lu & Archer,

2010). Further evidence shows that SP1 vehiculates the glucose-mediated activation of acetyl-CoA carboxylase expression, the rate-limiting enzyme in the biosynthesis of fatty-acids (Daniel & Kim, 1996). Moreover, glucose transporters that allow for the cellular uptake of glucose, have shown to be potentially regulated by SP1. More specifically, GLUT1, responsible for the low level of basal glucose uptake, and GLUT2, a glucose-sensing apparatus within liver and pancreatic β-cells, were shown to be responsive to SP1-control. In fact, their promoters contain SP1 sites that could be at the heart of the transcriptional regulation of these transporters across tissues (Ahn *et al.*, 1995; Hwang & Ismail-Beigi, 2006). Glucose- and insulin-stimulated leptin secretion is also under the control of SP1-binding sites (Moreno-Aliaga *et al.*, 2007), controlling thus hunger and appetite. Evidence also shows that the glucose concentration can modulate SP1 activity, however studies suggested both lower and higher levels of intracellular glucose can stimulate SP1 phosphorylation and lower its activity (Schafer *et al.*, 1997; Zhang *et al.*, 2011b). Insulin was also shown to increase SP1 phosphorylation in murine hepatoma and skeletal muscle cells (Horovitz-Fried & Sampson, 2007).

Furthermore, lines of evidence show that SP1 is involved in circadian rhythm regulation (**Figure 5.1.4**): SP1-binding sites show to be overexpressed in circadian gene promoters (Bozek *et al.*, 2009) and SP1 was shown to cooperate with NF-Y transcription factor in activating transcription of BMAL1, at CCAAT/GC-boxes (Xiao *et al.*, 2013).

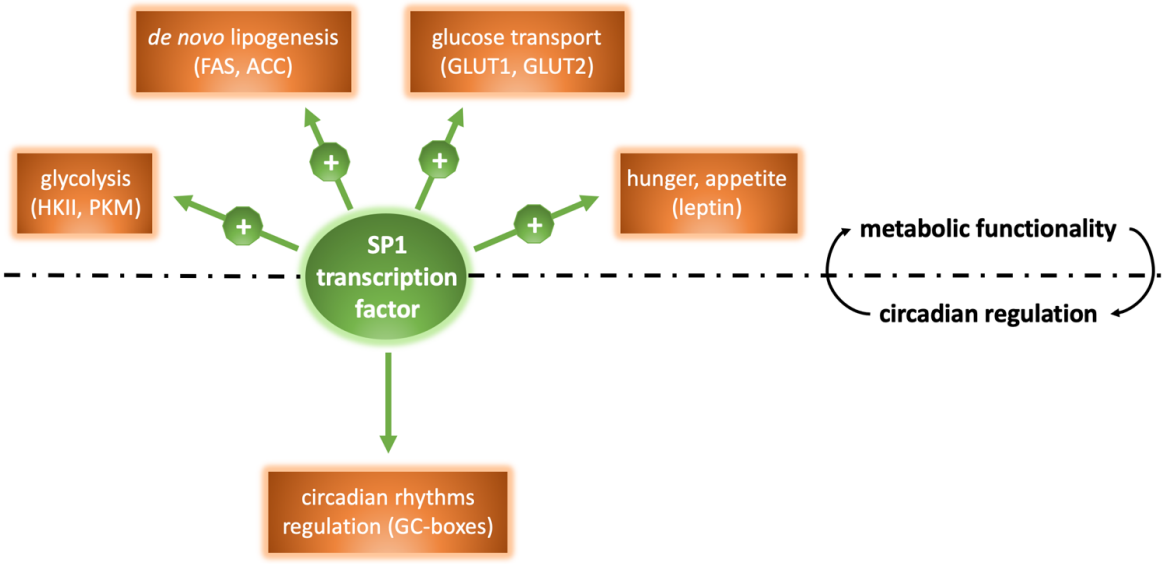


Figure 5.1.4 – Evidence-based representation of SP1 transcription factor impact on metabolic and circadian pathways. Graphic representation of metabolic and circadian targets that are regulated by Specificity-Protein 1 transcription factor. SP1 was shown to modulate glycolysis, de novo lipogenesis (through modulating the fatty-acid synthase and Acetyl-CoA Carboxylase genes) glucose transport and appetite, but was also shown to impact on circadian biology. The evidence is noted within the text and bibliography.

Under conditions of reduced cellular O_2 availability, the Hypoxia Inducible-Factor I (HIF1) acts as a transcriptional activator of genes which translate for proteins that are necessary to switch oxidative to glycolytic metabolism, as although more inefficient, it requires less oxygen for the cellular energy production (Semenza, 2011). Moreover, aberrant regulation of HIF1 could be involved in the development of obesity, obesity-induced inflammation, fatty liver disease and type-2 diabetes (T2D) (Ban *et al.*, 2014). It was indeed shown that knock-out of *Hif1α* in adipocytes ameliorates HFD-induced obesity, glucose-intolerance and insulin resistance (Jiang *et al.*, 2011), possibly through a decrease in the metabolic efficiency, and hypoxia (or *Hif1* overexpression) inhibits insulin signalling through a decrease in the phosphorylation of the insulin receptor (Regazzetti *et al.*, 2009). Moreover, HIF1 may be linked in the control of food intake and energy expenditure in the hypothalamus (Virtue & Vidal-Puig, 2011), as

proopiomelanocortin (POMC) hormonal release seems to integrate HIF1-based regulatory mechanisms. HIF1, a basic-helix-loop-helix (bHLH) transcription factor, is an important regulator of the response of cells to hypoxia (lack of oxygen). HIF1 was shown to increase the expression of a number of glycolytic enzymes (such as aldolase A, enolase 1, lactate dehydrogenase A, phosphofructokinase L, phosphoglycerate kinase 1 and pyruvate kinase M) (Dang & Semenza, 1999) and GLUT1 (Semenza, 2003), thus impacting on cellular glucose functionalities. Moreover, *Hif1α* promoter contains binding sites for SP1 (Iyer *et al.*, 1998) and it was shown that SP1 is necessary for *Hif1* transcription (Kim & Park, 2010). Evidence shows that SP1 and HIF1 are co-factors in regulating the expression of ATP-binding cassette A1 (ABCA1), which regulates cellular release of phospholipids and cholesterol (Schmitz & Langmann, 2005). This evidence, taken together, suggests HIF1 and SP1 are pivotal transcription factors in the regulation of glucose metabolism and have both been shown to be regulated by IBET-762 administration (**Figure 5.1.5**).

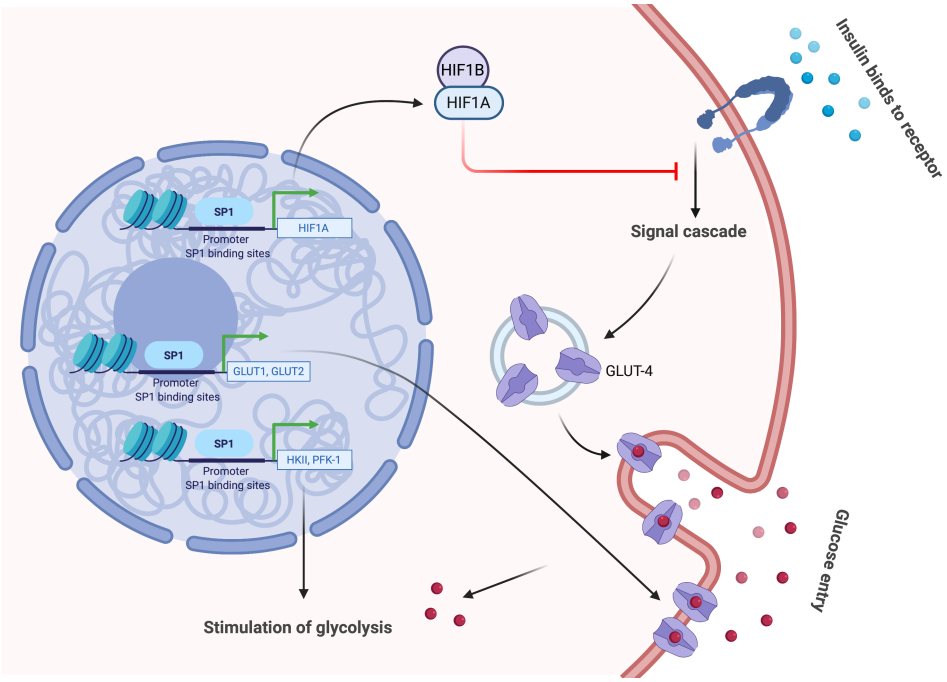


Figure 5.1.5 – Role of SP1 and HIF1 in cellular glucose-metabolism. Graphic representation of the role of SP1 and HIF1 transcription factors in modulating glucose metabolism. Evidence suggests HIF1α could inhibit the insulin signaling cascade and inflict on the GLUT4 receptor migration to the plasma membrane. *Glut1* and *Glut2* expression were shown to be potentially regulated by the SP1 binding on SP1-binding sites on their promoter, and on the promoter of other genes important for glycolysis, such as HKII and PFK-1.

Several reports demonstrate that bromodomains can modulate metabolic pathways. As *Brd2* and *Brd4* knockouts (brd2$^{-/-}$, brd4$^{-/-}$) bring embryonic lethality (Houzelstein *et al.*, 2002; Shang *et al.*, 2009), mice with reduced *Brd2* whole-body expression (brd2$^{w/lo}$) have been generated. These mice indeed have shown to be associated with a severe obesity and diabetes phenotype, pancreatic islet expansion, hyperinsulinemia and hepatic steatosis in mice on a regular chow, though it also enhanced glucose tolerance, stimulated mitochondrial uncoupling and heat production. These contrasting effects translated into a 'healthy' obesogenic phenotype (Wang *et al.*, 2009a), in which metabolic inflammatory pathways were found to be reduced. The culprit for the higher weight in the knockdown of brd2 is thought to be due to an increased appetite, which in part stimulates a higher fat metabolic rate and an increase in the expression and production of adiponectin, an

insulin sensitizing hormone. Molecularly, *Brd2* knockdown has been associated with an increase in expression of *PPARɣ* and adipogenesis in 3T3-L1 cells, partially explaining the adipogenic phenotype of a whole-body knockdown. As a possible mechanism of action, PPARɣ was shown to be transactivated by E2F elongation factor family (Lin *et al.*, 1996), which is known to interact with BRD2/4 and SP1 (Miard & Fajas, 2005; Sinha *et al.*, 2005). Furthermore, bromodomain inhibitors were shown to have anti-inflammatory properties, with I-BET drugs potentially reducing expression of pro-inflammatory cytokines and chemokines such as IL-6 and IL-1β and rescued mice from endotoxin-induced death (Nicodeme *et al.*, 2010). Moreover, BRD4 was also shown to co-activate pro-inflammatory pathways through NFkβ (Huang *et al.*, 2009). These results are in line with a possible BET-inhibitor metabolic anti-inflammatory effect that could influence a higher insulin sensitivity in circumstances of enhanced food consumption (Karelis *et al.*, 2005).

5.2 RESULTS

5.2.1 Regulation of metabolic gene expression by IBET-762

Having established IBET-762 as a circadian modulator, to understand the influence of IBET-762 on metabolic pathways in U2OS cells, we tested the effects of this drug on several metabolic genes (**Figure 5.2.1**), following from previous U2OS cell results (**Figure 4.2.7**) and literature (Bordone & Guarente, 2005; Cheng *et al.*, 2018; Evans *et al.*, 2004). The effect of IBET-762 (p<0.0001, $F_{(1, 70)}$=357.2) and time (p=0.004, $F_{(8, 70)}$=3.17) on *PPARγ* (**Figure 5.2.1A**) were shown to be statistically significant, with the drug decreasing gene expression at almost all timepoints. Similar results were registered for PPARγ-Coactivator 1-α (*Pgc1α*) (**Figure 5.2.1B**) (p<0.0001, $F_{(1, 70)}$=109) and time (p<0.0001, $F_{(8, 70)}$=5.74), with the drug dampening its expression. IBET-762 was shown to reduce the expression of *Tfeb* (**Figure 5.2.1C**) (p<0.0001, $F_{(1, 77)}$=72.49), in a time-sensitive manner (p=0.0002, $F_{(9, 77)}$=4.198). With respect to *Sirt1* (**Figure 5.2.1D**), IBET-762 was shown to increase the gene expression (p<0.0001, $F_{(1, 75)}$=71.11), in a time-sensitive manner (p<0.0001, $F_{(9, 75)}$=8.94), at most timepoints, however the effect seems to be abolished by 32-36 hours after drug administration. The effect of IBET-762 on *Sp1* (**Figure 5.2.1E**) was also assessed, with the drug reducing the expression of *Sp1* significantly (p<0.0008, $F_{(1, 77)}$=12.11), in a timely manner (p<0.0001, $F_{(9, 77)}$=6.332). Gene expression of *Hif1*, on the other hand, was stimulated by the addition of IBET-762 (**Figure 5.2.1F**) (p=0.0014, $F_{(1, 76)}$=11.06), in a time-sensitive manner (p<0.0001, $F_{(9, 76)}$=12.77).

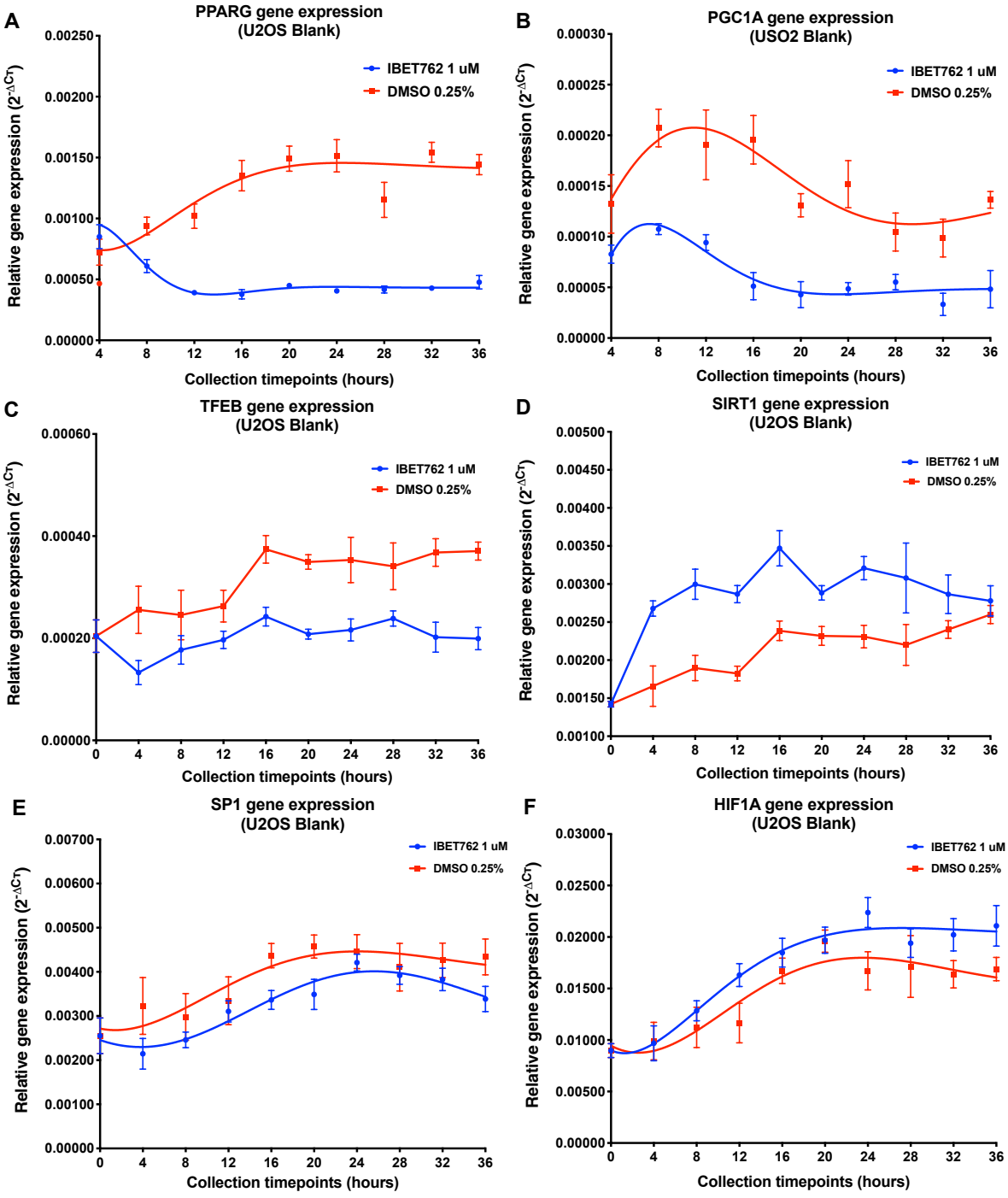


Figure 5.2.1 – Effects of IBET-762 on the metabolic gene expression. Metabolic genes were quantified in U2OS cells: *PPARɣ* (**A**), *Pgc1α* (**B**), *Tfeb* (**C**), *Sirt1* (**D**), *Sp1* (**E**), *Hif1α* (**F**). Data was expressed as average ± SEM (n=4-6). The possible divergence between the two curves was statistically tested using a two-way ANOVA and a Sidak-powered post-hoc multiple comparisons analysis. The impact of time and treatment were assessed over all timepoints taken together, as well as individually over each of the timepoints.

5.2.2 Mediation of PPARɣ gene expression effects

As evidence shows *PPARɣ* gene expression can be modulated by *Sirt1* (Picard *et al.*, 2004), and given we have shown IBET-762 is able to increase *Sirt1* expression early-on after drug administration (**Figure 3.3.1D**), we wanted to test whether *Sirt1* could influence the effects of the epigenetic modulator on the expression of PPARɣ.

We first confirmed the reduction of expression of *PPARɣ* upon administration of 0.5μM of IBET-762 (-45%, p=0.0005) (**Figure 5.2.2A).** This effect was removed by the knockdown of *Sirt1* (-10%, ns) (**Figure 5.2.2B**). We also confirmed previous results showing that IBET-762 was able to increase *Sirt1* expression (+39%, p=0.0142) (**Figure 5.2.2C)** and that the knock-down of *Sirt1* was indeed efficient (-94%, p<0.0001) (**Figure 5.2.2D**).

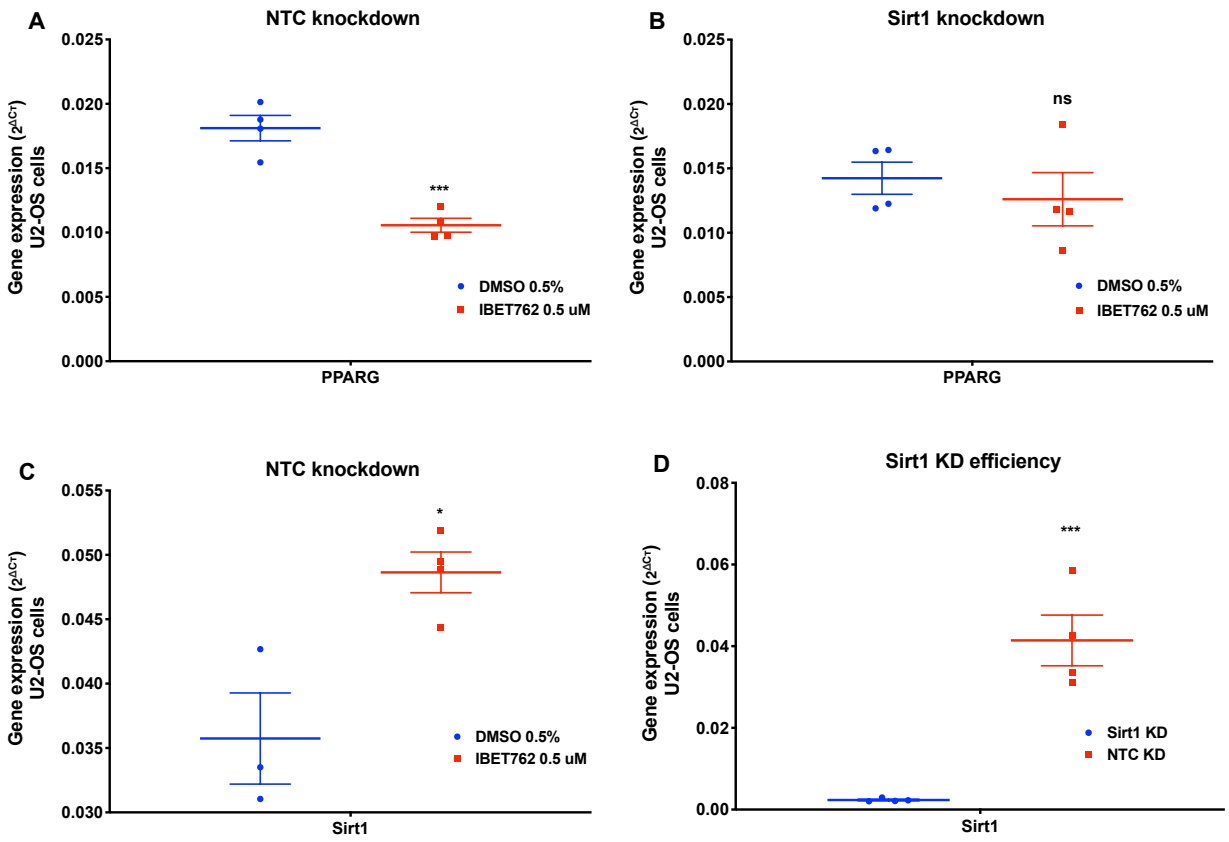


Figure 5.2.2 – Effects of IBET-762 and *Sirt1* knockdown on *PPARɣ* gene expression; the effect of a non-targeting knock-down was assessed on PPARɣ gene expression (**A**). This effect of *Sirt1* increase in expression (**C**) was removed by the *Sirt1* knock-down (**B**). *Sirt1* is shown to be efficiently knocked-down (**D**). Data was expressed as average ± SEM (n=4). The statistical significance was tested using an unpaired T-test analysis.

5.2.3 Modulation of adipocyte differentiation by IBET-762

Given the widespread effects of IBET-762 on metabolic genes and markers of adipogenesis, such as *PPARγ*, *Pgc1α* and *Tfeb*, we evaluated whether IBET-762 would be able to modulate adipogenesis in differentiating 3T3-L1 cells. We therefore tested the effects of administering IBET-762 (1μM) on a two-week differentiation assay using two routinely used differentiation protocols, to evaluate its effects on adipogenesis (**Figure 5.2.3**).

Results are shown in **Figure 5.2.3A-D**, where it is possible to qualitatively assess the impact of IBET-762 on adipocyte differentiation. Following differentiation, cells demonstrate a decrease in lipids (represented in pink by oil-red staining), in relation to cell numbers (represented by nuclear stain in blue).

The results were also quantitatively assessed through Nile Red/DAPI staining (**Figure 5.2.3E**), which confirmed our previous findings that adipocyte differentiation is indeed reduced by the co-administration of IBET-762, together with either insulin and IBMX (29% reduction as compared to DMSO, p=0.0125), or insulin, IBMX and rosiglitazone (42% reduction as compared to DMSO, p=0.0013). Moreover, adipocyte differentiation does not show any difference between the two IBET-762-treated groups, that is, between the two differentiation protocols. Furthermore, IBET-762 does not show to reduce adipogenesis differentiation in the control group, where the cells have not been exposed to adipogenesis differentiation factors.

Further, we also tested whether the *PPARγ* downregulation brought forward by IBET-762 (**Figure 5.2.1**), which might mediate the IBET-762-stimuated reduction in adipocyte differentiation is bromodomain-mediated. We have therefore knocked-down each bromodomain known to be inhibited by IBET-762, with the exception of BRD-T, which did not show an amplitude enhancing effect on the circadian clock (**Figure 4.2.1-4.2.2**).

The results showed that both BRD2 and BRD4 knockdown reduced *PPARγ* gene expression significantly (-40%, p=0.0286 and -77%, p<0.0001 respectively) (**Figure 5.2.3F**). Furthermore, upon the concomitant treatment with both bromodomain inhibition and IBET-762, the effect of the drug in inhibiting *PPARγ* was confirmed. Additionally, IBET-762 did not further inhibit *PPARγ* over the levels of inhibition brought forward by BRD4 inhibition (-77%, p<0.0001 vs -80%, p<0.0001), suggesting the effects of *PPARγ* inhibition brought forward by IBET-762 are BRD4-mediated.

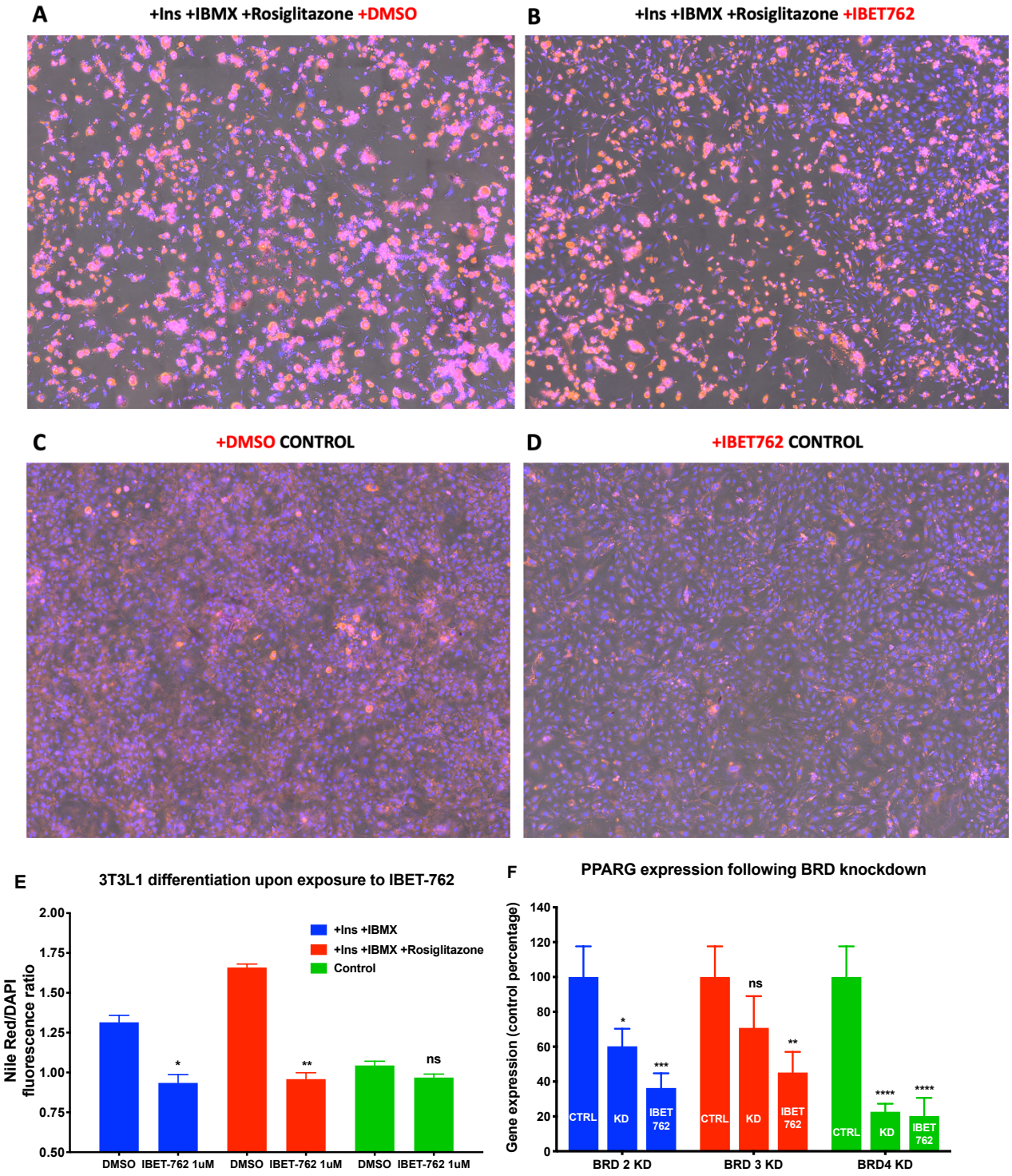


Figure 5.2.3 – IBET-762 reduces adipocyte differentiation. The effects of IBET-762 on 3T3-L1 differentiation were tested. The 3T3-L1 cells were differentiated with either Insulin, IBMX and Rosiglitazone or with Insulin and IBMX only. Examples of cellular differentiation can be seen under the Insulin+ IBMX + Rosiglitazone protocol (**A, B**) and the control protocol (**C, D**), where the pink colour symbolises the fatty acids and adipose cell differentiation, whereas the blue colour represents stained nuclei, under the Nile red staining protocol. Upon a two-way ANOVA analysis and Sidak-powered multi-comparison analysis, we can see that IBET-762 can inhibit cellular differentiation in both differentiation protocols (p=0.0125, p=0.0013 respectively), but not in the control protocol (ns) (**E**) (n=3, data expressed as mean and SEM). Further, bromodomain knockdown mimics the *PPARγ* reduction brought by IBET-762, specifically when BRD-4 is inhibited, with no further reduction brought by IBET-762 (**F**).

5.2.4 IBET-762 modulation of metabolic markers in adipogenesis

Given that IBET-762 inhibited adipocyte differentiation (**Figure 5.2.3**), we further examined whether we could pinpoint the modulation in differentiation to specific gene markers involved in adipogenesis. We tested a series of adipogenesis markers (**Figure 5.2.4**) and their expression with two differentiating protocols with Insulin and IBMX (treatment A) or with insulin, IBMX and rosiglitazone (treatment B), and DMSO-only control treatment, with or without IBET-762 1μM.

In many cases, the down-regulation in adipogenesis markers is stark; *Retn* showed a decrease in expression of 93% (p=0.0001) and 91% (p<0.0001) in treatment A and treatment B respectively, whereas the control treatment showed a no difference (-5%, ns) (**Figure 5.2.4A**). *Cd36* showed a similar trend towards a diminished expression in treatment A (-22%, ns), and treatment B (-33%, p<0.0001) and a trend towards an increase for the treatment control (+28%, ns) (**Figure 5.2.4B**). Similarly, *CEBPα* showed a trend towards a decrease in treatment A (-42%, ns) and a significant decrease in treatment B (-50%, p<0.0001), with a trend towards an increase in the treatment control (+52%, ns) (**Figure 5.2.4C**). Adiponectin also showed a significant decrease for both treatment A (-73%, p<0.0001) and treatment B (-75%, p<0.0098) and no change for the treatment control (+6%, ns) (**Figure 5.2.4D**). The fatty-acid synthase (*Fas*) also showed a decrease in expression, with a diminishing trend for treatment A (-13%, ns) and a significant decrease for treatment B (-49%, p=0.0002), and a non-significant increase in the control treatment (+83%, ns) (**Figure 5.2.4E**). Leptin has showed significant gene expression decrease for both treatment A (-74%, p=0.0229) and treatment B (-87%, p<0.0001), but no significant change for the treatment control (-

15%, ns) (**Figure 5.2.4F**). The hormone-sensitive lipase (*Hsl*) was shown to be decreased in treatment A (-33% , ns) and significantly downregulated in treatment B (-51% , $p<0.0001$), with a trend towards an increase for the treatment control (+69%, ns) (**Figure 5.2.4G**). *PPARγ* was also shown to be significantly downregulated by IBET-762, both for treatment A (-59%, $p<0.0001$) and treatment B (-48%, $p<0.0001$), with no difference in the treatment control (+8%, ns) (**Figure 5.2.4H**). Finally, Phosphoserine Aminotransferase 1 (*Psat1*) shows a significant increase in gene expression for treatment A (+37%, $p=0.0021$) and a decrease in gene expression for treatment B (-21%, $p=0.0004$), and no significant differences for the treatment control (-9%, ns) (**Figure 5.2.4I**).

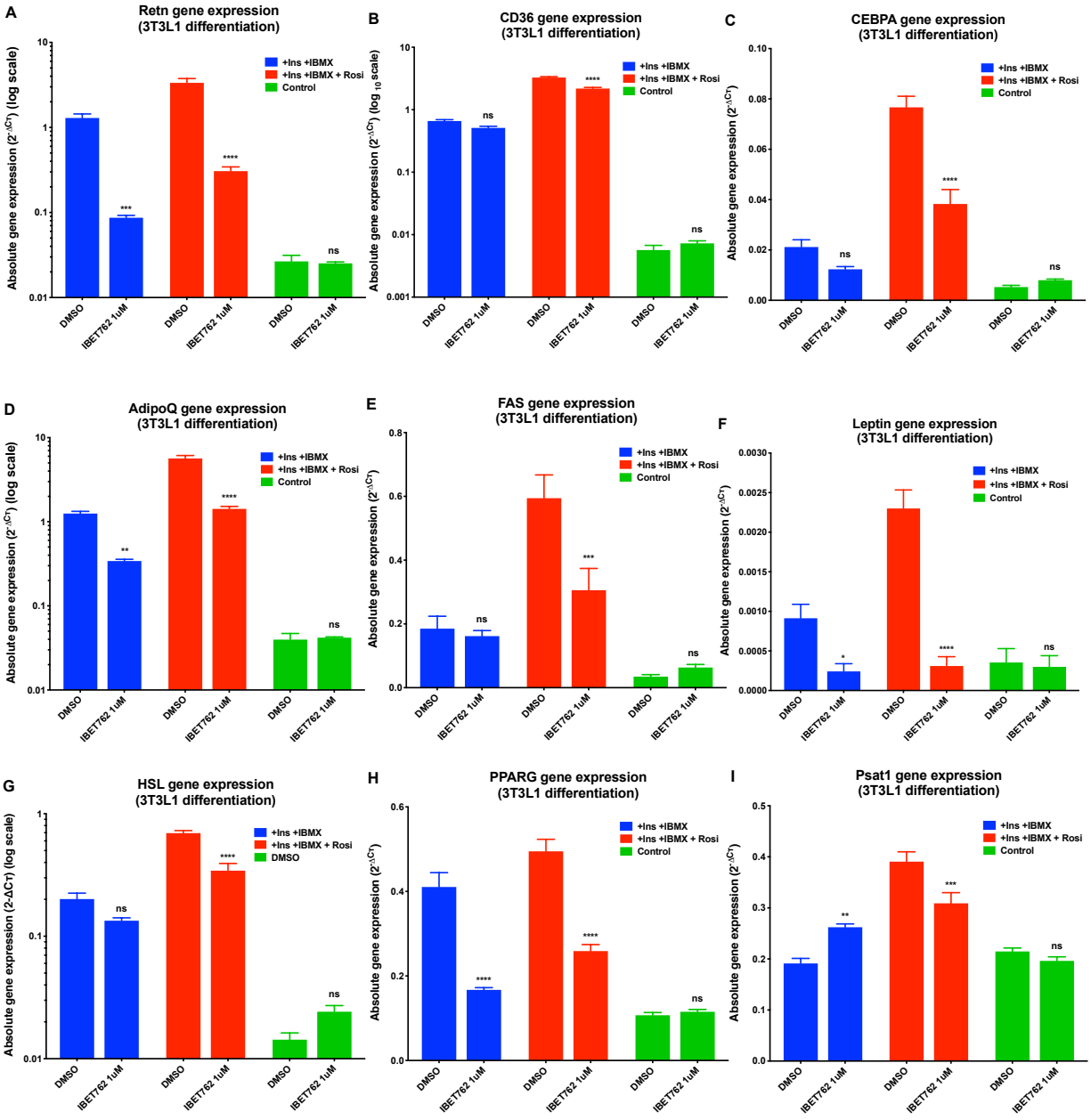


Figure 5.2.4 - Effects of IBET-762 on the gene expression of markers of white-fat adipogenesis (A-I); data was expressed as average ± SEM (n=3-6). The data was analysed using a two-way ANOVA method and a Sidak posthoc multiple comparisons test. The effects of IBET-762 were analysed against the DMSO control on 3T3-L1 cells treated for two weeks with either Insulin and IBMX or with Insulin, IBMX and Rosiglitazone, to induce adipogenesis.

5.2.5 IBET-762 modulation of key metabolic pathways in adipocytes

To further assess whether specific metabolic pathways were affected by IBET-762 treatment, we further analyzed a series of genes that are known to be modulated in oxidative stress regulation (**Figure 5.2.5A-C**), brown-adipose tissue differentiation (**Figure 5.2.5D-F**) and glucose metabolism (**Figure 5.2.5G-I**).

To assess the importance of IBET-762 in modulating oxidative stress regulatory pathways, we have analyzed the expression of three specific gene markers: *Cox7a1*, *Pgc1α* and *Idh3a*. *Cox7a1* showed a significant reduction when treated with IBET-762 for both treatment A (-99%, $p<0.0001$) and treatment B (98%, $p<0.0001$) and an increase for the treatment control (+393%, ns) (**Figure 5.2.5A**). *Pgc1α* showed no change for treatment A (+16%, ns) and a significant decrease for both treatment B (-64%, $p<0.0001$) and the treatment control (-31%, $p=0.0119$) (**Figure 5.2.5B**). *Idh3a* showed a significant gene expression decrease for treatment A (-68% , $p<0.0001$) and treatment B (-67% , $p<0.0001$), but no change for the treatment control (-4%, ns) (**Figure 5.2.5C**). Furthermore, to assess a possible shift towards brown-adipose tissue differentiation, we have analyzed a series of markers associated with BAT-differentiation: *Ucp1*, *Dio2* and *Pparα* (**Figure 5.2.5D-F**). However, the levels of these could not be detected in several instances, upon IBET-762 and as a baseline, respectively for both *Ucp1* and *Dio2* (**Figure 5.2.5D-E**). We could however assess a significant gene expression decrease for *Dio2* in the undifferentiated control treatment (-98% , $p<0.0001$). *Pparα* showed a statistically significant decrease in expression under both treatment A (-73%, $p=0.0067$) and treatment B (-94%, $p<0.0001$) but no significant change under control treatment (+27%,

ns) (**Figure 5.2.5F**). With regards to glucose metabolism, we observed IBET-762 downregulated the expression of *Slc2a1* (Solute Carrier Family 2 Member 1, also known as GLUT1 receptor) for both treatment A (-59% , p=0.0001) and treatment B (-59% , p=0.0024) as well as for the treatment control group (-35% , p=0.0101) (**Figure 5.2.5G**). Similarly, *Slc2a4* (GLUT4) expression was also downregulated by IBET-762 upon treatment A (-94%, p<0.0001) and treatment B (-91% , p<0.0001), however, the treatment control did not seem to change the expression of this gene significantly (+20%, ns) (**Figure 5.2.5H**). Glucokinase (*Gck*) expression was also downregulated by IBET-762 for both treatment A (-83% , p<0.0001) and treatment B (-89% ,p<0.0001), however, its levels were undetectable for the treatment control (**Figure 5.2.5I**).

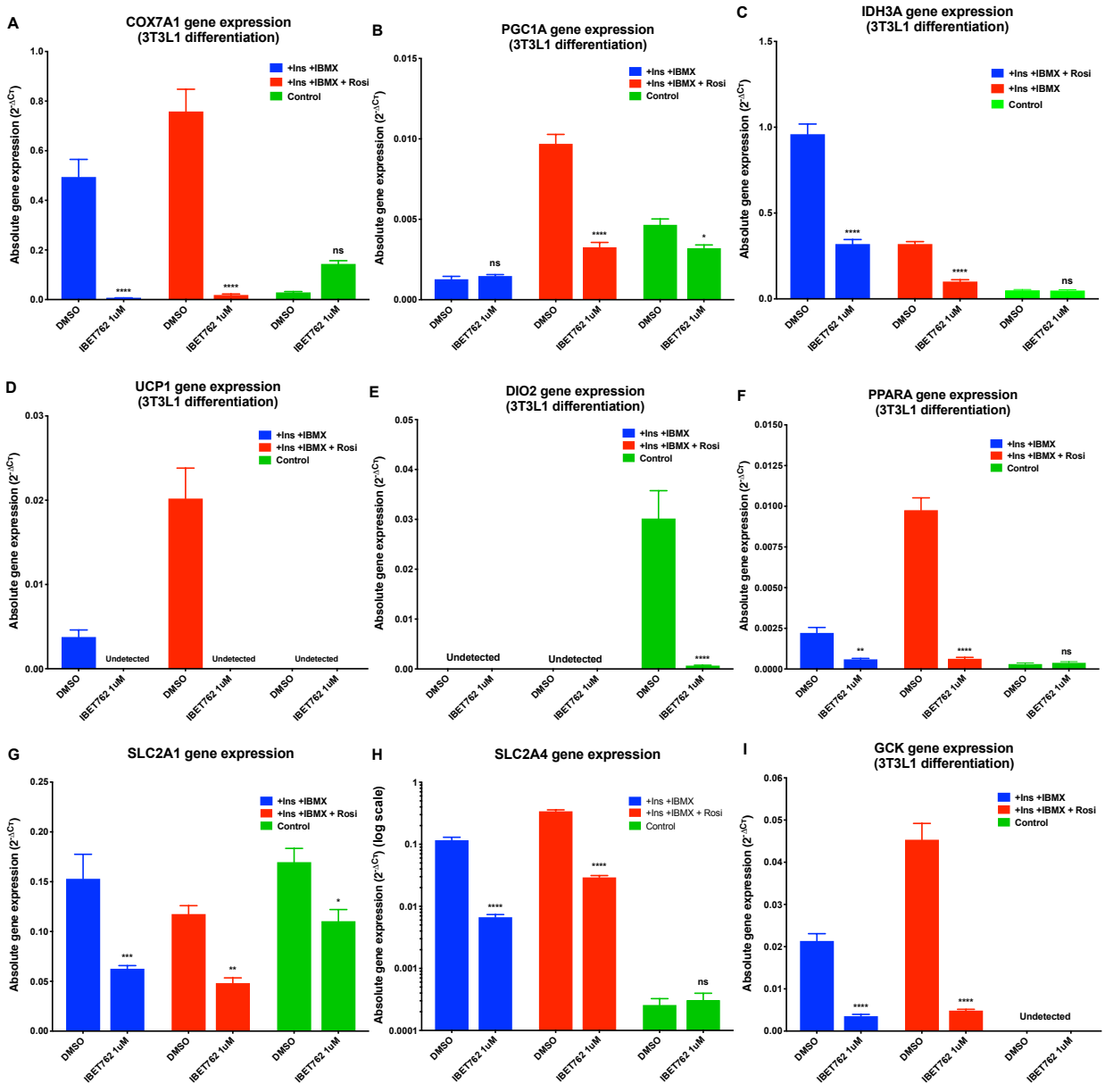


Figure 5.2.5 - Effects of IBET-762 on the gene expression of markers of oxidative stress (A-C), brown-adiposity (D-F) and glucose regulation (G-I); data was expressed as average ± SEM (n=3-6). The data was analysed using a two-way ANOVA method and a Sidak posthoc multiple comparisons test. The effects of IBET-762 were analysed against the DMSO control on 3T3-L1 cells treated for two weeks with either Insulin and IBMX or with Insulin, IBMX and Rosiglitazone, to induce

5.2.6 IBET-762 modulation of metabolic regulation in adipocytes

To assess the impact of IBET-762 on metabolic pathways, we evaluated the gene expression of markers of adipogenesis (**Figure 5.2.6A**), adipokines (**Figure 5.2.6B**), oxidative stress (**Figure 5.2.6C**) and glucose regulation (**Figure 5.2.6D**) on differentiated adipocytes, over a two-weeks chronic administration, informing us on the effects of the bromodomain inhibitor on mature adipocytes.

We initially evaluated the white-adipose markers expression (**Figure 5.2.6A**), with IBET-762 stimulating a significant increase in expression of *Cd36* (+144%, $p<0.0001$), *CEBPα* (+88%, ns) and *PPARγ* (+23%, $p=0.0469$).

We also tested the expression of different adipokines, with respect to the effects of IBET-762 (**Figure 5.2.6B**). Adiponectin (+268%, $p<0.0001$), Leptin (+86%, ns) and *Pparα* (+105%, ns) all showed an increase in their expression upon application of IBET-762.

We also tested the gene expression levels of oxidative stress (**Figure 5.2.6C**). IBET-762 increased the gene expression of *Cox7a1* (+1265% , $p<0.0001$) and *Idh3a* (+30%, $p=0.0126$) and showed a trend towards an increase of *Pgc1α* (+108% , ns). Lastly, the glucose regulation markers showed a decrease in expression of *Slc2a1* (GLUT1) (-78%, $p<0.0001$), and an increase in the expression of *Slc2a4* (GLUT4) (+433% , ns). The gene expression of glucokinase could not be detected in the differentiated adipocytes (**Figure 5.2.6D**).

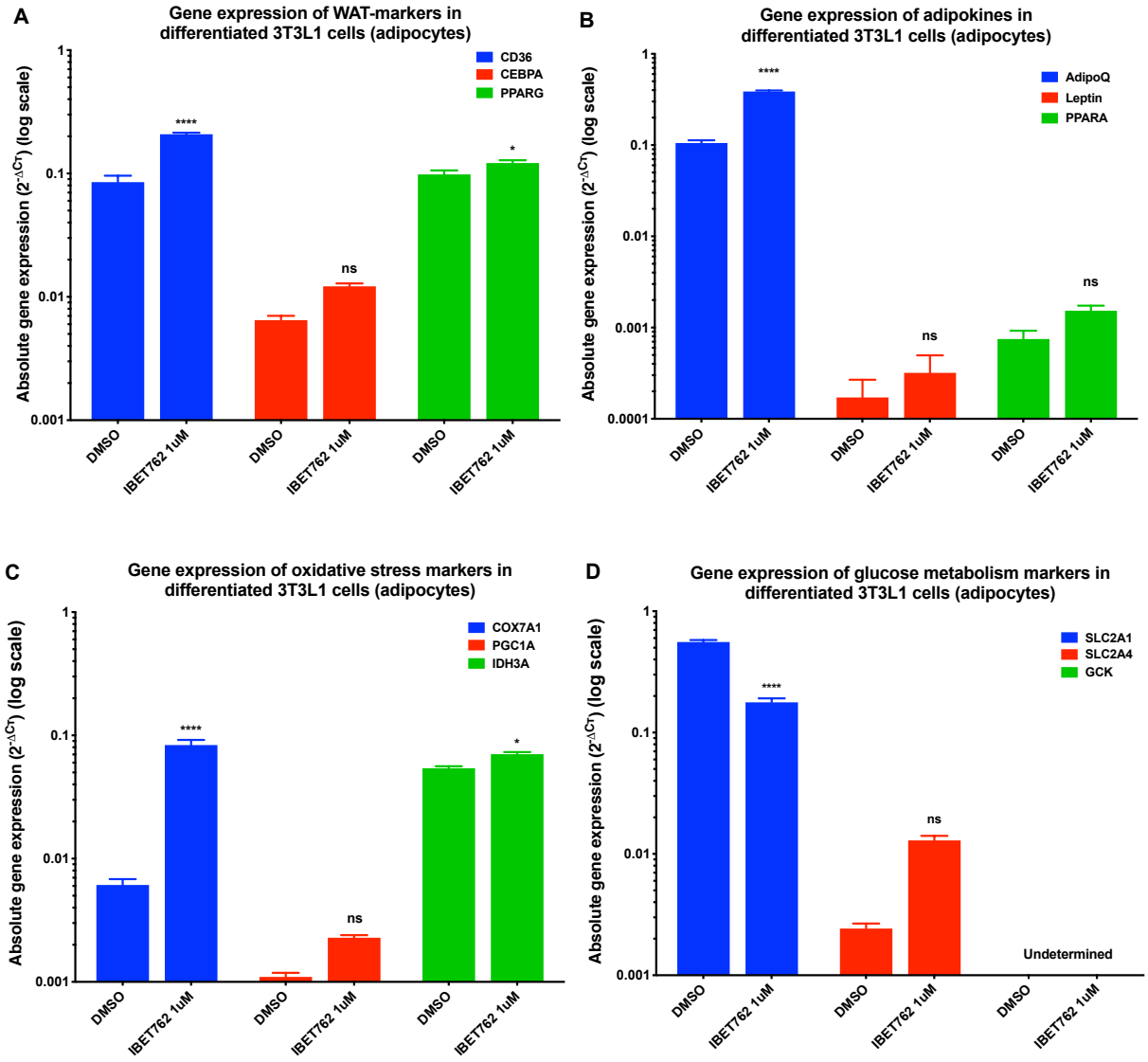


Figure 5.2.6 - Effects of IBET-762 on the gene expression of markers of adipogenesis (A), levels of adipokines (B), oxidative stress (C) and glucose metabolism (D) in differentiated 3T3-L1 cells (adipocytes); data was expressed as average ± SEM (n=3-6). The data was analysed using a two-way ANOVA method and a Sidak posthoc multiple comparisons test. The effects of IBET-762 were analysed against the DMSO control on differentiated 3T3-L1 cells.

5.2.7 Effects of IBET-762 on lipolysis and lactate production

Given the effects of IBET-762 on adipogenesis (Figure 3.3.2) and lipogenesis gene expression (**Figure 5.2.4**, **Figure 5.2.5** and **Figure 5.2.6**), we investigated the effects of IBET-762 on lipolysis and glycolysis. We had therefore assessed the effects of the bromodomain inhibitor on the adipocyte glycerol production and concentration, as compared to a DMSO control, in adipocytes. The effects of IBET-762 were registered at 1 hour and 24 hours after drug administration, and at 4-hour isoproterenol co-administration (**Figure 5.2.7**).

The results showed a decrease in glycerol concentration upon treatment with IBET-762. The trending decrease after 1 hour of IBET-762 1μM addition (21% decrease, ns) was statistically confirmed after 24 hours of drug treatment (45% decrease, $p<0.0001$).

Lactate production was also assessed as a proxy of glycolytic function, as it follows the glycolysis step, in anaerobic conditions. The lactate production was also found to be dampened after a 24-hour administration of 1μM of IBET-762 vs DMSO (-8%, $p=0.0040$) (**Figure 5.2.7**).

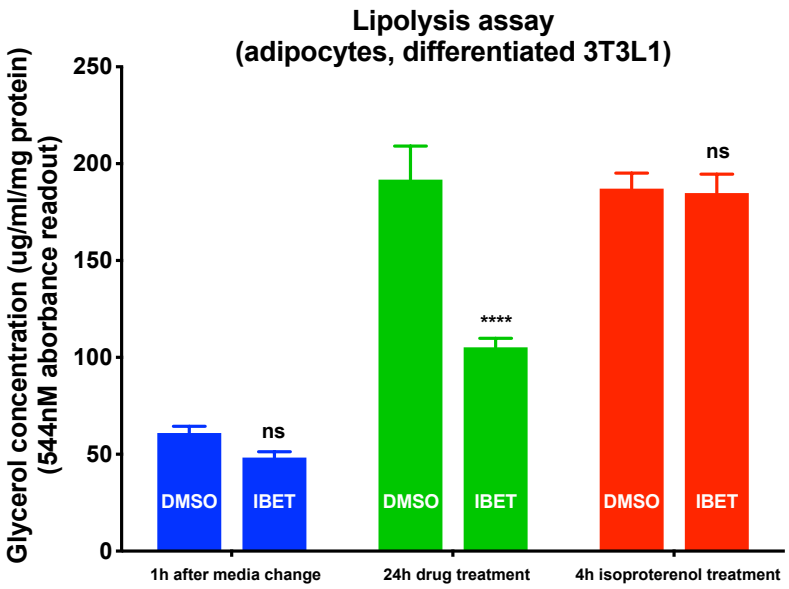


Figure 5.2.7 - Effects of IBET-762 on cellular lipolysis as measured on differentiated adipocytes; the assay allowed for the exposure of IBET-762 or control DMSO for either 1 hour, 24 hours or 4 hours with isoproterenol co-treatment, to allow for a baseline increase. The concentration of glycerol was assessed as a function of absorbance at 544nM. Data was expressed as average ± SEM (n=10) and analysed using a two-way ANOVA method and a Sidak posthoc multiple comparisons test. The effects of IBET-762 were analysed against the DMSO control on adipocytes (differentiated 3T3-L1 cells).

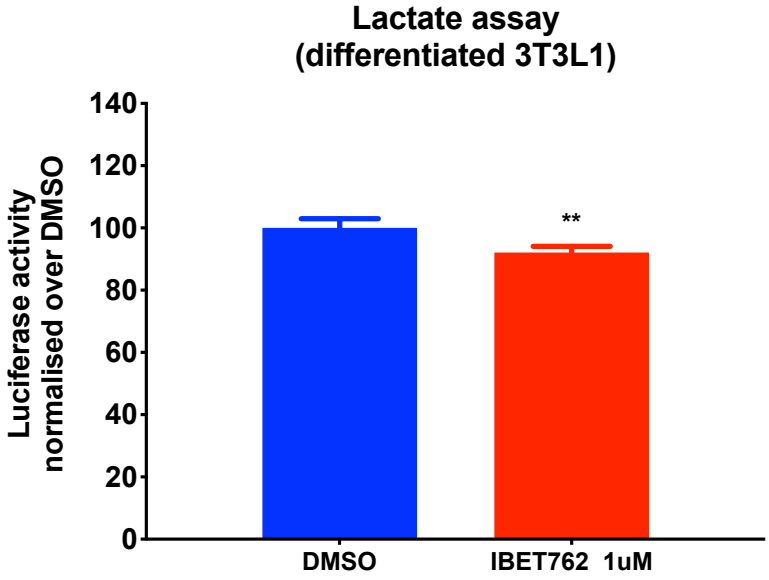


Figure 5.2.8 - Effects of IBET-762 on lactate production; the assay allowed for the exposure of IBET-762 or control DMSO for 24 hours and the quantification of lactate within the media. The concentration of extracellular lactate was assessed as a function of luciferase activity. Data was expressed as average ± SEM (n=6 for the glucose uptake) and analysed through an unpaired two-tailed T-Test.

5.2.8 CLOCK and SP1 effects of IBET-762 on adipocyte glucose uptake

Given the modulation of several glucose markers in adipocytes (**Figure 5.2.5** and **Figure 5.2.6**), such as *Slc2a1* (GLUT1*)*, *SlC2a4* (GLUT4), important in the uptake of glucose and glycolysis, we wanted to further understand the effects of IBET-762 on glucose regulation. We have therefore tested the effects of the bromodomain inhibitor on the uptake of glucose from the media (**Figure 5.2.9**).

The results showed a decrease in glucose uptake in adipocytes (-13%, $p<0.0001$), after a 24 hour IBET-762 exposure, when compared to the DMSO control (**Figure 5.2.9A**).

To understand whether the effects of IBET-762 on the dampening of glucose uptake were modulated by *Clock* or *Sp1* genes, we have knocked-down each of them individually and assessed the effects of IBET-762 on adipocytes lacking each of these genes (**Figure 5.2.9B-D**).

The non-targeting control had no influence on the ability of 1μM IBET-762 to reduce glucose uptake (**Figure 5.2.9B**), resulting in a similar reduction in uptake (-12%, $p=0.0259$). Similarly, the *Clock* knockdown did not influence the IBET-762 reduction in glucose uptake (-11%, $p=0.0115$) (**Figure 5.2.9C**). On the other hand, the *Sp1* knockdown markedly reversed the effects of IBET-762 on glucose uptake, by significantly increasing the uptake of glucose, rather than decreasing it (+39%, $p<0.0001$) (**Figure 5.2.9D**).

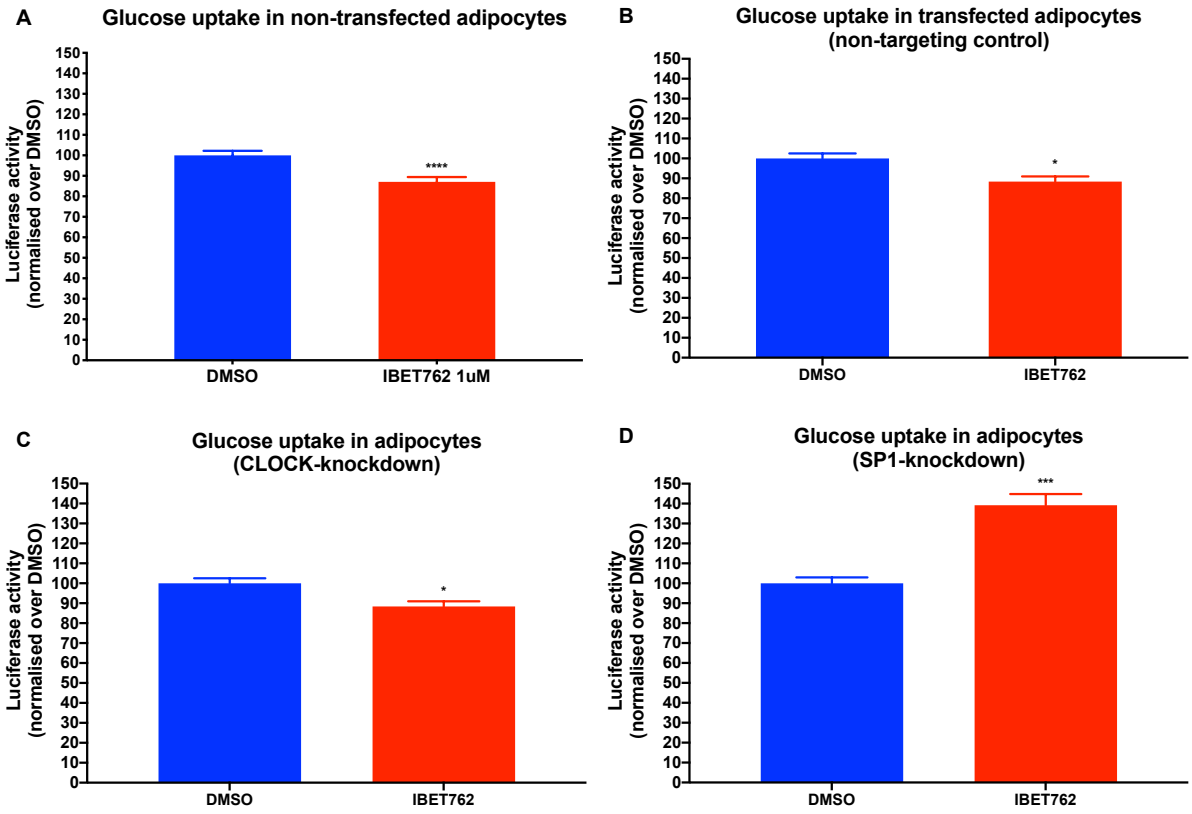


Figure 5.2.9 - Effects of IBET762 on glucose uptake; the assay allowed for the exposure of IBET-762 or control DMSO under a non-transfection (**A**) and transient-transfection protocol (**B-D**). The transient-transfection protocol saw the knockdown of a non-targeting control (NTC) (**B**), the *Clock* gene (**C**) and the *Sp1* gene (**D**). The concentration of intracellular glucose were assessed as a function of luciferase activity. Data was expressed as average ± SEM (n=6 for the glucose uptake) and analysed through an unpaired two-tailed T-Test.

5.2.9 Effects of IBET-762 on ATP energy production

Furthermore, the effects of IBET-762 could also be assessed on ATP production, as an indication of a potential shift between mitochondrial and glycolytic energy production. We therefore dissected the impact of both glycolytic and mitochondrial ATP production (**Figure 5.2.10-Figure 5.2.11**), on adipocytes. ATP originating from glycolysis was quantified in **Figure 5.2.9C**, with IBET-762 decreasing it by both a 500nM (-22%, p=0.0123) and a 1μM dose (-28%, p=0.0008). The positive control Molidustat, was shown to not change glycolytic ATP production significantly (-10%, ns). Molidustat was chosen as a positive control due to its role in mimicking hypoxia and increasing HIF1 activity (Beck *et al.*, 2018), phenomena known to shift ATP energy production from oxidative phosphorylation to glycolysis (Nagao *et al.*, 2019). Mitochondrial ATP production was also quantified in **Figure 5.2.10D**, with IBET-762 reducing it at both 500nM (-40%, p<0.0001) and 1μM (-27%, p=0.0002). Molidustat significantly decreased MitoATP (-37%, p<0.0001). Total ATP production has diminished for both 500nM (-26%, p=0.0002) and 1μM of IBET-762 (-27%, p<0.0001) and Molidustat also (-15%, p=0.0145) when compared to DMSO control (**Figure 5.2.10E**), however the mitochondrial to glycolytic ATP production ratio was not changed significantly by IBET-762 at 500nM (-26%, ns) and 1μM (-4%, ns) (**Figure 5.2.10F**)

The OCR and ECAR values informed on a series of parameters useful to evaluate the mitochondrial functionality (**Figure 5.2.11**). Basal respiration was shown unchanged by IBET-762 500nM (+14%, ns) but significantly increased by the 1μM dose (+29%, p=0.002) and decreased by Molidustat (-27%, p=0.0027) (**Figure 5.2.11A**).

Mitochondrial stress capacity was unchanged by both doses of IBET-762 (+4%, ns), but was decreased by Molidustat (-46%, p<0.0001) (**Figure 5.2.11B**). Spare capacity was decreased by both 500nM (-11%, ns) and 1μM IBET-762 (-26%, p=0.0137) and Molidustat (-72%, p<0.0001) (**Figure 5.2.11C**). Proton leak was also evaluated, with IBET-762 increasing it at both the 500nM (+65%, p<0.0001) and 1μM (+83%, p<0.0001) doses but not by Molidustat (-17%, ns) (**Figure 5.2.11D**).

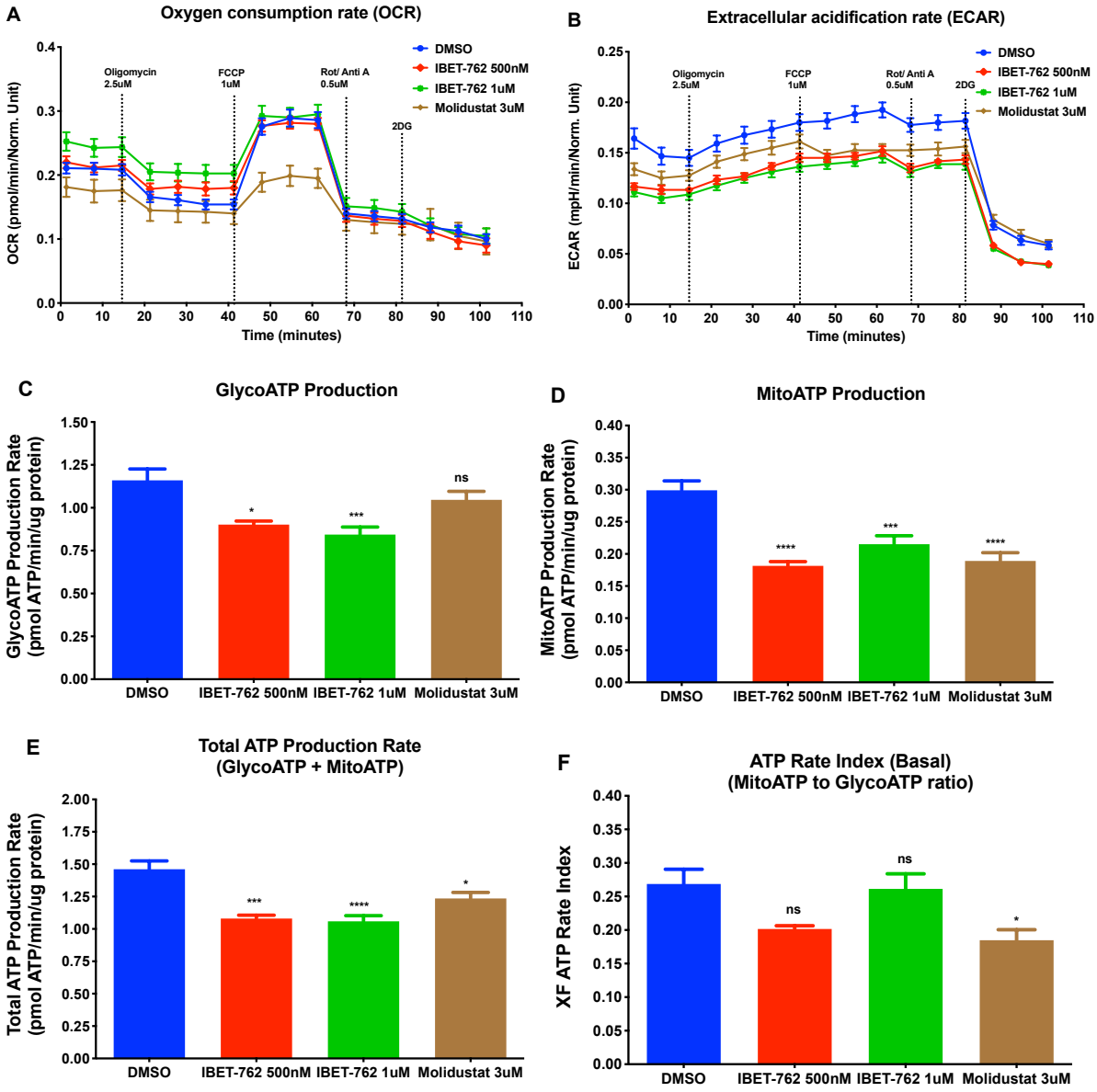


Figure 5.2.10 - Effects of IBET762 on cellular energy production; the assay allowed for the exposure of IBET-762 at 1µM and 0.5µM, DMSO control and 3µM of Molidustat as a positive control. The oxygen consumption rate (OCR) (**A**) and the extracellular acidification rate (ECAR) (**B**) were assessed through Seahorse as main outputs. The GlycoATP production rate (**C**) and MitoATP production rate (**D**) were calculated from OCR/ECAR. Total ATP production rate (MitoATP+GlycoATP) (**E**) and ATP Rate Index (MitoATP/GlycoATP) (**F**), were also assessed. Data was normalised over total protein concentration and expressed as average ± SEM (n=6-12) and analysed through a one-way ANOVA test and Dunnett-powered multiple comparisons.

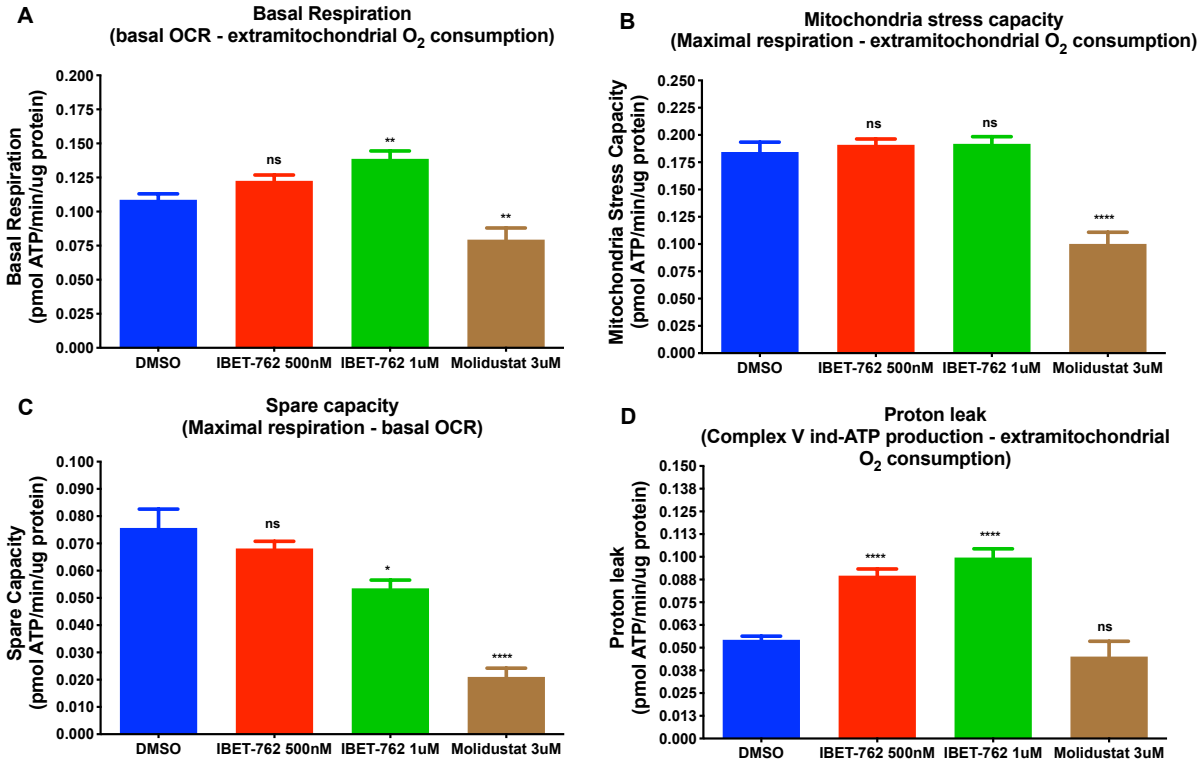


Figure 5.2.11 - Effects of IBET-762 on mitochondrial functionality; the assay allowed for the exposure of IBET-762 at 1µM and 0.5µM, DMSO control and 3µM of Molidustat as a positive control. The rates were calculated based on the OCR/ECAR data outlined in **Figure 3.3.8**. Basal respiration was calculated by subtracting the extramitochondrial O_2 consumption (following rotenone treatment) from the baseline OCR (**A**). Mitochondrial stress capacity was calculated by subtracting extramitochondrial O_2 consumption (rotenone treatment) from the maximal respiration (FCCP treatment) (**B**). The spare capacity was calculated subtracting the baseline OCR from the maximal respiration (FCCP treatment) (**C**) and the proton leak was calculated subtracting the extramitochondrial O_2 consumption (rotenone treatment) from the Complex V-independent ATP production (oligomycin treatment) (**D**). Data was normalised over total protein concentration and expressed as average ± SEM (n=6-12) and analysed through a one-way ANOVA test and Dunnett-powered multiple comparisons.

5.2.10 Effects of IBET-762 on NAD^+ and NADH levels in adipocytes

Given the effects of IBET-762 on both mitochondrial and glycolytic ATP production (**Figure 5.2.10-Figure 5.2.11**), we have assessed the effects of the drug on NAD^+ and NADH production. As shown in **Figure 5.2.12**, IBET-762 1μM reduced the concentrations of NADH (-21%, $p<0.0001$), but not of NAD^+ (-6%, ns), at 30 minutes after the analysis (**Figure 5.2.12A**). Therefore, the NAD^+/NADH ratio increased, given the decrease in NADH, in the IBET-762 group, when compared to the DMSO control (+19%, $p=0.0030$) (**Figure 5.2.12B**).

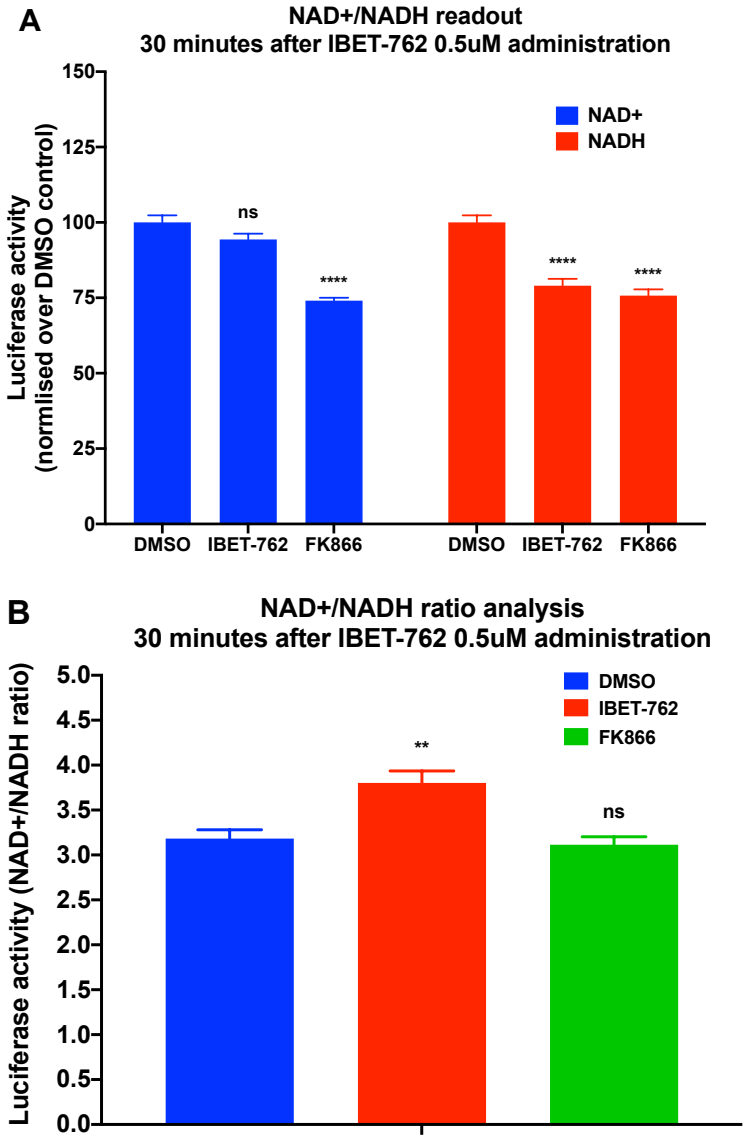


Figure 5.2.12 – NAD+/NADH modulation by IBET-762 administration; NAD^+ and NADH levels were assessed and expressed as normalised on the DMSO control, 30 minutes after the addition of IBET-762 0.5uM (**A**). A ratio between the NAD+ and NADH readings was calculated (**B**). Data was expressed as average ± SEM (n=5) and analysed through a one-way ANOVA and Sidak-powered post-hoc multiple comparisons analysis.

5.3 DISCUSSION

The effects of several genes at the forefront of the interaction between metabolic pathways and circadian rhythms were shown to be modulated by IBET-762 in U2OS cells (**Figure 5.2.1**); *PPARγ* and *PPARγc1α* (PGC1α) expression was severely reduced within the first hours and throughout the 36 hour period of drug administration. PPARγ is in fact a key factor in adipogenesis and glucose metabolism, and is at the centre of the interaction between circadian rhythms and metabolism, with Nocturnin (*Noc*), a rhythmic (circadian) gene expressed in peripheral tissue, shown to enhance PPARγ activity and involved in lipid homeostasis. *Noc*-deficient mice demonstrate a drastic decrease in *PPARγ* expression, similarly to the effects of IBET-762, and were protected against diet-induced obesity (Kawai *et al.*, 2010a; Kawai *et al.*, 2010b). PPARγ is also known to play a role in epigenetic modulation as it forms dimers with nuclear-receptor co-repressor 1/2 (NCoR1/2) and HDACs, when is transcriptionally silent, and HATs when is transcriptionally active (Guan *et al.*, 2005). SIRT1, an HDAC, can also modulate PPARγ transcription by repressing its expression and promoting fat mobilisation in adipocytes (Picard *et al.*, 2004). *PPARγ* was also shown to be transactivated by the elongation factor E2F (Miard & Fajas, 2005), which associates with BRD4 (Dong *et al.*, 2018) and SP1 (Lin *et al.*, 1996), both key factors in relaying the circadian effects of IBET-762. Further, BRD4, whose inhibition we showed to mimic the IBET-762's circadian amplitude enhancement (**Figure 4.2.1 – Figure 4.2.2**), was shown to stimulate the expression of *PPARγ* and therefore adipocyte differentiation (Brown *et al.*, 2018). PGC1A co-regulates PPARγ activity and is fundamental in physiological circadian

functions such as locomotor activity, body temperature oscillations and energy metabolism, with CLOCK, BMAL1 and PER1 expression altered by its decrease in expression (Liu *et al.*, 2007). At a more phyisiological level, PPARɣ modulation was also shown to be influencial in both diabetes and obesity. In fact, thiazolidinediones (TZDs), acting as PPARɣ-agonists, are a class of insulin-sensitizer drugs that lower blood glucose and are used in the management of type-2 diabetes. However, their use has become limited due to serious side-effects, including weight-gain due to an increase in fat mass and fluid retention, which was associated to be directly related to its PPARɣ-agonism mechanism of action and to an increase in risk of miocardial infarction and cardiovascular mortality (Nissen & Wolski, 2007). Given that PPARɣ-agonism was associated with both insulin sensitisation, pivotal in the management of T2D and with an increase in obesity, it is therefore key to modulate the expression and activity of PPARɣ such that it promotes the best outcome in relation to both pathologies. It is apparent that the downstream impact of PPARɣ modulation can be differentially activated depending on the molecule used to interact with the receptor, possibly due to the partial agonism phenomenon that could see the activation of specific downstream pathways and the inactivation of others, with PPARɣ-modulators having a wide array of differential effectiveness and safety profiles (Hong *et al.*, 2018).

IBET-762 also reduced the expression of *Tfeb*, a bHLH regulator of PPARɣ (Salma *et al.*, 2017) also at the forefront between circadian rhythms and metabolic regulation. TFEB was indeed shown to stimulate the expression of *Nr1d1* (REV-ERBa) (Pastore *et al.*, 2019), a transcriptional repressor of the molecular clock and directly involved in metabolic functionality. IBET-762 increased the expression of *Sirt1*, a NAD^+-dependent

HDAC that has a key emerging functionality as a metabolic sensor, controling glucose and lipid metabolism in the liver and insulin secretion in the pancreas possibly through suppression of PPARɣ (Picard *et al.*, 2004). Treatment with activators of SIRT1 were shown to protect against high-fat-diet induced obesity and T2D (Baur *et al.*, 2006; Milne *et al.*, 2007). Sirt1 activation was also shown to ameliorate the diabetic phenotype in a streptozotocin-induced diabetic mouse model, suggesting its expression upregulation by IBET-762 might be beneficial in metabolic disorders (Zhang *et al.*, 2018a). SIRT1 also modulates the activity of peripheral circadian clocks by co-recruiting NCor and regulating PER2 and BMAL1 activity (Asher *et al.*, 2008; Nakahata *et al.*, 2008).

The SP1 and HIF1α's role in energy metabolism and circadian rhtyhms were extensively described elsewhere (**Introduction 5.1.6**). Here we show that *Sp1* and *Hif1α* gene expression levels, although circadian, are not drastically changed by the addition of IBET-762. As the activity levels of SP1 and HIF1A were shown to be indeed modulated using functional assays (**Figure 5.2.11**), this effect of IBET-762 could be mediated by posttranslational processess, rather than transcriptional modifications. It was indeed shown that phosphorylation plays an important role in the posttranscriptional modulation of SP1's activity, which could inflict on SP1 nuclear translocation, protein stability, DNA binding affinity and interaction with other transcription factors. SP1 phosphorylation can both activate or repress its activity, depending on the cell line used, phosphorylation sites and phosphorilatory enzyme (Tan & Khachigian, 2009). Phosphorylation of SP1 seems to decrease its binding to HDACs such as HDAC1 and HDAC2, and thus stimulate transcription (Tsai *et al.*, 2011; Zhang *et al.*, 2006).

As several transcription factors implicated in adipogenesis and glucose regulation were shown to be modulated by IBET-762 in U2OS cells, we wanted to check whether the epigenetic modulator was able to inhibit adipogenesis in differentiating 3T3-L1 cells. The results showed that IBET-762 1μM was able to considerably reduce differentiation of pre-adipocytes, both when treated with IBMX and Insulin, and when treated with IBMX, Insulin and Rosiglitazone, a PPARɣ activator (**Figure 5.2.3**). These results confirmed previous findings in U2OS, of the epigenetic modulator reducing the expression of *Tfeb*, *PPARɣ* and *Pgc1α*. Further, it showed that *PPARɣ* gene expression downregulation, a key mechanism in adipocyte differentiation which could possibly mediate the IBET-762's effects on adipogenesis, is mediated by BRD4 inhibition (**Figure 5.2.3F).** This is in line with previous studies showing the binding of BRD4 to *PPARɣ* enhancers that drive the gene's expression, with disruptions of BRD4 driving *PPARɣ* downregulation and adipogenesis impairment (Brown *et al.*, 2018). Nonetheless, these findings could be in contrast with studies showing an increase in adipogenesis differentiation upon brd2 knockdown (Denis *et al.*, 2010). An explanation to this discrepancy might be due to the fact that BRD2 knockdown might promote opposite effects on differentiation per se, however, a complete BD knockdown or inhibition by IBET-762 could bring about contrasting effects from each of the inhibited bromodomains, culminating in an overall reduction in adipogenesis.

To further confirm IBET-762's reduction in adipogenesis, we have tested the expression of several markers of adipogenesis, under both pro-differentiating stimuli as well as under a control experiment in which 3T3-L1 cells were only added DMSO (**Figure 5.2.4**). The gene expression experiment confirmed that IBET-762 was able to reduce

the expression of 8 out of 9 markers of differentiation by several fold, with the exception of *Psat1*, which showed an increase in its expression under the Insulin + IBMX condition. This confirms our previous findings, placing IBET-762 at the forefront of adipogenesis modulation, as it reduces their expression.

We have further tested the effects of IBET-762 on oxidative stress markers, such as *Cox7a1*, *Pgc1α* and *Idh3a,* showing that IBET-762 decreased the expression of these markers significantly, with the exception of *Pgc1α* under the Insulin + IBMX treatment. This confirms that IBET-762 protects against the increase seen in oxidative stress in adipogenesis (Furukawa *et al.*, 2004). We have also tested the expression of several specific markers of BAT, such as *Ucp1*, *Dio2* and *Ppara*. *Ucp1* and *Pparα* were shown to be downregulated by IBET-762, whereas levels of *Dio2* expression were undetectable. These results underlined that BAT differentiation was also inhibited by IBET-762, possibly due to a general decrease in differentiation from pre-adipocytes to adipocytes. We also evaluated glucose regulation markers such as *Slc2a1* (GLUT1), *Slc24* (GLUT4) and *Gck,* as they are both pivotal in glucose metabolism as well as adipogenic differentiation markers. Their expression was reduced by IBET-762 in both differentiation protocols. The *Slc2a1* and *Slc2a4* reduction, as shown previously, is most likely due to a reduction of PPARɣ expression (Liao *et al.*, 2007; Wu *et al.*, 1998).

Furthermore, we wanted to understand the expression of key adipogenesis genes in mature adipocytes. We thus tested IBET-762 on differentiated 3T3-L1 cells (**Figure 5.2.6**). The effects of the epigenetic inhibitor were largely contrastant to the effects it had in differentiating 3T3-L1 cells (**Figure 5.2.5**), increasing rather than decreasing the expression of these genes. IBET-762 was shown to indeed increase the expression of

WAT-markers, such as *PPARɣ*, *CEBPα* and *Cd36* (**Figure 5.2.6A**). This could be due to the longer term effects of IBET-762 (as the drug was given for about two weeks) and compensatory mechanisms, or to differential metabolic networks between mature adipocytes and pre-adipocytes. Clinically, PPARɣ activation was shown to improve insulin sensitivity and induce browning of white fat, as it was shown to be essential for WAT survival (Imai *et al.*, 2004), though it was also associated with an increase in adiposity and weight gain. However, it is not clear whether the increase is due to the effects of PPARɣ on precursor or mature adipocytes. Furthermore, it was shown that CEBPα and PPARɣ overlap and cooperate in the activation of key metabolic adipocyte genes, such as *Cd36* and *Retn*, among others (Madsen *et al.*, 2014). The effects of IBET-762 on adipokynes was also tested in adipocytes, the main source of these hormones, with both leptin and adiponectin seeing an increase in their expression upon IBET-762 administration (**Figure 5.2.6B**). Higher serum levels of adiponectin were shown to work as a protective factor against obesity and T2D (Arita *et al.*, 1999; Hotta *et al.*, 2000). *Pparα* was shown to increase the expression of both adiponectin and AdipoR (Tsuchida *et al.*, 2005), and its expression levels were upregulated by IBET-762 indeed. Leptin is a satiety-inducing hormone, produced by adipocytes when levels of nutrients are abundant. Higher levels of leptin were associated with obesity, likely due to leptin-resistance and insensitiveness (Considine *et al.*, 1996), and not due to a negative effect of the adipokine per se. This is confirmed by data showing that leptin treatment brings beneficial effects on appetite, fat mass, hyperinsulinaemia and hyperlipidaemia in leptin-deficient humans (Farooqi *et al.*, 2002). IBET-762 was also shown to increase the expression of several genes linked to oxidative stress, such as *Cox7a1*, *Pgc1α* and *Idh3a* (**Figure 5.2.6C**). This might indicate a possible inflammatory status within the adipocytes, or an increase in

uncoupling, or a shift in energy production towards oxidative phosphorylation. With respect to glucose metabolism (**Figure 5.2.6D**), IBET-762 showed an increase in *Slc2a4* expression, hinting towards an increase in insulin-sensitivity in adipocytes, in line with literature (Hauner *et al.*, 1998). Exercise was shown to at least partially counteract the effects of T2D by stimulating the expression of *Slc2a4* receptors in skeletal muscle cells (Rodnick *et al.*, 1990) and that GLUT4 overexpression improved on insulin sensitivity in mice (Atkinson *et al.*, 2013). However, GLUT1 receptor expression was shown to be reduced in adipocytes. If its effects were to be widespread throughout the body and also present in skeletal muscle cells, this could be a reason of wary, as reduced GLUT1 levels were associated with type-1-diabetes mellitus (Garg *et al.*, 2014).

Given the widespread effects of IBET-762 on adipogenesis and the expression of genes involved in fatty acid metabolism in differentiated adipocytes (**Figure 5.2.6**), we decided to further test the effects of the epigenetic modulator on lypolysis, the catabolic process which breaks fatty acids in triglycerides and glycerol, with triglycerides being used as an energy source (**Figure 5.2.7**). The results showed that IBET-762 decreased lypolysis both after 1 hour and after 24 hours of drug addition. However, the isoproterenol-stimulated cells did not show a difference with IBET-762, possibly as the β_3-agonist overseeded the effects of IBET-762 in inhibiting lypolysis, as it possibly acted through mechanisms that do not overlap with the ones of IBET-762's. IBET-762's lipolysis decrease might be due to the downregulation of some of the key hydrolysing enzymes involved in lipolysis, such as the hormone-sensitive lipase (HSL), which was shown to be involved in maintaining adequate levels of fatty-acid release (Haemmerle *et al.*, 2002; Schwartz & Jungas, 1971). The downregulation of HSL would thus explain the observed

reduction in lypolysis activity. Although this is in apparent contrast with previous data in which IBET-762 shows to inhibit adipogenesis and lipogenesis, it has been previously shown that a decrease in fatty acid esterification can stoichiometrically compensate for the reduced lypolytic activity in HSL-deficient WAT (Zimmermann *et al.*, 2003).

Given the effects of IBET-762 on glucose regulation markers, as *Slc2a1* and *Slc2a4* were all modulated both in differentiating 3T3-L1 cells (**Figure 5.2.5**) and mature adipocytes (**Figure 5.2.6**), we wanted to test the effects of the epigenetic modulator on glycolysis. Lactate production was shown to be reduced by IBET-762 (**Figure 5.2.8**), however it is unclear if the effect was due to an aerobic redirectioning effect of energy production or to a lowering of glucose-fuelled energy production overall. Nonetheless, a reduction in lactate production was associated with a decreased risk of developing obesity and insulin resistance (Nellemann *et al.*, 2012).

Given the modulation of both *Slc2a1* and *Slc2a4* receptor expression, we decided to assess glucose uptake. As mentioned before, GLUT1 is a baseline glucose-uptake receptor expressed throughout the body, whereas GLUT4 is an insulin-sensitive receptor which gets predominantly activated postprandially, and is predominant in liver, skeletal muscle and adipocytes. We tested the glucose uptake levels in adipocytes and showed that the overall effect of glucose regulation translated into a lowering of glucose-uptake after 24 hours of IBET-762 treatment (**Figure 5.2.9A**). As we identified glucose uptake downregulated by IBET-762 in adipocytes, we wanted to understand whether these effects were mediated by the molecular clock or by mechanisms that bring forward the circadian changes in amplitude we saw in U2OS cells. We therefore tested the

influence of knocking-down CLOCK and SP1 individually on glucose-uptake in adipocytes upon administering IBET-762 1μM (**Figure 5.2.9B-D**). We used the *Clock* knock-down as a way to alter circadian rhythmicity without completely disrupting key molecular metabolic pathways, as would have happened with a *Bmal1* knock-down (Ameneiro *et al.*, 2020). The *Sp1* knockdown was a way to assess the importance of SP1 transcription factor in mediating the glucose uptake effects, given it was shown essential in mediating the circadian amplitude increase (**Figure 5.2.10**). We could see a direct impact of SP1 transcription factor in mediating the reduction of glucose-uptake, but not of CLOCK. The increase in glucose-uptake upon IBET-762 administration seen in the *Sp1*-knocked down adipocytes could be attributed by overarching effects of the epigenetic modulator on other targets that could influence glucose uptake independently of the SP1 knockdown. SP1 was indeed shown to have an important influence in a plethora of metabolic pathways across tissues and regulate the expression of key genes in fatty b-oxidation, cholesterol and phospholipid homeostatis, among others (Krey *et al.*, 1995; Schmitz & Langmann, 2005). This underlines the importance of SP1 in mediating both circadian amplitude effects as well as IBET-762's metabolic effects on glucose regulatory mechanisms. In fact, it was previously shown in 3T3-L1 cells that SP1 is essential as a transcription factor to mediate the increase in transcription of leptin (**Figure 5.2.6B**) in insulin-stimulated metabolism, possibly by binding to an identified SP1-binding site on the leptin promoter (Moreno-Aliaga *et al.*, 2007). *Clock* knockdown failed to remove IBET-762's effects on the molecular clock, possibly due to the fact that CLOCK function can be compensated by its paralogues such as Neruonal PAS Domain Protein 2 (NPAS2), as shown in both the SCN and peripheral tissues (Landgraf *et al.*, 2016).

As lactate production was downregulated by IBET-762, we wanted to assess whether the effect is due to a downregulation of glycolysis or a redirectioning of energy production from glycolysis to oxidative phosphorylation. To assess if there is a redirectioning of energy production between aerobic and anaerobic modalities, we performed a seahorse assay which measures glycolysis and oxidative phosphorylation levels in the citoplasm and mitochondria of cells (**Figure 5.2.10-Figure 5.2.11**). The results showed that IBET-762 decreased both glycoATP and mitoATP production significantly, at both doses (**Figure 5.2.10C-D**), thus lowering the overall total ATP production significantly (**Figure 5.2.10E**). However, the MitoATP to GlycoATP ratio portrayed in the ATP rate index (**Figure 5.2.10F**) was not significantly decreased by IBET-762 at any of the two doses, suggesting there is not a significant shift towards mitochondrial ATP production. However, 3T3-L1 differentiated adipocytes may use glycolysis as a preferial way of energy production (Sabater *et al.*, 2014), possibly as a short-term strategy to energy expenditure in conditions of normoxia and abundant glucose. Thus, the shift between glycolitic and mitochondrial ATP production might not have happened due to the 3T3-L1 cells characteristic preference on glycolysis for energy production. IBET-762 showed decreased levels of extracellular acidification, at both the 500nM and 1μM dosages (**Figure 5.2.11B**). The lowering in extracellular acidification is in line with evidence showing a lowering of the lactate production in the media of adipocytes exposed to IBET-762 (**Figure 5.2.8**), which has been recognized as a major source of extracellular acidification (Wu *et al.*, 2007), together with the production of CO_2 and H^+ through the aerobic TCA cycle and oxidative phosphorylation (which was also shown to be increased by IBET-762, see below). The reduction in glucose uptake

(**Figure 5.2.9A**), potentially due to a reduction in expression of *Slc2a1* (**Figure 5.2.6**), could explain the reduction in overall glucose-fuelled energy production seen through both a reduction of glycolysis, a lowering in production of lactate and a reduction in oxidative phosphorylation (**Figure 5.2.10D**).

Mitochondria are the biggest energy producers of our cells, in most circumstances, and have shown to be able to adapt to acute and chronic conditions (Soubannier & McBride, 2009). Abnormal mitochondrial functionality is associated with several conditions, such as cardiomyopathy (Sharov *et al.*, 2000) and diabetes (Mogensen *et al.*, 2007). Several of its metabolic parameters calculated based on the oxygen consumption rate (OCR) can thus inform on mitochondrial functionality, in normal conditions or under stress:

- Basal respiration relates to mitochondrial respiration minus the non-mitochondrial O_2 consumption, in baseline conditions
- Mitochondrial stress capacity measures maximal respiration minus the non-mitochondrial O_2 consumption, and is important under stress conditions
- Spare capacity is the maximal respiration minus the basal respiration
- The proton leak measures the inefficiency of energy conversion by the mitochondria

Thus, oxygen consumption rate (OCR) (**Figure 5.2.10A**) has been used to calculate the above parameters (**Figure 5.2.11**). As such, basal mitochondrial respiration supplying mitochondrial ATP synthesis exclusively, was shown to be increased by IBET-762 at both doses (**Figure 5.2.11A**). Basal respiration increase can be given by a series of cellular changes, availability of substrates, such as fatty acids, pyruvate or lactate (Korzeniewski

et al., 1995; Nobes *et al.*, 1990) or by an increased need of ATP production, possibly due to a reduction in glycolysis. Looking at the mitochondrial stress capacity, that is, the amount of energy surplus the mitochondria are able to produce in case of stressors, has not been changed by IBET-762 at any of the two doses (**Figure 5.2.11B**). This suggests that the mitochondria kept their functionality and were not damaged by the epigenetic modulator, as opposed to the effects of molidustat. However, spare mitochondrial capacity was dimished by IBET-762 significantly at the 1μM dose (**Figure 5.2.11C**), which might indicate mitochondrial disfunction. Spare capacity is directly dependent on basal OCR, thus an increased basal oxygen consumption stimulated by IBET-762 1μM influenced the decrease in spare capacity. This indicates that adipocytes operate at a tighter bioenergetic limit, but not necessarily that the bioenergetic ceiling itself has decreased, in presence of 1μM of IBET-762. Proton leakage was also shown to be increased by IBET-762 at both doses (**Figure 5.2.11D**), suggesting a decrease in the efficiency of mitochondrial ATP production, possibly mediated by an increased activity of uncoupling proteins such as UCP1, involved in adipocyte browning and heat production, or UCP2, involved in the regulation of glucose-stimulated insulin secretion in pancreatic β-cells (Robson-Doucette *et al.*, 2011; Zhang *et al.*, 2001) and in the switch between fatty acid and glucose metabolism (Pecqueur *et al.*, 2008). Higher UCP activity might diminish thus mitochondrial superoxide production and protect against ROS-induced diseases and oxidative damage at the expense of loss of energy production (Brand *et al.*, 2004). Furthermore, caloric restriction diets have been associated with a lower superoxide production, possibly as a mechanism of metabolic-fitness and retardation of ageing (Sohal *et al.*, 1994).

As the NAD^+/NADH ratio was recognized as an important factor linking energy consumption with circadian rhythms (Rutter *et al.*, 2001) and ageing, we wanted to test if IBET-762 promoted any direct effects on the production of these two metabolites (**Figure 5.2.12**). We could indeed see that IBET-762 did not impact on the levels of NAD^+, but it did lower the levels of NADH significantly. The lowering of NADH levels suggests a reduction in glycolysis and Krebs cycle pathways as major sources for NADH, without a major change in oxidative phosphorylation, pathway which would replenish NAD^+ reserves. Thus, the lowering of NADH production, significantly increased the NAD^+/NADH ratio, the redox rate within cells, which controls the activity of several bottle-neck enzymes such as the glyceraldehyde-3-phosphate dehydrogenase and pyruvate dehydrogenase. The physiologycal ratio of total NAD^+/NADH within cells is estimated to be between 3 to 10 (Swierczynski *et al.*, 2001), and in our case, it is shown to be around 3.18 in the DMSO control and 3.8 in the IBET-762-treated group (+20% increase). NAD levels feedback on both metabolism (impacting on glycolysis and oxidative phosphorylation) as well as on the circadian clock. Although NAD^+ levels did not change per se, NADH levels dimished, with potentially decreasing the oxidative stress on cells.

Key findings of this chapter:

The physiological data, taken together, demonstrates IBET-762 modulates cellular metabolism, outlined by its impact on several key metabolic genes in U2OS cells (**Figure 5.2.1**), 3T3-L1 cells (**Figure 5.2.4** and **Figure 5.2.5**) and differentiated adipocytes (**Figure 5.2.6**). Moreover, IBET-762 was shown to inflict on metabolic physiology by

both diminishing adipocyte differentiation and adipogenesis markers (**Figure 5.2.3-Figure 5.2.5**) and impacting on key metabolic pathways such as lypolysis (**Figure 5.2.7**) and lactate production (**Figure 5.2.8**). The decrease in lypolysis and lactate production could be ascribed to both a modulation of glucose receptors' expression of *Slc2a1*, *Slc2a4* and *Gck* (**Figure 5.2.6D**) and a decrease in cellular glucose uptake (**5.2.9A**), which was shown to be mediated by the expression of *Sp1* transcription factor (**Figure 5.2.9B-D**), also key in mediating the epigenetic modulator's effects on circadian amplitude (**Figure 4.2.9 and Figure 4.2.10**). The glucose uptake reduction further inflicted on ATP production rates of both glycolytic and mitochondrial production, with no significant shift towards any of the two (**Figure 5.2.10**). IBET-762 has also impacted on the mitochondrial functionality by increasing both basal respiration and proton leakage. It has also decreased mitochondrial spare capacity though without influencing its' stress capacity (**Figure 5.2.11).** The lowering in NADH activity confirms the decrease in glycolysis and Krebs cycle, however the unchanged NAD^+ activity suggests a non significant or less impactful change in oxidative phosphorylation rates (**Figure 5.2.12**), possibly due to the specific physiological architecture of the cellular model used. The metabolic changes in cellular physiology here outlined by the effects of IBET-762 could have profound effects on the metabolism of whole organisms, presumably influencing both obesity and diabetes phenotypes.

CHAPTER IV

IN-VIVO EFFECTS OF IBET-762 ON METABOLISM

main findings:

IBET-762 protects against weight gain in a HFD induced obesity C57BL/6 mouse model

IBET-762 promotes high blood glucose concentrations, which subside at halting of treatment

IBET-762-promoted glucose intolerance not due to insulin-insensitivity or pancreatic toxicity

IBET-762 protects against hepatosteatosis and the metabolic syndrome

IBET-762-stimulated glucose intolerance can be ascribed to an acute MODY-like phenotype

IBET-762 lowers leptin and improves on leptin resistance and ER stress

6 Chapter IV: *IN-VIVO* EFFECTS OF IBET-762 ON METABOLISM

6.1 INTRODUCTION

6.1.1 Markers and types of diabetes

Diabetes can be subdivided into two main types: type 1 diabetes, whereby the b-islets in the pancreas are attacked by the body such that they do not produce or release enough insulin and type 2 diabetes, or the inability of cells to make or respond to the release of insulin. Molecularly, total plasma free fatty acid levels are increased in T2D, modulating the regulation of lipolysis, lipogenesis and inflammation and is a hallmark contributor to insulin resistance (Boden, 2011; Wilding, 2007). Moreover, hypertriglyceridemia and dyslipidaemia (higher levels of LDL cholesterol, the low-density lipoprotein cholesterol associated with atherosclerosis and higher risks of cardiovascular disease and lower levels of HDL, the high-density lipoprotein that acts as a protective factor against CVDs) have also been associated with diabetes (T1D and late T2D) and the metabolic syndrome (Bitzur *et al.*, 2009). High triglyceride levels and a reduced HDL to LDL ratio as the possible culprit of the cardiovascular complications seen in diabetes. Insulin would normally reduce circulating free fatty acids, which are substrates of VLDL (very low density lipoproteins, precursors of LDL) (Malmstrom *et al.*, 1998), and would promote the cleareance of LDL (Mazzone *et al.*, 1984). Moreover, insulin would also enhance the activity and synthesis of lipoprotein lipases (LPLs), which would promote the catabolism of triglycerides and thus limit its levels (Fried *et al.*, 1993) and stimulate the increase in HDL (Ruotolo *et al.*, 1994).

Glucose receptors' gene expression were also tested in relation to the diabetes status of the subjects. GLUT1 expression (promoting basal glucose uptake across most organs) was shown to be decreased in most organs, though increased in liver samples of T2D-induced mice. The expression of GLUT4 receptor (which promotes an insulin-dependent cellular glucose uptake) was shown to be decreased in most organs of diabetic animal models (Jurysta *et al.*, 2013), with the exception of skeletal muscle. GLUT1 is also expressed in skeletal muscle and liver cells and potentially hold a major influence in the glucose uptake in those tissues. However, tissue-specific depletion of GLUT4 receptors in the adipose tissue showed a diabetes-like phenotype of insulin resistance and glucose intolerance, although most insulin-regulated glucose is uptaken by the skeletal muscle (Abel *et al.*, 2001; Zisman *et al.*, 2000).

A third type of diabetes is constituted by the maturity-onset diabetes of the young (MODY) class. It is characterized by a type 2-like noninsulin dependent diabetes and shows autosomal dominant inheritance which typically presents itself before the age of 25 in humans and account for about 1-2% of all diagnosed diabetes cases (Shepherd *et al.*, 2001). The genetic mutations result in a diabetes-phenotype due to their effects on β-cell dysfunction, that is, loss-of-function mutations in genes that are implicated in the production and release of insulin. We are currently aware of 9 genetic mutations that can bring forward the MODY-phenotype, all with different population prevalence, however only 4 of them have been described extensively (**Table 6.1.1**). The other five genes show a lower than 1% prevalence across MODY cases (*Ins*, *Ipf1*, *Neurod1*, *Cel* and *Pax4*).

Gene	Role of gene	Prevalence of MODY in diabetes	Distinct clinical features
Hnf1A	Glucose transport and metabolism – defects in islet glucosensing (Pontoglio *et al.*, 1998)	30-50%	MODY3 - Common and highly penetrant mutation with a large effect on blood glucose after glucose intake (>6mmol/L) (Stride *et al.*, 2002). Progressive -CE failure and reduced mitochondrial metabolism (Wang *et al.*, 1998).
Gck	Glucose phosphorylation – defects in islet glucosensing (Matschinsky, 1993)	30-50%	MODY2 - Common and with raised fasting glucose levels but limited effect on blood glucose after glucose intake (<3mmol/L) as insulin production is adequate (Stride *et al.*, 2002).
Hnf4A	B-cell defect	2-5%	MODY1 - Similar to *Hnf1a*. Progressive B-cell failure.
Hnf1B	HIF1A gene expression regulation across organs	5-10%	MODY 5 - Similar to *Hnf1A*, with an increase in renal disease (Ulinski *et al.*, 2006).

Table 6.1.1 – Genetic mutations, prevalence and clinical features of the four most common causes of MODY.

As it occurs, many MODY cases are initially diagnosed as either type 1 or type 2 diabetes, given their similarities with the two types and the lack of molecular testing. However, MODY differentiates itself from type 1 diabetes as it is insulin independent, does not produce autoantibodies against β-pancreatic cells, and there is a lack of initial ketoacidosis (production of ketonic bodies in absence of neuronal glucose uptake) (McDonald *et al.*, 2011). It also shows differential aspects to type 2 diabetes, such as the absence of insulin resistance, lack of obesity and normal triglyceride levels.

6.1.2 Circadian rhythms influence in diabetes

Shift work is one of the main sources of modern circadian misalignment, with up to 20% of the workforce engaged in shift-work, in the industrialised societies (Alterman *et al.*, 2013). At an epidemiological level, circadian rhythm disruptions were associated with glucose intolerance and type-2 diabetes (Kervezee *et al.*, 2020; Morris *et al.*, 2015). A 14-year prospective study showed an increase in HbA1c levels, as a marker of chronic blood glucose concentrations, in Japanese shift workers (Suwazono *et al.*, 2009). Other studies also confirmed these findings, with rotational shift workers showing a 166% increase in glucose intolerance with respect to the day-shift workers (Mikuni *et al.*, 1983). Healthcare rotational shift workers have also showed increased postprandial glycaemic excursions and a delayed increase in insulin release during night-shifts, findings which were supported by an impairment of pancreatic β-cells and a reduced sensitivity to glucose, in the respective night-shift workers (Sharma *et al.*, 2017). Furthermore, permanent night workers were also shown to have increased likelihood of developing the metabolic syndrome (Biggi *et al.*, 2008).

These epidemiological findings are not surprising as it has been reported how circadian rhythms can influence on metabolism and metabolic pathways and vice-versa (Masri & Sassone-Corsi, 2013; Sinturel *et al.*, 2019). Moreover, night shifts and circadian rhythm disruptions were shown to be associated to changes in the metabolome and expression of key metabolic pathways, with the majority of metabolites being misaligned in the night shift condition (Kervezee *et al.*, 2019). As discussed in **Introduction 1.14**, the disruption of *Clock* and *Bmal1*, key genes of the molecular clock, were shown to promote hyporinsulinaemia and diabetes. In fact, insulin release was shown to be dysregulated in

humans with diabetes due to a un-rhythmicity in the pancreatic β-cells (Marcheva *et al.*, 2010; Peschke & Peschke, 1998). Liver mutants of *Bmal1* showed an altered glucose metabolism (Lamia *et al.*, 2008) and pancreatic mutants of *Bmal1* and *Clock* impacted on the oscillation of insulin release and gene transcription of pathways fundamental in insulin secretion (Marcheva *et al.*, 2010; Perelis *et al.*, 2015; Saini *et al.*, 2016) and skeletal muscle knockdowns of *Bmal1* were associated with a reduction in insulin-stimulated glucose uptake, with a reduction in GLUT4 activity (Dyar *et al.*, 2014).

A study looking into the mechanisms associated with the metabolic consequences of circadian misalignment found several hormones to be dysregulated in subjects who ate and slept out of phase with their circadian clock. Among these we can encounter lower blood levels of leptin and higher blood levels of glucose and insulin as well as completely deregulated circadian blood concentrations of cortisol across the whole behavioural cycle, causing pre-diabetic like postprandial glucose concentrations in part of the subjects studied that did not verify before the start of the trial (Scheer *et al.*, 2009). Further, HbA1c levels in biopsy fibroblasts from patients affected by type-2-diabetes were inversely correlated to period length. At a more molecular level, the expression levels of *Icam1* gene (encoding for the endothelial adhesion protein that was shown to be rhythmically activated by CLOCK) was differentially expressed in T2D and non-diabetic patients and also inversely correlated with cellular period length. These findings suggest a possible mechanistic link between diabetes and the molecular clock, as the binding of CLOCK to *Icam1* showed to be enhanced in patients affected by T2D (Sinturel *et al.*, 2019).

6.1.3 Models to study obesity and HFD in mice

The prevalence of obesity is currently high, affecting over 750 million people worldwide and steadily increasing (WHO, April 2020). An increase in fat intake and fatty diets has been associated with an increased likelihood of developing obesity and insulin resistance, possibly due to the fact that fatty meals induce less satiety than carbohydrate-rich meals, inducing overconsumption and weight gain (Golay & Bobbioni, 1997). Furthermore, the increase in obesity is associated with both an increase in morbidity and mortality (Hruby & Hu, 2015). In fact, high-fat diet induced obesity was also shown to cause adipose tissue inflammation, insulin resistance and predispose towards the metabolic syndrome and type 2 diabetes (Eckel *et al.*, 2005), and an increase in oxidative stress, dyslipidaemia, high-blood pressure (Grundy, 2006), and non-alcoholic fatty liver disease (NAFLD) (Ragab *et al.*, 2015), among other pathologies.

Several obesity animal models can be employed, ranging from models that present specific genetic mutations that make them more susceptible to gaining weight, or by administering a high fat diet to wild-background models. Popular genetically-mutated models of obesity (and consequently diabetes) are animals that see mutations in the signalling of leptin. Leptin is an adipokine produced by the fat tissue, now considered an endocrine organ, given it releases a series of hormones that regulate various metabolic functions, such as leptin and adiponectin (Zhang *et al.*, 1994). Moreover, high levels of leptin, a satiety-stimulating hormone, were associated with obesity and leptin-resistance, giving rise to a vicious cycle, and type-2 diabetes (Wang *et al.*, 2014). The mechanisms of leptin resistance can be multifaceted, such as defects in leptin synthesis and secretion (Knight *et al.*, 2010), signal transduction and trafficking (Bjornholm *et al.*, 2007; Wilsey

& Scarpace, 2004) and endoplasmic reticulum (ER) stress (Hosoi *et al.*, 2008). Leptin thus stimulates POMC neurons to secrete anorexigenic neuropeptides such as POMC, whereas AgRP neurons are inhibited by leptin, leading to a reduced release of orexigenic peptides such as NPY and AgRP (Kim *et al.*, 2014a).

One of the main and most employed animal models of obesity among the leptin-signalling models are the db/db and ob/ob mice. The db/db mice have the leptin receptor gene mutated and thus show reduced satiety levels upon food consumption. However, the leptin mutation implicates a wide phenotype outside of metabolic disorders, including reproductive and immune system alterations, impacting on the dissection of the molecular impact linked to the metabolic effects. Thus, although is considered as a very good model of type-2 diabetes, it has limitations with regards to its construct validity, as leptin resistance develops in obese patients as a desensitisation consequence of an increased leptin production due to an increased food intake, rather than a mutation in the leptin receptor itself. Recessive leptin receptor mutations are in fact rarely identified in individuals and do not constitute a preponderant cause of obesity (Hannema *et al.*, 2016). The ob/ob mice are another genetic model of mutations in leptin-signalling, giving rise to an obese phenotype. This model presents a mutation in the leptin gene and thus influences the satiety response to food and stimulating overall food intake and weight gain (Ingalls *et al.*, 1950). As the db/db model, the ob/ob mutation also impacts on other pathophysiological aspects, such as angiogenesis, malignancies and reproduction and it constitutes a restricted model in obesity due to its limited validity. The ob/ob model is better suited for the study of the effects of leptin on obesity and metabolism (Lindstrom, 2007).

Diet-induced obesity (DIO) mice are believed to be a close mimic of the obesogenic state in humans owing it to the fact obesity is caused as a result of dietary imbalance and, as an extension, a good choice for evaluating therapeutics against obesity. These mice demonstrate increased body-mass as a result of increase in fat intake, representing parallels with human pathophysiology (Wang & Liao, 2012). Studies have indeed shown that a 12-week long high fat diet can increase weight gain by almost 200% and predispose towards insulin resistance and glucose tolerance (both in fasting glucose concentrations as well as post prandial glucose in C57BL/6 mice (Lang *et al.*, 2019). Moreover, just 8 to 12 weeks of high fat diet were shown to influence the reduction of β-oxidation and an increase in hepatic lipogenesis and hepatic damage, precursors of NAFLD, in C57BL/6 mice (Bargut *et al.*, 2014)·(Chamma *et al.*, 2017). The high fat diet induced obesity model was used to study the effects of some circadian amplitude enhancers on the development of obesity, insulin resistance and dyslipidaemia. An example of this is nobiletin, a flavone that was shown to both increase circadian amplitude and improve the metabolic profile of C57BL/6 mice that were exposed to a 8 to 10 week-long high fat diet regime (He *et al.*, 2016; Lee *et al.*, 2013). One of the criticisms of the model has been the monotonous nature of providing high fat diet at 40% or 60% ratio over a long time and the rapid manner in which the metabolic phenotype is induced. This indeed may or may not accurately represent the pathophysiology of the human state. Nevertheless, given this model mimics several attributes of human metabolic disorder, this model should give valuable insights and reveal possible mechanisms underlying metabolic disorders, which in the future can be considered with additional models. Furthermore, C57BL/6 mice are a good model of NAFLD, given their genetic predisposition towards developing obesity, type-2 diabetes, dyslipidaemias and NAFLD, when administered a HFD or subject to

mutations in specific obesogenic genes (Van Herck *et al.*, 2017). This phenotype is similar to the one developed by humans with NAFLD (Rocchini *et al.*, 1997), allowing for an increased face validity of the model.

6.2 RESULTS

6.2.1 Effects of IBET-762 on weight in chronic HFD mouse model

In the previous chapter, it was observed that IBET-762 not only reduced adipogenesis (**Figure 5.2.2-Figure 5.2.4**) but also lipolysis (**Figure 5.2.6**) and modulated the expression of several key metabolic genes (**Figure 5.2.5**). Further IBET-762 also reduced glucose uptake (**Figure 5.2.8**) and ATP production (**Figure 5.2.9-Figure 5.2.10**. These results suggest the epigenetic modulator is capable of regulating several metabolic pathways implicated in adipogenesis, lipogenesis and body fat storage and possibly modulate glucose uptake and energy production. We therefore decided to evaluate the effects of IBET-762 in modulating the adipogenesis in a diet-induced-obesity high fat diet C57BL/6 mouse model.

The mice were subdivided into three groups: 1) high-fat-diet only (Vehicle control), 2) IBET-762-treated mice on high-fat-diet and 3) diet control (a regular normocaloric chow diet). IBET-762 was administered for the first 10 weeks at 20mg/kg. Following this 10 week treatment period administration of IBET-762 was stopped and the mice were allowed to continue on the high-fat diet to probe the reversibility (vs toxicity) of IBET-762

As can be seen from **Figure 6.2.1A**, mice on IBET-762 failed to gain significant weight in comparison to the vehicle HFD group from week 2 (-12% weight, p=0.0111) all the way to the completion of the experiment in week 10 (-24%, p<0.0001). This indeed holds

true also at the level of individual weight gain in addition to the overall weight of the mice (**Figure 6.2.1B**). The ability of IBET-762 to prevent weight gain was so striking that the weekly weight gain and the overall weight of mice on IBET-762 – HFD, resembled mice on normal chow and were starkly different from HFD control. Further to evaluate that the failure to gain weight in the IBET-762 were reversible and not due to significant toxicity, IBET-762 treatment was stopped following 10 weeks and the mice were allowed to continue ad libitum feeding of HFD. The effects of interrupting the IBET-762 treatment were analysed in comparison to weight-matched vehicle treated HFD control mice (**Figure 6.2.1C**). As can be observed, the average intraweek weight gain (W11-17) following the interruption of IBET-762 was no different to the weigh-gain demonstrated by mice on vehicle control between W4-W10, (ns, pooled slope 1.297, pooled intercept 28.05) (**Figure 6.2.1D**).

The percentage increase in weight gain of the week before culling (as normalised onto the baseline week) was also analysed, allowing us to pinpoint chronic effects of the intervention. In fact, we can notice lower weight gains in both the diet control (-12%, $p<0.0001$)) and IBET-762 treatment (-12%, $p<0.0001$), between week 9 and week 10 of drug administration, when compared to HFD vehicle control. Moreover, following the interruption of IBET-762 treatment (week 10), significant weight gain was evident as soon as week 12 (week 2 w/o IBET, +10%, $p=0.0361$) all the way to the end of this procedure at week 18 (week 8 w/o IBET +24%, $p<0.0001$) (**Figure 6.2.1E**). An analysis of the food consumption (normalised as kcal/weight) throughout the first ten weeks, showed that there was no difference in caloric intake between the three cohorts analysed (**Figure 6.2.1F**).

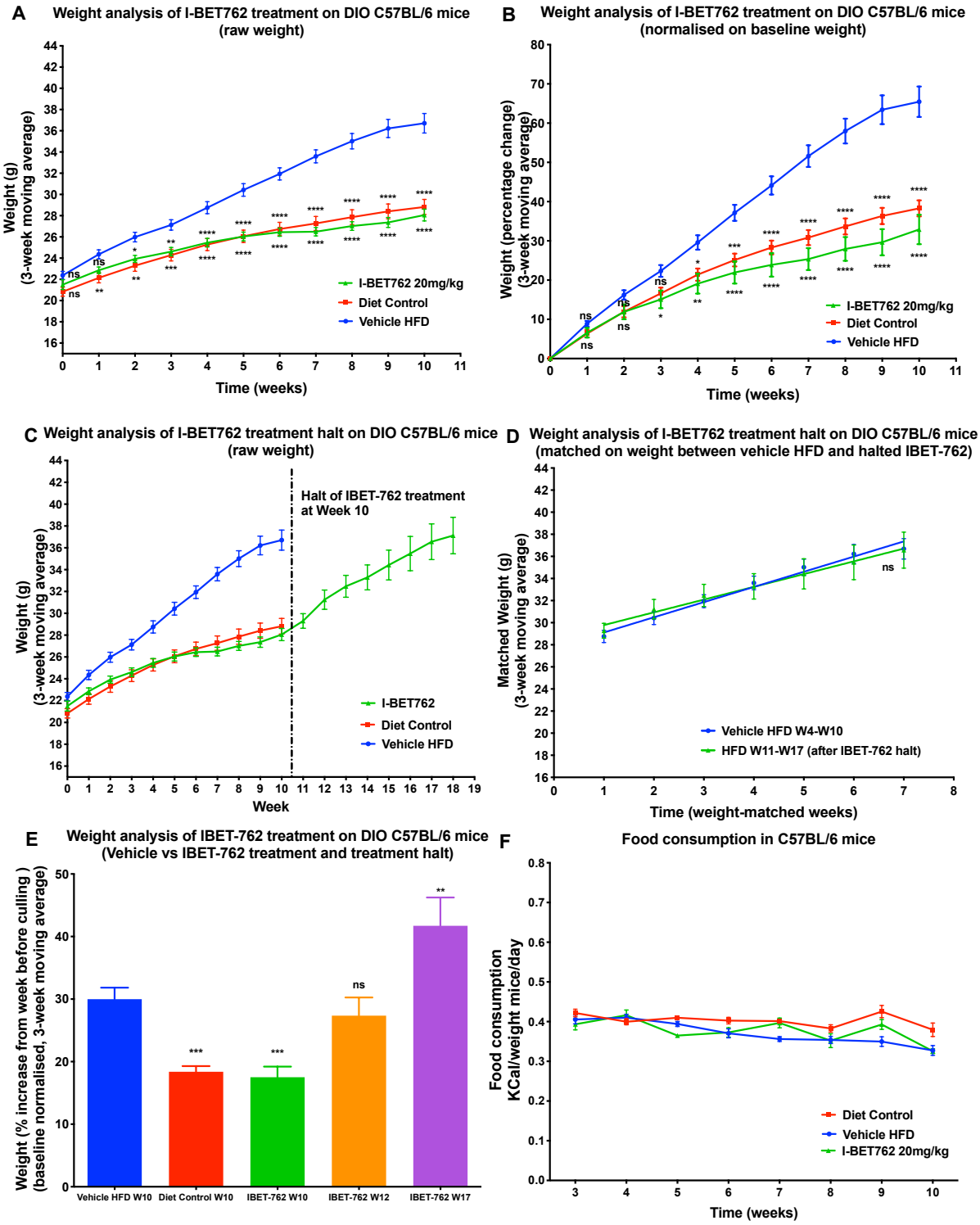


Figure 6.2.1 – Effects of 20mg/kg IBET-762 on weight gain in DIO C57BL/6 mice; data was expressed as a 3-week moving average to reduce week to week variations, ± SEM (n=8-16). Weight is represented as both raw data (**A**) and individual weight percentage change from baseline (**B**) before and after IBET-762 treatment interruption (**C**). The weight was matched between vehicle HFD control and IBET-762 treatment halt groups and plotted against each other (**D**). Weight gain was also analysed in the last week before culling and normalised on baseline weight (**E**). The effect of IBET-762 treatment on caloric intake is also shown and normalised on kcal/weight of mice (**F**). Significance was tested through a one-way ANOVA followed by a post-hoc Dunnett-powered multiple comparisons analysis.

6.2.2 Effects of IBET-762 on glucose tolerance in chronic HFD mice

Given the effects of IBET-762 on glucose uptake in adipocytes (**Figure 5.2.8**), an overall decrease in energy production (**Figure 5.2.9-Figure 5.2.10**) and reduction of weight gain in a high-fat diet-induced obesity C57BL/6 mouse model (**Figure 6.2.1**), we decided to assess the glucose tolerance of a chronic exposure to IBET-762, in mice exposed to a high-fat diet (**Figure 6.2.2**). In the IBET-762-treated group we could see a stark increase in glucose concentrations at all timepoints (**Figure 6.2.2A**) when compared to the vehicle HFD control, and specifically at baseline (+39%, $p<0.0001$) (**Figure 6.2.2C**) and at the 15 minutes peak (+29%, $p<0.0001$), after the administration of a glucose bolus (**Figure 6.2.2D**). The increase in glucose in IBET762-treated mice persisted even after two hours following drug administration (+59%, $p<0.0001$). Glucose concentrations in the diet control were lower, when compared to HFD vehicle, at baseline (-36%, $p<0.0001$) and peak (-23%, $p=0.0005$) (**Figure 6.2.2A, C, D**). Conversely, the effects of halting IBET-762 after 10 weeks were apparent, as the interruption of the drug decreased the glucose concentrations at all timepoints, when compared to W9 IBET-762 treated mice (**Figure 6.2.2B**).

Moreover, both after 2 weeks and 8 weeks following treatment halt, glucose concentration decreased at both baseline and peak (-36%, $p=0.0005$; -54%, $p<0.0001$) when compared to vehicle control and to IBET-762 W9 treatment respectively (**Figure 6.2.2B, C, D**). After normalising the glucose tolerance test on baseline glucose concentrations, IBET-762 has similar effects on glucose concentration increase at week 9, when compared to the vehicle control (**Figure 6.2.2E**) and the halt of treatment reverses the increase at both 2 and 8 weeks after treatment interruption (**Figure 6.2.2F**).

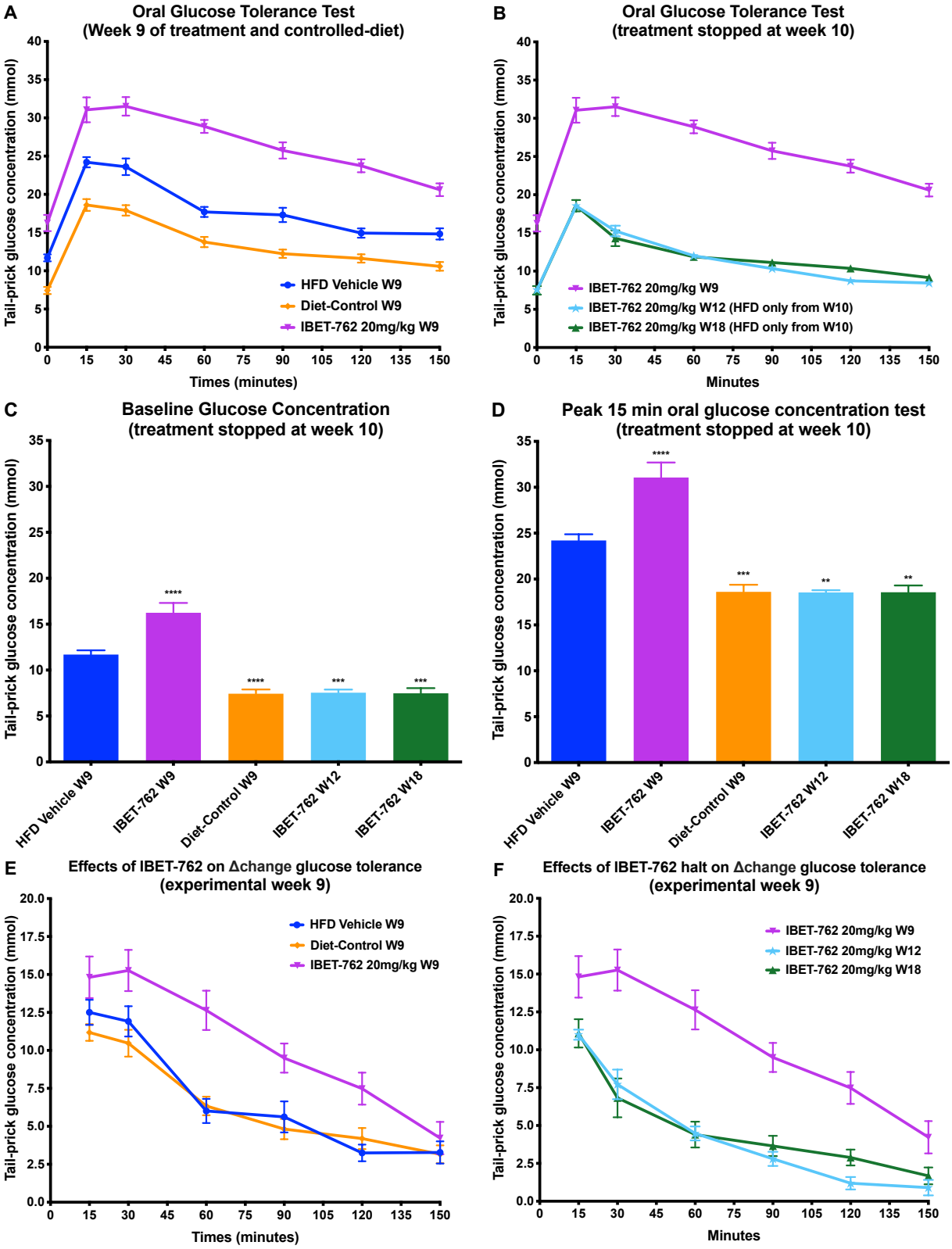


Figure 6.2.2 – Effects of 20mg/kg IBET-762 on glucose tolerance test in DIO C57BL/6 mice; data was expressed as an average ± SEM (n=8-15). The data shows the effects of 10 week long IBET-762 20mg/kg on a glucose tolerance test (**A**), the effects of interruption of IBET-762 treatment on the treated mice at week 12 and week 18 (**B**) the analysis of the glucose concentration at baseline, before glucose administration (**C**) and at the 15-minutes peak after glucose administration (**D**). The Δchange in glucose concentration was also tested as the baseline glucose levels were subtracted from the glucose challenge readings (**E, F**). The glucose concentration was expressed in mmol.

6.2.3 Effects of IBET-762 on insulin tolerance in chronic HFD mice

Following on results from plasma glucose concentrations in mice models subjected to a glucose tolerance test (**Figure 6.2.2**), we wanted to test whether the changes were driven by alterations in insulin sensitivity or the release of insulin. We thus subjected all our groups to an insulin tolerance test, assessing the concentration of glucose after an IP bolus of insulin (**Figure 6.2.3**).

As can be seen below, IBET-762 administration did not significantly affect insulin's ability to reduce blood glucose. Specifically, the results showed an overall decrease in the glucose concentration upon insulin administration in the IBET-762-treated mice at week 9, when compared to the vehicle control (**Figure 6.2.3A**). Further, although the baseline glucose concentration was increased in the IBET-762 group in comparison to vehicle control (+26%, p=0.0008) (**Figure 6.2.3C**), after the insulin bolus, it saw a greater decrease in comparison to vehicle control (-11%, ns) (**Figure 6.2.3D**). The diet control had a bigger effect on the trough glucose concentration (-40%, p<0.0001), although the baseline was only modestly decreased (-13%, ns) (**Figure 6.2.3C-D**). The IBET-762 treatment halt decreased the baseline glucose concentration at 2 weeks (-30%, p=0.011) and 8 weeks after treatment interruption (-18%, ns) (**Figure 6.2.3C**). It also severely impacted on the trough glucose concentration after insulin administration at both 2 and 8 weeks after (-53%, p<0.0001; -36%, p<0.0001, respectively) (**Figure 6.2.3.D**). When normalised on baseline glucose concentrations, IBET-762 showed to promote a decrease in the trough of glucose concentration at week 9 (**Figure 6.2.3.E**) with respect to vehicle control, with the treatment halt partially eliminating the effect (**Figure 6.2.3F**).

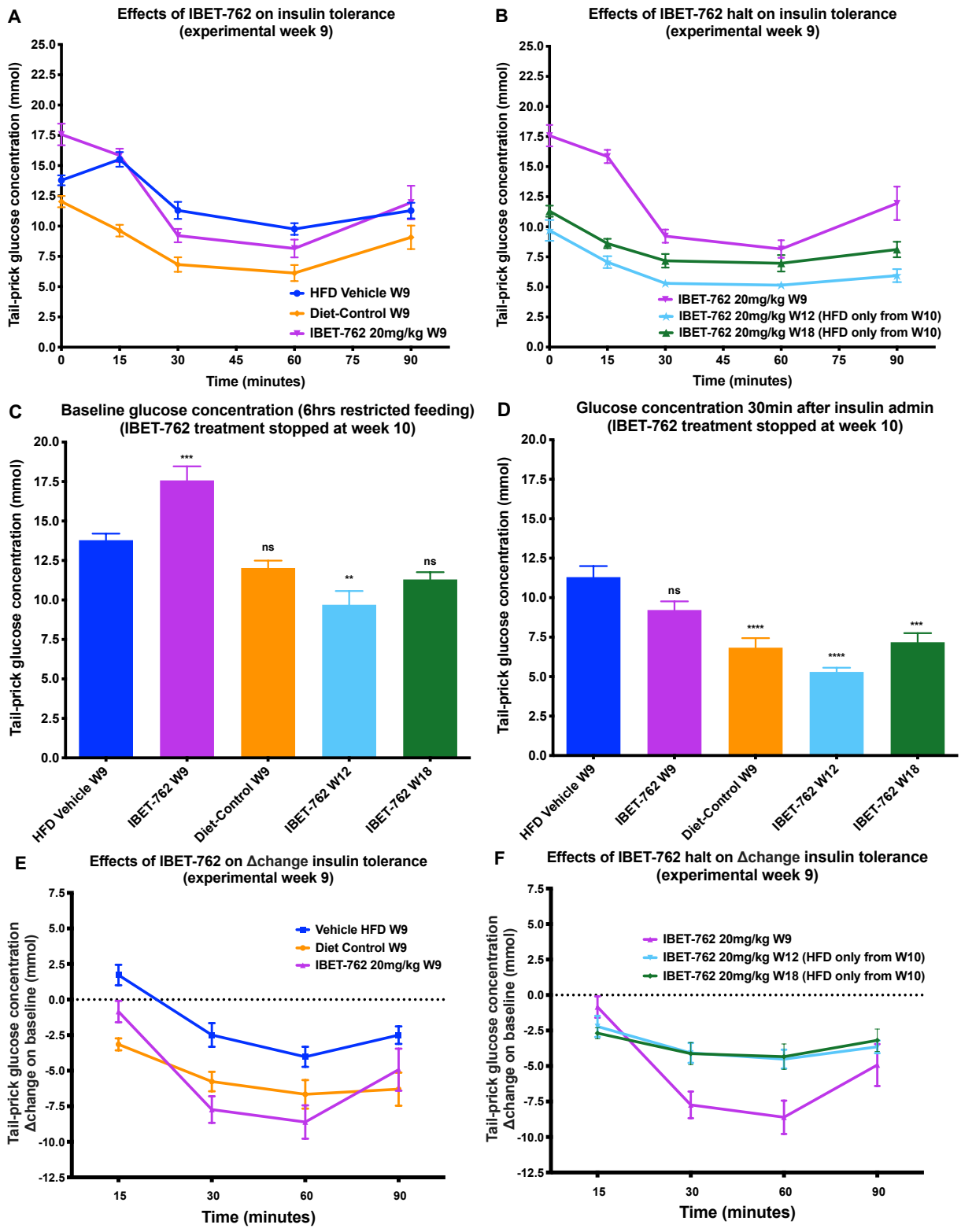


Figure 6.2.3 – Effects of 20mg/kg IBET-762 on insulin tolerance in DIO C57BL/6 mice; data was expressed as an average ± SEM (n=8-11). The data shows the effects of 10 week long IBET-762 20mg/kg on the insulin tolerance test (**A**), the effects of interruption of IBET-762 treatment on the treated mice at week 12 and week 18 (**B**), the analysis of the glucose concentration at baseline, before insulin administration (**C**) and 30 minutes after insulin administration (**D**). The Δchange in glucose concentration was also tested as the baseline glucose levels were subtracted from the insulin challenge readings (**E, F**). The glucose concentration was expressed in mmol and significance was tested through a one-way ANOVA followed by a post-hoc Dunnett-powered multiple comparisons analysis.

6.2.4 Effects of IBET-762 on liver weight and steatosis in HFD mice

Given the aforementioned widespread effects of IBET-762 on weight (**Figure 6.2.1)** and insulin and glucose tolerance (**Figure 6.2.2-Figure 6.2.3**), we wanted to further assess the effects of the IBET-762 on the liver and on other factors that could be involved in mediating these phenotypic changes. We thus weighted the livers of all groups and normalised their weight to the tibia length, as a way to dissect the effects of different physiognomies (**Figure 6.2.4A**). The results show that IBET-762 20mg/kg promotes a reduction in the weight of the liver after 10 weeks of treatment (-24%, p=0.003), however the effect of the drug dissipated 8 weeks after the interruption of IBET-762 (+7%, ns), when compared to the vehicle control at week 10.

Hepatosteatosis was also quantified in cryo-conserved sections of liver samples. The results confirmed a significant increase of liver steatosis in the HFD-vehicle control group, when compared to the diet control group fed with a normal chow (2.6% as opposed to 20.3% hepatosteatosis in the HFD group), as expected in relation to the high fat diet administration in C57BL/6 mice. Most importantly, IBET-762 was shown to mitigate the effects of the high-fat diet on hepatosteatosis, reducing it to 2.9%, 10 weeks after the treatment. Furthermore, although IBET-762 was halted at week 10 and the mice were administered a high-fat diet throughout until week 18, the IBET-762 W18 group showed low levels of liver lipid presence (0.9%), as found in the IBET-762 W10 cohort (**Figure 6.2.4B**).

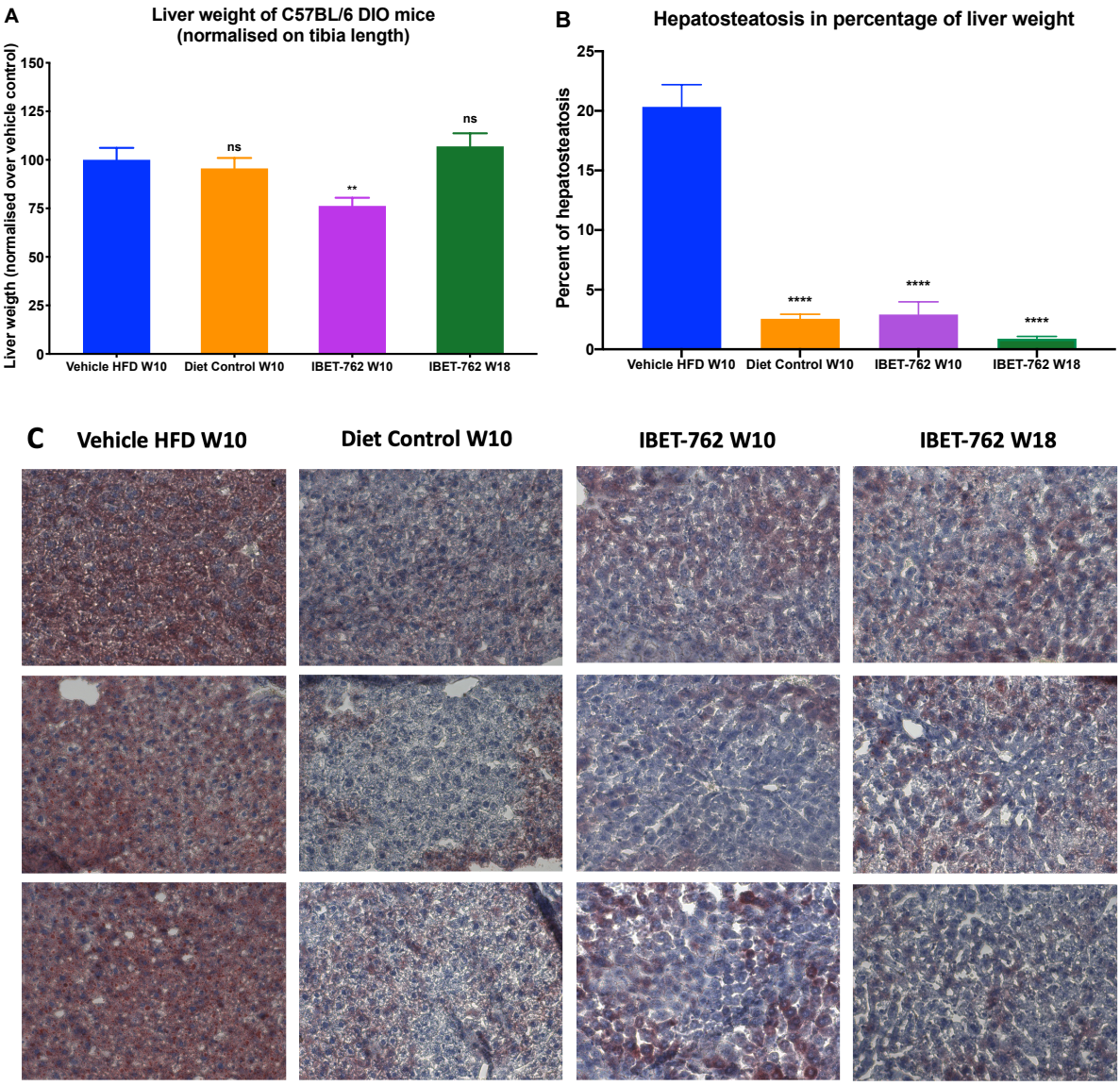


Figure 6.2.4 – Effects of 20mg/kg IBET-762 on liver weight and hepatosteatosis DIO C57BL/6 mice; (**A**) The effects of IBET-762 on liver weight were quantified and the data was normalised over individual tibia length to account for different physiognomy and was expressed as a percentage average over vehicle control ± SEM (n=6-15). (**B**) Hepatosteatosis was also measured and lipids were stained in liver samples with oil-red-o (**C**), which was then quantified and expressed as percentage of hepatosteatosis over same-size slides. Treatment was halted at week 10, thus IBET-762 W18 includes W10-W18 of HFD treatment. Significance was tested through a one-way ANOVA followed by a post-hoc Dunnett-powered multiple comparisons analysis against Vehicle HFD W10.

6.2.5 Effects of IBET-762 on plasma metabolites in DIO mice

After culling, plasma was collected to allow for the testing of the levels of several blood metabolites pivotal in energy storage, production and release. Thus, levels of insulin, triglycerides, free-fatty acids and cholesterol were tested post-mortem, both at 10 weeks and 18 weeks (8 weeks after interrupting IBET-762 treatment) (**Figure. 6.2.5).** Plasma levels of insulin were shown to be diminished by IBET-762 at week 10 (-90%, ns), as compared to vehicle control, and increased at week 18 (+108%, p=0.0076) (**Figure 6.2.5A**). IBET-762 also promoted an increase in plasma triglycerides (+10%, p=0.025), and the effect was reversed upon removal of IBET-762 administration at week 10 (-11%, p=0.0151) (**Figure 6.2.5B**). IBET-762 did not change free fatty acid concentrations at week 10 (+10%, ns), as compared to vehicle control, but did have effects 8 weeks after treatment interruption (-33%, p=0.0007) (**Figure 6.2.5C**). Lastly, IBET-762 decreased levels of total cholesterol at both week 10 (-34%, p=0.0001) and week 18 (-22%, p=0.0073) (**Figure 6.2.5D**), when compared to HFD

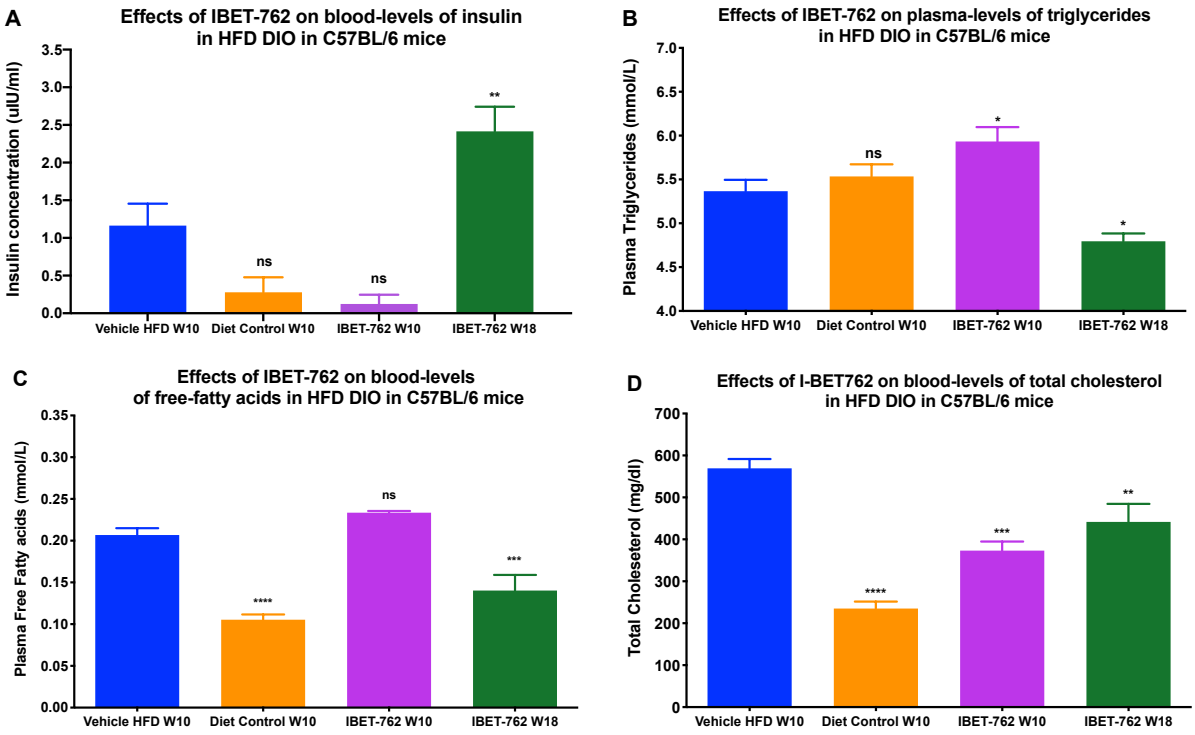


Figure 6.2.5 – Effects of 20mg/kg IBET-762 on plasma metabolites in DIO C57BL/6 mice; plasma metabolites were analysed *ex-vivo* in samples collected from mice, testing the levels of insulin (**A**), triglycerides (**B**), free fatty-acids (**C**) and total cholesterol (**D**). The data was expressed as an average ± SEM (n=5-13). Treatment was halted at week 10, thus IBET-762 W18 includes W10-W18 of solely high-fat diet administration. Significance was tested through a one-way ANOVA followed by a post-hoc Dunnett-powered multiple comparisons analysis against Vehicle HFD W10.

6.2.6 Adipogenesis markers expression in liver samples of DIO mice

As the reduction in liver size could possibly be due to a reduction in adipocytes as compared to vehicle control, we further tested the impact of IBET-762 on liver genes involved with hepatic steatosis and adipogenesis (**Figure. 6.2.6**).

We indeed found a significant downregulation of several adipogenic genes by IBET-762, including *PPARγ* (-92%, $p<0.0001$), the Insulin receptor (*Insr*) (-42%, $p=0.0056$), hepatic lipase (*Hlip*) (-74%, $p=0.0037$) and stearoyl-CoA desaturase 1 (*Scd1*) (-89%, $p=0.0007$), when compared to the vehicle control. Furthermore, several genes reduced, albeit non-significantly, such as D-Box Binding PAR BZIP Transcription Factor *(Dbp*, -37%, ns) and *CEBPα* (-24%, ns). *Cd36* (+3%, ns) and *Fasn* (+27%, ns) exhibited a non-significant increase.

In contrast to the IBET-762 treatment group, several genes were significantly upregulated in the high fat diet group, when compared to the diet control group, such as *PPARγ* (+230%, $p=0.0002$) and *Cd36* (+230%, $p=0.0024$). Others were significantly downregulated by the high fat diet, such as the *Hlip* (-34%, $p=0.0344$) and *Scd1* (-48%, $p=0.0004$), when compared to the diet control group. Others did not change significantly in expression: *Dbp* (-5%, ns), *CEBPα* (-6%, ns), *Fasn* (-34%, ns) and the *Insr* (+23%, ns).

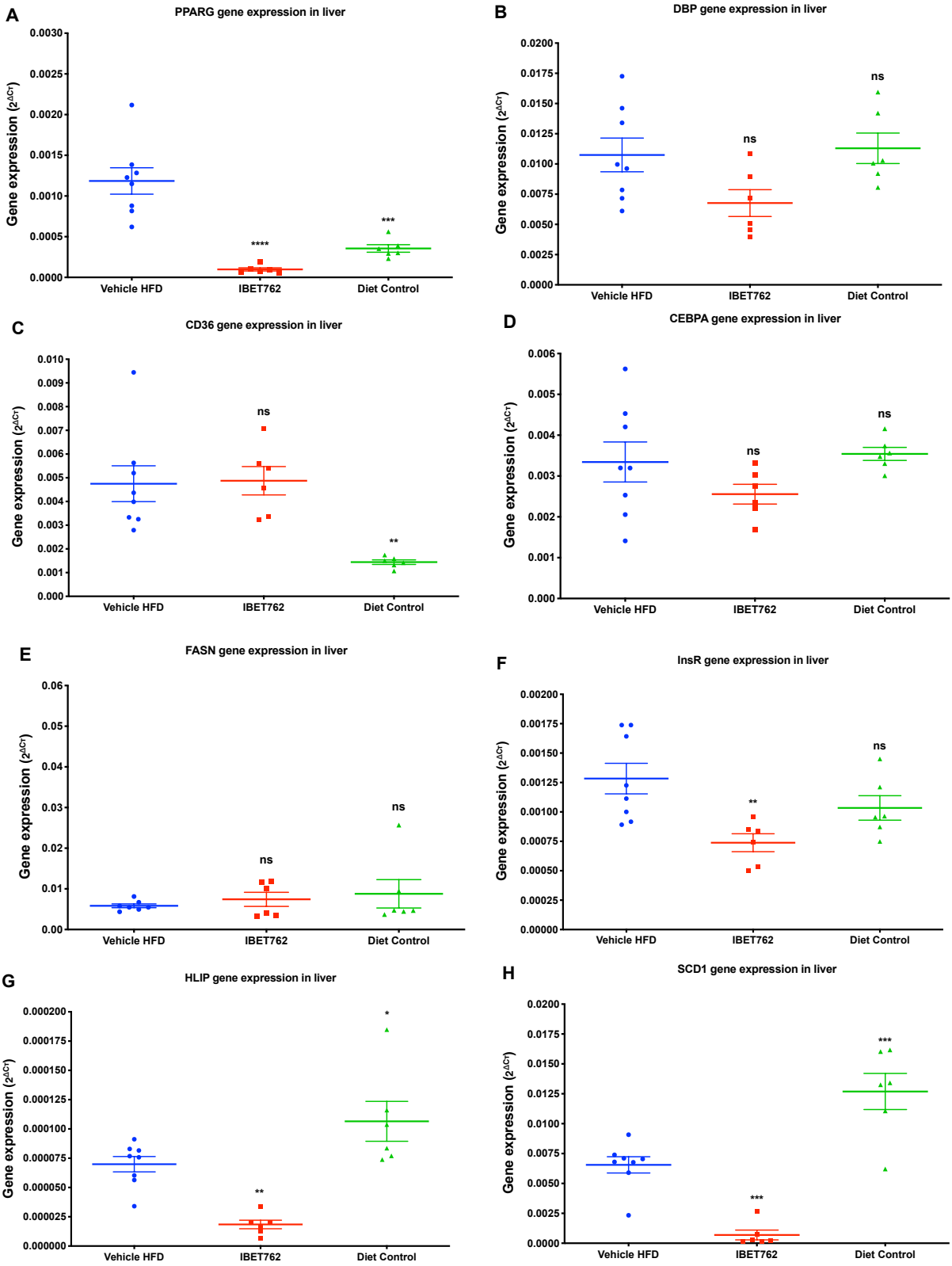


Figure 6.2.6 – Adipogenesis gene expression in liver samples of DIO C57BL/6 mice; gene expression of adipogenesis markers were analysed in *ex-vivo* samples collected from mice's liver tissue. The expression was normalised on the geometric mean of two housekeeping genes and the data was expressed as an average ± SEM (n=6-8). Significance was tested through a one-way ANOVA followed by a post-hoc Dunnett-powered multiple comparisons analysis against Vehicle HFD.

6.2.7 Glucose regulation gene expression in liver samples of DIO mice

Furthermore, the expression of genes implicated in glucose regulation (glucose uptake, glucose sensing, insulin signalling, insulin production and activity) were also tested, given the effects of IBET-762 on glucose (**Figure 6.2.2**) and insulin tolerance (**Figure 6.2.3**). We observed a wide effect of IBET-762 administration on the expression of genes involved in glucose metabolism (**Figure 6.2.7**). *Slc2a4* (GLUT4) (-88%, p=0.0159), *Irs1* (-47%, p=0.0277), *Hnf1a* (-45%, p=0.041), *Hnf1b* (-46%, p=0.0198) and *Gck* (-86%, p<0.0001) were all significantly downregulated by the chronic administration of the IBET-762, when compared to vehicle control. The rest of the genes tested did not show a significant modulation, such as *Slc2a1* (GLUT1) (-14%, ns), *Irs2* (+23, ns) and *Hnf4a* (-16%, ns).

High fat diet also influenced on the expression of these genes, when compared to diet control, but only *Gck* gene expression was significantly upregulated (+82%, p<0.0001). The other genes did not show a significant modulation brought forward by the diet change: *Slc2a1* (GLUT1) (+6%, ns), *Slc2a4* (GLUT4) (-23%, ns), *Irs1* (+10%, ns), *Irs2* (-6%, ns), *Hnf1a* (+25%, ns), *Hnf1b* (+41%%, ns) and *Hnf4a* (-3%, ns).

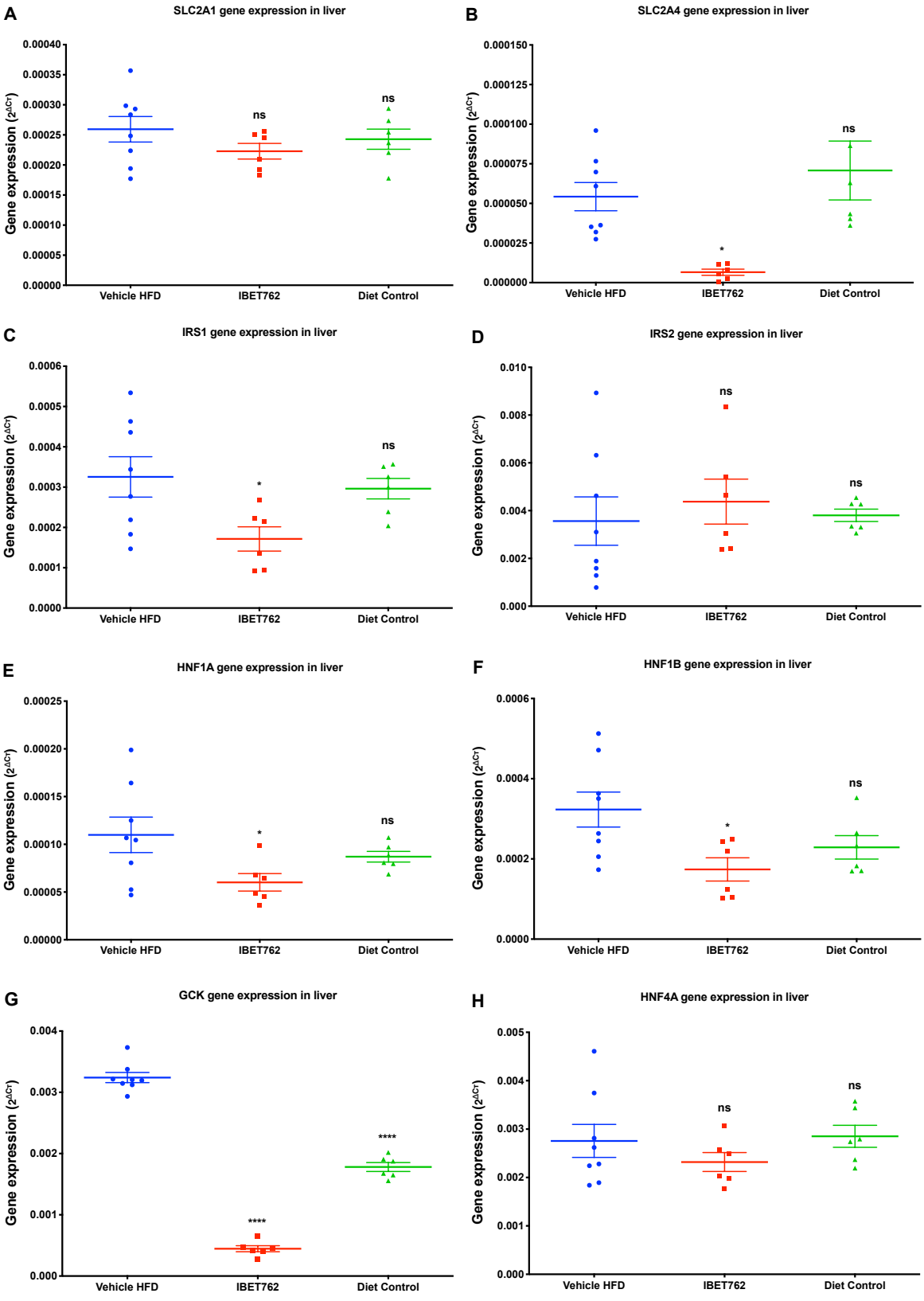


Figure 6.2.7 – Glucose regulation gene expression in liver samples DIO C57BL/6 mice; gene expression of glucose metabolism markers were analysed in *ex-vivo* samples collected from mice's liver tissue. The expression was normalised on the geometric mean of two housekeeping genes and the data was expressed as an average ± SEM (n=6-8). Significance was tested through a one-way ANOVA followed by a post-hoc Dunnett-powered multiple comparisons analysis against Vehicle HFD.

6.2.8 Glucose regulation gene expression in skeletal muscle of DIO mice

Given the importance of the skeletal muscle in glucose regulation, we have tested the expression of several genes associated with glucose metabolism in samples of skeletal muscle (**Figure 6.2.8**). IBET-762 administration significantly increased the expression of several genes such as *Slc2a1* (GLUT1) (+126%, $p<0.0001$), *Slc2a4* (GLUT4) (+43%, $p=0.0234$) and the insulin receptor (+131%, $p<0.0001$) whilst it significantly decreased the expression of *PPARγ* (-57%, $p=0.0232$), *Tfeb* (-54%, $p=0.0151$) and *Gck* (-96%, $p<0.0001$). It did not significantly modulate the expression of other tested genes, such as *Irs1* (+10%, ns) and *Irs2* (-20%, ns).

High fat diet significantly decreased the expression of several of these genes such as *Slc2a1* (GLUT1) (-66%, $p<0.0001$), *Slc2a4* (GLUT4) (-49%, $p<0.0001$), *Irs1* (-55%, $p=0.0001$), *Irs2* (-67%, $p<0.0001$), *Tfeb* (-50%, $p<0.0001$) and *Insr* (-61%, $p<0.0001$). Furthermore, it significantly increased the expression of *PPARγ* (+148%, $p=0.0232$). whilst it did not significantly change the expression of *Gck* (-8%, ns).

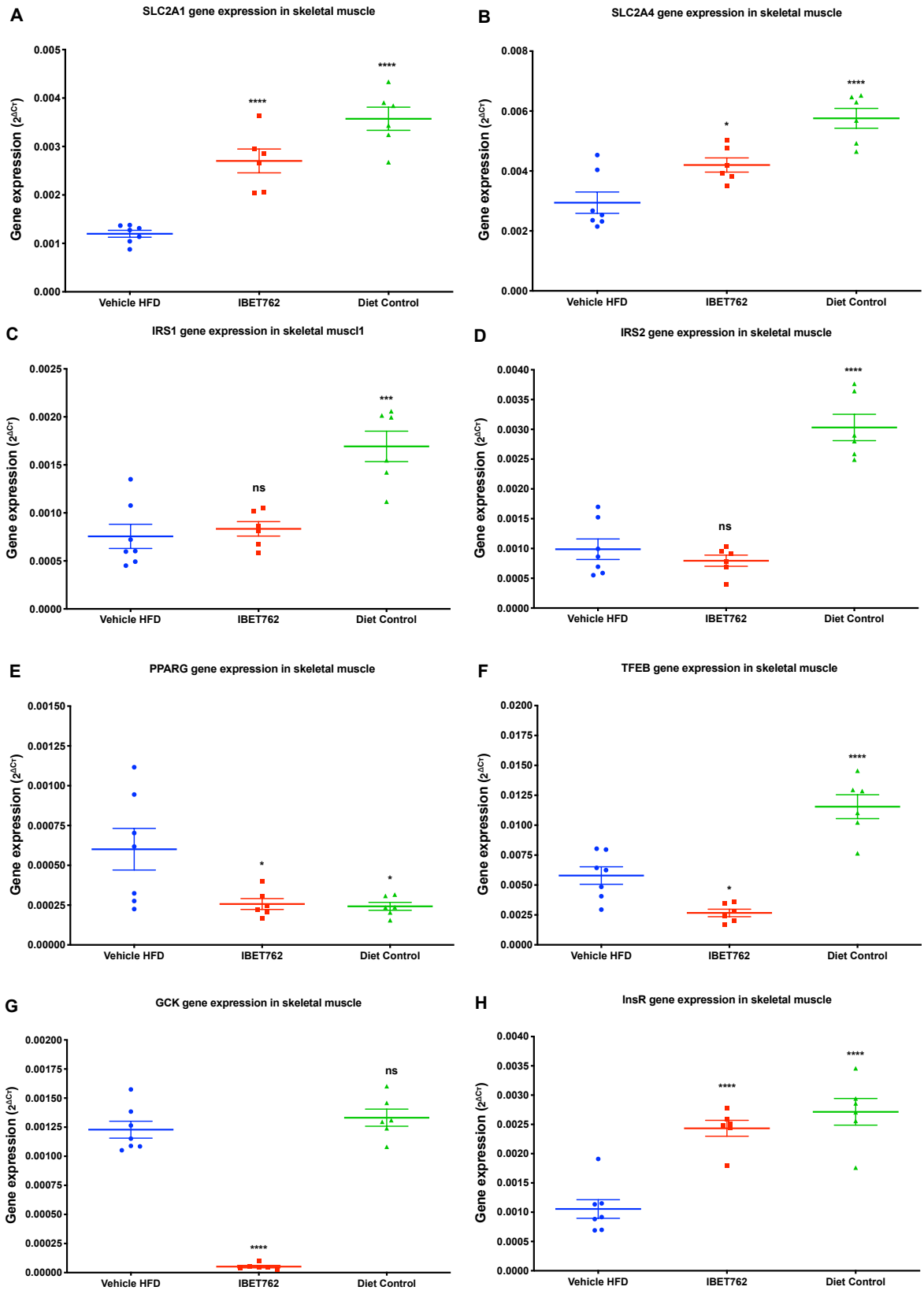


Figure 6.2.8 – Glucose regulation gene expression in skeletal muscle samples of high-fat diet-induced obesity of C57BL/6 mice; gene expression of glucose metabolism markers were analysed in *ex-vivo* samples collected from mice's skeletal muscle tissue. The expression was normalised on the geometric mean of two housekeeping genes and the data was expressed as an average ± SEM (n=6-8). Significance was tested through a one-way ANOVA followed by a post-hoc Dunnett-powered multiple comparisons analysis against Vehicle HFD.

6.2.9 Metabolomic regulation gene expression visceral fat of DIO mice

Given the widespread protective effects of IBET-762 against a high-fat diet (**Figure 6.2.1**), we investigated the effects of IBET-762 on the gene expression of several markers of metabolomic health in the visceral fat (**Figure 6.2.9**).

IBET-762 was shown to significantly decrease the expression of several genes such as *Slc2a1* (GLUT1) (-51%, p=0.0291) and leptin (-77%, p<0.0001), whereas it significantly increased the expression of *Slc2a4* (GLUT4) (+142%, p=0.0084), when compared to vehicle control, in the visceral fat. It did not change significantly the expression of other genes such as *Irs1* (+50%, ns), *Irs2* (+25%, ns), adiponectin (+29%, ns), *Fasn* (+13%, ns) and *PPARγ* (+29%, ns).

Furthermore, the high fat diet also showed an effect on metabolically-vital gene expression regulation, when compared to diet control. Several of the genes were significantly downregulated, such as *Slc2a4* (GLUT4) (-57%, p=0.0129), adiponectin (-48%, p=0.0024), *Fasn* (-73%, p=0.0079) and *PPARγ* (-31%, p=0.0075). Leptin was significantly upregulated (+305%, p<0.0001), whereas the rest of the genes tested did not show a significant modulation upon high fat diet: *Slc2a1* (GLUT1) (+80%, ns), *Irs1* (-36%, ns) and *Irs2* (-7%, ns).

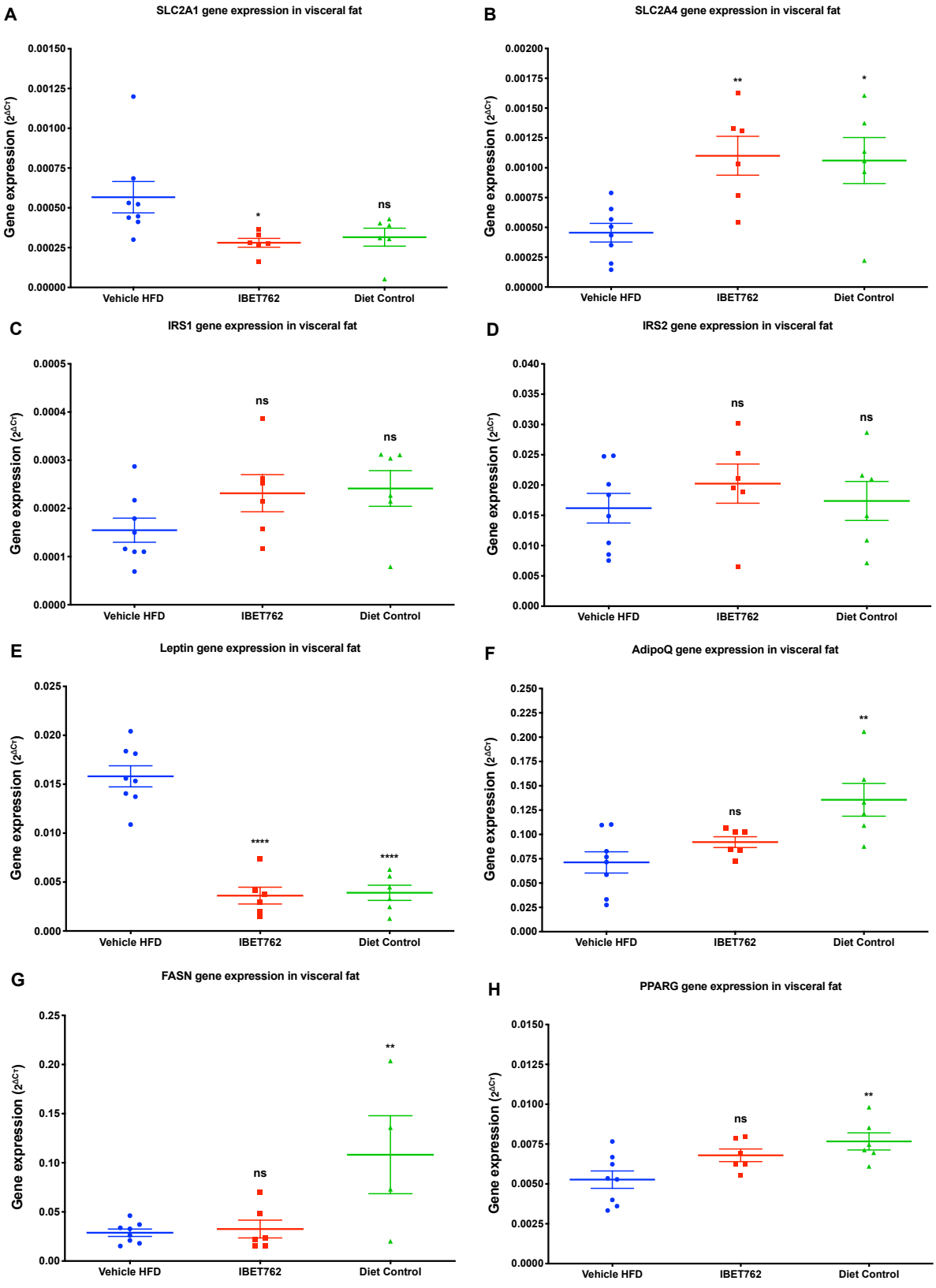


Figure 6.2.9 – Metabolomic regulation gene expression in visceral fat samples in DIO C57BL/6 mice; gene expression of metabolic markers were analysed in *ex-vivo* samples collected from mice's visceral fat tissue. The expression was normalised on the geometric mean of two housekeeping genes and the data was expressed as an average ± SEM (n=6-8). Significance was tested through a one-way ANOVA followed by a post-hoc Dunnett-powered multiple comparisons analysis against Vehicle HFD.

6.2.10 Inflammatory markers gene expression in visceral fat of DIO mice

To further understand the impact of the drug on inflammation, a hallmark of the metabolic syndrome in visceral fat, we have tested the expression of several inflammatory genes in the visceral fat (**Figure 6.2.10**).

Regarding the IBET-762's effects, only *Tnfα* was shown to decrease in expression (-77%, p=0.0008), whereas the other genes tested did not change significantly, such as *Il6* (-10%, ns), C-C Motif Chemokine 2 (*Ccl2*, -81%, ns) and Resistin (-35%, ns), although they did show a trend towards a reduction. High fat diet also showed to have an effect on inflammatory gene expression, with a significant increase in *Tnfα* expression (+253%, p=0.0015). Other genes were non-significantly modulated when compared to vehicle control: *Il6* (+28%, ns), *Ccl2* (-11%, ns) and Resistin (-44%, ns).

6.2.11 Effects of IBET-762 on the size of visceral adipocytes

To further understand whether there were any differences in the size of the adipocytes upon IBET-762 treatment, we analysed *ex-vivo* slices of visceral fat from the C57BL/6 mice.

Upon a qualitative analysis, there seems to be a trend towards a lower size area of visceral adipocytes of the mice treated with IBET-762, both at week 10 and week 18. However, adipocyte area seems to be slightly smaller in the diet control group, when compared to both groups of IBET-762-treated mice.

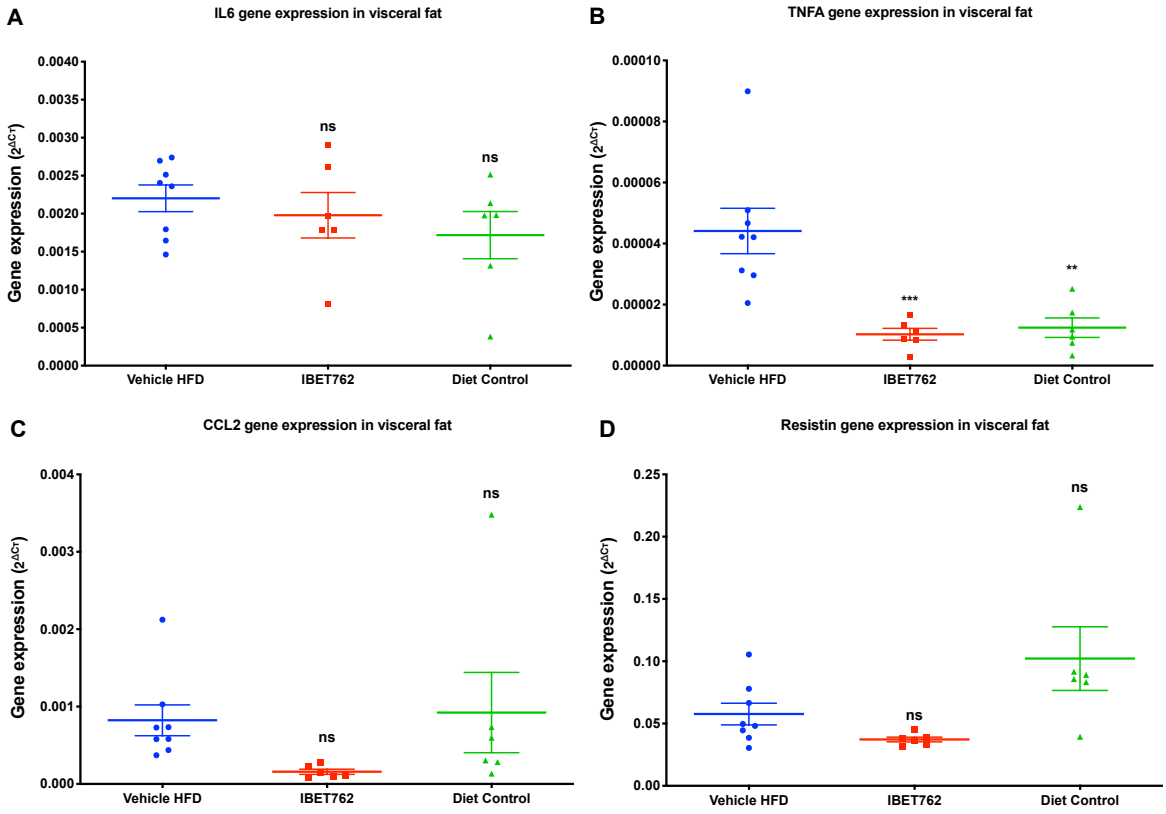


Figure 6.2.10 – Inflammatory markers gene expression in visceral fat samples in DIO C57BL/6 mice; gene expression of inflammatory markers were analysed in *ex-vivo* samples collected from mice's visceral fat tissue. The expression was normalised on the geometric mean of two housekeeping genes and the data was expressed as an average ± SEM (n=6-8). Significance was tested through a one-way ANOVA followed by a post-hoc Dunnett-powered multiple comparisons analysis against Vehicle HFD.

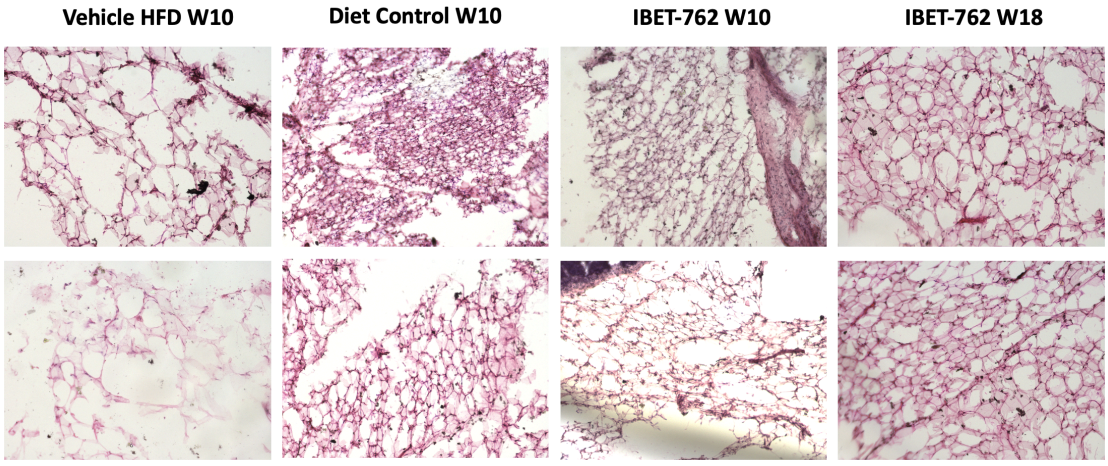


Figure 6.2.11 – H&E staining of adipocytes of DIO C57BL/6 mice; results show a 40x magnification of sliced tissues of visceral fat stained through H&E (n=2). The bigger the area of the eosin-delimited areas (in pink), the bigger the adipocytes. The tissue was collected at culling and was processed for *ex-vivo* imaging.

6.2.12 Anorexigenic markers gene expression in PVN of DIO mice

Given the effects of IBET-762 on diet-induced obesity (**Figure 6.2.1**) and the downregulation of leptin expression in visceral fat (**Figure 6.2.9**), we wanted to further test the effects of the drug on specific anorexigenic and ER stress gene expression that are markers of leptin resistance or risk towards leptin resistance (**Figure 6.2.12**).

IBET-762 was shown to significantly downregulate the gene expression of *Pomc* (-43%, p=0.0057) and Heat Shock 70 kDa Protein 1A *(Hspa1a*, -63%, p=0.0003) whilst significantly upregulating the expression of *Agrp* (+224%, p=0.0082) and *NPY* (+192%, p=0.0052). It did not influence on the gene expression of other tested genes, such as X-Box Binding Protein 1 (*Xbp1*, -1%, ns) and DNA Damage Inducible Transcript 3 (*Ddit3*, -6%, ns). High fat diet also influenced on the gene expression of several of these genes, when compared to the diet control. It significantly upregulated *Pomc* (+122%, p=0.0021), *Hspa1a* (+223%, p=0.0001) and *Xbp1* (+20%, p=0.0385). It did not impact on other tested genes in the PVN: *Agrp* (-34%, ns), *NPY* (-14%, ns) and *Ddit3* (+3%, ns).

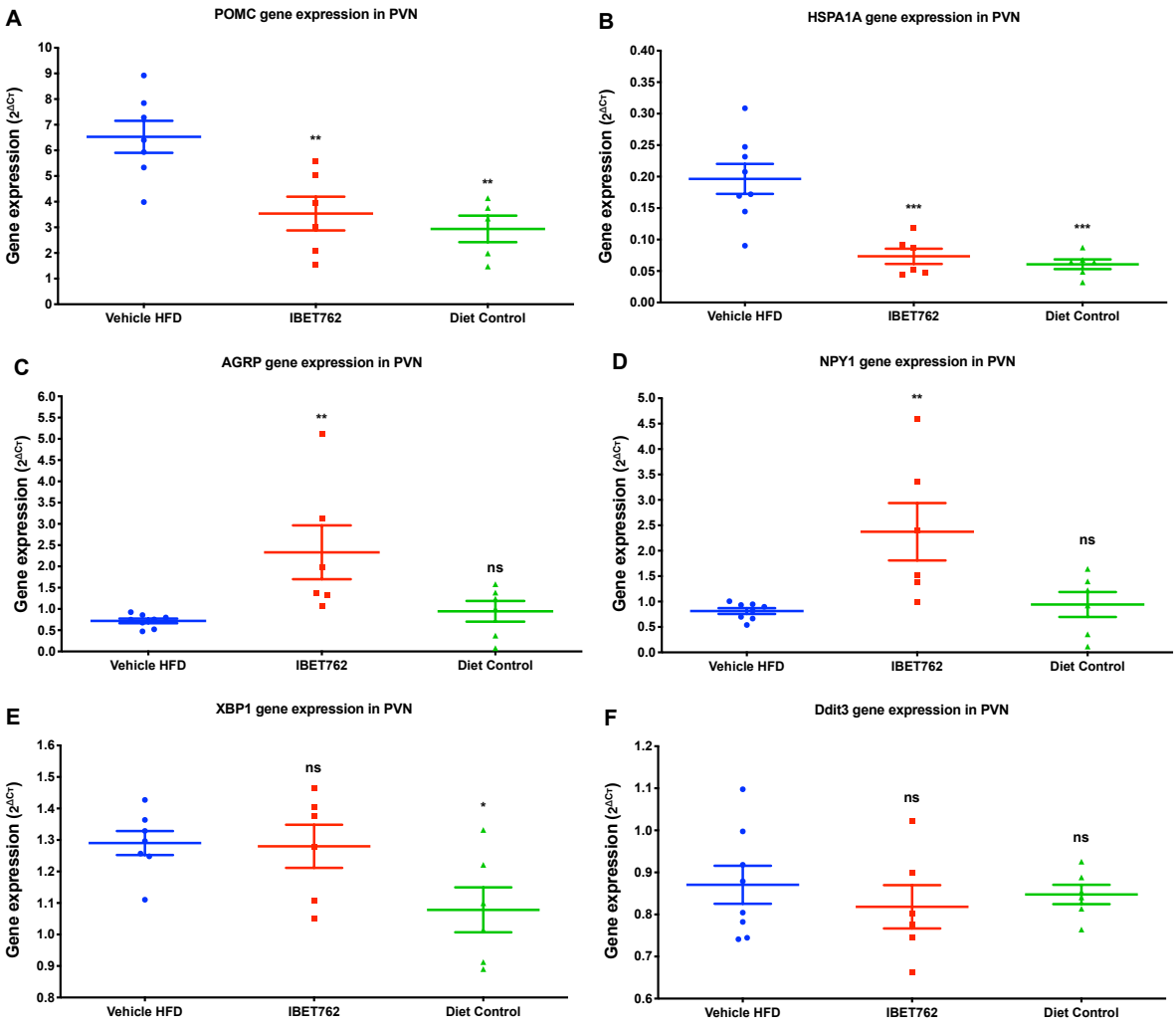


Figure 6.2.12 – Anorexigenic markers gene expression in PVN samples of DIO C57BL/6 mice; gene expression of anorexigenic markers were analysed in *ex-vivo* samples collected from mice's PVN tissue. The expression was normalised on the geometric mean of two housekeeping genes and the data was expressed as an average ± SEM (n=6-8). Significance was tested through a one-way ANOVA followed by a post-hoc Dunnett-powered multiple comparisons analysis against Vehicle HFD.

6.3 DISCUSSION

A high fat diet induced obesity C57BL/6 mouse model was used to assess the effects of IBET-762 in reversing the negative impact of the diet (**Figure 6.2.1**). The C57BL/6 DIO mice in the past have proved to be a well investigated model for studying agents capable of ameliorating weight gain effects, partially due to the predisposition of C57BL/6 models of gaining weight and developing type-2 diabetes disorders (Surwit *et al.*, 1988). Several diets in the past have been employed to mimic obesogenic dietary habits, such as the cafeteria diet (CAF, highly energetic and palatable foods mimicking western-style diets) and other high percentage fat diets (45% to 60% of kcal constituted by fat). Although lower percetage fat diets, such as the cafeteria diet and the 45% fat-content HFD are closer to unhealthy diets nowadays, they are also more limited in the lipid profile changes produced in mice. In fact, mice on 60% kcal fat HFD diets show higher levels of cholesterol and become obese at a higher rate (Higa *et al.*, 2014). Although both diets produce similar overt physiological effects, it is important to underline that they induce different molecular metabolite fingerprints. For instance it has been shown that the 45% fat and the 60% fat diets only share 35 of 80 metabolites that change in reponse to these the two high fat diets (Showalter *et al.*, 2018).

In line with past observation, the 60% Fat HFD caused a 170% weight gain in the first 10 weeks. In addition, as reported previously, glucose intolerance and type-2-diabetes-like phenotypes were evident within 8 weeks of exposing them to HFD (Surwit *et al.*, 1988; Winzell & Ahren, 2004). Our results showed that the high fat diet induced a statistically significant increase in body mass in the mice after 4 weeks of administration

of the high fat diet, as compared to the chow-fed control diet (**Figure 6.2.1B**), which is comparable with previous literature showing a significant increase in body weight-gain 4 weeks after the dietary intervention (Winzell & Ahren, 2004). Although the weights of the mice were slightly different (albeit not significantly) between groups at baseline, the baseline-normalised weight increase analysis has allowed for meaningful weight analysis. Furthermore, our data also showed an effect of IBET-762 in significantly protecting against the weight gain increase stimulated by the high fat diet. Indeed, we showed that the IBET-762-treated mice were able to significantly protect against body weight increase after three weeks of concomitant HFD and IBET-762 20mg/kg administration (**Figure 6.2.1B**). This data is in line with our previous findings in cells showing that the epigenetic modulator would decrease glucose uptake in adipocytes and reduce adipogenesis (**Figure 5.2.2** and **Figure 5.2.8**). The protection against weight increase was sustained throughout the first 10 weeks. Furthermore, we stopped IBET-762 treatment after week 10, to see if the weight increase was sustained even after the interruption of the treatment (possibly alluding to permanent epigenetic change or toxicity/tissue damage). We found this to not be the case, as the weight gain increased similarly to the weight-matched high-fat diet control (**Figure 6.2.1C-D**). A further analysis on the effect of the drug after 9 weeks of administration showed that the weight gain in the IBET-762 condition is significantly reduced against the vehicle control and similar to the diet control. An analysis looking at the effect of IBET-762 treatment interruption showed a significant increase in weekly weight change at week 12 and week 18, suggesting that the treatment interruption allowed for a recoup in weight increase in this group (**Figure 6.2.1E**). These changes suggest that, in order for IBET-762 to be effective as a weight loss therapy, it needs to be constantly administered throughout the

treatment, though it also assures that the weight loss effects can be removed upon termination of the BET-I treatment. Furthermore, a food consumption analysis showed that the mice did not eat different amounts of calories among the three groups studied, underlying that the effects of IBET-762 are independent of the food intake (**Figure 6.2.1F**). The dosage of 20mg/kg of IBET-762 administered through gavage was chosen based on past evidence of the drug being safe and well tolerated in mice. In fact, mice were safely treated with up to 60mg/kg of gavage IBET-762 (Leal *et al.*, 2017), for seven days, and up to 25mg/kg in a longer 30-day experiment and loss in body weight has not reported on a normal chow (Wyce *et al.*, 2013).

As the C57BL/6 DIO model stimulates a glucose intolerance and type-2 diabetes phenotype within 10-weeks of high-fat diet, and given that IBET-762 showed to reduce glucose uptake and energy metabolism in adipocytes (**Figure 5.2.8** and **Figure 5.2.9**), we further tested the *in-vivo* effects of the drug on glucose-tolerance and insulin-tolerance (**Figure 6.2.2**). In line with our observation from 3T3-L1 adipocyte cells where IBET-762 reduced glucose uptake, IBET-762 dramatically increased blood glucose concentration, both at baseline and throughout the glucose tolerance test (**Figure. 6.2.2A, Figure 6.2.2C, Figure 6.2.2D**). The blood glucose concentration increase seen by the high-fat diet treated with vehicle is in line with literature (Lang *et al.*, 2019).

Furthermore, we wanted to understand if the effects of the drugs were maintained after the interruption of the pharmacological agent. We had thus halted the administration of IBET-762 at week 10 and let the mice to continue on the previous high fat diet intervention for 8 weeks further. Although the animals were significantly older at week

18 since the beginning of the experiment, the IBET-762 effects of glucose intolerance vanished at both week 12 and week 18 (**Figure 6.2.2B**). It is important to underline that the older IBET-762 W12 and W18 analyses were not age-matched with the high fat diet control, however, it is known that age could have deleterious effects on glucose intolerance, generally on a longer time-scale of several months, allowing thus for a worsening rather than an improvement in glucose tolerance, in absence of any treatment (Reynolds *et al.*, 2019).

Upon stopping IBET-762 administration at week 10, we noticed that the animals started to gain weigh in a manner similar to HFD vehicle between week 4 and 10. In parallell, the increased glucose level seen at week 10 (baseline and tolerance test) were normalised and resembled glucose profile of mice on normal chow (**Figure 6.2.2C**). The glucose tolerance test is used to determine whether the animals have difficulty in metabolising an intake of carbohydrate. The test is useful in further shedding light, together with other information on pre-diabetes and insulin resistance. The peak glucose concentration at 15 minutes after glucose administration was also similar to the chow control at both 12 week and 18 weeks (**Figure 6.2.2D**), which were confirmed under a glucose-baseline normalisation analysis (**Figure 6.2.2F**).

These results suggest that IBET-762 promotes diabetic-like glucose intolerance for the duration of its administration, however its interruption shows a protective effect against diabetes, possibly as a result of the prevention in weight gain associated with the bromodomain inhibitor. Given the glucose concentrations are below the high-fat diet

control, 2 weeks from treatment interruption, suggest an acute diabetic-like phenotype and limited pancreatic β-cell toxicity.

We also analysed the glucose concentrations upon an insulin challenge (**Figure 6.2.3**). The insulin tolerance test is used to inform on the bodily insulin sensitivity. The results showed that the IBET-762's effects on insulin sensitivity were similar to high-fat diet alone, implying that the insulin sensitivity was not impaired compared to the vehicle group (**Figure 6.2.3A**). Although the glucose concentration at baseline seems higher in the IBET-762-treated group than in the vehicle control and diet control groups (**Figure 6.2.3C**) following 6 hours of food restriction, a trend towards improvement in the glucose concentration after 30 minutes, in the IBET-762 cohort, as compared to the vehicle control (**Figure 6.2.3D**) could be observed. Further upon normalising the glucose concentration to the initial intraindividual baseline values, we can reveal an increased sensitivity to insulin at all timepoints, in the IBET-762 group, comparably to the diet control group (**Figure 6.2.3E**). We have also tested the effects of halting the IBET-762-treatment in mice that were exposed to IBET-762 for 10 weeks. Upon the interruption of the drug, we observed a significant decrease in the baseline and peak concentrations of glucose at week 12 (2 weeks after the interruption of IBET-762), which has partially subsided at week 18 (8 weeks after the interruption of the epigenetic modulator) (**Figure 6.2.3C** and **Figure 6.2.3D**). This suggests that IBET-762 improves insulin sensivitiy during its administration, possibly due to its weight gain protection effects. As the drug was halted, we noticed a trend towards impaired insulin sensitivity, possibly due to the body weight increase as a result of HFD. Nevertheless, the overall insulin sensitivity even at this stage was improved over the HFD group.

Taken together, our evidence suggests that IBET-762 induction of a diabetic-like phenotype in mice is unrelated to the obesity-related type-2 diabetes phenotype, given that their body weight increase is limited (**Figure 6.2.1**) and that insulin sensitivity is improved (**Figure 6.2.3**). The diabetes-like phenotype is also different from type-1 diabetes as glucose concentrations return to normal (and are improved with respect to the vehicle control) upon interruption of IBET-762, at week 12 and week 18 (**Figure 6.2.2**), suggesting the drug does not inflict pancreatic β-cell toxicity, which could be a common outcome of both type-1 and type-2 diabetes (Cnop *et al.*, 2005). The improved glucose profile upon termination of IBET-762 treatment at week 12 and 18 are possibly influenced by the improvement in baseline glucose.

To further understand the impact of the decreased body weight, we also wanted to understand the impact on liver and hepatic steatosis. Firstly, we analysed the weight of the liver and normalised it to the tibial length, to dissect possible differences in physiognomy of our animal subjects. Liver weight had decreased in the IBET-762 cohort at week 10, however, the effect was not kept after the interruption of the drug, at week 18 (that is, 8 weeks after the interruption of the drug) (**Figure 6.2.4A**). These findings are in line with our findings of decreased weight increase in the IBET-762 group, which then subsided after the halt of the treatment (**Figure 6.2.1**). To further confirm our findings, we have analysed the presence of hepatosteatosis on *ex-vivo* liver slices from all groups (**Figure 6.2.4B**). It was indeed confirmed from lipid imaging and quantification that hepatosteatosis was averted in the IBET-762 group, after 10 weeks of treatment. Furthermore, hepatosteatosis was absent from the treated group, even after the IBET-762 treatment was interrupted, with the concomitant administration of the HFD, for 8

extra weeks, although the liver weight in the latter group was not lower than the HFD group. The increase in liver weight in the IBET-762 W18 cohort could therefore be ascribed to the expansion of hepatocytes as a function of supporting their weight gain.

To understand whether insulin release was truly downregulated in the IBET-762 group, we have tested the baseline insulin levels (after 5 hours of restricted feeding), in the C57BL/6 DIO mice (**Figure 6.2.5A**). The results showed that insulin levels were lower in the IBET-762-treated mice, when compared to the vehicle control, at week 10, however, the results were not statisticaly significant. This trend, together with our data showing an increase in insulin sensitivity (**Figure 6.2.4**), suggests the IBET-762 Week 10 cohort might have suffered a reduction in the release of insulin.

The IBET-762 treatment was halted at week 10 and the mice were also tested for baseline insulin levels after 8 weeks following IBET-762 treatment interruption, showing a significant increase in insulin levels, possibly due to the increase in weight gain in this group, though it was not accompanied by a decrease in insulin sensitivity. However, it is important to underline that the significance of these results is limited by the fact that these are the baseline insulin levels, rather than the insulin levels upon a glucose stimulation.

Furthermore, we also tested for other metabolites that were shown to be disregulated in diabetes, such as triglycerides, free fatty acids and cholesterol. The results showed that cholesterol levels were downregulated by IBET-762 (**Figure 6.2.5D**), in line with our lines of evidence showing a decrease in weight in C57BL/6 DIO mice (**Figure 6.2.1**)

and lipolysis in adipocytes (**Figure 5.2.6**). The lower levels in cholesterol could possibly be explained by the downregulation of *Hlip* expression in the liver, which is known to promote a lowering of LDL levels (Tilly-Kiesi *et al.*, 2004). Moreover, the levels of free fatty acids were unchanged in the IBET-762 group with respect to the vehicle control group (**Figure 6.2.5C**). Althogh fat accumulation was shown to be decreased in the IBET-762 group (**Figure 6.2.1**), free fatty acids and blood triglycerides (**Figure 6.2.5B** and **Figure 6.2.5C**) were not diminished, possibly due to the decrease in lipolysis. High triglyceride and free fatty acids were indeed associated with diabetes (Bitzur *et al.*, 2009) and our results suggest that, although the fatty acids are not deposited within adipocytes and across the organism, as a result, they appear in plasma. The decreased levels of insulin seen in the IBET-762 cohort could also be a culprit, as insulin enhances the activity of lipoprotein lipases, which break down triglycerides and limit their levels (Fried *et al.*, 1993). In fact, upon IBET-762-treatment halt, levels of insulin release increased, as seen in **Figure 6.2.5A**, and levels of both triglycerides and free fatty acids signficantly decreased (**Figure 6.2.4B-C**), in line with insulin decrease being the culprit of the increase in triglyceride and free fatty acids upon IBET-762 treatment.

As seen in **Figure 6.2.4A**, the weight of livers, as normalised on tibial length, decreased in the IBET-762 cohort. To further assess whether this was related to a decrease in hepatic steatosis, we analysed the presence of lipids within cryo-conserved liver slices (**Figure 4.3.4B**). These showed a stark effect of high fat diet in increasing hepatic steatosis, as expected, to about 20%, well above the 5% lower limit that defines the presence of NAFLD. More importantly, IBET-762 was shown to significantly reduce the presence of hepatosteatosis at both W10 and W18. To further confirm our findings,

we analysed the expression of several markers of adipogenesis (**Figure 6.2.6**). We have indeed seen the downregulation of *PPARγ* in IBET-762-treated mice, a key gene involved in adipogenesis (Lefterova *et al.*, 2014), confirming its downregulation in pre-adipocytes seen in previous studies **(Figure 5.2.3**). However, some of its co-regulators, such as *Cd36* and *CEBPα*, were not shown to be modulated by the drug. However, the downregulation of *PPARγ* alone could be sufficient to overt adipogenesis in the liver. Further analysing the diabetic phenotype in the liver, the insulin receptor expression was shown to be decreased in the IBET-762 cohort, possibly due to a defect in glucose transportation (Garvey *et al.*, 1985). Glucose uptake was indeed shown to be downregulated in 3T3-L1 cells in our data (**Figure 5.2.8**). To assess the impact of the modulation of insulin and triglycerides in the liver, we have also analysed the levels of the hepatic lipase (*Hlip*) and stearoyl-CoA 1 (*Scd1*). HLIP catalyses the hydrolysis of triglicerydes whereas SCD1 synthesises monounsaturated fats from saturated fats and its inhibition is protective against obesity (Ntambi *et al.*, 2002) and stimulates insulin signaling (Rahman *et al.*, 2003). Moreover, *Scd1* reduction in expression is associated with lean mice, through the action of leptin (Cohen *et al.*, 2003). Both *Hlip* and *Scd1* were significantly reduced in expression in liver, thus suggesting the increase in triglycerides could also be explained by a decrease in *Hlip*, whereas the decrease in *Scd1* reduction could explain the lower weight gain and increased insulin sensitivity seen in IBET-762 mice.

To understand the effects on increased glucose concentrations at baseline under IBET-762 administration, we have further examined the expression of glucose transporters *Slc2a1* (GLUT1) and *Slc2a4* (GLUT4) in the liver (**Figure 6.2.7**). As *Slc2a1* was

unchanged in expression, *Slc2a4* showed a decrease in expression in the IBET-762 cohort. Insulin signalling was also further studied, with *Irs1* significantly decreased in expression in the IBET-762 group. *Irs1* decreased levels were associated with patients affected by obesity and diabetes (Kovacs *et al.*, 2003) and impaired GLUT4 mobilisation and subsequently, insulin-stimulated glucose uptake (Wang *et al.*, 2009b). These findings are in line with the decrease in glucose uptake in adipocytes (**Figure 5.2.8**) and decrease expression of *Slc2a4*.

Given the high levels of glucose baseline concentrations after IBET-762 administration and a lack of phenotypic type-1 or type-2 diabetes due to an absence of pancreatic toxicity and insulin sensitivity, we wanted to further dwelve in the reasons behind the reduced glucose uptake as a potential explanation for the increased glucose concentrations. We thus tested the expression of several genes associated with maturity-onset diabetes of the young, a rare genetic form of diabetes that presents itself as a mutation in genes pivotal in insulin production and glucose transport functionalities. Three out of the four most common autosomal dominant mutation-prone genes were showed to be signifcantly reduced in gene expression (**Figure 6.2.7E-H**), such as *Hnf1a*, *Hnf1b* and *Gck*. A mutation in each of these genes alone might not justify the significant increase in baseline glucose concentrations in the IBET-762 mice, however, the downregulation of three of them could have a significant impact in glucose regulatory mechanisms.

Given the importance of the skeletal muscle in uptaking blood glucose and in energy production, especially regarding the insulin-sensitive uptake of glucose, we also wanted

to test the expression of key genes implicated in glucose uptake and metabolism in this tissue (Wasserman *et al.*, 2011) (**Figure 6.2.8**). Both *Slc2a1* and *Slc2a4* were shown to be upregulated by the IBET-762 treatment (**Figure 6.2.8A** and **Figure 6.2.8B**). *Glut1* may be upregulated possibly due to the lack of expression of the glucokinase gene (*Gck*), which normally irreversibly phosphorylates glucose to glucose-6-phosphate, trapping it intracellularly and completing the glucose uptake process. Its significant downregulation in the skeletal muscle (**Figure 6.2.8G**) suggests that glucose can easily exit the cell through the same transporters which it entered through, as they are bidirectional, mechanism which could possibly stimulate the expression of more receptors (**Figure 6.2.3**). Although GLUT4 is not upregulated in the liver, the skeletal muscle is known to account for the bulb of insulin-stimulated glucose uptake within the organism, thus possibly influencing the overall increase in insulin-sensitivity in the IBET-762-treated mice (Wasserman *et al.*, 2011). Furthermore, we also found *PPARɣ* and *Tfeb* genes to be substantially downregulated by the drug (**Figure 6.2.8E** and **Figure 6.2.8F**), confirming previous results in C57BL/6 mice liver samples (**Figure 6.2.6**).

Given the importance of visceral fat in the metabolic syndrome, and the effects of IBET-762 on weight gain (**Figure 6.2.1**), we further tested the expression of genes pivotal in metabolic regulation in the visceral fat (**Figure 6.2.9**). In this tissue *Slc2a1* (GLUT1) was significantly downregulated (possibly due to a lower baseline glucose demand), whereas *Slc2a4* was significantly upregulated (**Figure 6.2.9A** and **Figure 6.2.9B**), furthermore contributing to the increase in insulin sensitisation effect that IBET-762 had shown (**Figure 6.2.3**). We have also tested the gene expression of key adipokines, such as leptin and adiponectin (**Figure 6.2.9E** and **Figure 6.2.9F**). Leptin was found to be

significantly downregulated in the IBET-762 cohort, similarly to the levels of expression in the diet control group. As high fat diet was shown to influence an increase in expression of leptin (Handjieva-Darlenska & Boyadjieva, 2009), IBET-762 seems to protect against a leptin increase in expression and possibly a down-the-line leptin resistance, which is typical in conditions of persistent high levels of this hormone (Koch *et al.*, 2014).

The metabolic syndrome is dependent on the activation of inflammatory mechanisms within the visceral fat, possibly due to adipocyte hypertrophy and oxidative stress (Monteiro & Azevedo, 2010). This metabolically-triggered low-grade inflammation could be the cause of type-2 diabetes in obese patients. More specifically, an increase in free plasma saturated fatty acids was shown to increase expression of proinflammatory cytokines such as *Il-6* and *Tnfα (Qatanani & Lazar, 2007)* and aggravate the metabolic syndrome in obese patients (Wolowczuk *et al.*, 2008). In our hands, only *Tnfα* was shown to be upregulated in the HFD vehicle control group and downregulated by IBET-762 to levels similar to the diet control group (**Figure 6.2.10B**). *Ccl2* and Resistin also showed a trend towards decrease in the IBET-762-treated group, however this was not significant (**Figure 6.2.10C**, **Figure 6.2.10D**). Besides being associated with obesity and the metabolic syndrome, a *Tnfα* increase was also positively associated with the development of type-2 diabtes and insulin insensitivity (Alzamil, 2020). The lower levels of *Tnfα* expression in the IBET-762 group can be explained and explain their lower body mass and the increased insulin sensitivity. Taken together, visceral fat seems to indicate lower levels of inflammation in the IBET-762 group. To further our analysis, we looked at the size of visceral adipocytes in the treated animals (**Figure 6.2.11**). The size of

visceral adipocytes was indeed found to be predictive of insulin resistance, with bigger-sized adipocytes showing increased insulin insensitivity and predisposition towards obesity (Verboven *et al.*, 2018). Our findings also show that there is a qualitative trend towards smaller visceral adipocyte size than high fat diet control, further supporting our findings on decreased obesity levels of the IBET-762 mice and increased insulin sensitivity.

Given leptin is the satiety hormone directly correlated with leptin-resistence and obesity and obese people have unusually high levels of leptin, and given that IBET-762 was shown to decrease leptin gene expression significantly in the visceral fat, we further wanted to assess the impact this had on leptin sensitivity and ER stress markers (*Pomc*, *NPY*, *Agrp*, *Hspa1a*, *Xbp1* and *Ddit3*) in the PVN (**Figure 6.2.12**). As leptin stimulates the release of POMC and inhibits the release of AGRP and NPY (Kim *et al.*, 2014a), our results are in line with the decrease of leptin expression in the IBET-762 group (**Figure 6.2.9E**). In fact, *Pomc* was shown to significantly decrease in expression, given the lower leptin levels (**Figure 6.2.12A**), whereas both *Npy* and *Agrp* increased significantly (**Figure 6.2.12C-D**), given the lack of leptin inhibition in the IBET-762 cohort. *Hspa1a*, a marker of endoplasmic reticulum stress and obesity (Stygar *et al.*, 2019), was also shown to be signficantly downregulated in the IBET-762 cohort (**Figure 6.2.12B**), whereas other tested markers, such as *Xbp1* and *Ddit3* (**Figure 6.2.12E-F**) were unchanged. This data demonstrated the impact of the leptin decrease in diminishing the chances of developing leptin resistance and protecting against spiralling towards an obesity phenotype. As summarised in **Figure 6.3.1**, taken together, this data shows that IBET-762 is impactful in protecting against weight-gain in a high fat diet-induced obesity C57BL/6 mouse model, effects which disappeared after treatment interruption (**Figure**

6.2.1). The drug's effects impacted on glucose metabolism by negatively impacting on glucose tolerance and baseline levels of the mice exposed to the high fat diet and drugs, however this effect was dependent on the administration of the drug, as it dissipated at the interruption of the treatment (**Figure 6.2.2**).

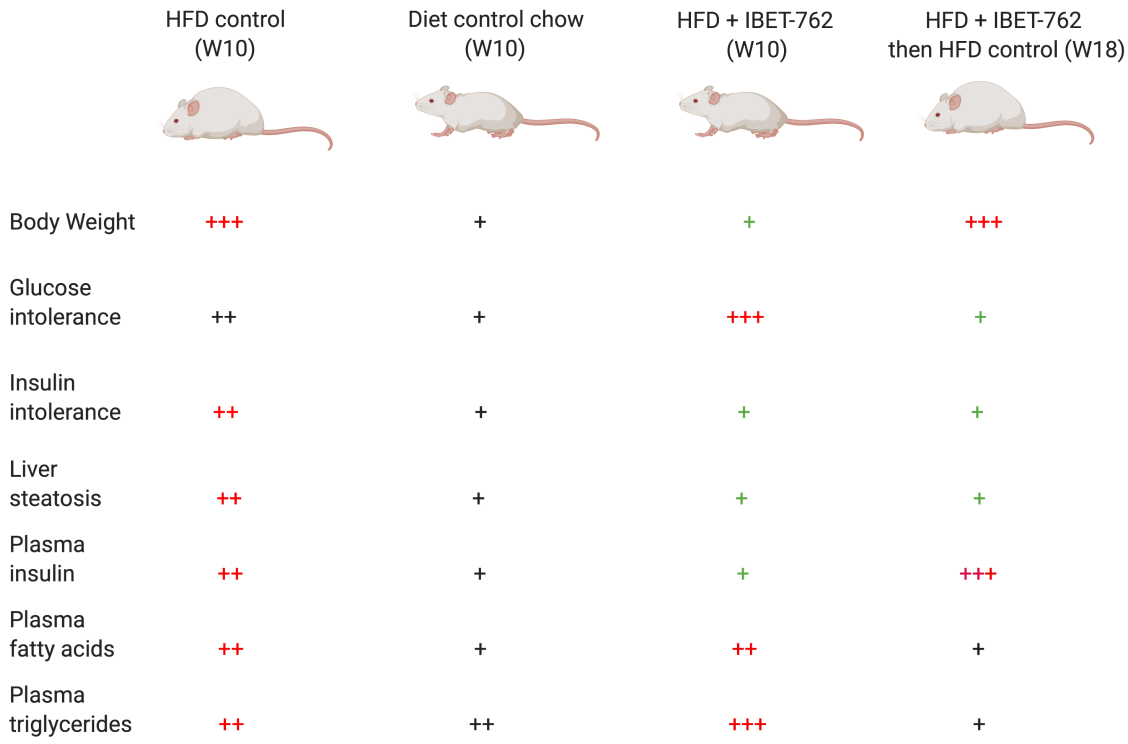


Figure 6.3.1 – Summary of long-term IBET-762 effects on mice exposed to high-fat diet; The figure above summarizes our findings on administering IBET-762 20mg/kg for 10 weeks under 60% high fat diet. Furthermore, the effects of IBET-762 interruption after week 10, whilst the mice were still under a high-fat diet regimen are presented. Parameters included in this summary: body weight, glucose intolerance, insulin intolerance, liver steatosis, plasma insulin, fatty acids and triglyceride concentrations. (+) – low, (++) – medium, (+++) – high.

Moreover, the diabetic-like effect could not be ascribed to insulin insensitivity, as IBET-762 mice were highly sensitive to the hormone and there was no long-term β-cell pancreatic toxicity (**Figure 6.2.3**). However, the levels of plasma insulin concentration were low in the IBET-762 cohort (**Figure 6.2.5**), possibly inflicting a reduction in gene expression of the hepatic lipase and *Scd1* enzymes (**Figure 6.2.6**), associated with a lean

and insulin-sensitive phenotype. Given the decrease in body mass in the IBET-762, leaner liver samples and no hepatosteatosis were also observed in this cohort (**Figure 6.2.4**), and, together with a downregulation in adipogenesis markers, such as *PPARγ*, (**Figure 6.2.6**), the data suggests a possible reduction in fat-induced hepatic steatosis in the treated subjects. The high blood glucose concentration levels seen in the IBET-762 mice could be ascribed to a defect in the release of insulin and glucose-sensing mechanisms, as three of the four most common gene mutations associated with the maturity-onset diabetes in the young, were significantly downregulated (**Figure 6.2.7**), with some of these confirmed in the skeletal muscle as well (**Figure 6.2.8**). Furthermore, gene expression in the visceral fat showed reduced levels of leptin (**Figure 6.2.9**), and a lower predisposition towards inflammation and the metabolic syndrome, in the IBET-762 cohort (**Figure 6.2.10**). The lower leptin gene expression and its impact on leptin-sensitivity was also confirmed through downstream markers, which were shown to be modulated as expected, in the PVN (**Figure 6.2.12**), confirming the impact of IBET-762 on obesity, insulin and leptin sensitivity (as summarised in **Figure 6.3.2**).

7 FINAL DISCUSSION

7.1 Implications of circadian amplitude enhancement of BET inhibitors

IBET-762 is an epigenetic modulator which elicits its actions by inhibition of bromodomain proteins of the BET family, including BRD2, BRD3, BRD4 and BRDT (Mirguet *et al.*, 2013). IBET-762 and other BET inhibitors are currently studied in an array of cancerous pathologies, including several types of leukaemias and lymphomas, given that they reduce cellular proliferation (Dawson *et al.*, 2011), and BET proteins were found to be overexpressed in several malignancies. Here we show that BET inhibition, mediated by the effects of drugs such as JQ-1 and IBET-762, also enhance gene expression amplitude of several genes of the circadian molecular clock dose-responsively, such as *Bmal1* and *Per2,* with a low EC_{50} of about 50nM (**Figure 3.2.5 - Figure 3.2.10**). Given in mice nearly half of the genes oscillate in at least one tissue and the fact that over half of the 100 top selling drugs have targets that are cyclic (Zhang *et al.*, 2014), the importance of rhythmic circadian physiology is becoming increasingly apparent. Molecules that could enhance circadian rhythms could therefore be potentially useful in improving metabolic health and potentially reduce the incidence of disorders such as T2D, obesity and NAFLD (Bernsmeier *et al.*, 2015; Karlsson *et al.*, 2001; Scheer *et al.*, 2009). Given that the circadian clock acts as a master regulator of gene expresion, it could be envisaged that circadian medicine under certain circumstances would be of use even in a non (circadian) disrupted individual to modulate the expression of certain proteins. The impact of circadian rhythm disruptions on metabolic integrity were further shown to involve epigenetic mechanisms (Cedernaes *et al.*, 2015), hence our efforts in enhancing circadian rhythm gene expression through the use of epigenetic modulators,

such as IBET-762. The hypothesis is that by enhancing the amplitude of the molecular clock with BET inhibitors, we could temporally subdivide physiological functions to reduce the incidence of circadian rhythm disruption-associated pathologies, but also to ameliorate other pathophysiological disruptions that could be given by an altered temporal expression of certain genes.

Modulators of the peripheral and central circadian clock have been identified in several previous screens, with drugs reported to target proteins such as casein kinase Iε (CkIε), Glycogen Synthase Kinase 3β (GSK-3β), CRY and ROR (Badura *et al.*, 2007; He *et al.*, 2016; Hirota *et al.*, 2008). Interestingly, among the amplitude enhancing molecules identified in a previous publication, one specific molecule possessed a structure based on the benzodiazepine scaffold (Chen *et al.*, 2012b), which was pivotal in bringing about the drug's effects on the clock. Similarly, IBET-762's structure is also based on a benzodiazepine scaffold and is thought to be essential in the drug's effect as a bromodomain inhibitor (Filippakopoulos *et al.*, 2012a). Furthermore, the molecules found to enhance amplitude of circadian genes were also associated with a period shortening of the circadian clock. As the targets of these period-shortening, amplitude enhancing drugs are unknown from the published work (Chen *et al.*, 2012b), it is not possible to compare them to the putative mechanism of action of IBET-762. A further circadian amplitude enhancing and period lenghtening drug, nobiletin, and its effects were attributed to an action on the retinoid receptor (He *et al.*, 2016). However, in contrast with previous findings, it is important to underline that the effects of IBET-762 on amplitude dissociate from any effects on the period of the circadian clock. As IBET-762 was shown to increase circadian amplitude by activating SP1 binding on the *Bmal1*

promoter, it is possible an upstream effector such as BMAL1 could stoichiometrically increase the expression of downstream genes of the negative arm, such as Per1/2 and Cry1/2, which would keep the positive to negative arms of the clock in balance thus not inflicting on the length of the circadian period. An amplitude enhancing effect devoit of changes of the circadian period is hypothesized as optimal in tackling disorders associated with circadian rhythm disruptions and dampening of the expression of the molecular clock genes, as the effects of the drug would not further destabilize the possibly already precarious balance between the components of the clock. Further, the effects of IBET-762 on amplitude enhancement had shown an EC_{50} of about 50nM, showing a 20-100x more potent effect than other molecules that have been identified as circadian rhythm modulators, with EC_{50s} in the 1-5μM range. These findings suggest that is more likely to replicate the cellular effects of IBET-762 *in-vivo* at doses compatible with experimentation and possibly therapeutic treatment.

7.2 SP1-mediated circadian amplitude increase of IBET-762

SP1 is a transcription factor ubiquitously expressed in mammalian cells that binds to GC-rich promoters of genes and promotes their transcription. SP1-binding sites were found across over 12,000 sites across the human genome, including in the BMAL1 promoter. Our analysis indeed showed that the knockdown of SP1 removed the amplitude enhancing effects of IBET-762 (**Figure 4.2.9 – Figure 4.2.12**). Furthermore, a site-mutagenesis experiment done in our lab as part of another project showed that the two identified SP1-binding sites identified in the BMAL1 promoter are essential for IBET-762's amplitude enhancing effects (data not shown). Mechanistically, the effect

could be ascribed to the indirect interaction between BRD4 and SP1 through E2F, which was also shown to interact with BMAL1 (**Figure 4.1.2**). Former studies suggest that the elongation factor E2F acts as a facilitator in the binding of SP1 to SP1-binding sites and thus the inhibition of BRD4-E2F complex brought forward by IBET-762 would dampen SP1's ability to bind to SP1-binding sites and reduce gene transcription activation (Lin *et al.*, 1996; Wong *et al.*, 2005). Furthermore, SP1-binding sites were also found in the promoters and regulatory regions of addition genes of the molecular clock, besides the *Bmal1*, such as in the *Per1* and *Per2* promoters, however, experimental binding evidence is limited (Yamajuku *et al.*, 2010).

7.3 IBET-762 effects on cellular metabolism

Further to its role in enhancing amplitude of the circadian clock, SP1 was shown to play a significant role in processes ranging from cellular growth, cell cycle regulation, and differentiation, hormonal activation, apoptosis, and angiogenesis, with a potential role in cancer (Black *et al.*, 2001) and metabolic functions. In fact, TIEG1, a transcription factor of the SP1 family transactivated by the BMAL1-CLOCK complex, was identified to bind to two enriched GC-rich elements within the *Bmal1* promoter and dampen its transcription in a circadian fashion and partially dependent on glucose concentrations (Hirota *et al.*, 2010). Animal experiments showed that *Tieg1* knockout mice show a postprandial and baseline hyperglycaemia, with modulated target genes involved in glucose, lipid metabolism and the molecular clock (Guillaumond *et al.*, 2010).

In our hands, IBET-762 was able to significantly reduce adipogenesis in 3T3-L1 cells, possibly through BRD2/4 inhibition, given that we could see a significant *PPARγ*

downregulation upon BRD2/4 knockdown (**Figure 5.2.3-5.2.5**). PPARɣ is indeed an essential transcription factor in adipogenesis (Lefterova *et al.*, 2008) and *PPARɣ* gene transcription inhibition was associated with an inhibition of BRD4 (Brown *et al.*, 2018). SIRT1, an HDAC inhibitor that is recognized as a metabolic sensor that associates with CLOCK-BMAL1 in regulating circadian clock transcription (Asher *et al.*, 2008; Nakahata *et al.*, 2008), was also shown to bind to *PPARɣ* regulatory sites and inhibit its expression, thus attenuating adipogenesis (Picard *et al.*, 2004). In fact, *Sirt1* gene expression was upregulated by IBET-762 and *Sirt1* knockdown removed the *PPARɣ* expression decrease brought forward by the epigenetic modulator (**Figure 5.2.1 – Figure 5.2.2**), potentially regarding this mechanism as an alternative or concomitant pathway of adipogenesis inhibition by IBET-762.

PPARɣ activation is a known mechanism of the glitazones, a class of insulin sensitizers that activate PPARɣ and allow for a reduction in the blood levels of glucose and aid type-2 diabetic phenotypes. Nonetheless, the glitazones are associated with serious side effects, including weight gain and obesity (Fonseca, 2003). However, PPARɣ modulation can be differential, with the resulting selective activation of an array of downstream effectors depending on the molecules employed. Troglitazone and rosiglitazone were in fact shown to have differential effects due to conformational differences upon PPARɣ activation, allowing thus for the modulation of the receptor activity and physiological output through partial agonism (Camp *et al.*, 2000). Similarly, the reduction in *PPARɣ* expression by IBET-762 could inflict on downstream pathways differently than its total knockdown, which was associated with severe hyperglycaemia and diabetes mellitus (Barroso *et al.*, 1999).

To further assess the impact of IBET-762 on cellular metabolism, we have tested its effects on lactate production, glucose uptake and energy production in differentiated adipocytes (**Figure 5.2.7- 5.2-10**). The results showed that IBET-762 significantly reduced glucose uptake through SP1, putting the transcription factor once again at the forefront of the interaction between circadian rhythms and metabolism. The reduction in glucose uptake was later attributed to a reduced expression of *Gck* (**Figure 5.2.5, Figure 6.2.7, Figure 6.2.8**), which is converted in a pivotal enzyme in the phosphorylation and entrapment of glucose within the cell. Further, the downregulation in *Gck* expression and glucose uptake might have influenced the reduction in ATP production, both from glycolytic and oxidative phosphorylation pathways, with no apparent shift between the two. Notwithstanding the reduction in ATP production, mitochondrial functionality was assessed as physiological. Alterations in GCK expression or activity across tissues have been associated with a diabetes-like phenotype in blood glucose concentrations called maturity-onset diabetes of the young (MODY), accounting for about 1 to 3% of all diabetes cases worldwide (Shields *et al.*, 2010). The downregulation of GCK was shown to be potentially inflicted by the reduction in PPARɣ activity in pancreatic β-cells, inflicting thus alterations in the glucose-sensing mechanisms and promoting a diabetic phenotype (Kim & Ahn, 2004). Glucose uptake reduction in the fat tissue were associated with both insulin resistance and a putative anti-diabetic effect (Ferrannini *et al.*, 2018). However, given the potential heterogeneity of the penetrance of IBET-762 and the potential differential effects of the epigenetic modulator in different tissues across a whole organism, a whole body effect of the aforementioned cellular outcomes could not be anticipated.

7.4 Effects of IBET-762 on DIO C57BL/6 mouse model

In order to fully assess the impact of IBET-762 on the metabolic syndrome, we have tested the drug on a diet-induced obesity mouse model and evaluated several parameters of importance in metabolic health (**Figure 6.2.1-Figure 6.2.3**). The epigenetic modulator was able to significantly reduce weight gain in the group that were co-administered the high-fat diet and IBET-762, to the levels of the diet control. The effects of IBET-762 on weight gain were stark, especially given that the mice ate as much as their non-treated counterpart, when normalised per mouse weight and kcal of energy provided by the food. This suggests the decrease in weight gain was due to metabolic effects of the drug rather than a reduction in food intake. Further, the effects were removed by the interruption of the drug, suggesting the effects are acute throughout the administration of the therapeutic. Given its effects on weight gain, we wanted to understand if these were able to impact on glucose metabolism, thus tested both glucose and insulin tolerance in mice. The results were contradictory, with IBET-762 significantly increasing baseline blood glucose levels upon fasting, mimicking a diabetes-like phenotype. This is in line with further evidence from *ex-vivo* genotyping analyses showing a reduction in the expression of *Gck*, *Hnf1a* and other enzymes that are pivotal in glucose sensing and glucose trapping, in the liver and skeletal muscle (**Figure 6.2.7-Figure 6.2.8**). Further, the downregulation of *Gck* in the pancreas would limit the glucose-stimulated insulin-release (Matschinsky & Wilson, 2019). In fact, blood insulin levels were found to be downregulated in IBET-762-treated mice (**Figure 6.2.5**), with possible alterations in insulin release rather than insulin sensitivity, given that the IBET-762-treated mice were found to be increasingly sensitive to insulin when compared to their control cohort (**Figure 6.2.3**). The increased insulin sensitivity is thought to be due

to the limited weight gain influenced by the IBET-762 treatment, as an over-expansion in visceral fat was associated to microinflammation and β-cell impairment (Qatanani & Lazar, 2007). Upon IBET-762 interruption, although the mice were further exposed to another 8 weeks of high-fat diet, blood glucose levels returned to normal, indicating no pancreatic toxicity and an acute mechanism of action of IBET-762 in inducing the diabetic-like phenotype, possibly through *Gck* downregulation.

The altered insulin-release was also potentially pivotal in the lack of activation of transcription of several lipases that are fundamental in metabolism, such as *Scd1 (Waters & Ntambi, 1994),* which was found downregulated in the liver (**Figure 6.2.6**). SCD1 catalyzes the rate-limiting step of conversion of saturated fats into monounsaturated fats (MUFAs), which are major components of tissue lipids. As *Scd1* inhibition is protective against obesity and was shown to be required in the synthesis of lipids, including triglycerides and cholesterol esters (Miyazaki *et al.*, 2000), its reduction could have influenced the lean phenotype seen in the IBET-762-treated mice (Brown *et al.*, 2010; Ntambi *et al.*, 2002). Inhibition of *Scd1* was proposed as a potential mechanism of action for drug development against the metabolic syndrome, although some concerns were risen with respect to a possible pro-inflammatory side effect of *Scd1* inhibition due to substrate accumulation (Brown & Rudel, 2010). However, this was not the case in our experience, as IBET-762 was shown to reduce inflammation in the visceral fat (**Figure 6.2.10**), possibly due to the fact that *Scd1* was not completely knocked down by IBET-762. Orlistat, the only drug approved for obesity in the United Kingdom at the time of writing, is known to work as a reversible inhibitor of the gastric and pancreatic lipases, inhibiting thus the absorption of dietary fatty acids in the gut (Guerciolini, 1997). IBET-

762 might promote a differential mechanism of action in its effects as an anti-obesity drug, by inhibiting *Scd1*.

Cholesterol was also shown to be affected by IBET-762 (**Figure 6.2.5**), with a significant decrease in total cholesterol. We do not know whether the lowering interests either the levels of HDL or LDL, or both, and given that they have opposing effects, we cannot assess its impact on cardiovascular health. However, the reduction in expression of the liver lipase *Hlip* suggests the reduction in levels might interest predominantly the LDL levels, as the hepatic lipase is involved in the hydrolysis of Intermediate Density Lipoprotein (IDL) to LDL cholesterol, which builds up in arteries and is the culprit of atherosclerosis. A deficiency in *Hlip* was indeed associated with a delayed prognosis of cardiovascular disorders such as atherosclerosis, myocardial infarction and an extended lifespan in knockout mice (Karackattu *et al.*, 2006). However, we have not further tested cardiovascular health in our mice.

Finally, gene expression in the visceral fat showed reduced levels of leptin (**Figure 6.2.9**), also confirmed through downstream markers, which were shown to be modulated as expected, in the PVN (**Figure 6.2.12**). Low levels of leptin were associated with reduced body weight, given this adipokine is predominantly produced by body fat. As low levels of leptin would promote themselves hunger and obesity, due to an increased appetite and lack of satiety, these findings further confirm that the limited gain in weight seen in the IBET-762 cohort is not due to a limited food intake or a decrease in appetite, but to a change in metabolic pathways of food processing. As insulin stimulates leptin synthesis and secretion, a downregulated expression in insulin could be the culprit for low levels

of leptin production. In fact, it was shown that a drop in both leptin and insulin levels is necessary for shifting the metabolism from using glucose to burning fat, and hence losing weight (Perry *et al.*, 2018). A lowering in both leptin and insulin is thus signalling the body that blood levels of glucose are reduced, thus potentially mimicking the effects of caloric restriction and chronicly lowering the rates of hepatic mitochondrial oxidation and gluconeogenesis. This reduction is explicable by the downregulation in several glucose-sensing and trapping mechanisms, such as the mutation in the *Gck* gene previously discussed.

The effects of IBET-762 on the metabolic syndrome were apparent, and accounted to a lowering of weight gain and an increased insulin sensitization in the diet-induced obesity mouse model used. However, the increased glucose tolerance was also evident, with the drug mimicking a maturity-onset diabetes in the young (MODY) phenotype. Further to these effects, a lowering in the liver weight, as normalised per tibial length, was also observed (**Figure 6.2.4**), suggesting a possible decrease in hepatosteatosis, which was then confirmed by the absence of lipid storage in the liver samples of the IBET-762-treated group. The reduction in *Hlip* and *Scd1* expression levels seen in the liver (**Figure 6.2.6**) could be potentially linked to a reduction in hepatic steatosis, as its activity was directly correlated with NAFLD in patients (Kotronen *et al.*, 2009; Miksztowicz *et al.*, 2012). Importantly, the reduction in liver steatosis lasted further after the interruption of IBET-762 administration, although the mice were still exposed to the high-fat diet, suggesting the changes in the expression of these genes could be more permanent. Please see **Figure 7.1** for a summary of our cellular and *in-vivo* findings of IBET-762 administration.

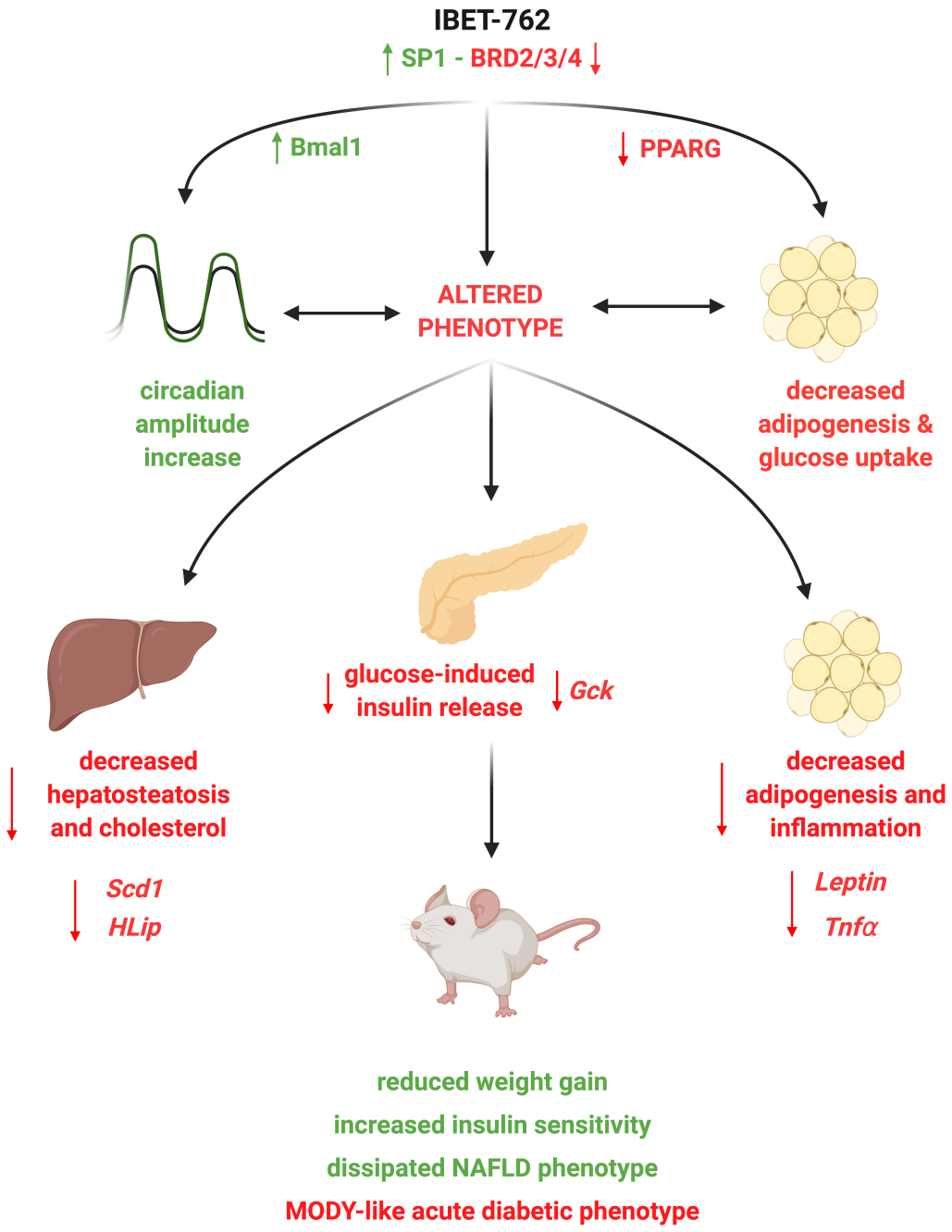


Figure 7.1 – Summary of overall effects of IBET-762 in cells and animal models; a summary of the effects of IBET-762 sees an enhancement of circadian amplitude and a decrease in adipogenesis, mediated by the increase in SP1. The *in-vivo* effects of IBET-762 might have been influenced by the modulation of circadian amplitude and adipogenesis, both mediated by SP1. *Gck* downregulation could justify the decrease in glucose-induced insulin release due to an alteration of the pancreatic glucose-sensing mechanisms, which might have directly impacted on the decreased hepatosteatosis and decreased weight gain seen in the IBET-762-treated C57BL/6 mice.

7.5 Conclusions and final remarks

NALFD is considered to be the hepatic manifestation of the metabolic syndrome and can be a serious affliction and mutate into NASH, a more dangerous form of the pathology, which may progress to cirrhosis and hepatocellular carcinoma. As discussed previously, there are no current therapies approved for this disease, with the exception of a few drugs that have a limited efficacy in tackling the symptomatology. As NASH can see the development of hepatic fibrosis as one of the more worrying symptoms, it would be interesting to assess whether IBET-762 would be able to tackle hepatic fibrosis after it has established, following a long-term high-fat diet induced obesity experiment. As there is a good potential of the drug in limiting or even reversing the fibrotic phenotype in NASH, this would make of IBET-762 a potential candidate in the fight against the disease.

As the MODY phenotype is temporary, there would need to be a cautious evaluation of the risk-benefits analysis and assess whether the side-effects of the drug are worth its putative therapeutic ones. Further, it would be essential to evaluate whether the two phenotypes, that is the diabetic-like phenotype and the anti-obesogenic phenotype, are mediated through differential pathways or if they are two outputs of the same common effector. By dissecting the effects of the drug on a cellular / physiological level, we could target one rather than the other pathway in the quest to develop therapeutic molecules in the fight against obesity and the metabolic syndrome. As an example, it is not clear which of the four bromodomains inhibited by IBET-762 could bring forward its metabolic effects, and if their inhibitory effects could counteract each other. Evidence has indeed shown that the sole whole-body disruption of brd2 could bring about pro-

obesity and anti-diabetic effects in an animal model (Wang *et al.*, 2009a). As the effects of brd2 knockout are diametrically opposite to the effects seen in our experience, with IBET-762, this further supports the need of dissecting the role of each of the bromodomains on metabolism and the circadian clock. Supporting this, it was shown that BRD3 and BRD4 proteins differentially regulate skeletal myogenesis, with BRD3 and BRD4 downregulation resulting in enhanced and inhibited myogenic differentiation respectively, as the overall effect of BET bromodomain inhibition was anti-myogenic (Roberts *et al.*, 2017). Also, it will be important to assess the functional overlap and induced expression of other bromodomains of the BET family as compensatory mechanisms, upon their downregulation or inhibition. There is in fact evidence of functional overlap between BRD2 and BRD3 (Stonestrom *et al.*, 2015), however it is not clear to what degree and the effects the functional overlaps have on cellular and physiological metabolism among the four BET proteins.

It was shown that IBET-762 stimulated an increase in activity on SP1-binding sites and increased circadian amplitude through SP1 signalling, as its downregulation completely removed the effect (**Figure 4.2.8 – Figure 4.2.9**). Experiments done in our laboratory showed that the SP1 sites in the Bmal1 promoter are fundamental in bringing forward the amplitude increase (data not shown). Metabolically, it was shown that the pivotal reduction in glucose uptake brought forward by IBET-762 was also SP1-mediated, as its knockdown promoted an opposite effect after the administration of the epigenetic modulator (**Figure 5.2.8**). BRD4, which was shown to increase circadian amplitude upon downregulation (**Figure 4.2.1 – Figure 4.2.3**), mimicking thus the effects of IBET-762, was also important in bringing about the *PPARγ* reduction in expression,

which was associated with a decrease in adipogenesis and the *PPARγ* gene expression reduction was further associated with SIRT1 (**Figure 5.2.2 – Figure 5.2.3**), which is also known to impact on the circadian clock. However, the *in-vivo* evidence of the effects of IBET-762 on the interaction between circadian rhythms and metabolism is limited, thus several experiments could be aimed at further characterising this relationship; as an example, a mouse jet-lag experiment would allow to test the *in-vivo* effects of strengthening the circadian clock through IBET-762 administration, and a tissue-specific knockout of SP1 would further correlate the effects of the transcription factor on both the circadian clock and metabolism.

8 BIBLIOGRAPHY

Abel ED, Peroni O, Kim JK, Kim YB, Boss O, Hadro E*, et al.* (2001). Adipose-selective targeting of the GLUT4 gene impairs insulin action in muscle and liver. Nature 409**:** 729-733.

Abrahamson EE, & Moore RY (2001). Suprachiasmatic nucleus in the mouse: retinal innervation, intrinsic organization and efferent projections. Brain Res 916**:** 172-191.

Ahn YH, Kim JW, Han GS, Lee BG, & Kim YS (1995). Cloning and characterization of rat pancreatic β-cell/liver type glucose transporter gene: a unique exon/intron organization. Arch Biochem Biophys 323**:** 387-396.

Alenghat T, Meyers K, Mullican SE, Leitner K, Adeniji-Adele A, Avila J*, et al.* (2008). Nuclear receptor corepressor and histone deacetylase 3 govern circadian metabolic physiology. Nature 456**:** 997-1000.

Allfrey VG, Faulkner R, & Mirsky AE (1964). Acetylation and Methylation of Histones and Their Possible Role in the Regulation of Rna Synthesis. Proc Natl Acad Sci U S A 51**:** 786-794.

Alqahtani A, Choucair K, Ashraf M, Hammouda DM, Alloghbi A, Khan T*, et al.* (2019). Bromodomain and extra-terminal motif inhibitors: a review of preclinical and clinical advances in cancer therapy. Future Sci OA 5**:** FSO372.

Alrob OA, Sankaralingam S, Ma C, Wagg CS, Fillmore N, Jaswal JS*, et al.* (2014). Obesity-induced lysine acetylation increases cardiac fatty acid oxidation and impairs insulin signalling. Cardiovasc Res 103**:** 485-497.

Alterman T, Luckhaupt SE, Dahlhamer JM, Ward BW, & Calvert GM (2013). Prevalence rates of work organization characteristics among workers in the U.S.: data from the 2010 National Health Interview Survey. Am J Ind Med 56**:** 647-659.

Alzamil H (2020). Elevated Serum TNF-α Is Related to Obesity in Type 2 Diabetes Mellitus and Is Associated with Glycemic Control and Insulin Resistance. J Obes 2020**:** 5076858.

Ameneiro C, Moreira T, Fuentes-Iglesias A, Coego A, Garcia-Outeiral V, Escudero A*, et al.* (2020). BMAL1 coordinates energy metabolism and differentiation of pluripotent stem cells. Life Sci Alliance 3.

American Diabetes A (2009). Diagnosis and classification of diabetes mellitus. Diabetes Care 32 Suppl 1**:** S62-67.

Anderson DR, Meyers MJ, Kurumbail RG, Caspers N, Poda GI, Long SA*, et al.* (2009). Benzothiophene inhibitors of MK2. Part 1: structure-activity relationships, assessments of selectivity and cellular potency. Bioorg Med Chem Lett 19**:** 4878-4881.

Ando H, Kumazaki M, Motosugi Y, Ushijima K, Maekawa T, Ishikawa E*, et al.* (2011). Impairment of peripheral circadian clocks precedes metabolic abnormalities in ob/ob mice. Endocrinology 152**:** 1347-1354.

Arendt J, Hampton S, English J, Kwasowski P, & Marks V (1982). 24-hour profiles of melatonin, cortisol, insulin, C-peptide and GIP following a meal and subsequent fasting. Clin Endocrinol (Oxf) 16**:** 89-95.

Arita Y, Kihara S, Ouchi N, Takahashi M, Maeda K, Miyagawa J*, et al.* (1999). Paradoxical decrease of an adipose-specific protein, adiponectin, in obesity. Biochem Biophys Res Commun 257**:** 79-83.

Arslanian S, Ohki Y, Becker DJ, & Drash AL (1990). Demonstration of a dawn phenomenon in normal adolescents. Horm Res 34**:** 27-32.

Asai M, Yoshinobu Y, Kaneko S, Mori A, Nikaido T, Moriya T*, et al.* (2001). Circadian profile of Per gene mRNA expression in the suprachiasmatic nucleus, paraventricular nucleus, and pineal body of aged rats. J Neurosci Res 66**:** 1133-1139.

Asangani IA, Dommeti VL, Wang X, Malik R, Cieslik M, Yang R*, et al.* (2014). Therapeutic targeting of BET bromodomain proteins in castration-resistant prostate cancer. Nature 510**:** 278-282.

Aschoff J (1960). Exogenous and endogenous components in circadian rhythms. Cold Spring Harb Symp Quant Biol 25**:** 11-28.

Aschoff J (1965). CIRCADIAN RHYTHMS IN MAN. Science 148**:** 1427-1432.

Asher G, Gatfield D, Stratmann M, Reinke H, Dibner C, Kreppel F*, et al.* (2008). SIRT1 regulates circadian clock gene expression through PER2 deacetylation. Cell 134**:** 317-328.

Athyros VG, Mikhailidis DP, Didangelos TP, Giouleme OI, Liberopoulos EN, Karagiannis A*, et al.* (2006). Effect of multifactorial treatment on non-alcoholic fatty liver disease in metabolic syndrome: a randomised study. Curr Med Res Opin 22**:** 873-883.

Atkinson BJ, Griesel BA, King CD, Josey MA, & Olson AL (2013). Moderate GLUT4 overexpression improves insulin sensitivity and fasting triglyceridemia in high-fat diet-fed transgenic mice. Diabetes 62**:** 2249-2258.

Azzi A, Dallmann R, Casserly A, Rehrauer H, Patrignani A, Maier B*, et al.* (2014). Circadian behavior is light-reprogrammed by plastic DNA methylation. Nat Neurosci 17**:** 377-382.

Babu MM, Luscombe NM, Aravind L, Gerstein M, & Teichmann SA (2004). Structure and evolution of transcriptional regulatory networks. Curr Opin Struct Biol 14**:** 283-291.

Badura L, Swanson T, Adamowicz W, Adams J, Cianfrogna J, Fisher K*, et al.* (2007). An inhibitor of casein kinase I epsilon induces phase delays in circadian rhythms under free-running and entrained conditions. J Pharmacol Exp Ther 322**:** 730-738.

Balsalobre A, Brown SA, Marcacci L, Tronche F, Kellendonk C, Reichardt HM*, et al.* (2000). Resetting of circadian time in peripheral tissues by glucocorticoid signaling. Science 289**:** 2344-2347.

Ban JJ, Ruthenborg RJ, Cho KW, & Kim JW (2014). Regulation of obesity and insulin resistance by hypoxia-inducible factors. Hypoxia (Auckl) 2**:** 171-183.

Baratta MG, Schinzel AC, Zwang Y, Bandopadhayay P, Bowman-Colin C, Kutt J*, et al.* (2015). An in-tumor genetic screen reveals that the BET bromodomain protein, BRD4, is a potential therapeutic target in ovarian carcinoma. Proc Natl Acad Sci U S A 112**:** 232-237.

Barbieri I, Cannizzaro E, & Dawson MA (2013). Bromodomains as therapeutic targets in cancer. Brief Funct Genomics 12**:** 219-230.

Bargut TC, Frantz ED, Mandarim-de-Lacerda CA, & Aguila MB (2014). Effects of a diet rich in n-3 polyunsaturated fatty acids on hepatic lipogenesis and β-oxidation in mice. Lipids 49**:** 431-444.

Barroso I, Gurnell M, Crowley VE, Agostini M, Schwabe JW, Soos MA*, et al.* (1999). Dominant negative mutations in human PPARgamma associated with severe insulin resistance, diabetes mellitus and hypertension. Nature 402**:** 880-883.

Baur JA, Pearson KJ, Price NL, Jamieson HA, Lerin C, Kalra A*, et al.* (2006). Resveratrol improves health and survival of mice on a high-calorie diet. Nature 444**:** 337-342.

Becares N, Gage MC, Voisin M, Shrestha E, Martin-Gutierrez L, Liang N*, et al.* (2019). Impaired LXRα Phosphorylation Attenuates Progression of Fatty Liver Disease. Cell Rep 26**:** 984-995 e986.

Beck H, Jeske M, Thede K, Stoll F, Flamme I, Akbaba M*, et al.* (2018). Discovery of Molidustat (BAY 85-3934): A Small-Molecule Oral HIF-Prolyl Hydroxylase (HIF-PH) Inhibitor for the Treatment of Renal Anemia. ChemMedChem 13**:** 988-1003.

Beishline K, & Azizkhan-Clifford J (2015). Sp1 and the 'hallmarks of cancer'. FEBS J 282**:** 224-258.

Belfort R, Harrison SA, Brown K, Darland C, Finch J, Hardies J*, et al.* (2006). A placebo-controlled trial of pioglitazone in subjects with nonalcoholic steatohepatitis. N Engl J Med 355**:** 2297-2307.

Bernsmeier C, Weisskopf DM, Pflueger MO, Mosimann J, Campana B, Terracciano L*, et al.* (2015). Sleep Disruption and Daytime Sleepiness Correlating with Disease Severity and Insulin Resistance in Non-Alcoholic Fatty Liver Disease: A Comparison with Healthy Controls. PLoS One 10**:** e0143293.

Bernstein E, Caudy AA, Hammond SM, & Hannon GJ (2001). Role for a bidentate ribonuclease in the initiation step of RNA interference. Nature 409**:** 363-366.

Biggi N, Consonni D, Galluzzo V, Sogliani M, & Costa G (2008). Metabolic syndrome in permanent night workers. Chronobiol Int 25**:** 443-454.

Bitzur R, Cohen H, Kamari Y, Shaish A, & Harats D (2009). Triglycerides and HDL cholesterol: stars or second leads in diabetes? Diabetes Care 32 Suppl 2**:** S373-377.

Bjornholm M, Munzberg H, Leshan RL, Villanueva EC, Bates SH, Louis GW*, et al.* (2007). Mice lacking inhibitory leptin receptor signals are lean with normal endocrine function. J Clin Invest 117**:** 1354-1360.

Black AR, Black JD, & Azizkhan-Clifford J (2001). Sp1 and kruppel-like factor family of transcription factors in cell growth regulation and cancer. J Cell Physiol 188**:** 143-160.

Boden G (2011). Obesity, insulin resistance and free fatty acids. Curr Opin Endocrinol Diabetes Obes 18**:** 139-143.

Bondarenko VA, Liu YV, Jiang YI, & Studitsky VM (2003). Communication over a large distance: enhancers and insulators. Biochem Cell Biol 81**:** 241-251.

Borbely G, Haldosen LA, Dahlman-Wright K, & Zhao C (2015). Induction of USP17 by combining BET and HDAC inhibitors in breast cancer cells. Oncotarget 6**:** 33623-33635.

Bordone L, & Guarente L (2005). Calorie restriction, SIRT1 and metabolism: understanding longevity. Nat Rev Mol Cell Biol 6**:** 298-305.

Bozek K, Relogio A, Kielbasa SM, Heine M, Dame C, Kramer A*, et al.* (2009). Regulation of clock-controlled genes in mammals. PLoS One 4**:** e4882.

Brand MD, Affourtit C, Esteves TC, Green K, Lambert AJ, Miwa S*, et al.* (2004). Mitochondrial superoxide: production, biological effects, and activation of uncoupling proteins. Free Radic Biol Med 37**:** 755-767.

Brennan AM, & Mantzoros CS (2006). Drug Insight: the role of leptin in human physiology and pathophysiology--emerging clinical applications. Nat Clin Pract Endocrinol Metab 2**:** 318-327.

Brion MJ, Ness AR, Rogers I, Emmett P, Cribb V, Davey Smith G*, et al.* (2010). Maternal macronutrient and energy intakes in pregnancy and offspring intake at 10 y: exploring parental comparisons and prenatal effects. Am J Clin Nutr 91**:** 748-756.

Brown JD, Feldman ZB, Doherty SP, Reyes JM, Rahl PB, Lin CY*, et al.* (2018). BET bromodomain proteins regulate enhancer function during adipogenesis. Proc Natl Acad Sci U S A 115**:** 2144-2149.

Brown JM, Chung S, Sawyer JK, Degirolamo C, Alger HM, Nguyen TM*, et al.* (2010). Combined therapy of dietary fish oil and stearoyl-CoA desaturase 1 inhibition prevents the metabolic syndrome and atherosclerosis. Arterioscler Thromb Vasc Biol 30**:** 24-30.

Brown JM, & Rudel LL (2010). Stearoyl-coenzyme A desaturase 1 inhibition and the metabolic syndrome: considerations for future drug discovery. Curr Opin Lipidol 21**:** 192-197.

Brundtland GH (2002). From the World Health Organization. Reducing risks to health, promoting healthy life. JAMA 288**:** 1974.

Buck-Koehntop BA, & Defossez PA (2013). On how mammalian transcription factors recognize methylated DNA. Epigenetics 8**:** 131-137.

Button EL, Bersten DC, & Whitelaw ML (2017). HIF has Biff - Crosstalk between HIF1a and the family of bHLH/PAS proteins. Exp Cell Res 356**:** 141-145.

Buxton OM, Cain SW, O'Connor SP, Porter JH, Duffy JF, Wang W*, et al.* (2012). Adverse metabolic consequences in humans of prolonged sleep restriction combined with circadian disruption. Sci Transl Med 4**:** 129ra143.

Cai L, Wang Z, Ji A, Meyer JM, & van der Westhuyzen DR (2012). Scavenger receptor CD36 expression contributes to adipose tissue inflammation and cell death in diet-induced obesity. PLoS One 7**:** e36785.

Calo E, & Wysocka J (2013). Modification of enhancer chromatin: what, how, and why? Mol Cell 49**:** 825-837.

Camp HS, Li O, Wise SC, Hong YH, Frankowski CL, Shen X*, et al.* (2000). Differential activation of peroxisome proliferator-activated receptor-gamma by troglitazone and rosiglitazone. Diabetes 49**:** 539-547.

Campodonico-Burnett W, Hetrick B, Wesolowski SR, Schenk S, Takahashi DL, Dean TA*, et al.* (2020). Maternal Obesity and Western-Style Diet Impair Fetal and Juvenile Offspring Skeletal Muscle Insulin-Stimulated Glucose Transport in Nonhuman Primates. Diabetes 69**:** 1389-1400.

Carmeliet P, Dor Y, Herbert JM, Fukumura D, Brusselmans K, Dewerchin M*, et al.* (1998). Role of HIF-1α in hypoxia-mediated apoptosis, cell proliferation and tumour angiogenesis. Nature 394**:** 485-490.

Cedernaes J, Osler ME, Voisin S, Broman JE, Vogel H, Dickson SL*, et al.* (2015). Acute Sleep Loss Induces Tissue-Specific Epigenetic and Transcriptional Alterations to Circadian Clock Genes in Men. J Clin Endocrinol Metab 100**:** E1255-1261.

Chakravarty B, Gu Z, Chirala SS, Wakil SJ, & Quiocho FA (2004). Human fatty acid synthase: structure and substrate selectivity of the thioesterase domain. Proc Natl Acad Sci U S A 101**:** 15567-15572.

Chamma CM, Bargut TC, Mandarim-de-Lacerda CA, & Aguila MB (2017). A rich medium-chain triacylglycerol diet benefits adiposity but has adverse effects on the markers of hepatic lipogenesis and β-oxidation. Food Funct 8**:** 778-787.

Chang HC, & Guarente L (2013). SIRT1 mediates central circadian control in the SCN by a mechanism that decays with aging. Cell 153**:** 1448-1460.

Chen G, Cheng Y, Tang Y, Martinka M, & Li G (2012a). Role of Tip60 in human melanoma cell migration, metastasis, and patient survival. J Invest Dermatol 132**:** 2632-2641.

Chen Z, Yoo SH, Park YS, Kim KH, Wei S, Buhr E*, et al.* (2012b). Identification of diverse modulators of central and peripheral circadian clocks by high-throughput chemical screening. Proc Natl Acad Sci U S A 109**:** 101-106.

Cheng CF, Ku HC, & Lin H (2018). PGC-1α as a Pivotal Factor in Lipid and Metabolic Regulation. Int J Mol Sci 19.

Cheng Z, Gong Y, Ma Y, Lu K, Lu X, Pierce LA*, et al.* (2013). Inhibition of BET bromodomain targets genetically diverse glioblastoma. Clin Cancer Res 19**:** 1748-1759.

Cheung P, Allis CD, & Sassone-Corsi P (2000). Signaling to chromatin through histone modifications. Cell 103**:** 263-271.

Chiang CM (2014). Nonequivalent response to bromodomain-targeting BET inhibitors in oligodendrocyte cell fate decision. Chem Biol 21**:** 804-806.

Chiang PK (1998). Biological effects of inhibitors of S-adenosylhomocysteine hydrolase. Pharmacol Ther 77**:** 115-134.

Choudhary C, Kumar C, Gnad F, Nielsen ML, Rehman M, Walther TC*, et al.* (2009). Lysine acetylation targets protein complexes and co-regulates major cellular functions. Science 325**:** 834-840.

Cinti S (2009). Transdifferentiation properties of adipocytes in the adipose organ. Am J Physiol Endocrinol Metab 297**:** E977-986.

Clarke JM, Hamer J, Shelton JR, Taylor S, & Venning GR (1976). The rhythm of the normal human heart. Lancet 1**:** 508-512.

Cnop M, Welsh N, Jonas JC, Jorns A, Lenzen S, & Eizirik DL (2005). Mechanisms of pancreatic β-cell death in type 1 and type 2 diabetes: many differences, few similarities. Diabetes 54 Suppl 2**:** S97-107.

Cohen P, Ntambi JM, & Friedman JM (2003). Stearoyl-CoA desaturase-1 and the metabolic syndrome. Curr Drug Targets Immune Endocr Metabol Disord 3**:** 271-280.

Considine RV, Sinha MK, Heiman ML, Kriauciunas A, Stephens TW, Nyce MR*, et al.* (1996). Serum immunoreactive-leptin concentrations in normal-weight and obese humans. N Engl J Med 334**:** 292-295.

Corbalan-Tutau D, Madrid JA, Nicolas F, & Garaulet M (2014). Daily profile in two circadian markers "melatonin and cortisol" and associations with metabolic syndrome components. Physiol Behav 123**:** 231-235.

Covello KL, Kehler J, Yu H, Gordan JD, Arsham AM, Hu CJ*, et al.* (2006). HIF-2α regulates Oct-4: effects of hypoxia on stem cell function, embryonic development, and tumor growth. Genes Dev 20**:** 557-570.

da Motta LL, Ledaki I, Purshouse K, Haider S, De Bastiani MA, Baban D*, et al.* (2017). The BET inhibitor JQ1 selectively impairs tumour response to hypoxia and downregulates CA9 and angiogenesis in triple negative breast cancer. Oncogene 36**:** 122-132.

Daan S, & Pittendrigh CS (1976). A Functional analysis of circadian pacemakers in nocturnal rodents. Journal of comparative physiology 106**:** 253-266.

Dang CV, & Semenza GL (1999). Oncogenic alterations of metabolism. Trends Biochem Sci 24**:** 68-72.

Daniel S, & Kim KH (1996). Sp1 mediates glucose activation of the acetyl-CoA carboxylase promoter. J Biol Chem 271**:** 1385-1392.

Dashwood RH, & Ho E (2007). Dietary histone deacetylase inhibitors: from cells to mice to man. Semin Cancer Biol 17**:** 363-369.

Dawson MA, Prinjha RK, Dittmann A, Giotopoulos G, Bantscheff M, Chan WI*, et al.* (2011). Inhibition of BET recruitment to chromatin as an effective treatment for MLL-fusion leukaemia. Nature 478**:** 529-533.

de Goede P, Foppen E, Ritsema W, Korpel NL, Yi CX, & Kalsbeek A (2019). Time-Restricted Feeding Improves Glucose Tolerance in Rats, but Only When in Line With the Circadian Timing System. Front Endocrinol (Lausanne) 10**:** 554.

DeFronzo RA, & Tripathy D (2009). Skeletal muscle insulin resistance is the primary defect in type 2 diabetes. Diabetes Care 32 Suppl 2**:** S157-163.

Denis GV, Nikolajczyk BS, & Schnitzler GR (2010). An emerging role for bromodomain-containing proteins in chromatin regulation and transcriptional control of adipogenesis. FEBS Lett 584**:** 3260-3268.

Dhalluin C, Carlson JE, Zeng L, He C, Aggarwal AK, & Zhou MM (1999). Structure and ligand of a histone acetyltransferase bromodomain. Nature 399**:** 491-496.

Di Micco R, Fontanals-Cirera B, Low V, Ntziachristos P, Yuen SK, Lovell CD*, et al.* (2014). Control of embryonic stem cell identity by BRD4-dependent transcriptional elongation of super-enhancer-associated pluripotency genes. Cell Rep 9**:** 234-247.

Dibner C, & Schibler U (2018). Body clocks: Time for the Nobel Prize. Acta Physiol (Oxf) 222.

Diez JJ, & Iglesias P (2003). The role of the novel adipocyte-derived hormone adiponectin in human disease. Eur J Endocrinol 148**:** 293-300.

Dijk DJ, Duffy JF, Silva EJ, Shanahan TL, Boivin DB, & Czeisler CA (2012). Amplitude reduction and phase shifts of melatonin, cortisol and other circadian rhythms after a gradual advance of sleep and light exposure in humans. PLoS One 7**:** e30037.

Divakaruni AS, Paradyse A, Ferrick DA, Murphy AN, & Jastroch M (2014). Analysis and interpretation of microplate-based oxygen consumption and pH data. Methods Enzymol 547**:** 309-354.

Doi M, Hirayama J, & Sassone-Corsi P (2006). Circadian regulator CLOCK is a histone acetyltransferase. Cell 125**:** 497-508.

Dong X, Hu X, Chen J, Hu D, & Chen LF (2018). BRD4 regulates cellular senescence in gastric cancer cells via E2F/miR-106b/p21 axis. Cell Death Dis 9**:** 203.

Duan Q, McMahon S, Anand P, Shah H, Thomas S, Salunga HT*, et al.* (2017). BET bromodomain inhibition suppresses innate inflammatory and profibrotic transcriptional networks in heart failure. Sci Transl Med 9.

Duffield GE, Best JD, Meurers BH, Bittner A, Loros JJ, & Dunlap JC (2002). Circadian programs of transcriptional activation, signaling, and protein turnover revealed by microarray analysis of mammalian cells. Curr Biol 12**:** 551-557.

Dyar KA, Ciciliot S, Wright LE, Bienso RS, Tagliazucchi GM, Patel VR*, et al.* (2014). Muscle insulin sensitivity and glucose metabolism are controlled by the intrinsic muscle clock. Mol Metab 3**:** 29-41.

Eckel RH, Grundy SM, & Zimmet PZ (2005). The metabolic syndrome. Lancet 365**:** 1415-1428.

Eckel-Mahan K, & Sassone-Corsi P (2009). Metabolism control by the circadian clock and vice versa. Nat Struct Mol Biol 16**:** 462-467.

Ekstedt M, Franzen LE, Mathiesen UL, Holmqvist M, Bodemar G, & Kechagias S (2007). Statins in non-alcoholic fatty liver disease and chronically elevated liver enzymes: a histopathological follow-up study. J Hepatol 47**:** 135-141.

Etchegaray JP, Lee C, Wade PA, & Reppert SM (2003). Rhythmic histone acetylation underlies transcription in the mammalian circadian clock. Nature 421**:** 177-182.

Etchegaray JP, Yang X, DeBruyne JP, Peters AH, Weaver DR, Jenuwein T*, et al.* (2006). The polycomb group protein EZH2 is required for mammalian circadian clock function. J Biol Chem 281**:** 21209-21215.

Evans RM, Barish GD, & Wang YX (2004). PPARs and the complex journey to obesity. Nat Med 10**:** 355-361.

Farooqi IS, Matarese G, Lord GM, Keogh JM, Lawrence E, Agwu C*, et al.* (2002). Beneficial effects of leptin on obesity, T cell hyporesponsiveness, and neuroendocrine/metabolic dysfunction of human congenital leptin deficiency. J Clin Invest 110**:** 1093-1103.

Feng D, Liu T, Sun Z, Bugge A, Mullican SE, Alenghat T*, et al.* (2011). A circadian rhythm orchestrated by histone deacetylase 3 controls hepatic lipid metabolism. Science 331**:** 1315-1319.

Feng Q, Zhang Z, Shea MJ, Creighton CJ, Coarfa C, Hilsenbeck SG*, et al.* (2014). An epigenomic approach to therapy for tamoxifen-resistant breast cancer. Cell Res 24**:** 809-819.

Ferezou-Viala J, Roy AF, Serougne C, Gripois D, Parquet M, Bailleux V*, et al.* (2007). Long-term consequences of maternal high-fat feeding on hypothalamic leptin sensitivity and diet-induced obesity in the offspring. Am J Physiol Regul Integr Comp Physiol 293**:** R1056-1062.

Ferrannini E, Iozzo P, Virtanen KA, Honka MJ, Bucci M, & Nuutila P (2018). Adipose tissue and skeletal muscle insulin-mediated glucose uptake in insulin resistance: role of blood flow and diabetes. Am J Clin Nutr 108**:** 749-758.

Filippakopoulos P, & Knapp S (2014). Targeting bromodomains: epigenetic readers of lysine acetylation. Nat Rev Drug Discov 13**:** 337-356.

Filippakopoulos P, Picaud S, Fedorov O, Keller M, Wrobel M, Morgenstern O*, et al.* (2012a). Benzodiazepines and benzotriazepines as protein interaction inhibitors targeting bromodomains of the BET family. Bioorg Med Chem 20**:** 1878-1886.

Filippakopoulos P, Picaud S, Mangos M, Keates T, Lambert JP, Barsyte-Lovejoy D*, et al.* (2012b). Histone recognition and large-scale structural analysis of the human bromodomain family. Cell 149**:** 214-231.

Filippakopoulos P, Qi J, Picaud S, Shen Y, Smith WB, Fedorov O*, et al.* (2010). Selective inhibition of BET bromodomains. Nature 468**:** 1067-1073.

Findeisen HM, Pearson KJ, Gizard F, Zhao Y, Qing H, Jones KL*, et al.* (2011). Oxidative stress accumulates in adipose tissue during aging and inhibits adipogenesis. PLoS One 6**:** e18532.

Floras JS, Jones JV, Johnston JA, Brooks DE, Hassan MO, & Sleight P (1978). Arousal and the circadian rhythm of blood pressure. Clin Sci Mol Med Suppl 4**:** 395s-397s.

Fogg PC, O'Neill JS, Dobrzycki T, Calvert S, Lord EC, McIntosh RL*, et al.* (2014). Class IIa histone deacetylases are conserved regulators of circadian function. J Biol Chem 289**:** 34341-34348.

Fonseca V (2003). Effect of thiazolidinediones on body weight in patients with diabetes mellitus. Am J Med 115 Suppl 8A**:** 42S-48S.

Fowler SD, & Greenspan P (1985). Application of Nile red, a fluorescent hydrophobic probe, for the detection of neutral lipid deposits in tissue sections: comparison with oil red O. J Histochem Cytochem 33**:** 833-836.

Fox CS, Massaro JM, Hoffmann U, Pou KM, Maurovich-Horvat P, Liu CY*, et al.* (2007). Abdominal visceral and subcutaneous adipose tissue compartments: association with metabolic risk factors in the Framingham Heart Study. Circulation 116**:** 39-48.

French CA, Ramirez CL, Kolmakova J, Hickman TT, Cameron MJ, Thyne ME*, et al.* (2008). BRD-NUT oncoproteins: a family of closely related nuclear proteins that block epithelial differentiation and maintain the growth of carcinoma cells. Oncogene 27**:** 2237-2242.

Fried SK, Russell CD, Grauso NL, & Brolin RE (1993). Lipoprotein lipase regulation by insulin and glucocorticoid in subcutaneous and omental adipose tissues of obese women and men. J Clin Invest 92**:** 2191-2198.

Friedman SL, Neuschwander-Tetri BA, Rinella M, & Sanyal AJ (2018). Mechanisms of NAFLD development and therapeutic strategies. Nat Med 24**:** 908-922.

Froy O, & Miskin R (2007). The interrelations among feeding, circadian rhythms and ageing. Prog Neurobiol 82**:** 142-150.

Fujimoto K, Hamaguchi H, Hashiba T, Nakamura T, Kawamoto T, Sato F*, et al.* (2007). Transcriptional repression by the basic helix-loop-helix protein Dec2: multiple mechanisms through E-box elements. Int J Mol Med 19**:** 925-932.

Furukawa S, Fujita T, Shimabukuro M, Iwaki M, Yamada Y, Nakajima Y*, et al.* (2004). Increased oxidative stress in obesity and its impact on metabolic syndrome. J Clin Invest 114**:** 1752-1761.

Gacias M, Gerona-Navarro G, Plotnikov AN, Zhang G, Zeng L, Kaur J*, et al.* (2014). Selective chemical modulation of gene transcription favors oligodendrocyte lineage progression. Chem Biol 21**:** 841-854.

Gallo M (2013). Thyroid safety in patients treated with liraglutide. J Endocrinol Invest 36**:** 140-145.

Ganapathy V, Thangaraju M, & Prasad PD (2009). Nutrient transporters in cancer: relevance to Warburg hypothesis and beyond. Pharmacol Ther 121**:** 29-40.

Garaulet M, & Gomez-Abellan P (2014). Timing of food intake and obesity: a novel association. Physiol Behav 134**:** 44-50.

Garg M, Thamotharan M, Becker DJ, & Devaskar SU (2014). Adolescents with clinical type 1 diabetes display reduced red blood cell glucose transporter isoform 1 (GLUT1). Pediatr Diabetes 15**:** 511-518.

Gartel AL, Ye X, Goufman E, Shianov P, Hay N, Najmabadi F*, et al.* (2001). Myc represses the p21(WAF1/CIP1) promoter and interacts with Sp1/Sp3. Proc Natl Acad Sci U S A 98**:** 4510-4515.

Garvey WT, Maianu L, Zhu JH, Brechtel-Hook G, Wallace P, & Baron AD (1998). Evidence for defects in the trafficking and translocation of GLUT4 glucose transporters in skeletal muscle as a cause of human insulin resistance. J Clin Invest 101**:** 2377-2386.

Garvey WT, Olefsky JM, & Marshall S (1985). Insulin receptor down-regulation is linked to an insulin-induced postreceptor defect in the glucose transport system in rat adipocytes. J Clin Invest 76**:** 22-30.

Gesta S, Tseng YH, & Kahn CR (2007). Developmental origin of fat: tracking obesity to its source. Cell 131**:** 242-256.

Gilham D, Wasiak S, Tsujikawa LM, Halliday C, Norek K, Patel RG*, et al.* (2016). RVX-208, a BET-inhibitor for treating atherosclerotic cardiovascular disease, raises ApoA-I/HDL and represses pathways that contribute to cardiovascular disease. Atherosclerosis 247**:** 48-57.

Goda N, Ryan HE, Khadivi B, McNulty W, Rickert RC, & Johnson RS (2003). Hypoxia-inducible factor 1α is essential for cell cycle arrest during hypoxia. Mol Cell Biol 23**:** 359-369.

Godoy-Matos AF, Silva Junior WS, & Valerio CM (2020). NAFLD as a continuum: from obesity to metabolic syndrome and diabetes. Diabetol Metab Syndr 12**:** 60.

Golay A, & Bobbioni E (1997). The role of dietary fat in obesity. Int J Obes Relat Metab Disord 21 Suppl 3**:** S2-11.

Goodarzi AA, Noon AT, Deckbar D, Ziv Y, Shiloh Y, Lobrich M*, et al.* (2008). ATM signaling facilitates repair of DNA double-strand breaks associated with heterochromatin. Mol Cell 31**:** 167-177.

Gordon DE, Jang GM, Bouhaddou M, Xu J, Obernier K, O'Meara MJ*, et al.* (2020). A SARS-CoV-2-Human Protein-Protein Interaction Map Reveals Drug Targets and Potential Drug-Repurposing. bioRxiv.

Green H, & Kehinde O (1975). An established preadipose cell line and its differentiation in culture. II. Factors affecting the adipose conversion. Cell 5**:** 19-27.

Greenspan P, Mayer EP, & Fowler SD (1985). Nile red: a selective fluorescent stain for intracellular lipid droplets. J Cell Biol 100**:** 965-973.

Greenwald RJ, Tumang JR, Sinha A, Currier N, Cardiff RD, Rothstein TL*, et al.* (2004). E mu-BRD2 transgenic mice develop B-cell lymphoma and leukemia. Blood 103**:** 1475-1484.

Greer EL, & Shi Y (2012). Histone methylation: a dynamic mark in health, disease and inheritance. Nat Rev Genet 13**:** 343-357.

Grundy SM (2006). Atherogenic dyslipidemia associated with metabolic syndrome and insulin resistance. Clin Cornerstone 8 Suppl 1**:** S21-27.

Gu YZ, Hogenesch JB, & Bradfield CA (2000). The PAS superfamily: sensors of environmental and developmental signals. Annu Rev Pharmacol Toxicol 40**:** 519-561.

Guan HP, Ishizuka T, Chui PC, Lehrke M, & Lazar MA (2005). Corepressors selectively control the transcriptional activity of PPARgamma in adipocytes. Genes Dev 19**:** 453-461.

Guerciolini R (1997). Mode of action of orlistat. Int J Obes Relat Metab Disord 21 Suppl 3**:** S12-23.

Guillaumond F, Grechez-Cassiau A, Subramaniam M, Brangolo S, Peteri-Brunback B, Staels B*, et al.* (2010). Kruppel-like factor KLF10 is a link between the circadian clock and metabolism in liver. Mol Cell Biol 30**:** 3059-3070.

Haemmerle G, Zimmermann R, Strauss JG, Kratky D, Riederer M, Knipping G*, et al.* (2002). Hormone-sensitive lipase deficiency in mice changes the plasma lipid profile by affecting the tissue-specific expression pattern of lipoprotein lipase in adipose tissue and muscle. J Biol Chem 277**:** 12946-12952.

Halberg N, Khan T, Trujillo ME, Wernstedt-Asterholm I, Attie AD, Sherwani S*, et al.* (2009). Hypoxia-inducible factor 1α induces fibrosis and insulin resistance in white adipose tissue. Mol Cell Biol 29**:** 4467-4483.

Hales CN, & Barker DJ (2001). The thrifty phenotype hypothesis. Br Med Bull 60**:** 5-20.

Hales CN, Barker DJ, Clark PM, Cox LJ, Fall C, Osmond C*, et al.* (1991). Fetal and infant growth and impaired glucose tolerance at age 64. BMJ 303**:** 1019-1022.

Handjieva-Darlenska T, & Boyadjieva N (2009). The effect of high-fat diet on plasma ghrelin and leptin levels in rats. J Physiol Biochem 65**:** 157-164.

Hannema SE, Wit JM, Houdijk ME, van Haeringen A, Bik EC, Verkerk AJ*, et al.* (2016). Novel Leptin Receptor Mutations Identified in Two Girls with Severe Obesity Are Associated with Increased Bone Mineral Density. Horm Res Paediatr 85**:** 412-420.

Hauner H, Rohrig K, Spelleken M, Liu LS, & Eckel J (1998). Development of insulin-responsive glucose uptake and GLUT4 expression in differentiating human adipocyte precursor cells. Int J Obes Relat Metab Disord 22**:** 448-453.

Haus E, & Smolensky M (2006). Biological clocks and shift work: circadian dysregulation and potential long-term effects. Cancer Causes Control 17**:** 489-500.

He B, Nohara K, Park N, Park YS, Guillory B, Zhao Z*, et al.* (2016). The Small Molecule Nobiletin Targets the Molecular Oscillator to Enhance Circadian Rhythms and Protect against Metabolic Syndrome. Cell Metab 23**:** 610-621.

He Y, Jones CR, Fujiki N, Xu Y, Guo B, Holder JL, Jr.*, et al.* (2009). The transcriptional repressor DEC2 regulates sleep length in mammals. Science 325**:** 866-870.

Henssen A, Thor T, Odersky A, Heukamp L, El-Hindy N, Beckers A*, et al.* (2013). BET bromodomain protein inhibition is a therapeutic option for medulloblastoma. Oncotarget 4**:** 2080-2095.

Hida A, Kitamura S, Ohsawa Y, Enomoto M, Katayose Y, Motomura Y*, et al.* (2013). In vitro circadian period is associated with circadian/sleep preference. Sci Rep 3**:** 2074.

Higa TS, Spinola AV, Fonseca-Alaniz MH, & Evangelista FS (2014). Comparison between cafeteria and high-fat diets in the induction of metabolic dysfunction in mice. Int J Physiol Pathophysiol Pharmacol 6**:** 47-54.

Hirota T, Kon N, Itagaki T, Hoshina N, Okano T, & Fukada Y (2010). Transcriptional repressor TIEG1 regulates Bmal1 gene through GC box and controls circadian clockwork. Genes Cells 15**:** 111-121.

Hirota T, Lewis WG, Liu AC, Lee JW, Schultz PG, & Kay SA (2008). A chemical biology approach reveals period shortening of the mammalian circadian clock by specific inhibition of GSK-3β. Proc Natl Acad Sci U S A 105**:** 20746-20751.

Hnilicova J, Hozeifi S, Stejskalova E, Duskova E, Poser I, Humpolickova J*, et al.* (2013). The C-terminal domain of Brd2 is important for chromatin interaction and regulation of transcription and alternative splicing. Mol Biol Cell 24**:** 3557-3568.

Holliday R (1987). The inheritance of epigenetic defects. Science 238**:** 163-170.

Hong F, Xu P, & Zhai Y (2018). The Opportunities and Challenges of Peroxisome Proliferator-Activated Receptors Ligands in Clinical Drug Discovery and Development. Int J Mol Sci 19.

Hong S, Dutta A, & Laimins LA (2015). The acetyltransferase Tip60 is a critical regulator of the differentiation-dependent amplification of human papillomaviruses. J Virol 89**:** 4668-4675.

Honma S, Kawamoto T, Takagi Y, Fujimoto K, Sato F, Noshiro M*, et al.* (2002). Dec1 and Dec2 are regulators of the mammalian molecular clock. Nature 419**:** 841-844.

Hood S, & Amir S (2017). The aging clock: circadian rhythms and later life. J Clin Invest 127**:** 437-446.

Horovitz-Fried M, & Sampson SR (2007). Involvement of PKCα in insulin-induced PKCdelta expression: Importance of SP-1 and NFkappaB transcription factors. Biochem Biophys Res Commun 352**:** 78-83.

Hosoi T, Sasaki M, Miyahara T, Hashimoto C, Matsuo S, Yoshii M*, et al.* (2008). Endoplasmic reticulum stress induces leptin resistance. Mol Pharmacol 74**:** 1610-1619.

Hotamisligil GS, Shargill NS, & Spiegelman BM (1993). Adipose expression of tumor necrosis factor-α: direct role in obesity-linked insulin resistance. Science 259**:** 87-91.

Hotta K, Funahashi T, Arita Y, Takahashi M, Matsuda M, Okamoto Y*, et al.* (2000). Plasma concentrations of a novel, adipose-specific protein, adiponectin, in type 2 diabetic patients. Arterioscler Thromb Vasc Biol 20**:** 1595-1599.

Houzelstein D, Bullock SL, Lynch DE, Grigorieva EF, Wilson VA, & Beddington RS (2002). Growth and early postimplantation defects in mice deficient for the bromodomain-containing protein Brd4. Mol Cell Biol 22**:** 3794-3802.

Hruby A, & Hu FB (2015). The Epidemiology of Obesity: A Big Picture. Pharmacoeconomics 33**:** 673-689.

Hu Y, Spengler ML, Kuropatwinski KK, Comas-Soberats M, Jackson M, Chernov MV*, et al.* (2011). Selenium is a modulator of circadian clock that protects mice from the toxicity of a chemotherapeutic drug via upregulation of the core clock protein, BMAL1. Oncotarget 2**:** 1279-1290.

Huang B, Yang XD, Zhou MM, Ozato K, & Chen LF (2009). Brd4 coactivates transcriptional activation of NF-kappaB via specific binding to acetylated RelA. Mol Cell Biol 29**:** 1375-1387.

Hussong M, Borno ST, Kerick M, Wunderlich A, Franz A, Sultmann H*, et al.* (2014). The bromodomain protein BRD4 regulates the KEAP1/NRF2-dependent oxidative stress response. Cell Death Dis 5**:** e1195.

Hwang DY, & Ismail-Beigi F (2006). Control of Glut1 promoter activity under basal conditions and in response to hyperosmolarity: role of Sp1. Am J Physiol Cell Physiol 290**:** C337-344.

Imai T, Takakuwa R, Marchand S, Dentz E, Bornert JM, Messaddeq N*, et al.* (2004). Peroxisome proliferator-activated receptor gamma is required in mature white and brown adipocytes for their survival in the mouse. Proc Natl Acad Sci U S A 101**:** 4543-4547.

Ingalls AM, Dickie MM, & Snell GD (1950). Obese, a new mutation in the house mouse. J Hered 41**:** 317-318.

Ito T, Kitamura H, Uwatoko C, Azumano M, Itoh K, & Kuwahara J (2010). Interaction of Sp1 zinc finger with transport factor in the nuclear localization of transcription factor Sp1. Biochem Biophys Res Commun 403**:** 161-166.

Iyer NV, Leung SW, & Semenza GL (1998). The human hypoxia-inducible factor 1α gene: HIF1A structure and evolutionary conservation. Genomics 52**:** 159-165.

Jacobi D, Liu S, Burkewitz K, Kory N, Knudsen NH, Alexander RK*, et al.* (2015). Hepatic Bmal1 Regulates Rhythmic Mitochondrial Dynamics and Promotes Metabolic Fitness. Cell Metab 22**:** 709-720.

Jiang BH, Semenza GL, Bauer C, & Marti HH (1996). Hypoxia-inducible factor 1 levels vary exponentially over a physiologically relevant range of O2 tension. Am J Physiol 271**:** C1172-1180.

Jiang C, Qu A, Matsubara T, Chanturiya T, Jou W, Gavrilova O*, et al.* (2011). Disruption of hypoxia-inducible factor 1 in adipocytes improves insulin sensitivity and decreases adiposity in high-fat diet-fed mice. Diabetes 60**:** 2484-2495.

Jiang YW, Veschambre P, Erdjument-Bromage H, Tempst P, Conaway JW, Conaway RC*, et al.* (1998). Mammalian mediator of transcriptional regulation and its possible role as an end-point of signal transduction pathways. Proc Natl Acad Sci U S A 95**:** 8538-8543.

Jin J, Lian T, Gu C, Yu K, Gao YQ, & Su XD (2016). The effects of cytosine methylation on general transcription factors. Sci Rep 6**:** 29119.

Jonkers I, & Lis JT (2015). Getting up to speed with transcription elongation by RNA polymerase II. Nat Rev Mol Cell Biol 16**:** 167-177.

Jung M, Gelato KA, Fernandez-Montalvan A, Siegel S, & Haendler B (2015). Targeting BET bromodomains for cancer treatment. Epigenomics 7**:** 487-501.

Jurysta C, Nicaise C, Giroix MH, Cetik S, Malaisse WJ, & Sener A (2013). Comparison of GLUT1, GLUT2, GLUT4 and SGLT1 mRNA expression in the salivary glands and six other organs of control, streptozotocin-induced and Goto-Kakizaki diabetic rats. Cell Physiol Biochem 31**:** 37-43.

Kahn SE (2003). The relative contributions of insulin resistance and β-cell dysfunction to the pathophysiology of Type 2 diabetes. Diabetologia 46**:** 3-19.

Kamine J, Elangovan B, Subramanian T, Coleman D, & Chinnadurai G (1996). Identification of a cellular protein that specifically interacts with the essential cysteine region of the HIV-1 Tat transactivator. Virology 216**:** 357-366.

Kanno T, Kanno Y, LeRoy G, Campos E, Sun HW, Brooks SR*, et al.* (2014). BRD4 assists elongation of both coding and enhancer RNAs by interacting with acetylated histones. Nat Struct Mol Biol 21**:** 1047-1057.

Kapuscinski J (1995). DAPI: a DNA-specific fluorescent probe. Biotech Histochem 70**:** 220-233.

Karackattu SL, Trigatti B, & Krieger M (2006). Hepatic lipase deficiency delays atherosclerosis, myocardial infarction, and cardiac dysfunction and extends lifespan in SR-BI/apolipoprotein E double knockout mice. Arterioscler Thromb Vasc Biol 26**:** 548-554.

Karelis AD, Faraj M, Bastard JP, St-Pierre DH, Brochu M, Prud'homme D*, et al.* (2005). The metabolically healthy but obese individual presents a favorable inflammation profile. J Clin Endocrinol Metab 90**:** 4145-4150.

Karlsson B, Knutsson A, & Lindahl B (2001). Is there an association between shift work and having a metabolic syndrome? Results from a population based study of 27,485 people. Occup Environ Med 58**:** 747-752.

Katada S, & Sassone-Corsi P (2010). The histone methyltransferase MLL1 permits the oscillation of circadian gene expression. Nat Struct Mol Biol 17**:** 1414-1421.

Katewa SD, Akagi K, Bose N, Rakshit K, Camarella T, Zheng X*, et al.* (2016). Peripheral Circadian Clocks Mediate Dietary Restriction-Dependent Changes in Lifespan and Fat Metabolism in Drosophila. Cell Metab 23**:** 143-154.

Kawai M, Green CB, Horowitz M, Ackert-Bicknell C, Lecka-Czernik B, & Rosen CJ (2010a). Nocturnin: a circadian target of Pparg-induced adipogenesis. Ann N Y Acad Sci 1192**:** 131-138.

Kawai M, Green CB, Lecka-Czernik B, Douris N, Gilbert MR, Kojima S*, et al.* (2010b). A circadian-regulated gene, Nocturnin, promotes adipogenesis by stimulating PPAR-gamma nuclear translocation. Proc Natl Acad Sci U S A 107**:** 10508-10513.

Keck KM, Moquin SA, He A, Fernandez SG, Somberg JJ, Liu SM*, et al.* (2017). Bromodomain and extraterminal inhibitors block the Epstein-Barr virus lytic cycle at two distinct steps. J Biol Chem 292**:** 13284-13295.

Kelly T, Yang W, Chen CS, Reynolds K, & He J (2008). Global burden of obesity in 2005 and projections to 2030. Int J Obes (Lond) 32**:** 1431-1437.

Kervezee L, Cermakian N, & Boivin DB (2019). Individual metabolomic signatures of circadian misalignment during simulated night shifts in humans. PLoS Biol 17**:** e3000303.

Kervezee L, Kosmadopoulos A, & Boivin DB (2020). Metabolic and cardiovascular consequences of shift work: The role of circadian disruption and sleep disturbances. Eur J Neurosci 51**:** 396-412.

Kim HI, & Ahn YH (2004). Role of peroxisome proliferator-activated receptor-gamma in the glucose-sensing apparatus of liver and β-cells. Diabetes 53 Suppl 1**:** S60-65.

Kim JD, Leyva S, & Diano S (2014a). Hormonal regulation of the hypothalamic melanocortin system. Front Physiol 5**:** 480.

Kim JM, Hong K, Lee JH, Lee S, & Chang N (2009). Effect of folate deficiency on placental DNA methylation in hyperhomocysteinemic rats. J Nutr Biochem 20**:** 172-176.

Kim MS, Pinto SM, Getnet D, Nirujogi RS, Manda SS, Chaerkady R*, et al.* (2014b). A draft map of the human proteome. Nature 509**:** 575-581.

Kim SY, & Park JW (2010). Modulation of hypoxia-inducible factor-1α expression by mitochondrial NADP+-dependent isocitrate dehydrogenase. Biochimie 92**:** 1908-1913.

Kim YH, Marhon SA, Zhang Y, Steger DJ, Won KJ, & Lazar MA (2018). Rev-erbα dynamically modulates chromatin looping to control circadian gene transcription. Science 359**:** 1274-1277.

Kitabchi AE, Umpierrez GE, Miles JM, & Fisher JN (2009). Hyperglycemic crises in adult patients with diabetes. Diabetes Care 32**:** 1335-1343.

Knight ZA, Hannan KS, Greenberg ML, & Friedman JM (2010). Hyperleptinemia is required for the development of leptin resistance. PLoS One 5**:** e11376.

Knutson KL, Spiegel K, Penev P, & Van Cauter E (2007). The metabolic consequences of sleep deprivation. Sleep Med Rev 11**:** 163-178.

Ko CH, & Takahashi JS (2006). Molecular components of the mammalian circadian clock. Hum Mol Genet 15 Spec No 2**:** R271-277.

Ko J, Kim JY, Kim JW, & Yoon JS (2020). Anti-oxidative and anti-adipogenic effects of caffeine in an in vitro model of Graves' orbitopathy. Endocr J 67**:** 439-447.

Kobayashi M, Morinibu A, Koyasu S, Goto Y, Hiraoka M, & Harada H (2017). A circadian clock gene, PER2, activates HIF-1 as an effector molecule for recruitment of HIF-1α to promoter regions of its downstream genes. FEBS J 284**:** 3804-3816.

Koch CE, Lowe C, Pretz D, Steger J, Williams LM, & Tups A (2014). High-fat diet induces leptin resistance in leptin-deficient mice. J Neuroendocrinol 26**:** 58-67.

Kohsaka A, Laposky AD, Ramsey KM, Estrada C, Joshu C, Kobayashi Y*, et al.* (2007). High-fat diet disrupts behavioral and molecular circadian rhythms in mice. Cell Metab 6**:** 414-421.

Koike N, Yoo SH, Huang HC, Kumar V, Lee C, Kim TK*, et al.* (2012). Transcriptional architecture and chromatin landscape of the core circadian clock in mammals. Science 338**:** 349-354.

Kolker DE, Fukuyama H, Huang DS, Takahashi JS, Horton TH, & Turek FW (2003). Aging alters circadian and light-induced expression of clock genes in golden hamsters. J Biol Rhythms 18**:** 159-169.

Konopka RJ, & Benzer S (1971). Clock mutants of Drosophila melanogaster. Proc Natl Acad Sci U S A 68**:** 2112-2116.

Korzeniewski B, Harper ME, & Brand MD (1995). Proportional activation coefficients during stimulation of oxidative phosphorylation by lactate and pyruvate or by vasopressin. Biochim Biophys Acta 1229**:** 315-322.

Koshiji M, To KK, Hammer S, Kumamoto K, Harris AL, Modrich P*, et al.* (2005). HIF-1α induces genetic instability by transcriptionally downregulating MutSα expression. Mol Cell 17**:** 793-803.

Kotronen A, Seppanen-Laakso T, Westerbacka J, Kiviluoto T, Arola J, Ruskeepaa AL*, et al.* (2009). Hepatic stearoyl-CoA desaturase (SCD)-1 activity and diacylglycerol but not ceramide concentrations are increased in the nonalcoholic human fatty liver. Diabetes 58**:** 203-208.

Kouzarides T (2007). Chromatin modifications and their function. Cell 128**:** 693-705.

Kovacs P, Hanson RL, Lee YH, Yang X, Kobes S, Permana PA*, et al.* (2003). The role of insulin receptor substrate-1 gene (IRS1) in type 2 diabetes in Pima Indians. Diabetes 52**:** 3005-3009.

Krey G, Mahfoudi A, & Wahli W (1995). Functional interactions of peroxisome proliferator-activated receptor, retinoid-X receptor, and Sp1 in the transcriptional regulation of the acyl-coenzyme-A oxidase promoter. Mol Endocrinol 9**:** 219-231.

Kulaeva OI, Nizovtseva EV, Polikanov YS, Ulianov SV, & Studitsky VM (2012). Distant activation of transcription: mechanisms of enhancer action. Mol Cell Biol 32**:** 4892-4897.

Kyle UG, & Pichard C (2006). The Dutch Famine of 1944-1945: a pathophysiological model of long-term consequences of wasting disease. Curr Opin Clin Nutr Metab Care 9**:** 388-394.

Lafontan M, & Girard J (2008). Impact of visceral adipose tissue on liver metabolism. Part I: heterogeneity of adipose tissue and functional properties of visceral adipose tissue. Diabetes Metab 34**:** 317-327.

Lamia KA, Storch KF, & Weitz CJ (2008). Physiological significance of a peripheral tissue circadian clock. Proc Natl Acad Sci U S A 105**:** 15172-15177.

Lamonica JM, Deng W, Kadauke S, Campbell AE, Gamsjaeger R, Wang H*, et al.* (2011). Bromodomain protein Brd3 associates with acetylated GATA1 to promote its chromatin occupancy at erythroid target genes. Proc Natl Acad Sci U S A 108**:** E159-168.

Landgraf D, Wang LL, Diemer T, & Welsh DK (2016). NPAS2 Compensates for Loss of CLOCK in Peripheral Circadian Oscillators. PLoS Genet 12**:** e1005882.

Lang P, Hasselwander S, Li H, & Xia N (2019). Effects of different diets used in diet-induced obesity models on insulin resistance and vascular dysfunction in C57BL/6 mice. Sci Rep 9**:** 19556.

Langmead B, & Salzberg SL (2012). Fast gapped-read alignment with Bowtie 2. Nat Methods 9**:** 357-359.

Lau DC, Dhillon B, Yan H, Szmitko PE, & Verma S (2005). Adipokines: molecular links between obesity and atheroslcerosis. Am J Physiol Heart Circ Physiol 288**:** H2031-2041.

Laurencikiene J, Skurk T, Kulyte A, Heden P, Astrom G, Sjolin E*, et al.* (2011). Regulation of lipolysis in small and large fat cells of the same subject. J Clin Endocrinol Metab 96**:** E2045-2049.

Lawless MW, O'Byrne KJ, & Gray SG (2009). Oxidative stress induced lung cancer and COPD: opportunities for epigenetic therapy. J Cell Mol Med 13**:** 2800-2821.

Le Martelot G, Canella D, Symul L, Migliavacca E, Gilardi F, Liechti R*, et al.* (2012). Genome-wide RNA polymerase II profiles and RNA accumulation reveal kinetics of transcription and associated epigenetic changes during diurnal cycles. PLoS Biol 10**:** e1001442.

Leal AS, Williams CR, Royce DB, Pioli PA, Sporn MB, & Liby KT (2017). Bromodomain inhibitors, JQ1 and I-BET 762, as potential therapies for pancreatic cancer. Cancer Lett 394**:** 76-87.

Lee MG, & Pedersen PL (2003). Glucose metabolism in cancer: importance of transcription factor-DNA interactions within a short segment of the proximal region og the type II hexokinase promoter. J Biol Chem 278**:** 41047-41058.

Lee Y, Chen R, Lee HM, & Lee C (2011). Stoichiometric relationship among clock proteins determines robustness of circadian rhythms. J Biol Chem 286**:** 7033-7042.

Lee YS, Cha BY, Choi SS, Choi BK, Yonezawa T, Teruya T*, et al.* (2013). Nobiletin improves obesity and insulin resistance in high-fat diet-induced obese mice. J Nutr Biochem 24**:** 156-162.

Lefterova MI, Haakonsson AK, Lazar MA, & Mandrup S (2014). PPARgamma and the global map of adipogenesis and beyond. Trends Endocrinol Metab 25**:** 293-302.

Lefterova MI, Zhang Y, Steger DJ, Schupp M, Schug J, Cristancho A*, et al.* (2008). PPARgamma and C/EBP factors orchestrate adipocyte biology via adjacent binding on a genome-wide scale. Genes Dev 22**:** 2941-2952.

Lemon B, & Tjian R (2000). Orchestrated response: a symphony of transcription factors for gene control. Genes Dev 14**:** 2551-2569.

Lemus-Varela ML, Flores-Soto ME, Cervantes-Munguia R, Torres-Mendoza BM, Gudino-Cabrera G, Chaparro-Huerta V*, et al.* (2010). Expression of HIF-1 α, VEGF and EPO in peripheral blood from patients with two cardiac abnormalities associated with hypoxia. Clin Biochem 43**:** 234-239.

Leproult R, Holmback U, & Van Cauter E (2014). Circadian misalignment augments markers of insulin resistance and inflammation, independently of sleep loss. Diabetes 63**:** 1860-1869.

LeRoy G, Rickards B, & Flint SJ (2008). The double bromodomain proteins Brd2 and Brd3 couple histone acetylation to transcription. Mol Cell 30**:** 51-60.

Li H, Handsaker B, Wysoker A, Fennell T, Ruan J, Homer N*, et al.* (2009). The Sequence Alignment/Map format and SAMtools. Bioinformatics 25**:** 2078-2079.

Li Z, Guo J, Wu Y, & Zhou Q (2013). The BET bromodomain inhibitor JQ1 activates HIV latency through antagonizing Brd4 inhibition of Tat-transactivation. Nucleic Acids Res 41**:** 277-287.

Liao W, Nguyen MT, Yoshizaki T, Favelyukis S, Patsouris D, Imamura T*, et al.* (2007). Suppression of PPAR-gamma attenuates insulin-stimulated glucose uptake by affecting both GLUT1 and GLUT4 in 3T3-L1 adipocytes. Am J Physiol Endocrinol Metab 293**:** E219-227.

Lin SY, Black AR, Kostic D, Pajovic S, Hoover CN, & Azizkhan JC (1996). Cell cycle-regulated association of E2F1 and Sp1 is related to their functional interaction. Mol Cell Biol 16**:** 1668-1675.

Lindstrom P (2007). The physiology of obese-hyperglycemic mice [ob/ob mice]. ScientificWorldJournal 7**:** 666-685.

Linhart HG, Ishimura-Oka K, DeMayo F, Kibe T, Repka D, Poindexter B*, et al.* (2001). C/EBPα is required for differentiation of white, but not brown, adipose tissue. Proc Natl Acad Sci U S A 98**:** 12532-12537.

Lister R, Pelizzola M, Dowen RH, Hawkins RD, Hon G, Tonti-Filippini J*, et al.* (2009). Human DNA methylomes at base resolution show widespread epigenomic differences. Nature 462**:** 315-322.

Liu C, & Chung M (2015). Genetics and epigenetics of circadian rhythms and their potential roles in neuropsychiatric disorders. Neurosci Bull 31**:** 141-159.

Liu C, Li S, Liu T, Borjigin J, & Lin JD (2007). Transcriptional coactivator PGC-1α integrates the mammalian clock and energy metabolism. Nature 447**:** 477-481.

Liu L, Ji P, Qu N, Pu WL, Jiang DW, Liu WY*, et al.* (2016). The impact of high co-expression of Sp1 and HIF1α on prognosis of patients with hepatocellular cancer. Oncol Lett 12**:** 504-512.

Liu W, Ma Q, Wong K, Li W, Ohgi K, Zhang J*, et al.* (2013). Brd4 and JMJD6-associated anti-pause enhancers in regulation of transcriptional pause release. Cell 155**:** 1581-1595.

Lo KA, & Sun L (2013). Turning WAT into BAT: a review on regulators controlling the browning of white adipocytes. Biosci Rep 33.

Lochrin SE, Price DK, & Figg WD (2014). BET bromodomain inhibitors--a novel epigenetic approach in castration-resistant prostate cancer. Cancer Biol Ther 15**:** 1583-1585.

Lonn M, Mehlig K, Bengtsson C, & Lissner L (2010). Adipocyte size predicts incidence of type 2 diabetes in women. FASEB J 24**:** 326-331.

Loudni L, Roche J, Potiron V, Clarhaut J, Bachmann C, Gesson JP*, et al.* (2007). Design, synthesis and biological evaluation of 1,4-benzodiazepine-2,5-dione-based HDAC inhibitors. Bioorg Med Chem Lett 17**:** 4819-4823.

Loven J, Hoke HA, Lin CY, Lau A, Orlando DA, Vakoc CR*, et al.* (2013). Selective inhibition of tumor oncogenes by disruption of super-enhancers. Cell 153**:** 320-334.

Lu P, Qu X, Shen Y, Jiang Z, Wang P, Zeng H*, et al.* (2016). The BET inhibitor OTX015 reactivates latent HIV-1 through P-TEFb. Sci Rep 6**:** 24100.

Lu S, & Archer MC (2010). Sp1 coordinately regulates de novo lipogenesis and proliferation in cancer cells. Int J Cancer 126**:** 416-425.

Luger K, Dechassa ML, & Tremethick DJ (2012). New insights into nucleosome and chromatin structure: an ordered state or a disordered affair? Nat Rev Mol Cell Biol 13**:** 436-447.

Machado M, Marques-Vidal P, & Cortez-Pinto H (2006). Hepatic histology in obese patients undergoing bariatric surgery. J Hepatol 45**:** 600-606.

Macotela Y, Emanuelli B, Mori MA, Gesta S, Schulz TJ, Tseng YH*, et al.* (2012). Intrinsic differences in adipocyte precursor cells from different white fat depots. Diabetes 61**:** 1691-1699.

Madsen MS, Siersbaek R, Boergesen M, Nielsen R, & Mandrup S (2014). Peroxisome proliferator-activated receptor gamma and C/EBPα synergistically activate key metabolic adipocyte genes by assisted loading. Mol Cell Biol 34**:** 939-954.

Maksylewicz A, Bysiek A, Lagosz KB, Macina JM, Kantorowicz M, Bereta G*, et al.* (2019). BET Bromodomain Inhibitors Suppress Inflammatory Activation of Gingival Fibroblasts and Epithelial Cells From Periodontitis Patients. Front Immunol 10**:** 933.

Malik VS, Popkin BM, Bray GA, Despres JP, & Hu FB (2010). Sugar-sweetened beverages, obesity, type 2 diabetes mellitus, and cardiovascular disease risk. Circulation 121**:** 1356-1364.

Malmstrom R, Packard CJ, Caslake M, Bedford D, Stewart P, Yki-Jarvinen H*, et al.* (1998). Effects of insulin and acipimox on VLDL1 and VLDL2 apolipoprotein B production in normal subjects. Diabetes 47**:** 779-787.

Manoogian ENC, & Panda S (2017). Circadian rhythms, time-restricted feeding, and healthy aging. Ageing Res Rev 39**:** 59-67.

Marchesini G, Petta S, & Dalle Grave R (2016). Diet, weight loss, and liver health in nonalcoholic fatty liver disease: Pathophysiology, evidence, and practice. Hepatology 63**:** 2032-2043.

Marcheva B, Ramsey KM, Buhr ED, Kobayashi Y, Su H, Ko CH*, et al.* (2010). Disruption of the clock components CLOCK and BMAL1 leads to hypoinsulinaemia and diabetes. Nature 466**:** 627-631.

Marsin AS, Bouzin C, Bertrand L, & Hue L (2002). The stimulation of glycolysis by hypoxia in activated monocytes is mediated by AMP-activated protein kinase and inducible 6-phosphofructo-2-kinase. J Biol Chem 277**:** 30778-30783.

Martino TA, & Sole MJ (2009). Molecular time: an often overlooked dimension to cardiovascular disease. Circ Res 105**:** 1047-1061.

Masri S (2015). Sirtuin-dependent clock control: new advances in metabolism, aging and cancer. Curr Opin Clin Nutr Metab Care 18**:** 521-527.

Masri S, & Sassone-Corsi P (2010). Plasticity and specificity of the circadian epigenome. Nat Neurosci 13**:** 1324-1329.

Masri S, & Sassone-Corsi P (2013). The circadian clock: a framework linking metabolism, epigenetics and neuronal function. Nat Rev Neurosci 14**:** 69-75.

Matkovic V, Ilich JZ, Badenhop NE, Skugor M, Clairmont A, Klisovic D*, et al.* (1997). Gain in body fat is inversely related to the nocturnal rise in serum leptin level in young females. J Clin Endocrinol Metab 82**:** 1368-1372.

Matschinsky FM (1993). Evolution of the glucokinase glucose sensor paradigm for pancreatic β cells. Diabetologia 36**:** 1215-1217.

Matschinsky FM, & Wilson DF (2019). The Central Role of Glucokinase in Glucose Homeostasis: A Perspective 50 Years After Demonstrating the Presence of the Enzyme in Islets of Langerhans. Front Physiol 10**:** 148.

Mattson MP (2010). Perspective: Does brown fat protect against diseases of aging? Ageing Res Rev 9**:** 69-76.

Mazzone T, Foster D, & Chait A (1984). In vivo stimulation of low-density lipoprotein degradation by insulin. Diabetes 33**:** 333-338.

McCarthy JJ, Andrews JL, McDearmon EL, Campbell KS, Barber BK, Miller BH*, et al.* (2007). Identification of the circadian transcriptome in adult mouse skeletal muscle. Physiol Genomics 31**:** 86-95.

McDonald TJ, Colclough K, Brown R, Shields B, Shepherd M, Bingley P*, et al.* (2011). Islet autoantibodies can discriminate maturity-onset diabetes of the young (MODY) from Type 1 diabetes. Diabet Med 28**:** 1028-1033.

McGowan D, Nyanguile O, Cummings MD, Vendeville S, Vandyck K, Van den Broeck W*, et al.* (2009). 1,5-Benzodiazepine inhibitors of HCV NS5B polymerase. Bioorg Med Chem Lett 19**:** 2492-2496.

McMullan CJ, Schernhammer ES, Rimm EB, Hu FB, & Forman JP (2013). Melatonin secretion and the incidence of type 2 diabetes. JAMA 309**:** 1388-1396.

Meng QJ, Maywood ES, Bechtold DA, Lu WQ, Li J, Gibbs JE*, et al.* (2010). Entrainment of disrupted circadian behavior through inhibition of casein kinase 1 (CK1) enzymes. Proc Natl Acad Sci U S A 107**:** 15240-15245.

Meng S, Zhang L, Tang Y, Tu Q, Zheng L, Yu L*, et al.* (2014). BET Inhibitor JQ1 Blocks Inflammation and Bone Destruction. J Dent Res 93**:** 657-662.

Miard S, & Fajas L (2005). Atypical transcriptional regulators and cofactors of PPARgamma. Int J Obes (Lond) 29 Suppl 1**:** S10-12.

Miksztowicz V, Lucero D, Zago V, Cacciagiu L, Lopez G, Gonzalez Ballerga E*, et al.* (2012). Hepatic lipase activity is increased in non-alcoholic fatty liver disease beyond insulin resistance. Diabetes Metab Res Rev 28**:** 535-541.

Mikuni E, Ohoshi T, Hayashi K, & Miyamura K (1983). Glucose intolerance in an employed population. Tohoku J Exp Med 141 Suppl**:** 251-256.

Milne JC, Lambert PD, Schenk S, Carney DP, Smith JJ, Gagne DJ*, et al.* (2007). Small molecule activators of SIRT1 as therapeutics for the treatment of type 2 diabetes. Nature 450**:** 712-716.

Mirabella AC, Foster BM, & Bartke T (2016). Chromatin deregulation in disease. Chromosoma 125**:** 75-93.

Mirguet O, Gosmini R, Toum J, Clement CA, Barnathan M, Brusq JM*, et al.* (2013). Discovery of epigenetic regulator I-BET762: lead optimization to afford a clinical candidate inhibitor of the BET bromodomains. J Med Chem 56**:** 7501-7515.

Mittal V (2004). Improving the efficiency of RNA interference in mammals. Nat Rev Genet 5**:** 355-365.

Miyazaki M, Kim YC, Gray-Keller MP, Attie AD, & Ntambi JM (2000). The biosynthesis of hepatic cholesterol esters and triglycerides is impaired in mice with a disruption of the gene for stearoyl-CoA desaturase 1. J Biol Chem 275**:** 30132-30138.

Miyazaki Y, Mahankali A, Matsuda M, Mahankali S, Hardies J, Cusi K*, et al.* (2002). Effect of pioglitazone on abdominal fat distribution and insulin sensitivity in type 2 diabetic patients. J Clin Endocrinol Metab 87**:** 2784-2791.

Mogensen M, Sahlin K, Fernstrom M, Glintborg D, Vind BF, Beck-Nielsen H*, et al.* (2007). Mitochondrial respiration is decreased in skeletal muscle of patients with type 2 diabetes. Diabetes 56**:** 1592-1599.

Monteiro R, & Azevedo I (2010). Chronic inflammation in obesity and the metabolic syndrome. Mediators Inflamm 2010.

Montenegro RC, Clark PG, Howarth A, Wan X, Ceroni A, Siejka P*, et al.* (2016). BET inhibition as a new strategy for the treatment of gastric cancer. Oncotarget 7**:** 43997-44012.

Moreno-Aliaga MJ, Swarbrick MM, Lorente-Cebrian S, Stanhope KL, Havel PJ, & Martinez JA (2007). Sp1-mediated transcription is involved in the induction of leptin by insulin-stimulated glucose metabolism. J Mol Endocrinol 38**:** 537-546.

Morris CJ, Yang JN, Garcia JI, Myers S, Bozzi I, Wang W*, et al.* (2015). Endogenous circadian system and circadian misalignment impact glucose tolerance via separate mechanisms in humans. Proc Natl Acad Sci U S A 112**:** E2225-2234.

Muller JE, Stone PH, Turi ZG, Rutherford JD, Czeisler CA, Parker C*, et al.* (1985). Circadian variation in the frequency of onset of acute myocardial infarction. N Engl J Med 313**:** 1315-1322.

Myers RM, Tilly K, & Maniatis T (1986). Fine structure genetic analysis of a β-globin promoter. Science 232**:** 613-618.

Nagao A, Kobayashi M, Koyasu S, Chow CCT, & Harada H (2019). HIF-1-Dependent Reprogramming of Glucose Metabolic Pathway of Cancer Cells and Its Therapeutic Significance. Int J Mol Sci 20.

Nakahata Y, Kaluzova M, Grimaldi B, Sahar S, Hirayama J, Chen D*, et al.* (2008). The NAD+-dependent deacetylase SIRT1 modulates CLOCK-mediated chromatin remodeling and circadian control. Cell 134**:** 329-340.

Nakahata Y, Sahar S, Astarita G, Kaluzova M, & Sassone-Corsi P (2009). Circadian control of the NAD+ salvage pathway by CLOCK-SIRT1. Science 324**:** 654-657.

Nakamura TJ, Nakamura W, Yamazaki S, Kudo T, Cutler T, Colwell CS*, et al.* (2011). Age-related decline in circadian output. J Neurosci 31**:** 10201-10205.

Nakashima A, Kawamoto T, Honda KK, Ueshima T, Noshiro M, Iwata T*, et al.* (2008). DEC1 modulates the circadian phase of clock gene expression. Mol Cell Biol 28**:** 4080-4092.

Naruse Y, Oh-hashi K, Iijima N, Naruse M, Yoshioka H, & Tanaka M (2004). Circadian and light-induced transcription of clock gene Per1 depends on histone acetylation and deacetylation. Mol Cell Biol 24**:** 6278-6287.

Navale AM, & Paranjape AN (2016). Glucose transporters: physiological and pathological roles. Biophys Rev 8**:** 5-9.

Nellemann B, Gormsen LC, Sorensen LP, Christiansen JS, & Nielsen S (2012). Impaired insulin-mediated antilipolysis and lactate release in adipose tissue of upper-body obese women. Obesity (Silver Spring) 20**:** 57-64.

Nelson A, Torres DM, Morgan AE, Fincke C, & Harrison SA (2009). A pilot study using simvastatin in the treatment of nonalcoholic steatohepatitis: A randomized placebo-controlled trial. J Clin Gastroenterol 43**:** 990-994.

Nicholls SJ, Ray KK, Johansson JO, Gordon A, Sweeney M, Halliday C*, et al.* (2018). Selective BET Protein Inhibition with Apaβlone and Cardiovascular Events: A Pooled Analysis of Trials in Patients with Coronary Artery Disease. Am J Cardiovasc Drugs 18**:** 109-115.

Nicodeme E, Jeffrey KL, Schaefer U, Beinke S, Dewell S, Chung CW*, et al.* (2010). Suppression of inflammation by a synthetic histone mimic. Nature 468**:** 1119-1123.

Nissen SE, & Wolski K (2007). Effect of rosiglitazone on the risk of myocardial infarction and death from cardiovascular causes. N Engl J Med 356**:** 2457-2471.

Nobes CD, Hay WW, Jr., & Brand MD (1990). The mechanism of stimulation of respiration by fatty acids in isolated hepatocytes. J Biol Chem 265**:** 12910-12915.

Ntambi JM, Miyazaki M, Stoehr JP, Lan H, Kendziorski CM, Yandell BS*, et al.* (2002). Loss of stearoyl-CoA desaturase-1 function protects mice against adiposity. Proc Natl Acad Sci U S A 99**:** 11482-11486.

Ntranos A, & Casaccia P (2016). Bromodomains: Translating the words of lysine acetylation into myelin injury and repair. Neurosci Lett 625**:** 4-10.

Nunes-Souza V, Cesar-Gomes CJ, Da Fonseca LJ, Guedes Gda S, Smaniotto S, & Rabelo LA (2016). Aging Increases Susceptibility to High Fat Diet-Induced Metabolic Syndrome in C57BL/6 Mice: Improvement in Glycemic and Lipid Profile after Antioxidant Therapy. Oxid Med Cell Longev 2016**:** 1987960.

Nuttall FQ (2015). Body Mass Index: Obesity, BMI, and Health: A Critical Review. Nutr Today 50**:** 117-128.

Orozco-Solis R, & Sassone-Corsi P (2014). Epigenetic control and the circadian clock: linking metabolism to neuronal responses. Neuroscience 264**:** 76-87.

Ow JR, Tan YH, Jin Y, Bahirvani AG, & Taneja R (2014). Stra13 and Sharp-1, the non-grouchy regulators of development and disease. Curr Top Dev Biol 110**:** 317-338.

Page KC, Malik RE, Ripple JA, & Anday EK (2009). Maternal and postweaning diet interaction alters hypothalamic gene expression and modulates response to a high-fat diet in male offspring. Am J Physiol Regul Integr Comp Physiol 297**:** R1049-1057.

Palumbo S, Mariotti V, Iofrida C, & Pellegrini S (2018). Genes and Aggressive Behavior: Epigenetic Mechanisms Underlying Individual Susceptibility to Aversive Environments. Front Behav Neurosci 12**:** 117.

Panda S, Antoch MP, Miller BH, Su AI, Schook AB, Straume M*, et al.* (2002). Coordinated transcription of key pathways in the mouse by the circadian clock. Cell 109**:** 307-320.

Park M, Upton D, Blackmon M, Dixon V, Craver S, Neal D*, et al.* (2018). Anacardic acid inhibits pancreatic cancer cell growth, and potentiates chemotherapeutic effect by Chmp1A - ATM - p53 signaling pathway. BMC Complement Altern Med 18**:** 71.

Paschos GK, Ibrahim S, Song WL, Kunieda T, Grant G, Reyes TM*, et al.* (2012). Obesity in mice with adipocyte-specific deletion of clock component Arntl. Nat Med 18**:** 1768-1777.

Pastore N, Vainshtein A, Herz NJ, Huynh T, Brunetti L, Klisch TJ*, et al.* (2019). Nutrient-sensitive transcription factors TFEB and TFE3 couple autophagy and metabolism to the peripheral clock. EMBO J 38.

Pastori C, Daniel M, Penas C, Volmar CH, Johnstone AL, Brothers SP*, et al.* (2014). BET bromodomain proteins are required for glioblastoma cell proliferation. Epigenetics 9**:** 611-620.

Patel JH, Du Y, Ard PG, Phillips C, Carella B, Chen CJ*, et al.* (2004). The c-MYC oncoprotein is a substrate of the acetyltransferases hGCN5/PCAF and TIP60. Mol Cell Biol 24**:** 10826-10834.

Pathak S, Stewart WCL, Burd CE, Hester ME, & Greenberg DA (2020). Brd2 haploinsufficiency extends lifespan and healthspan in C57B6/J mice. PLoS One 15**:** e0234910.

Patterson CC, Dahlquist GG, Gyurus E, Green A, Soltesz G, & Group ES (2009). Incidence trends for childhood type 1 diabetes in Europe during 1989-2003 and predicted new cases 2005-20: a multicentre prospective registration study. Lancet 373**:** 2027-2033.

Pazin MJ, Kamakaka RT, & Kadonaga JT (1994). ATP-dependent nucleosome reconfiguration and transcriptional activation from preassembled chromatin templates. Science 266**:** 2007-2011.

Pecqueur C, Bui T, Gelly C, Hauchard J, Barbot C, Bouillaud F*, et al.* (2008). Uncoupling protein-2 controls proliferation by promoting fatty acid oxidation and limiting glycolysis-derived pyruvate utilization. FASEB J 22**:** 9-18.

Peek CB, Levine DC, Cedernaes J, Taguchi A, Kobayashi Y, Tsai SJ*, et al.* (2017). Circadian Clock Interaction with HIF1α Mediates Oxygenic Metabolism and Anaerobic Glycolysis in Skeletal Muscle. Cell Metab 25**:** 86-92.

Peirson SN, Butler JN, & Foster RG (2003). Experimental validation of novel and conventional approaches to quantitative real-time PCR data analysis. Nucleic Acids Res 31**:** e73.

Pengelley ET, Asmundson SJ, Aloia RC, & Barnes B (1976). Circannual rhythmicity in a non-hibernating ground squirrel, Citellus leucurus. Comp Biochem Physiol A Comp Physiol 54**:** 233-237.

Perelis M, Marcheva B, Ramsey KM, Schipma MJ, Hutchison AL, Taguchi A*, et al.* (2015). Pancreatic β cell enhancers regulate rhythmic transcription of genes controlling insulin secretion. Science 350**:** aac4250.

Perry RJ, Wang Y, Cline GW, Rabin-Court A, Song JD, Dufour S*, et al.* (2018). Leptin Mediates a Glucose-Fatty Acid Cycle to Maintain Glucose Homeostasis in Starvation. Cell 172**:** 234-248 e217.

Peschke E, & Peschke D (1998). Evidence for a circadian rhythm of insulin release from perifused rat pancreatic islets. Diabetologia 41**:** 1085-1092.

Petkau N, Budak H, Zhou X, Oster H, & Eichele G (2019). Acetylation of BMAL1 by TIP60 controls BRD4-P-TEFb recruitment to circadian promoters. Elife 8.

Petrenko V, Gandasi NR, Sage D, Tengholm A, Barg S, & Dibner C (2020). In pancreatic islets from type 2 diabetes patients, the dampened circadian oscillators lead to reduced insulin and glucagon exocytosis. Proc Natl Acad Sci U S A 117**:** 2484-2495.

Picard F, Kurtev M, Chung N, Topark-Ngarm A, Senawong T, Machado De Oliveira R*, et al.* (2004). Sirt1 promotes fat mobilization in white adipocytes by repressing PPAR-gamma. Nature 429**:** 771-776.

Picaud S, Wells C, Felletar I, Brotherton D, Martin S, Savitsky P*, et al.* (2013). RVX-208, an inhibitor of BET transcriptional regulators with selectivity for the second bromodomain. Proc Natl Acad Sci U S A 110**:** 19754-19759.

Piha-Paul SA, Hann CL, French CA, Cousin S, Brana I, Cassier PA*, et al.* (2020). Phase 1 Study of Molibresib (GSK525762), a Bromodomain and Extra-Terminal Domain Protein Inhibitor, in NUT Carcinoma and Other Solid Tumors. JNCI Cancer Spectr 4**:** pkz093.

Plagemann A, Harder T, Kohlhoff R, Rohde W, & Dorner G (1997). Overweight and obesity in infants of mothers with long-term insulin-dependent diabetes or gestational diabetes. Int J Obes Relat Metab Disord 21**:** 451-456.

Polonsky KS, Given BD, Hirsch LJ, Tillil H, Shapiro ET, Beebe C*, et al.* (1988). Abnormal patterns of insulin secretion in non-insulin-dependent diabetes mellitus. N Engl J Med 318**:** 1231-1239.

Pontoglio M, Sreenan S, Roe M, Pugh W, Ostrega D, Doyen A*, et al.* (1998). Defective insulin secretion in hepatocyte nuclear factor 1α-deficient mice. J Clin Invest 101**:** 2215-2222.

Prinjha RK, Witherington J, & Lee K (2012). Place your BETs: the therapeutic potential of bromodomains. Trends Pharmacol Sci 33**:** 146-153.

Pulivarthy SR, Tanaka N, Welsh DK, De Haro L, Verma IM, & Panda S (2007). Reciprocity between phase shifts and amplitude changes in the mammalian circadian clock. Proc Natl Acad Sci U S A 104**:** 20356-20361.

Qatanani M, & Lazar MA (2007). Mechanisms of obesity-associated insulin resistance: many choices on the menu. Genes Dev 21**:** 1443-1455.

Qatanani M, Szwergold NR, Greaves DR, Ahima RS, & Lazar MA (2009). Macrophage-derived human resistin exacerbates adipose tissue inflammation and insulin resistance in mice. J Clin Invest 119**:** 531-539.

Ragab SM, Abd Elghaffar S, El-Metwally TH, Badr G, Mahmoud MH, & Omar HM (2015). Effect of a high fat, high sucrose diet on the promotion of non-alcoholic fatty liver disease in male rats: the ameliorative role of three natural compounds. Lipids Health Dis 14**:** 83.

Rahman S, Sowa ME, Ottinger M, Smith JA, Shi Y, Harper JW*, et al.* (2011). The Brd4 extraterminal domain confers transcription activation independent of pTEFb by recruiting multiple proteins, including NSD3. Mol Cell Biol 31**:** 2641-2652.

Rahman SM, Dobrzyn A, Dobrzyn P, Lee SH, Miyazaki M, & Ntambi JM (2003). Stearoyl-CoA desaturase 1 deficiency elevates insulin-signaling components and down-regulates protein-tyrosine phosphatase 1B in muscle. Proc Natl Acad Sci U S A 100**:** 11110-11115.

Ramsey KM, Yoshino J, Brace CS, Abrassart D, Kobayashi Y, Marcheva B*, et al.* (2009). Circadian clock feedback cycle through NAMPT-mediated NAD+ biosynthesis. Science 324**:** 651-654.

Reed BC, & Lane MD (1980). Insulin receptor synthesis and turnover in differentiating 3T3-L1 preadipocytes. Proc Natl Acad Sci U S A 77**:** 285-289.

Regazzetti C, Peraldi P, Gremeaux T, Najem-Lendom R, Ben-Sahra I, Cormont M*, et al.* (2009). Hypoxia decreases insulin signaling pathways in adipocytes. Diabetes 58**:** 95-103.

Reid TS, & Beese LS (2004). Crystal structures of the anticancer clinical candidates R115777 (Tipifarnib) and BMS-214662 complexed with protein farnesyltransferase suggest a mechanism of FTI selectivity. Biochemistry 43**:** 6877-6884.

Ren K, Zhang W, Chen X, Ma Y, Dai Y, Fan Y*, et al.* (2016). An Epigenetic Compound Library Screen Identifies BET Inhibitors That Promote HSV-1 and -2 Replication by Bridging P-TEFb to Viral Gene Promoters through BRD4. PLoS Pathog 12**:** e1005950.

Reppert SM, & Weaver DR (2002). Coordination of circadian timing in mammals. Nature 418**:** 935-941.

Rey G, Cesbron F, Rougemont J, Reinke H, Brunner M, & Naef F (2011). Genome-wide and phase-specific DNA-binding rhythms of BMAL1 control circadian output functions in mouse liver. PLoS Biol 9**:** e1000595.

Reynolds TH, Dalton A, Calzini L, Tuluca A, Hoyte D, & Ives SJ (2019). The impact of age and sex on body composition and glucose sensitivity in C57BL/6J mice. Physiol Rep 7**:** e13995.

Richter L, de Graaf C, Sieghart W, Varagic Z, Morzinger M, de Esch IJ*, et al.* (2012). Diazepam-bound GABAA receptor models identify new benzodiazepine binding-site ligands. Nat Chem Biol 8**:** 455-464.

Riemersma-van der Lek RF, Swaab DF, Twisk J, Hol EM, Hoogendijk WJ, & Van Someren EJ (2008). Effect of bright light and melatonin on cognitive and noncognitive function in elderly residents of group care facilities: a randomized controlled trial. JAMA 299**:** 2642-2655.

Ripperger JA, & Schibler U (2006). Rhythmic CLOCK-BMAL1 binding to multiple E-box motifs drives circadian Dbp transcription and chromatin transitions. Nat Genet 38**:** 369-374.

Riserus U, Willett WC, & Hu FB (2009). Dietary fats and prevention of type 2 diabetes. Prog Lipid Res 48**:** 44-51.

Roberts TC, Etxaniz U, Dall'Agnese A, Wu SY, Chiang CM, Brennan PE*, et al.* (2017). BRD3 and BRD4 BET Bromodomain Proteins Differentially Regulate Skeletal Myogenesis. Sci Rep 7**:** 6153.

Robson-Doucette CA, Sultan S, Allister EM, Wikstrom JD, Koshkin V, Bhattacharjee A*, et al.* (2011). B-cell uncoupling protein 2 regulates reactive oxygen species production, which influences both insulin and glucagon secretion. Diabetes 60**:** 2710-2719.

Rocchini AP, Marker P, & Cervenka T (1997). Time course of insulin resistance associated with feeding dogs a high-fat diet. Am J Physiol 272**:** E147-154.

Rodnick KJ, Holloszy JO, Mondon CE, & James DE (1990). Effects of exercise training on insulin-regulatable glucose-transporter protein levels in rat skeletal muscle. Diabetes 39**:** 1425-1429.

Roeder RG (1996). The role of general initiation factors in transcription by RNA polymerase II. Trends Biochem Sci 21**:** 327-335.

Roenneberg T, Allebrandt KV, Merrow M, & Vetter C (2012). Social jetlag and obesity. Curr Biol 22**:** 939-943.

Roy D, Farabaugh KT, Wu J, Charrier A, Smas C, Hatzoglou M*, et al.* (2017). Coordinated transcriptional control of adipocyte triglyceride lipase (Atgl) by transcription factors Sp1 and peroxisome proliferator-

activated receptor gamma (PPARgamma) during adipocyte differentiation. J Biol Chem 292**:** 14827-14835.

Rucker D, Padwal R, Li SK, Curioni C, & Lau DC (2007). Long term pharmacotherapy for obesity and overweight: updated meta-analysis. BMJ 335**:** 1194-1199.

Ruotolo G, Parlavecchia M, Taskinen MR, Galimberti G, Zoppo A, Le NA*, et al.* (1994). Normalization of lipoprotein composition by intraperitoneal insulin in IDDM. Role of increased hepatic lipase activity. Diabetes Care 17**:** 6-12.

Rutter J, Reick M, Wu LC, & McKnight SL (2001). Regulation of clock and NPAS2 DNA binding by the redox state of NAD cofactors. Science 293**:** 510-514.

Sabater D, Arriaran S, Romero Mdel M, Agnelli S, Remesar X, Fernandez-Lopez JA*, et al.* (2014). Cultured 3T3L1 adipocytes dispose of excess medium glucose as lactate under abundant oxygen availability. Sci Rep 4**:** 3663.

Saeedi P, Petersohn I, Salpea P, Malanda B, Karuranga S, Unwin N*, et al.* (2019). Global and regional diabetes prevalence estimates for 2019 and projections for 2030 and 2045: Results from the International Diabetes Federation Diabetes Atlas, 9(th) edition. Diabetes Res Clin Pract 157**:** 107843.

Sahar S, & Sassone-Corsi P (2013). The epigenetic language of circadian clocks. Handb Exp Pharmacol**:** 29-44.

Saini C, Petrenko V, Pulimeno P, Giovannoni L, Berney T, Hebrok M*, et al.* (2016). A functional circadian clock is required for proper insulin secretion by human pancreatic islet cells. Diabetes, Obesity and Metabolism 18**:** 355-365.

Sakuraba K, Yokomizo K, Shirahata A, Goto T, Saito M, Ishibashi K*, et al.* (2011). TIP60 as a potential marker for the malignancy of gastric cancer. Anticancer Res 31**:** 77-79.

Salma N, Song JS, Kawakami A, Devi SP, Khaled M, Cacicedo JM*, et al.* (2017). Tfe3 and Tfeb Transcriptionally Regulate Peroxisome Proliferator-Activated Receptor gamma2 Expression in Adipocytes and Mediate Adiponectin and Glucose Levels in Mice. Mol Cell Biol 37.

Sancar G, & Brunner M (2014). Circadian clocks and energy metabolism. Cell Mol Life Sci 71**:** 2667-2680.

Sanghani HR, Jagannath A, Humberstone T, Ebrahimjee F, Thomas JM, Churchill GC*, et al.* (2020). Patient fibroblast circadian rhythms predict lithium sensitivity in bipolar disorder. Mol Psychiatry.

Sanusi I, Sarnowski A, Russell-Jones D, & Forni LG (2020). A potential diagnostic problem on the ICU: Euglycaemic diabetic Ketoacidosis associated with SGLT2 inhibition. J Crit Care 57**:** 19-22.

Schafer D, Hamm-Kunzelmann B, & Brand K (1997). Glucose regulates the promoter activity of aldolase A and pyruvate kinase M2 via dephosphorylation of Sp1. FEBS Lett 417**:** 325-328.

Scheer FA, Hilton MF, Mantzoros CS, & Shea SA (2009). Adverse metabolic and cardiovascular consequences of circadian misalignment. Proc Natl Acad Sci U S A 106**:** 4453-4458.

Schibler U, & Sassone-Corsi P (2002). A web of circadian pacemakers. Cell 111**:** 919-922.

Schmitz G, & Langmann T (2005). Transcriptional regulatory networks in lipid metabolism control ABCA1 expression. Biochim Biophys Acta 1735**:** 1-19.

Schoeman D, & Fielding BC (2019). Coronavirus envelope protein: current knowledge. Virol J 16**:** 69.

Schulz D, Mugnier MR, Paulsen EM, Kim HS, Chung CW, Tough DF*, et al.* (2015). Bromodomain Proteins Contribute to Maintenance of Bloodstream Form Stage Identity in the African Trypanosome. PLoS Biol 13**:** e1002316.

Schwartz JP, & Jungas RL (1971). Studies on the hormone-sensitive lipase of adipose tissue. J Lipid Res 12**:** 553-562.

Schweiger M, Eichmann TO, Taschler U, Zimmermann R, Zechner R, & Lass A (2014). Measurement of lipolysis. Methods Enzymol 538**:** 171-193.

Schweizer M, Roder K, Zhang L, & Wolf SS (2002). Transcription factors acting on the promoter of the rat fatty acid synthase gene. Biochem Soc Trans 30**:** 1070-1072.

Sei H, Oishi K, Chikahisa S, Kitaoka K, Takeda E, & Ishida N (2008). Diurnal amplitudes of arterial pressure and heart rate are dampened in Clock mutant mice and adrenalectomized mice. Endocrinology 149**:** 3576-3580.

Seisenberger S, Peat JR, Hore TA, Santos F, Dean W, & Reik W (2013). Reprogramming DNA methylation in the mammalian life cycle: building and breaking epigenetic barriers. Philos Trans R Soc Lond B Biol Sci 368**:** 20110330.

Semenza GL (2003). Targeting HIF-1 for cancer therapy. Nat Rev Cancer 3**:** 721-732.

Semenza GL (2011). Regulation of metabolism by hypoxia-inducible factor 1. Cold Spring Harb Symp Quant Biol 76**:** 347-353.

Semenza GL, Jiang BH, Leung SW, Passantino R, Concordet JP, Maire P*, et al.* (1996). Hypoxia response elements in the aldolase A, enolase 1, and lactate dehydrogenase A gene promoters contain essential binding sites for hypoxia-inducible factor 1. J Biol Chem 271**:** 32529-32537.

Shang E, Nickerson HD, Wen D, Wang X, & Wolgemuth DJ (2007). The first bromodomain of Brdt, a testis-specific member of the BET sub-family of double-bromodomain-containing proteins, is essential for male germ cell differentiation. Development 134**:** 3507-3515.

Shang E, Wang X, Wen D, Greenberg DA, & Wolgemuth DJ (2009). Double bromodomain-containing gene Brd2 is essential for embryonic development in mouse. Dev Dyn 238**:** 908-917.

Sharma A, Laurenti MC, Dalla Man C, Varghese RT, Cobelli C, Rizza RA*, et al.* (2017). Glucose metabolism during rotational shift-work in healthcare workers. Diabetologia 60**:** 1483-1490.

Sharov VG, Todor AV, Silverman N, Goldstein S, & Sabbah HN (2000). Abnormal mitochondrial respiration in failed human myocardium. J Mol Cell Cardiol 32**:** 2361-2367.

Sharp FR, & Bernaudin M (2004). HIF1 and oxygen sensing in the brain. Nat Rev Neurosci 5**:** 437-448.

Shaw JE, Sicree RA, & Zimmet PZ (2010). Global estimates of the prevalence of diabetes for 2010 and 2030. Diabetes Res Clin Pract 87**:** 4-14.

Shepherd M, Ellis I, Ahmad AM, Todd PJ, Bowen-Jones D, Mannion G*, et al.* (2001). Predictive genetic testing in maturity-onset diabetes of the young (MODY). Diabet Med 18**:** 417-421.

Shi J, & Vakoc CR (2014). The mechanisms behind the therapeutic activity of BET bromodomain inhibition. Mol Cell 54**:** 728-736.

Shi Y, Lan F, Matson C, Mulligan P, Whetstine JR, Cole PA*, et al.* (2004). Histone demethylation mediated by the nuclear amine oxidase homolog LSD1. Cell 119**:** 941-953.

Shields BM, Hicks S, Shepherd MH, Colclough K, Hattersley AT, & Ellard S (2010). Maturity-onset diabetes of the young (MODY): how many cases are we missing? Diabetologia 53**:** 2504-2508.

Shimamura T, Chen Z, Soucheray M, Carretero J, Kikuchi E, Tchaicha JH*, et al.* (2013). Efficacy of BET bromodomain inhibition in Kras-mutant non-small cell lung cancer. Clin Cancer Res 19**:** 6183-6192.

Showalter MR, Nonnecke EB, Linderholm AL, Cajka T, Sa MR, Lonnerdal B*, et al.* (2018). Obesogenic diets alter metabolism in mice. PLoS One 13**:** e0190632.

Siebel AL, Trinh SK, Formosa MF, Mundra PA, Natoli AK, Reddy-Luthmoodoo M*, et al.* (2016). Effects of the BET-inhibitor, RVX-208 on the HDL lipidome and glucose metabolism in individuals with prediabetes: A randomized controlled trial. Metabolism 65**:** 904-914.

Sinha A, Faller DV, & Denis GV (2005). Bromodomain analysis of Brd2-dependent transcriptional activation of cyclin A. Biochem J 387**:** 257-269.

Sinha MK, Ohannesian JP, Heiman ML, Kriauciunas A, Stephens TW, Magosin S*, et al.* (1996). Nocturnal rise of leptin in lean, obese, and non-insulin-dependent diabetes mellitus subjects. J Clin Invest 97**:** 1344-1347.

Sinturel F, Makhlouf AM, Meyer P, Tran C, Pataky Z, Golay A*, et al.* (2019). Cellular circadian period length inversely correlates with HbA1c levels in individuals with type 2 diabetes. Diabetologia 62**:** 1453-1462.

Skurk T, Alberti-Huber C, Herder C, & Hauner H (2007). Relationship between adipocyte size and adipokine expression and secretion. J Clin Endocrinol Metab 92**:** 1023-1033.

Sohail S, Yu L, Bennett DA, Buchman AS, & Lim AS (2015). Irregular 24-hour activity rhythms and the metabolic syndrome in older adults. Chronobiol Int 32**:** 802-813.

Sohal RS, Ku HH, Agarwal S, Forster MJ, & Lal H (1994). Oxidative damage, mitochondrial oxidant generation and antioxidant defenses during aging and in response to food restriction in the mouse. Mech Ageing Dev 74**:** 121-133.

Sonksen P, & Sonksen J (2000). Insulin: understanding its action in health and disease. Br J Anaesth 85**:** 69-79.

Soto N, Bazaes RA, Pena V, Salazar T, Avila A, Iniguez G*, et al.* (2003). Insulin sensitivity and secretion are related to catch-up growth in small-for-gestational-age infants at age 1 year: results from a prospective cohort. J Clin Endocrinol Metab 88**:** 3645-3650.

Soubannier V, & McBride HM (2009). Positioning mitochondrial plasticity within cellular signaling cascades. Biochim Biophys Acta 1793**:** 154-170.

Stewart HJ, Horne GA, Bastow S, & Chevassut TJ (2013). BRD4 associates with p53 in DNMT3A-mutated leukemia cells and is implicated in apoptosis by the bromodomain inhibitor JQ1. Cancer Med 2**:** 826-835.

Stonestrom AJ, Hsu SC, Jahn KS, Huang P, Keller CA, Giardine BM*, et al.* (2015). Functions of BET proteins in erythroid gene expression. Blood 125**:** 2825-2834.

Stride A, Vaxillaire M, Tuomi T, Barbetti F, Njolstad PR, Hansen T*, et al.* (2002). The genetic abnormality in the β cell determines the response to an oral glucose load. Diabetologia 45**:** 427-435.

Stygar D, Skrzep-Poloczek B, Romuk E, Chelmecka E, Poloczek J, Sawczyn T*, et al.* (2019). The influence of high-fat, high-sugar diet and bariatric surgery on HSP70 and HSP90 plasma and liver concentrations in diet-induced obese rats. Cell Stress Chaperones 24**:** 427-439.

Surwit RS, Kuhn CM, Cochrane C, McCubbin JA, & Feinglos MN (1988). Diet-induced type II diabetes in C57BL/6J mice. Diabetes 37**:** 1163-1167.

Suwazono Y, Dochi M, Oishi M, Tanaka K, Kobayashi E, & Sakata K (2009). Shiftwork and impaired glucose metabolism: a 14-year cohort study on 7104 male workers. Chronobiol Int 26**:** 926-941.

Swierczynski J, Slominska E, Smolenski RT, & Mayer D (2001). Increase in NAD but not ATP and GTP concentrations in rat liver by dehydroepiandrosterone feeding. Pol J Pharmacol 53**:** 125-130.

Takahashi JS (2017). Transcriptional architecture of the mammalian circadian clock. Nat Rev Genet 18**:** 164-179.

Tamai TK, Nakane Y, Ota W, Kobayashi A, Ishiguro M, Kadofusa N*, et al.* (2018). Identification of circadian clock modulators from existing drugs. EMBO Mol Med 10.

Tan NY, & Khachigian LM (2009). Sp1 phosphorylation and its regulation of gene transcription. Mol Cell Biol 29**:** 2483-2488.

Tanaka T, Yoshida N, Kishimoto T, & Akira S (1997). Defective adipocyte differentiation in mice lacking the C/EBPβ and/or C/EBPdelta gene. EMBO J 16**:** 7432-7443.

Tang W, Zeve D, Suh JM, Bosnakovski D, Kyba M, Hammer RE*, et al.* (2008). White fat progenitor cells reside in the adipose vasculature. Science 322**:** 583-586.

Tarnowski BI, Spinale FG, & Nicholson JH (1991). DAPI as a useful stain for nuclear quantitation. Biotech Histochem 66**:** 297-302.

Tek C (2016). Naltrexone HCI/bupropion HCI for chronic weight management in obese adults: patient selection and perspectives. Patient Prefer Adherence 10**:** 751-759.

Thiebaud D, Jacot E, DeFronzo RA, Maeder E, Jequier E, & Felber JP (1982). The effect of graded doses of insulin on total glucose uptake, glucose oxidation, and glucose storage in man. Diabetes 31**:** 957-963.

Thorens B, Weir GC, Leahy JL, Lodish HF, & Bonner-Weir S (1990). Reduced expression of the liver/β-cell glucose transporter isoform in glucose-insensitive pancreatic β cells of diabetic rats. Proc Natl Acad Sci U S A 87**:** 6492-6496.

Tilly-Kiesi M, Schaefer EJ, Knudsen P, Welty FK, Dolnikowski GG, Taskinen MR*, et al.* (2004). Lipoprotein metabolism in subjects with hepatic lipase deficiency. Metabolism 53**:** 520-525.

Timmermann S, Lehrmann H, Polesskaya A, & Harel-Bellan A (2001). Histone acetylation and disease. Cell Mol Life Sci 58**:** 728-736.

Tomaru T, Steger DJ, Lefterova MI, Schupp M, & Lazar MA (2009). Adipocyte-specific expression of murine resistin is mediated by synergism between peroxisome proliferator-activated receptor gamma and CCAAT/enhancer-binding proteins. J Biol Chem 284**:** 6116-6125.

Tong Q, Dalgin G, Xu H, Ting CN, Leiden JM, & Hotamisligil GS (2000). Function of GATA transcription factors in preadipocyte-adipocyte transition. Science 290**:** 134-138.

Tontonoz P, Hu E, & Spiegelman BM (1994). Stimulation of adipogenesis in fibroblasts by PPAR gamma 2, a lipid-activated transcription factor. Cell 79**:** 1147-1156.

Tough DF, Tak PP, Tarakhovsky A, & Prinjha RK (2016). Epigenetic drug discovery: breaking through the immune barrier. Nat Rev Drug Discov 15**:** 835-853.

Tran TT, Yamamoto Y, Gesta S, & Kahn CR (2008). Beneficial effects of subcutaneous fat transplantation on metabolism. Cell Metab 7**:** 410-420.

Tremmel M, Gerdtham UG, Nilsson PM, & Saha S (2017). Economic Burden of Obesity: A Systematic Literature Review. Int J Environ Res Public Health 14.

Trinklein ND, Aldred SJ, Saldanha AJ, & Myers RM (2003). Identification and functional analysis of human transcriptional promoters. Genome Res 13**:** 308-312.

Tsai PF, Lin SJ, Weng PL, Tsai SC, Lin JH, Chou YC*, et al.* (2011). Interplay between PKCdelta and Sp1 on histone deacetylase inhibitor-mediated Epstein-Barr virus reactivation. J Virol 85**:** 2373-2385.

Tsuchida A, Yamauchi T, Takekawa S, Hada Y, Ito Y, Maki T*, et al.* (2005). Peroxisome proliferator-activated receptor (PPAR)α activation increases adiponectin receptors and reduces obesity-related inflammation in adipose tissue: comparison of activation of PPARα, PPARgamma, and their combination. Diabetes 54**:** 3358-3370.

Tsujikawa LM, Fu L, Das S, Halliday C, Rakai BD, Stotz SC*, et al.* (2019). Apaβlone (RVX-208) reduces vascular inflammation in vitro and in CVD patients by a BET-dependent epigenetic mechanism. Clin Epigenetics 11**:** 102.

Tsume M, Kimura-Yoshida C, Mochida K, Shibukawa Y, Amazaki S, Wada Y*, et al.* (2012). Brd2 is required for cell cycle exit and neuronal differentiation through the E2F1 pathway in mouse neuroepithelial cells. Biochem Biophys Res Commun 425**:** 762-768.

Turek FW, Joshu C, Kohsaka A, Lin E, Ivanova G, McDearmon E*, et al.* (2005). Obesity and metabolic syndrome in circadian Clock mutant mice. Science 308**:** 1043-1045.

Turner BM (2000). Histone acetylation and an epigenetic code. Bioessays 22**:** 836-845.

Ulinski T, Lescure S, Beaufils S, Guigonis V, Decramer S, Morin D*, et al.* (2006). Renal phenotypes related to hepatocyte nuclear factor-1β (TCF2) mutations in a pediatric cohort. J Am Soc Nephrol 17**:** 497-503.

Um JH, Yang S, Yamazaki S, Kang H, Viollet B, Foretz M*, et al.* (2007). Activation of 5'-AMP-activated kinase with diabetes drug metformin induces casein kinase Iepsilon (CKIepsilon)-dependent degradation of clock protein mPer2. J Biol Chem 282**:** 20794-20798.

Van Cauter E, Leproult R, & Kupfer DJ (1996). Effects of gender and age on the levels and circadian rhythmicity of plasma cortisol. J Clin Endocrinol Metab 81**:** 2468-2473.

Van Den Broeck A, Nissou D, Brambilla E, Eymin B, & Gazzeri S (2012). Activation of a Tip60/E2F1/ERCC1 network in human lung adenocarcinoma cells exposed to cisplatin. Carcinogenesis 33**:** 320-325.

Van Herck MA, Vonghia L, & Francque SM (2017). Animal Models of Nonalcoholic Fatty Liver Disease-A Starter's Guide. Nutrients 9.

van Marken Lichtenbelt WD, Vanhommerig JW, Smulders NM, Drossaerts JM, Kemerink GJ, Bouvy ND*, et al.* (2009). Cold-activated brown adipose tissue in healthy men. N Engl J Med 360**:** 1500-1508.

Vazquez R, Riveiro ME, Astorgues-Xerri L, Odore E, Rezai K, Erba E*, et al.* (2017). The bromodomain inhibitor OTX015 (MK-8628) exerts anti-tumor activity in triple-negative breast cancer models as single agent and in combination with everolimus. Oncotarget 8**:** 7598-7613.

Venkataraman S, Alimova I, Balakrishnan I, Harris P, Birks DK, Griesinger A*, et al.* (2014). Inhibition of BRD4 attenuates tumor cell self-renewal and suppresses stem cell signaling in MYC driven medulloblastoma. Oncotarget 5**:** 2355-2371.

Verboven K, Wouters K, Gaens K, Hansen D, Bijnen M, Wetzels S*, et al.* (2018). Abdominal subcutaneous and visceral adipocyte size, lipolysis and inflammation relate to insulin resistance in male obese humans. Sci Rep 8**:** 4677.

Virtanen KA, Lidell ME, Orava J, Heglind M, Westergren R, Niemi T*, et al.* (2009). Functional brown adipose tissue in healthy adults. N Engl J Med 360**:** 1518-1525.

Virtue S, & Vidal-Puig A (2011). Nothing Iffy about HIF in the Hypothalamus. PLoS Biol 9**:** e1001116.

Vitaterna MH, Ko CH, Chang AM, Buhr ED, Fruechte EM, Schook A*, et al.* (2006). The mouse Clock mutation reduces circadian pacemaker amplitude and enhances efficacy of resetting stimuli and phase-response curve amplitude. Proc Natl Acad Sci U S A 103**:** 9327-9332.

Vollmers C, Gill S, DiTacchio L, Pulivarthy SR, Le HD, & Panda S (2009). Time of feeding and the intrinsic circadian clock drive rhythms in hepatic gene expression. Proc Natl Acad Sci U S A 106**:** 21453-21458.

Vologodskii A, & Cozzarelli NR (1996). Effect of supercoiling on the juxtaposition and relative orientation of DNA sites. Biophys J 70**:** 2548-2556.

Wang B, Chandrasekera PC, & Pippin JJ (2014). Leptin- and leptin receptor-deficient rodent models: relevance for human type 2 diabetes. Curr Diabetes Rev 10**:** 131-145.

Wang CY, & Liao JK (2012). A mouse model of diet-induced obesity and insulin resistance. Methods Mol Biol 821**:** 421-433.

Wang F, Liu H, Blanton WP, Belkina A, Lebrasseur NK, & Denis GV (2009a). Brd2 disruption in mice causes severe obesity without Type 2 diabetes. Biochem J 425**:** 71-83.

Wang GL, Jiang BH, Rue EA, & Semenza GL (1995). Hypoxia-inducible factor 1 is a basic-helix-loop-helix-PAS heterodimer regulated by cellular O2 tension. Proc Natl Acad Sci U S A 92**:** 5510-5514.

Wang GL, & Semenza GL (1995). Purification and characterization of hypoxia-inducible factor 1. J Biol Chem 270**:** 1230-1237.

Wang H, Maechler P, Hagenfeldt KA, & Wollheim CB (1998). Dominant-negative suppression of HNF-1α function results in defective insulin gene transcription and impaired metabolism-secretion coupling in a pancreatic β-cell line. EMBO J 17**:** 6701-6713.

Wang J, Li GL, Ming SL, Wang CF, Shi LJ, Su BQ*, et al.* (2020). BRD4 inhibition exerts anti-viral activity through DNA damage-dependent innate immune responses. PLoS Pathog 16**:** e1008429.

Wang QA, Tao C, Gupta RK, & Scherer PE (2013). Tracking adipogenesis during white adipose tissue development, expansion and regeneration. Nat Med 19**:** 1338-1344.

Wang RH, Zhao T, Cui K, Hu G, Chen Q, Chen W*, et al.* (2016). Negative reciprocal regulation between Sirt1 and Per2 modulates the circadian clock and aging. Sci Rep 6**:** 28633.

Wang Y, Nishina PM, & Naggert JK (2009b). Degradation of IRS1 leads to impaired glucose uptake in adipose tissue of the type 2 diabetes mouse model TALLYHO/Jng. J Endocrinol 203**:** 65-74.

Wasserman DH, Kang L, Ayala JE, Fueger PT, & Lee-Young RS (2011). The physiological regulation of glucose flux into muscle in vivo. J Exp Biol 214**:** 254-262.

Waterland RA, Travisano M, Tahiliani KG, Rached MT, & Mirza S (2008). Methyl donor supplementation prevents transgenerational amplification of obesity. Int J Obes (Lond) 32**:** 1373-1379.

Waters KM, & Ntambi JM (1994). Insulin and dietary fructose induce stearoyl-CoA desaturase 1 gene expression of diabetic mice. J Biol Chem 269**:** 27773-27777.

Watts AG, & Donovan CM (2010). Sweet talk in the brain: glucosensing, neural networks, and hypoglycemic counterregulation. Front Neuroendocrinol 31**:** 32-43.

Weaver DR (1998). The suprachiasmatic nucleus: a 25-year retrospective. J Biol Rhythms 13**:** 100-112.

Wehrli NE, Bural G, Houseni M, Alkhawaldeh K, Alavi A, & Torigian DA (2007). Determination of age-related changes in structure and function of skin, adipose tissue, and skeletal muscle with computed tomography, magnetic resonance imaging, and positron emission tomography. Semin Nucl Med 37**:** 195-205.

Whitfield TW, Wang J, Collins PJ, Partridge EC, Aldred SF, Trinklein ND*, et al.* (2012). Functional analysis of transcription factor binding sites in human promoters. Genome Biol 13**:** R50.

Wierstra I (2008). Sp1: emerging roles--beyond constitutive activation of TATA-less housekeeping genes. Biochem Biophys Res Commun 372**:** 1-13.

Wilding JP (2007). The importance of free fatty acids in the development of Type 2 diabetes. Diabet Med 24**:** 934-945.

Wilsey J, & Scarpace PJ (2004). Caloric restriction reverses the deficits in leptin receptor protein and leptin signaling capacity associated with diet-induced obesity: role of leptin in the regulation of hypothalamic long-form leptin receptor expression. J Endocrinol 181**:** 297-306.

Winzell MS, & Ahren B (2004). The high-fat diet-fed mouse: a model for studying mechanisms and treatment of impaired glucose tolerance and type 2 diabetes. Diabetes 53 Suppl 3**:** S215-219.

Wolowczuk I, Verwaerde C, Viltart O, Delanoye A, Delacre M, Pot B*, et al.* (2008). Feeding our immune system: impact on metabolism. Clin Dev Immunol 2008**:** 639803.

Wong CF, Barnes LM, Dahler AL, Smith L, Popa C, Serewko-Auret MM*, et al.* (2005). E2F suppression and Sp1 overexpression are sufficient to induce the differentiation-specific marker, transglutaminase type 1, in a squamous cell carcinoma cell line. Oncogene 24**:** 3525-3534.

Wu J, Cohen P, & Spiegelman BM (2013a). Adaptive thermogenesis in adipocytes: is beige the new brown? Genes Dev 27**:** 234-250.

Wu M, Neilson A, Swift AL, Moran R, Tamagnine J, Parslow D*, et al.* (2007). Multiparameter metabolic analysis reveals a close link between attenuated mitochondrial bioenergetic function and enhanced glycolysis dependency in human tumor cells. Am J Physiol Cell Physiol 292**:** C125-136.

Wu SY, & Chiang CM (2007). The double bromodomain-containing chromatin adaptor Brd4 and transcriptional regulation. J Biol Chem 282**:** 13141-13145.

Wu SY, Lee AY, Lai HT, Zhang H, & Chiang CM (2013b). Phospho switch triggers Brd4 chromatin binding and activator recruitment for gene-specific targeting. Mol Cell 49**:** 843-857.

Wu T, Kamikawa YF, & Donohoe ME (2018). Brd4's Bromodomains Mediate Histone H3 Acetylation and Chromatin Remodeling in Pluripotent Cells through P300 and Brg1. Cell Rep 25**:** 1756-1771.

Wu Y, Tang D, Liu N, Xiong W, Huang H, Li Y*, et al.* (2017). Reciprocal Regulation between the Circadian Clock and Hypoxia Signaling at the Genome Level in Mammals. Cell Metab 25**:** 73-85.

Wu Z, Xie Y, Morrison RF, Bucher NL, & Farmer SR (1998). PPARgamma induces the insulin-dependent glucose transporter GLUT4 in the absence of C/EBPα during the conversion of 3T3 fibroblasts into adipocytes. J Clin Invest 101**:** 22-32.

Wyce A, Degenhardt Y, Bai Y, Le B, Korenchuk S, Crouthame MC*, et al.* (2013). Inhibition of BET bromodomain proteins as a therapeutic approach in prostate cancer. Oncotarget 4**:** 2419-2429.

Xiao J, Zhou Y, Lai H, Lei S, Chi LH, & Mo X (2013). Transcription factor NF-Y is a functional regulator of the transcription of core clock gene Bmal1. J Biol Chem 288**:** 31930-31936.

Xu Y, & Vakoc CR (2017). Targeting Cancer Cells with BET Bromodomain Inhibitors. Cold Spring Harb Perspect Med 7.

Yamajuku D, Shibata Y, Kitazawa M, Katakura T, Urata H, Kojima T*, et al.* (2010). Identification of functional clock-controlled elements involved in differential timing of Per1 and Per2 transcription. Nucleic Acids Res 38**:** 7964-7973.

Yamazaki S, Numano R, Abe M, Hida A, Takahashi R, Ueda M*, et al.* (2000). Resetting central and peripheral circadian oscillators in transgenic rats. Science 288**:** 682-685.

Yan J, Wang H, Liu Y, & Shao C (2008). Analysis of gene regulatory networks in the mammalian circadian rhythm. PLoS Comput Biol 4**:** e1000193.

Yang Y, Hu X, Zhang Q, & Zou R (2016). Diabetes mellitus and risk of falls in older adults: a systematic review and meta-analysis. Age Ageing 45**:** 761-767.

Yin FC, Spurgeon HA, Rakusan K, Weisfeldt ML, & Lakatta EG (1982). Use of tibial length to quantify cardiac hypertrophy: application in the aging rat. Am J Physiol 243**:** H941-947.

Yin L, & Lazar MA (2005). The orphan nuclear receptor Rev-erbα recruits the N-CoR/histone deacetylase 3 corepressor to regulate the circadian Bmal1 gene. Mol Endocrinol 19**:** 1452-1459.

Yisireyili M, Wulamu W, Aili A, Li Y, Alimujiang A, Aipire A*, et al.* (2019). Chronic restraint stress induces esophageal fibrosis with enhanced oxidative stress in a murine model. Exp Ther Med 18**:** 1375-1383.

Younossi Z, Anstee QM, Marietti M, Hardy T, Henry L, Eslam M*, et al.* (2018). Global burden of NAFLD and NASH: trends, predictions, risk factors and prevention. Nat Rev Gastroenterol Hepatol 15**:** 11-20.

Younossi ZM, Koenig AB, Abdelatif D, Fazel Y, Henry L, & Wymer M (2016). Global epidemiology of nonalcoholic fatty liver disease-Meta-analytic assessment of prevalence, incidence, and outcomes. Hepatology 64**:** 73-84.

Yu S, Zhao T, Guo M, Fang H, Ma J, Ding A*, et al.* (2008). Hypoxic preconditioning up-regulates glucose transport activity and glucose transporter (GLUT1 and GLUT3) gene expression after acute anoxic exposure in the cultured rat hippocampal neurons and astrocytes. Brain Res 1211**:** 22-29.

Zebisch K, Voigt V, Wabitsch M, & Brandsch M (2012). Protocol for effective differentiation of 3T3-L1 cells to adipocytes. Anal Biochem 425**:** 88-90.

Zee BM, Levin RS, Xu B, LeRoy G, Wingreen NS, & Garcia BA (2010). In vivo residue-specific histone methylation dynamics. J Biol Chem 285**:** 3341-3350.

Zhang B, Song L, Cai J, Li L, Xu H, Li M*, et al.* (2019). The LIM protein Ajuba/SP1 complex forms a feed forward loop to induce SP1 target genes and promote pancreatic cancer cell proliferation. J Exp Clin Cancer Res 38**:** 205.

Zhang CY, Baffy G, Perret P, Krauss S, Peroni O, Grujic D*, et al.* (2001). Uncoupling protein-2 negatively regulates insulin secretion and is a major link between obesity, β cell dysfunction, and type 2 diabetes. Cell 105**:** 745-755.

Zhang FF, Cardarelli R, Carroll J, Zhang S, Fulda KG, Gonzalez K*, et al.* (2011a). Physical activity and global genomic DNA methylation in a cancer-free population. Epigenetics 6**:** 293-299.

Zhang L, Yang G, Tang G, Wu L, & Wang R (2011b). Rat pancreatic level of cystathionine gamma-lyase is regulated by glucose level via specificity protein 1 (SP1) phosphorylation. Diabetologia 54**:** 2615-2625.

Zhang R, Lahens NF, Ballance HI, Hughes ME, & Hogenesch JB (2014). A circadian gene expression atlas in mammals: implications for biology and medicine. Proc Natl Acad Sci U S A 111**:** 16219-16224.

Zhang Y, Liao M, & Dufau ML (2006). Phosphatidylinositol 3-kinase/protein kinase Czeta-induced phosphorylation of Sp1 and p107 repressor release have a critical role in histone deacetylase inhibitor-mediated derepression [corrected] of transcription of the luteinizing hormone receptor gene. Mol Cell Biol 26**:** 6748-6761.

Zhang Y, Liu T, Meyer CA, Eeckhoute J, Johnson DS, Bernstein BE*, et al.* (2008). Model-based analysis of ChIP-Seq (MACS). Genome Biol 9**:** R137.

Zhang Y, Proenca R, Maffei M, Barone M, Leopold L, & Friedman JM (1994). Positional cloning of the mouse obese gene and its human homologue. Nature 372**:** 425-432.

Zhang Y, Thai K, Jin T, Woo M, & Gilbert RE (2018a). SIRT1 activation attenuates α cell hyperplasia, hyperglucagonaemia and hyperglycaemia in STZ-diabetic mice. Sci Rep 8**:** 13972.

Zhang Y, Tian S, Xiong J, Zhou Y, Song H, & Liu C (2018b). JQ-1 Inhibits Colon Cancer Proliferation via Suppressing Wnt/β-Catenin Signaling and miR-21. Chem Res Toxicol 31**:** 302-307.

Zhao ZY, Xie Y, Fu YR, Bogdan A, & Touitou Y (2002). Aging and the circadian rhythm of melatonin: a cross-sectional study of Chinese subjects 30-110 yr of age. Chronobiol Int 19**:** 1171-1182.

Zimmermann R, Haemmerle G, Wagner EM, Strauss JG, Kratky D, & Zechner R (2003). Decreased fatty acid esterification compensates for the reduced lipolytic activity in hormone-sensitive lipase-deficient white adipose tissue. J Lipid Res 44**:** 2089-2099.

Zisman A, Peroni OD, Abel ED, Michael MD, Mauvais-Jarvis F, Lowell BB*, et al.* (2000). Targeted disruption of the glucose transporter 4 selectively in muscle causes insulin resistance and glucose intolerance. Nat Med 6**:** 924-928.

Zuber J, Shi J, Wang E, Rappaport AR, Herrmann H, Sison EA*, et al.* (2011). RNAi screen identifies Brd4 as a therapeutic target in acute myeloid leukaemia. Nature 478**:** 524-528.